Titre: Title:	Chemical Recycling of Poly Methyl Methacrylate (PMMA), Process and Economics
Auteur: Author:	Jacopo De Tommaso
Date:	2024
Type:	Mémoire ou thèse / Dissertation or Thesis
Référence: Citation:	De Tommaso, J. (2024). Chemical Recycling of Poly Methyl Methacrylate (PMMA), Process and Economics [Thèse de doctorat, Polytechnique Montréal]. PolyPublie. https://publications.polymtl.ca/61034/

POLYTECHNIQUE MONTRÉAL
affiliée à l'Université de Montréal

Chemical Recycling of Poly methyl methacrylate (PMMA), process and economics

JACOPO DE TOMMASO
Département de génie chimique

Thèse présentée en vue de l'obtention du diplôme de *Philosophiæ Doctor*
Génie chimique
Novembre 2024

POLYTECHNIQUE MONTRÉAL
affiliée à l'Université de Montréal

Cette thèse intitulée :

Chemical Recycling of Poly methyl methacrylate (PMMA), process and economics

présentée par **Jacopo DE TOMMASO**
en vue de l'obtention du diplôme de *Philosophiæ Doctor*
a été dûment acceptée par le jury d'examen constitué de :

Bruno BLAIS, président
Gregory PATIENCE, membre et directeur de recherche
Miroslav GRMELA, membre
Sebastian JOSEPH, membre externe

DEDICATION

A Benedetta ...

ACKNOWLEDGEMENTS

This work would have never been possible without the help and support from several people along the years.

In April 2019, two weeks before moving to Montreal to pursue a PhD between McGill and Polytechnique Montreal, the McGill supervisor took an extended sick leave, and I did not know what to do. By that time I had already quit my job, left my apartment, and was ready to move to Canada. Daria, who was supposed to be my Polytechnique supervisor, told me to come anyway, and we would figure it out. During our first meeting, as we were brainstorming projects, I met Gregory, who was passing by–his office was next to Daria's. He had an ongoing project with a "major French company" on plastic recycling. We had a quick chat, and I liked the project. As they say, the rest is history. I guess this long preamble is to say that no matter how much you plan, life is unpredictable. Things happen that are out of your control, and that's okay. Engineers work within handbooks, norms, and the rules of what is and what should be. But researchers know better: the world doesn't fit neatly into an n-dimensional box. Science, after all, is an open-ended journey.

The first person I need to thank is my supervisor, Gregory S. Patience. Gregory is one of the most curious people I've ever met, and he teaches engineers how to become independent thinkers, which is the most invaluable skill any researcher could have. I've learned more about business, life, and even myself from him than I could have ever imagined with another supervisor. Thank you, Gregory, for giving me the freedom to pursue the research I wanted and for always pushing me beyond my comfort zone.

Here's another twist: less than a year into the program, COVID-19 hit. The lab closed for over six months, and even after reopening, operated at limited capacity for another year. In July 2020, I received an email from our industrial partner at Arkema, Jean-Luc Dubois, who I had met briefly in September 2019 at a progress meeting in Montreal. He mentioned an opportunity for me to join Arkema France for a few months. That's when I really got to know Jean-Luc. He's the most knowledgeable–and kindest–person I've ever met. If there's one person without whom this project could never have been completed, it's him. Thank you, Jean-Luc, for your constant support over the years and for always making time to discuss research, even in your free time or after hours. I am forever in your debt. My year in France was the happiest time of my PhD, and it gave me the knowledge and confidence to go the distance.

Another special person I met on this journey is Federico Galli. Federico is not only an

outstanding researcher (and now a professor), but he's also incredibly caring and generous. Grazie mille Federico per la tua amicizia ed i preziosi consigli, oltre che l'aiuto ed il supporto in ambito accademico, e non. Special thanks to all my colleagues and friends from Polytechnique, Nooshin, Maoline, Mina, Dat, Yanfa, Tugce, Mahdi, and all the others. Thank you for always cheering me up and listening to me. Grazie mille a Dalma per i mille caffè, e sopratutto le nostre chiacchierate. Gracias especiales también a Paula, no sólo por hablar siempre español conmigo, sino por tu amistad y la alegría que aportaste al grupo. Special thanks to Nicolas, who made me realized that there was a way out, we are smart, and we deserve it. Un remerciement spécial à Jean-Ghantous, qui m'a enseigné presque toutes les compétences pratiques que j'ai, et m'a poussé à parler et à améliorer mon français.

Laura, Adrien, baby Paul, Alexandre and Juliette, my dearest friends and my family in Montreal, you supported me at every step of the way, and I never once felt alone so far from home. All my best memories in Montreal are shared with you, and I could've not asked to be surrounded by more caring people. Thank you Laura for the meals, pizza nights, the karaoke, and never giving up on our friendship. Merci à Juliette et Alex pour les voyages autour du Québec, pour m'avoir présenté à vos amis et à votre famille, et pour m'avoir aidé à me sentir accepté et aimé dans cette province.
Non sarei qui senza mamma, papà, nonna Lisa, mio fratello Christian, Giancarlo, Cristina, ed Alessandro, che hanno condiviso da lontano tutti i momenti di questi cinque anni, i tantissimi episodi di sconforto, tristezza, frustrazione, le piccole vittorie, ma anche, semplicemente, la quotidianità. Nonostante la distanza mi sono sempre sentito parte della vostra vita, grazie.
Michele, se sono qui è anche grazie al lavoro fatto in questi tre anni assieme, grazie.

Infine, grazie a Benedetta, mia moglie, che ha fatto sacrifici enormi per aiutarmi a raggiungere questo traguardo, si è trasferita dall'altra parte del mondo, ha aspettato tre anni per poter insegnare in Canada, e nel frattempo ha lavorato in un supermercato, o come nanny, imparato nuove lingue, e lasciato la sua famiglia e tutti i suoi amici. Affronti tutto con praticità e con un sorriso, sei il mio modello, la persona piú intelligente che conosco, e la compagna di mille (+1) avventure. Sei la mia famiglia, assieme a Remicc, ziglietto, la Tessa e tutti i nostri personaggi. Grazie a te per aver sempre creduto che ce l'avrei fatta, ed avermi aiutato a fare lo stesso.

RÉSUMÉ

Le Poly(méthacrylate de méthyle) (PMMA), également connu sous le nom de verre acrylique, ® Plexiglas, Persplex ®, ou Altuglas ™ est un thermoplastique transparent polyvalent, souvent utilisé comme alternative au verre dans les secteurs de la construction, de l'électronique et de l'automobile, en raison de sa résistance à la traction, à la flexion, aux UV, et de sa transparence. En 2021, le marché mondial du PMMA a dépassé 4,5 milliards de dollars. Le PMMA représente également un polymère idéal pour la transition vers une économie circulaire, en raison de son potentiel élevé de recyclage polymère à polymère (>90 %). Avec l'augmentation de la demande mondiale de PMMA et le renforcement des réglementations environnementales, les acteurs de l'industrie recherchent des solutions de recyclage efficaces. Cependant, le taux de recyclage du PMMA reste faible, avec moins de 10 % du matériau récupéré et recyclé en Europe, principalement en raison de contraintes techniques et économiques. En 2024, seules trois entreprises européennes recyclent le PMMA à une échelle industrielle, tandis que d'autres plus petites, situées en Asie du Sud et en Amérique du Sud, desservent surtout les marchés locaux.

Avant les interdictions d'importation de déchets plastiques imposées par la Chine et l'Inde en 2018-2019, le marché du méthacrylate de méthyle vierge (le monomère du PMMA) était cent fois plus grand que celui du r-MMA, et les fabricants occidentaux manifestaient peu d'intérêt pour intégrer des matériaux recyclés dans leurs lignes de production. De plus, le recyclage mécanique du PMMA est limité aux polymères propres, triés et post-industriels, issus de l'extrusion ou de l'injection. En revanche, la thermolyse du PMMA à 400 °C permet de traiter à la fois des PMMA coulés et extrudés ainsi que des déchets contaminés (par des pigments, inhibiteurs ou additifs), sans être limité par la couleur, puisque le r-MMA final est transparent.

Bien que plusieurs technologies de thermolyse du PMMA existent, un écart persiste entre la recherche académique et les pratiques industrielles. Les recycleurs industriels s'appuient souvent sur leur expérience pratique plutôt que sur des solutions fondées sur des données scientifiques, tandis que les chercheurs académiques se concentrent souvent sur des technologies moins applicables. Dans ce travail, nous développons des outils et des méthodologies pratiques pour promouvoir le recyclage du PMMA et combler ce fossé entre la théorie et l'application industrielle.

Pour ce faire, nous avons :

1. Analysé l'état actuel du recyclage du PMMA et identifié les risques techniques et

économiques associés ;

2. Développé des corrélations pour estimer l'investissement total (TCI) nécessaire pour la mise en place d'usines de recyclage chimique à un stade précoce du processus ; et

3. Dépolymérisé des composites complexes à base de PMMA.

Ce document sert de guide pour les ingénieurs, recycleurs et chercheurs impliqués dans la valorisation des déchets de PMMA. Il fournit des scénarios fondés sur des données, permettant aux recycleurs de justifier leurs décisions d'investissement tout en réduisant les risques, notamment ceux liés à l'incertitude des coûts en capital et à la qualité des produits. Le succès du recyclage à grande échelle du PMMA dépend des flux de déchets en fin de vie, qui ne sont souvent pas conçus pour être recyclés. Les chercheurs doivent réduire ces incertitudes et adapter les procédés de recyclage aux flux de déchets spécifiques – une solution one-size-fits-all ne convient pas au recyclage chimique.
Bien que le PMMA vierge soit relativement facile à recycler en théorie, les matériaux post-consommation, comme les composites à base de PMMA, posent des défis particuliers. Ils sont difficiles à broyer sans se dégrader, contiennent des co-produits qui favorisent des réactions secondaires indésirables, et doivent conserver toute leur valeur initiale pour justifier un retour économique et environnemental positif. Grâce aux méthodes que nous avons développées, les ingénieurs seront mieux équipés pour surmonter ces défis et recycler les composites à base de PMMA en fin de vie et post-consommation.

Nous avons d'abord étudié les pratiques actuelles de thermolyse du PMMA pour récupérer du MMA et identifié les facteurs clés qui influencent la viabilité économique d'une usine de recyclage type à l'aide de simulations Monte-Carlo. Nos résultats montrent que les usines les plus avancées coûtent environ 10 millions de dollars et peuvent traiter 5 000 tonnes de déchets PMMA par an, avec un rendement de 78 % en r-MMA, vendu au prix du matériau vierge. Toutefois, certains recycleurs préfèrent traiter des déchets moins coûteux et non triés dans des installations à moindre coût (á partir de 1,3 million de dollars), produisant un r-MMA de qualité inférieure (pureté $< 98{,}5$ %) pour minimiser le temps de retour sur investissement. Nos simulations montrent que cette approche est contre-productive à long terme. Les usines utilisant des déchets de faible qualité, produisant du r-MMA impur, sont les plus exposées à un risque de perte nette après dix ans. À l'inverse, viser un r-MMA de haute qualité (comparable au matériau vierge), réalisable avec un tri ou une purification supplémentaire, est la stratégie la plus rentable. Le scénario optimal consiste à traiter des déchets PMMA triés dans des installations de pointe, vendant le r-MMA au prix du matériau vierge ou à un prix supérieur, garantissant ainsi le meilleur retour sur investissement et le risque le plus faible.

En raison du manque de données fiables sur les usines de recyclage du PMMA, les décideurs ont besoin de méthodes rapides et précises d'estimation du capital pour évaluer de nouvelles technologies. Nous avons créé une base de données de 167 installations de recyclage chimique existantes ou prévues (incluant la pyrolyse, la gazéification et les technologies à base de solvants) et testé des modèles d'estimation des coûts en capital (AACE classe 5). Nous avons démontré que ces modèles manquaient de fiabilité et proposé de nouvelles corrélations basées sur la capacité de l'usine ou les pertes énergétiques, qui se sont révélées plus précises ($R^2 >$ 0,90). Pour une usine de recyclage de 5 000 tonnes de PMMA par an, le coût estimé se situe entre 5 et 8 millions de dollars, avec une plage de probabilité de [5 %, 95 %]. Cette estimation est proche de nos hypothèses initiales, mais la répartition des coûts est plus étroite. Lorsque le projet est à un stade précoce (moins de 10 % de maturité), les différentes technologies présentent des distributions de coûts similaires.

Malheureusement, ces résultats sont principalement valables pour les déchets post-industriels de PMMA propres. Les déchets post-consommation, en particulier sous forme de composites, nécessitent des prétraitements supplémentaires et sont souvent mal gérés. Le marbre artificiel, un composite de PMMA rempli d'hydroxyde d'aluminium (ATH), est l'un des plus difficiles à recycler, en raison de sa teneur en eau, qui favorise des réactions secondaires lors de la dégradation. Pour préserver au mieux la valeur de ce matériau, nous avons mis en place un processus de thermolyse en deux étapes : d'abord à 300 °C, pour éliminer l'eau de l'ATH, puis à 400 °C pour dépolymériser le PMMA en MMA. Cette approche permet de récupérer 66 % de MMA de la fraction organique et de la boehmite, précurseur de l'alumine γ, à partir de l'ATH. Ainsi, le recyclage du PMMA peut s'étendre à des flux de déchets plus diversifiés, démontrant que le recyclage chimique doit s'adapter aux spécificités de chaque matériau – qu'il s'agisse de polymères ou de composites – afin de garantir durabilité et viabilité économique.

ABSTRACT

Poly Methyl Methacrylate (PMMA), also known as acrylic glass, ® Plexiglas, Persplex ®, or Altuglas ™ is a versatile transparent thermoplastic, and an alternative to glass in construction, electronics, and the automotive industry due to its tensile and flexural strength, UV resistance, and transparency. The global PMMA market exceeded 4.5 billion USD in 2021. PMMA is also an ideal polymer for the transition to a circular economy, owing to its potentially high (>90%) polymer-to-polymer recycling yield. As global demand for PMMA rises, coupled with stricter environmental regulations, stakeholders across the value chain are calling for effective recycling solutions. Despite this, PMMA's recycling rate remains low, with less than 10% of PMMA being recovered and recycled in Europe due to both technical and economic constraints. As of 2024, only three companies in Europe recycle PMMA on a commercial scale, while smaller operations in southern Asia and South America primarily serve local markets.

Before China's and India's bans on plastic waste imports in 2018-2019, the market for virgin methyl methacrylate (PMMA's monomer) was a hundred times larger than the r-MMA market, with little interest from Western manufacturers to adapt their production lines and incorporate recycled materials. At the same time, mechanical recycling of PMMA is limited to clean, well-sorted, post-industrial extrusion and injection polymer grades. In contrast, PMMA thermolysis at 400 °C can treat both cast and extrusion-grade PMMA to r-MMA, including contaminated scraps (e.g., those containing pigments, inhibitors, or additives), without being limited by color, as the final r-MMA is transparent.

While various PMMA thermolysis technologies exist, a disconnect persists between academic research and industrial practice. Industrial recyclers often rely on experience rather than data-driven solutions, while academic researchers focus on unfeasible technologies. In this work, we develop practical tools and methodologies to advance PMMA recycling and bridge the gap between theoretical knowledge and real-world application.

To achieve this, we:

1. Analyzed the current state of the art in PMMA recycling and identified the associated technical and economic risks;

2. Developed plug-in correlations to estimate the total capital investment (TCI) of chemical recycling plants at the early stage of a process; and

3. Depolymerized complex PMMA-based composites.

This document serves as a guide for engineers, recyclers, and researchers working on PMMA waste valorization. Recyclers now have access to data-driven scenarios to justify investment decisions and minimize risks, particularly regarding capital cost uncertainties and consistent product quality, both of which hinder PMMA recycling at scale. This depends on the diverse, end-of-life PMMA waste feedstocks that are not necessarely "designed for recycling." Researchers must work to reduce capital cost uncertainties and tailor recycling processes to specific feedstocks – one-size-fits-all solutions are ineffective in chemical recycling.
While virgin, clean PMMA is theoretically "easy-to-recycle," post-consumer materials, such as PMMA composites, introduce specific challenges. These materials are hard to grind into fine powder without degradation, contain co-products that promote parasitic reactions, and must retain their full composite value to create both a positive business and environmental case. Engineers will learn how to overcome these challenges from the methods we developed to recycle end-of-life, post-consumer PMMA composites.

First, we analyzed current PMMA thermolysis practices for MMA recovery and identified key factors affecting the economic viability of a typical recycling plant using Monte Carlo simulations. We found that state-of-the-art plants cost around 10 million USD and can process 5,000 tons of PMMA waste annually, achieving a 78% r-MMA yield that sells at the virgin material price. However, recyclers often opt to treat cheaper, unsorted waste in low-cost facilities (as low as 1.3 million USD), which produces subpar r-MMA (purity $< 98.5\%$) to minimize payback time. When we compute historical distributions of PMMA scraps feedstock price, r-MMA price, capital investment, energy cost, plant waste handling costs, in the Monte Carlo simulation, we demonstrate that the current recycling approach is counterproductive over time. Plants using free, low-quality feedstocks to produce low-purity r-MMA face the highest risk of negative net present value over a 10-year period. Recyclers should instead aim for high-quality r-MMA (comparable to virgin material), which is achievable but requires additional investment in sorting or purification. The most profitable scenario processes clean, sorted PMMA scrap in a state-of-the-art facility and sells the r-MMA at virgin or premium prices, offering the highest return on investment and the lowest risk. Total capital investment and r-MMA pricing have the most significant impact on the economic viability of PMMA recycling projects. Deals with final buyers reduce r-MMA price uncertainties, and data-driven methods narrow the variability in capital investment estimates. However, chemical engineers still rely on outdated empirical methods from the oil and gas industry for early-stage capital investment estimation.

Reliable data on PMMA recycling plants are scarce, and decision-makers need quick, ac-

curate capital estimation methods to assess new technologies. Therefore, we developed a database of 167 existing or planned chemical recycling facilities (pyrolysis, gasification, and solvent-based technologies) and tested conventional early-stage capital cost estimation models (AACE class 5) against it. We found these models unreliable and proposed new ballpark correlations based on plant capacity or energy loss, which proved statistically more accurate ($R^2 > 0.90$). Given the similarities between PMMA thermolysis and mixed plastic pyrolysis (which dominates the database), a 5,000 tons/y PMMA recycling plant should cost between 5 and 8 M USD, in the [5%, 95%] probability range. The median is close to what we had guessed before for a typical facility, but the distribution is narrower. At low project maturity (less than 10%), all technologies exhibit similar capital investment distributions, regardless of feedstock, products, or reagents. At this stage, the number of cycles in which carbon retains 50% of its mass in the economy is an equally effective indicator for environmental screening. This reiterates that, PMMA, with a polymer-to-product mass yield of 90%, keeps 50% of the carbon in the economy after $0.5 = (0.9)^6$, 6 recycling operations, and is therefore the best polymer for a true circular economy transition.

Unfortunately, this is true only for clean, post-industrial, PMMA scraps, which are currently the only ones recycled. Post-consumer PMMA, particularly in composite form, requires additional pre-treatments, and it is mostly mismanaged. One such composite is artificial marble, an aluminium hydroxide (ATH) filled PMMA material, the most popular artificial stone globally but difficult to recycle due to water content, which promotes parasitic reactions during depolymerization. Regardless of the operative conditions (temperature, external water content, presence of catalyst, batch or semi-batch reaction), the inherent contact between ATH and PMMA promotes PMMA hydrolysis on its back-bone to poly methacrylic acid. To preserve the material full value, we thermolyzed it in a dual-stage process. First, at 300 °C, we released most of the water from ATH, and then, at 400 °C, we depolymerized PMMA to MMA. In this way, we recovered MMA (66 % yield) from the organic fraction, and boehmite, an γ-Alumina precursor, from ATH. This approach expands PMMA recycling to include diverse streams, and demonstrates that chemical recycling must be tailored to the unique characteristics of each material–whether composite or polymer–to ensure both sustainability and economic viability.

TABLE OF CONTENTS

LIST OF TABLES

LIST OF FIGURES

LIST OF SYMBOLS AND ACRONYMS

AACE	Association for the Advancement of Cost Engineering
ATH	Aluminium hydroxide $Al(OH)_3$
Bohemite	Aluminium hydroxide oxide AlOOH
CAPEX	Capital Expenditure
Crude MMA	Crude Methyl MethAcrylate
EA	Ethyl Acrylate
E/M Propionate	Ethyl/Methyl propionate
Gibbsite	Aluminium hydroxide $Al(OH)_3$
HDPE	High Density Polyethylene
LHV	Lower Heating Value
MA	Methyl Acrylate
MAA	Methacrylic Acid
MIB	Methyl Isobutyrate
MMA	Methyl Methacrylate
NPV	Net Present Value
PET	Poly Ethylene Terephthalate
PMAA	Poly Methacrylic Acid
PMMA	Poly Methyl Methacrylate
PS	Polystyrene
rMMA	Regenerated Methyl Methacrylate (Purified)
TCI	Total Capital Investment
$Al(OH)_3$	Aluminium hydroxide
Al_2O_3	Alumina
AlOOH	Aluminium hydroxide oxide

LIST OF APPENDICES

CHAPTER 1 INTRODUCTION

1.1 Plastic Recycling

Plastic pollution and overproduction have become a multi-generational challenge, surpassing 400 million tons of plastic produced in 2019 [1]. The COVID-19 outbreak worsened the plastic waste crisis, with a surge in peak production to more than 530 million tons per year in 2019-2020 [2, 3]. In the same biennium, the global annual GDP growth dropped by 7.5%, while plastic usage only declined by 2%, underscoring the increasing importance of plastic in the global economy [1]. The increasing demand for plastic, along with supply chain disruptions, are reducing post-industrial plastic waste while increasing the harder-to-manage post-consumer waste. The pandemic has also disrupted recycling efforts at both local and international levels, severely limiting the ability to manage the transition to a circular disposal system, [1, 4] especially for single-use healthcare waste streams, where the low cost of production outweighs the high costs of collection and pretreatment [5].

Right now, we estimate that only 9% of the total plastic waste is collected for recycling (chemically or mechanically) [1], with the rest littered, landfilled or incinerated in different proportions depending on the geographical areas. Landfilling is a threat for public health and wildlife [6], breaks the resource cycle, and it is ultimately unsustainable [7]. At the same time, because of its cost-effectiveness and low labor requirements, landfilling remains the preferred waste handling method across most of the world (49% of total waste) [8], with the exception of OECD Asian countries and EU member states [1]. Incineration (with energy recovery) reduces waste volumes up to 90% [9], and despite higher capital and operative costs, in the last 10 years, it has been replacing landfilling in EU and other densely populated areas where land is scarce [10, 11]. However, Directive (EU) 2018/850 and Regulation 2021/C of the European Parliament, endeavoured against the shift from landfill to incineration, and then included it under the activities 'considered to do significant harm to the circular economy, including waste prevention and recycling' [12]. Incineration facilities are now required to report to the EU emission trading system, a greenhouses gases carbon market to reduce EU emissions and finance the green transition [13].

Whenever feasible, mechanical recycling is the preferred option for handling plastic waste, as it is cost-effective, not energy-intensive, and theoretically applicable to all thermoplastics. However, plastic inevitably undergoes down-cycling over time [14,15], as the process degrades the material's mechanical and optical properties. Mechanical recycling is also susceptible to inhibitors and contaminants, requiring additional separation steps, and plastic blends, that

render the waste immiscible [16, 17]. Chemical recycling breaks down plastics at the molecular level into monomers, a variety of liquid or gaseous intermediates, or char [18]. This process bypasses the limitations of recycling cycles and material property degradation but requires more energy, capital, and labor compared to mechanical recycling. Currently, only 3% of waste plastic is chemically recycled [19]. Yet, chemical recycling could handle streams that are too contaminated, composed of mixed plastics, or have already been mechanically recycled [20]. Projections estimate that this recycling method will account for 25% of waste plastic processing by 2050 (and 15% by 2030) [19, 21].
Chemical recycling techniques vary based on their interaction with the plastic polymer chain. Pyrolysis and gasification are thermolysis processes: heat breaks the plastic chains in an inert or partially oxidized atmosphere, respectively. Pyrolysis typically operates at lower temperatures than gasification (e.g., 600 °C vs 1000 °C for polyolefins [22]), producing a wider spectrum of products, primarily liquids, waxes, and char. Gasification, on the other hand, converts plastic directly into gases. In contrast, solvolysis and selective dissolution require solvents, to interact with the plastic chains. Solvolysis occurs when the solvent reacts with the plastic, whereas in selective dissolution–positioned between mechanical and chemical recycling–the solvent dissolves the plastic without a molecular-level reaction.

Despite advancements in mechanical and chemical recycling, current practices do not achieve the plastic-to-plastic recycling rates necessary for sustainable waste management [20]. "Absolute sustainability" of human activities by 2030–defined as maintaining global operations without destabilizing the Earth's systems–requires a global plastic-to-plastic recycling rate of over 71% [23]. Even in an unrealistically optimistic scenario of 94% waste collection and recycling using existing technologies (39% through mechanical recycling and 55% via mixed plastic waste pyrolysis), this target is unattainable. This shortfall stems from material losses during mechanical recycling and the low plastic-to-plastic yields (30-35%) typical of mixed plastic pyrolysis. To meet this goal, a viable approach is to aim for a moderate yet achievable waste collection rate (e.g., 75%) and employ high-yielding recycling processes. This would involve maximizing mechanical recycling where feasible, supplemented by selective chemical recycling for streams with the highest potential for plastic-to-plastic conversion.

1.2 Poly Methyl Methacrylate

One, if not the best, candidate for high-yielding waste-to-plastic recycling is poly methyl methacrylate (PMMA), also known as acrylic glass, ® Plexiglas, Persplex ®, or Altuglas ™ , a versatile transparent thermoplastic and an alternative to glass due to its tensile and

flexural strength, UV resistance and transparency. The global PMMA market exceeds 4.5 billion USD (2021), equivalent to 2 M tonnes per year, foreseen to surpass 3 M tonnes by 2028 [24–26].

PMMA sells in form of cast or extruded sheets, injection molding, and granules resins, with four end-uses for products with a life span from several years to decades [26]: **(i)** building and construction – including signage (44%); **(ii)** automotive (26%); **(iii)** electronics (20%); **(iv)** others (6%). In particular:

- **Building and construction:** Shower panels, sound barriers, railings, building facade, and toilets [27] as well sanitary and interior decoration, signage and lighting, contributing to most of PMMA sheets market. Non-hazardous waste from the construction industry has low to zero market (except metals) and it's hardly recycled or reutilized (1%), [28]. In 2019, Europe only collected 11 kt of PMMA-based construction waste every year [29].

- **Signage and electronics**: PMMA accounts for 0.1 % of the global electronic waste [30, 31], or 9.5 kt/y and 3.5 kt/yof end-of-life PMMA from light signs and POP (point of purchase) in Europe and North America respectively [32]. Although presently less than 1 kt/y is collected, the supply chain is developing and volumes are expected to increase by an order of magnitude.

- **End-of-life vehicles**: Lightweight parts to attain fuel-efficiency, high weathering and UV resistance glazing owing, account for up to 2.3 kg of PMMA per vehicle, including rear lights and other fittings, contributing to most of the resin market. This translates to a end-of-life PMMA stream from vehicles in Europe of 12 kt/y (5 million units) in 2019, and 1 kt/y in the sole automobile market in Canada in the same period. [33].

Among those, a significant part (>15%) exists as composites or blends, such as aluminium hydroxide (ATH) filled PMMA, or dental resins, which complicates waste collection and subsequent treatments.

Accurate figures are uncertain due to trading among regions, but most of PMMA waste remains still unaddressed [34]. In Europe, 10% of PMMA waste is collected [35], and about 5% recycled [34]. If global PMMA collection mirrored European rates, recycling volumes could reach 250 kt/y to 500 kt/y, potentially creating a market worth billions of dollars. Unlike high-volume, low-value plastics such as polyolefins, PMMA is priced significantly higher (2500 USD/t to 3500 USD/t) and produced in quantities that support feasible collection and recycling logistics (Figure 1.1). The low margins associated with polyolefin or PET recycling often favours mechanical recycling, which is more cost-effective and technically viable where

applicable. In contrast, the untapped potential of the PMMA waste stream presents higher margins, and it favours approaches that preserve the full material value, like chemical, or advanced, recycling.

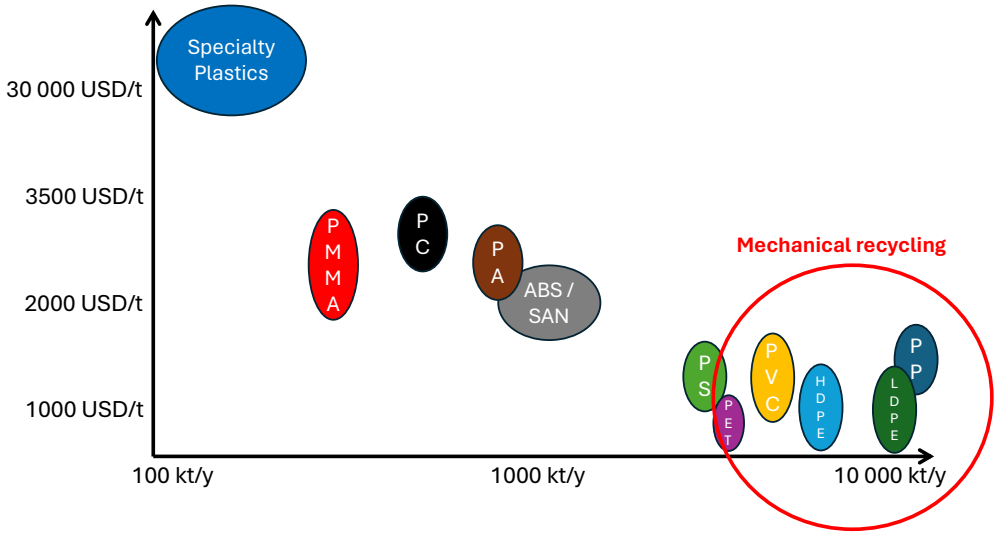

Figure (1.1) Prices versus production volume for common plastics in 2022-2023 [36]. Modified image from [37].

1.3 PMMA Recycling

For any plastic waste stream where both mechanical and chemical recycling are feasible and yield comparable products, mechanical recycling is the preferred option due to its lower energy and carbon footprint and higher process yields [38]. For PMMA, mechanical and chemical recycling are complementary and cater different needs.

1.3.1 Mechanical Recycling of PMMA

Mechanical recycling of PMMA involves one to two heating steps (180 °C to 250 °C) to melt and re-extrude ground waste scraps [35]. However, with a ceiling temperature of 192 °C [39, 40], PMMA is prone to degradation and depolymerization during mechanical reprocessing.

Even clean, properly sorted PMMA waste may not be ideal for mechanical recycling. PMMA waste from products with long lifespans often contains industrial additives or banned chemicals that mechanical recycling cannot remove [38, 41, 42]. Additionally, PMMA's frequent application alongside other materials complicates sorting into a homogeneous stream, and contamination with other plastics degrades its optical and mechanical properties when recy-

cled mechanically [35, 43]. Even with effective separation from other plastics, PMMA sorting by colour or grade (e.g. cast vs injection or extrusion grade) is not cost-effective, or feasible at all. This limits recycling to black products [43], and only for extrusion and injection PMMA grades, because cast PMMA degrades before melting due to a higher molecular weight [35].

1.3.2 Chemical Recycling of PMMA

Compared to mechanical, chemical recycling of PMMA is more energy intensive because the polymer needs to heat up, melt and react at 350 °C to 400 °C, followed by boiling the monomer at least once to purify it, and re-polymerizing it. Additionally, chemical recycling demands higher capital investment and more specialized personnel, particularly when producing high-quality monomers for premium markets. The expertise required for chemical recycling is distinct and not easily transferable from conventional polymer processing. However, chemical recycling treats indistinctly cast and extrusion grade PMMA, contaminated scraps (e.g. with pigments, inhibitors, or additives), and it is not limited by colour because the final r-MMA is transparent.

Otto Röhm first synthesized PMMA in 1928, and already in 1945, Gem Participations patented a "heat transfer bath process" to depolymerize "Lucite" scrap back to the monomer [44], as a response to the lack of virgin material for windshields and nose panels in german aircrafts during world war II. Since then, the chemical industry exploited PMMA's ability to unzip to its monomer (MMA) under heating through various techniques. The process is a radical polymer chain unzipping, with the scission mechanism that depends on the plastic nature, and the temperature. PMMA is prepared by free radical (FRP), or anionic polymerization (AP), with the first being the industrial standard [45]. Free radical polymerized (FRP) PMMA typically follows a three-step depolymerization, while anionically polymerized (AP) PMMA undergoes a single-step degradation [35, 46]. The reason is the presence of a thermal initiator for MMA polymerization via FPR, that introduces head-to-head defects and unsaturated chain ends in PMMA, that will in turn become radicals when the depolymerization starts [35]. Instead, in AP the polymerization proceeds exclusively via head-to-tail propagations, so that during depolymerization, the polymer unzips via head-to-tail fissions into tertiary radicals in only one step. AP is not industrially relevant, so in practice collected PMMA waste is most likely an FPR material.
When the depolymerization temperature is lower than 270 °C, head-to-head fission dominates, with the formation of two tertiary end-of-chain (ECR) radicals. MMA forms when a tertiary or primary ECR undergoes and end of chain β-scission. However, primary ECR are less stable radicals, and they can also undergo a group-side or methyl β-scission, which

will ultimately produce gas and oligomers. This means that for lower depolymerization temperatures, PMMA cracks around the head-to-head defects, producing two tertiary ECR, and MMA production is favoured thermodynamically, but not kinetically. Above 500 °C, head-to-tail fission dominates, but the temperature is high enough to activate the parasitic scissions of the primary ECR. Instead, around 350 °C to 400 °C, head-to-tail fission dominates, but the MMA yield is maximum because both tertiary and primary ECR mainly cleave on their end-chain [47]. In more practical terms, industrially, PMMA chemically thermolyse to its monomer methyl methacrylate (MMA) at 350 °C to 400 °C with over 90 % yield and purity [48, 49].

Depolymerization techniques vary in their heating delivery, residence time, and purification. The ideal process converts highly contaminated PMMA waste into pure MMA with the highest yield. However, historically, trade-offs between capital cost, target product quality, available waste streams, and local regulations have influenced the choice of technology, depending on the location and timing of the plant's construction. Processes such as dry-distillation and rotary drum systems require lower capital investment (e.g., 1-2 million USD for a 5 kt/y plant) but yield lower-quality recycled MMA (r-MMA) [24, 35]. These semi-batch processes load plastic into either static or rotating vessels that are externally heated. The uneven heating creates hot spots and char, which favour hydrogen-transfer reactions introducing impurities into the final product [35]. Dry-distillation plants are on the low-risk low-opportunity end of the spectrum [50], and more prevalent in markets where lower quality MMA is accepted, such as southern-east Asia or Brazil. Another existing variation of the dry-distillation is the stirred-tank, where the agitation increases heat and mass transfer, but with higher capital and operative costs to stir a highly-viscous medium [50].
In contrast, technologies like molten-lead beds, where PMMA scraps are fed into a molten metal tank, produce higher-quality MMA suitable for more regulated markets like the EU, but require a larger capital (e.g. 7-10 million USD for a 5 kt/y plant). Lead use imposes stricter environmental regulations too, and faces public opposition [51, 52]. More complex technologies, such as fluidized beds [53], microwave reactors [54], and superheated steam reactors [55], address specific technical challenges like heat transfer, product purificaton, and faster residence times. However, process stability, scalability, and operational costs limited their application at scale. For example, in 2008, Mitsubishi Rayon, the world's first PMMA producer, patented a fluidized bed process for PMMA pyrolysis [56]. Although they reported a 95% MMA yield with 94-95% purity [57], the process was discontinued after establishing pilot plants in Toyama, Japan (2 kt/y), and Hertfordshire, UK (4 kt/y), in collaboration with Lucite (formerly ICI Acrylics, now part of Mitsubishi) [58, 59]. Over the past 30 years,

molten-lead beds in Europe and dry-distillation or rotating drums in developing economies have dominated the industrial standard for PMMA recycling, with limited use of stirred-tank reactors and virtually no industrial relevance for the rest.

The European emphasis on recycling and material re-use, driven by both consumer demand and regulatory frameworks such as REACH, necessitates r-MMA quality that closely matches virgin PMMA. That is, a premium product at premium price, which has spurred renewed interest in high-risk, high-reward technologies like twin-screw extruders, auger-screws, and next-generation microwave reactors [60–63]. Ultimately, investment decisions hinge on the attractiveness of the business case rather than solely on chemical-engineering metrics such as purity or yield, to align technological choices with market demands.

PMMA chemical recycling to Methacrylic Acid (MAA)

r-MMA quality is catered to the market of choice, which means that although technically possible, producing r-MMA comparable to virgin MMA (99.7 %) while starting from highly contaminated feedstocks can be uneconomical. This is especially true in case of composites, like glass-fiber reinforced, or ATH-filled PMMA for interior design or wind-blades, where the plastic represent only a fraction of the material (e.g. 20-45 %). When recyclers target high-end optical application (e.g. automotive or electronic), a r-MMA impurity mass fraction as small as 0.2 % renders the final polymer opaque [35, 64, 65]. Same applies for other impurities like ethyl acrylate (EA) or 2,3-butanedione [66, 67], acrid molecules that will prevent commercialization if the odour intensity surpasses 3. When purification is non-viable or too expensive, the recycled polymer is downcycled to less profitable applications. Impurities in the r-MMA are numerous (Table 1.1), and they originate from:

(i) The PMMA scraps themselves: Impurities such as methyl acrylate, butyl acrylate, ethyl acrylate, or other acrylic esters come from co-monomers or additives present in the PMMA scrap formulation, for instance like in extruded sheets or solid surface materials. Same applies for chlorinated products coming from the PVC protection gaskets.

(ii) The depolymerization reaction [68]: Aromatics like benzene, xylene, or toluene originate either as part of the char formation mechanism [69], or from the pyrolysis of polyethylene films used to protect PMMA sheets from scratching [35]. The pyrolysis can also introduce additional impurities, such as methyl isobutyrate, which forms through the parasitic hydrogenation of MMA in contact with char for prolonged periods (e.g., in dry distillation reactors), as well as methyl pyruvate and 2,3-butanedione [66].

Automated or sometimes manual (e.g. PE films) sorting minimizes the external impurities **(i)**. Process-generated impurities depend, instead, on the technology of choice. Besides, some of these impurities (e.g. ethyl acrylate, or methyl isobutyrate) have a boiling within 5 °C to 10 °C to MMA, which further complicates the separation. An alternative to PMMA thermolysis to MMA, is PMMA hydrolysis to methacrylic acid (MAA), the correspondent acid of MMA. This alternative targets difficult to process PMMA scraps, unsuitable to thermolysis due to the prohibitive costs of upstream sorting and/or dowstream purification. Instead, in presence of water at temperatures similar to those of thermolysis (i.e. 350 °C to 400 °C), MMA hydrolyses to MAA, together with the acrylic impurities. For instance, methyl isobutyrate, a difficult to separate compound in MMA thermolysis, hydrolyses to isobutyric acid, which can be separated from MAA by crystallization (Table 1.1) [70]. Ethyl acrylate, another difficult to separate compound in thermolysis, converts to acrylic acid, that can be polymerized together with MAA in super-adsorbent materials, like diapers [71].

Compared to MMA, MAA has one-tenth the market size [75,76], most of which goes towards MMA production, but also paints, fabric treatment agents, adhesives and ion-exchange resins, and super-absorbent [77,78]. Due to its smaller market volumes and niche applications, MAA has fewer suppliers. There is growing interest from consumers to enhance market elasticity and decouple MAA dynamics from those of MMA by encouraging new producers, particularly those focusing on bio-sourced or renewable materials. There are no bio-based MAA routes due to thermodynamically intrinsic low yields, [79] which render potential MAA from waste PMMA even more attractive.

Over the past decade, research from both academia and industry has explored this route at the laboratory scale with mixed results. PMMA hydrolysis in a single-step fluidized bed process yields approximately 30% MAA by mass at 280 °C, using a large excess of zeolite Y catalyst (1:2 ratio compared to the plastic) [80]. Under similar conditions, MAA yields improve to around 50% in a tandem fluidized bed-fixed bed reactor, where PMMA first depolymerizes in the fluidized bed and then hydrolyzes in the fixed bed with a catalyst [81]. When employing a similar polymer-to-catalyst ratio but with a onehundredfold excess of water, PMMA hydrolyzes in a single-pot fixed bed process, achieving yields over 70% [82]. Industrially, Arkema, previously the third-largest PMMA producer before divesting its PMMA business to Trinseo, patented a PMMA hydrolysis process claiming similar yields [70].

Table (1.1) Boiling and melting points of selected impurities in PMMA thermolysis to MMA [35, 66, 72]. Data for common compounds sourced from PubChem [73].

Compound	$\mathbf{T_{boiling}}$ (°C)	$\mathbf{T_{melting}}$ (°C)
Ethyl acrylate	100	-71
Methyl acrylate	80	-76
Methyl methacrylate	100	-48
Methyl isobutyrate	93	-85
Methyl pyruvate	138	-27
Methyl propionate	80	-88
Propanoic acid	141	-20.7
2,3-Butanedione	88	-3
Benzene	80	5
Toluene	111	-95
1,4-Cyclohexanedicarboxylic acid, dimethyl ester	323 [74]	77 [74]
Cyclopentanone	131	-51
Methacrylic acid	163	15
Isobutyric acid	154	-47
Acrylic acid	141	14
Methanol	64.7	-98
Water	100	0

1.4 Motivations

Before the ban of plastic scrap imports in 2018/2019, China and India imported roughly 200 kt/y of PMMA waste scraps [52]. As a result, and given that the virgin MMA market was a hundredfold larger than the r-MMA market [35], there was little interest from Western customers, particularly in Europe, for r-MMA before 2018. With exports to China and India now halved and central governments incentivizing reuse and recycling, recyclers have both an available feedstock and potential buyers for their products. However, as of 2024, only three companies in Europe recycle PMMA on a commercial scale, with additional, smaller-scale operations in southern Asia and South America, mostly serving local markets. Despite the availability of various PMMA recycling technologies, with new innovations emerging annually, two of the three industrial facilities in Europe still rely on molten lead baths–a technology

invented in the 1950s. Why is this the case?
Although the top 10 chemical companies by sales (representing 10% of industry revenue) are "committed to sustainability," only two of them own plastic recycling plants. The rest prefer to outsource the risk to start-ups as external investors or, in some cases, as end users [83]. This reluctance is largely due to capital costs, which rank among the top factors influencing a chemical plant's overall viability [84]. Capital cost estimation techniques, tailored to the oil and gas industry, typically underestimate costs by an average of 20%, following preliminary engineering designs that require several months and hundreds of thousands of dollars to develop [85]. In an environment where feedstock supply is unstable, the required product purity is high, and process economics remain uncertain, companies are understandably hesitant to invest.
In the specific case of PMMA, newer technologies do not necessarily guarantee improved yields, product quality, economics, or environmental benefits. There is a balance among these factors, which was still unclear at the start of this project. Additionally, the challenge of thermolyzing difficult PMMA scraps, particularly composites, persists. Solid surface materials (e.g., Dupont's Corian) are among the most challenging to thermolyze but are potentially more suitable for hydrolysis. These materials also have favorable recycling logistics, with concentrated production and consumption patterns. Solid surface, also known as artificial marble, is an ATH-filled PMMA (40/60 PMMA/ATH). Aluminium hydroxide (ATH) $Al(OH)_3$ dehydrates within the same temperature range as PMMA depolymerization [86], meaning that hot vaporizing water inevitably interacts with the depolymerizing PMMA, producing acids (e.g., MAA) and alcohols. What presents a challenge for thermolysis becomes an opportunity for hydrolysis.

This work is part of a collaborative project between Arkema France, NRC, and Groupe Lavergne, a Canadian recycler, aimed at valorizing difficult-to-recycle, end-of-life post-consumer PMMA scraps. The project initially involved two students: one identified the best bench-scale catalyst for MMA hydrolysis, and tested it in a fluidized bed, while the second screened catalysts for one-pot PMMA to MAA hydrolysis, later testing them in a twin-screw extruder. I joined the project 12-18 months after these students, with the original goal of scaling up the fluidized bed from lab to pilot scale (0.6 m diameter and 2 m height). However, less than a year into the program, the Covid-19 pandemic severely limited lab access for nearly a year. During this period, I was invited to contribute to the MMAtwo PMMA recycling program in Europe, led by Arkema. I relocated to France to work on the techno-economic analysis of existing PMMA recycling processes. Initially, I believed that the primary obstacles to PMMA recycling commercialization–whether thermolysis or hydrolysis–were purely techni-

cal, such as the challenges of producing high-grade MMA or efficiently hydrolyzing MMA to MAA. However, after retro-engineering and analyzing various technologies (fluidized beds, extruders, stirred tanks, dry distillation, rotating drums, molten beds, etc.), I discovered that more efforts were underway to recycle PMMA to MMA than I had previously realized, and that the technical hurdles were only part of the problem.

For example, academic literature mostly focuses on fluidized beds, which have been tested at scale on at least two distinct occasions, both trials failed due to system instability, specifically defluidization, as confirmed by a technical executive involved in ICI's attempt. Conversely, simpler techniques like dry distillation and molten beds were consistently producing r-MMA, albeit in small volumes or rudimentary systems.

The main barriers to large-scale commercialization of these technologies became clear: **(i)** Recyclers were more interested in recycling lower-quality scraps into lower-quality MMA for immediate local market use, rather than investing in more advanced systems to produce higher-grade MMA. **(ii)** These recyclers often lacked an understanding of the economic risks associated with PMMA depolymerization and had no reliable means to estimate the required investment for building a chemical recycling plant. At the same time, I also discovered how chemical recycling of PMMA was commercially limited to post-industrial scraps, with minimal focus on difficult to treat streams like composites, with few exceptions.

Upon returning to Canada, I set out to tackle both challenges: advancing large-scale PMMA recycling, regardless of the final product, and depolymerizing PMMA composites. I first analyzed the economic risks of PMMA recycling to determine the most significant factors. After confirming that total capital investment, product pricing, and feedstock costs had the greatest impact on economic viability, I focused on reducing the uncertainty around capital cost estimation. Because historical PMMA recycling plant data are scarce, this required building a database of chemical recycling plants for all plastics. At the same time, I thermolyzed and hydrolyzed end-of-life, post-consumer PMMA composite scraps in a stirred-tank, a technically more mature technology. I realized that this approach would provide researchers and executives the tools to promote PMMA recycling at large, but also provide a solution to the long-standing problem of PMMA composite recycling.

1.4.1 Problem statement and research objectives

The **main objective** of this work is to develop practical tools and methodologies to advance the recycling of PMMA by bridging the gap between theoretical knowledge and real-world application. To do so, we took an holistic approach and investigated the problem from macro to meso scale, dividing it into 3 sub-objectives.

1. **Identify the current state of the art in PMMA recycling and assess the associated technical and economic risks**. The results of this objective have been published in *Polymers* (IF=5.0). The driving hypothesis (HP) here was that the reaction part of the plant was as important as pre-treatment and purification. That is, product purity and capital cost had the most impact on the process viability:

   - Review of process technologies and identification of a representative PMMA-to-MMA chemical recycling process;
   - Market assessment of PMMA waste scraps and the associated depolymerization products (MMA) and by-products (solid and liquid waste);
   - Monte Carlo simulation to assess the economic viability of different recycling scenarios (e.g., with or without investment subsidies, premium product pricing, varying feedstock quality, and different equipment types).

   This sub-objective demonstrated the necessity for PMMA recycling at large. It established the techno-economic viability of processes that aim for high-quality recycling products comparable to virgin materials, even with higher capital or feedstock costs. It also highlighted capital investment as the primary factor impacting process viability.

2. **Develop plug-in correlations to estimate the total capital investment (TCI) of chemical recycling plants at the early stage of a process**. The results of this objective have been published in *ChemSusChem* (IF=8.4). The first sub-objective indicated the need to minimize errors on capital investment estimation for PMMA, or more in general, plastic recycling plants. The HP here was that conventional early-stage capital cost estimation techniques are inaccurate or inappropriate for chemical recycling plants.
   This part of the work identifies the best estimation methods for chemical recycling plants, and propose new simpler correlations based on plant capacity and global energy loss.

   - Developed a database of 160+ existing or existed plastic recycling plants worldwide, documenting TCI, place and year of construction, type of technology (pyrolysis, gasification, solvolysis, selective dissolution), global heat and mass balance;
   - Tested state-of-the-art correlations in deterministic and probabilistic analyses on selected benchmark projects for each technology;
   - Identified the most suitable estimation methods for different technology clusters;
   - Proposed a more accurate correlation for pyrolysis and gasification plants;

- Identified the challenges of solvolysis and selective dissolution capital estimation due to low technology maturity;

This sub-objective reviewed and tested existing estimation techniques, proving their inadequacy for chemical recycling. The analysis demonstrated that TCI for pyrolysis and gasification plants is highly correlated (R^2=0.92) with total energy losses across the plant, and developed a tool for AACE –class 5 (early-stage) estimation of new chemical recycling plants, including PMMA.

3. **Depolymerize complex PMMA-based composites, such as post-consumer end-of life ATH-filled PMMA (i.e. artificial marble) to MMA and/or MAA**, to demonstrate that targeted chemical recycling approaches can unlock sustainable and economically viable pathways for these materials. The results of this objective are under review in *Waste Management* (IF = 7.1). The main HP here was that artificial marble is the best candidate for PMMA hydrolysis, due to the concurrent presence of hot water, acid sites in the alumina system, and depolymerizing PMMA.
In this phase, I thermolyzed and hydrolyzed waste artificial marble to maximize its valorization in a 5l stirred tank reactor. The target products were γ-alumina from the inorganic fraction and MMA or MAA from the polymer fraction.

   - PMMA to MMA or MAA depolymerization in a 5l stirred-tank reactor;
   - Identified the intertwined thermolysis and hydrolysis mechanisms as functions of water, temperature, heating mode, and catalyst presence in both batch and semi-continuous operations;
   - Optimized dual-phase thermolysis to maximize MMA or MAA recovery from artificial marble waste;
   - Developed a recycling method to retain the full value chain of the composite material.

   In this sub-objective, we demonstrated the proof of concept for a depolymerization process that converts PMMA to MAA or MMA using real end-of-life post-consumer waste. Temperature and water partial pressure drives the hydrolysis of PMMA, but the intimate contact between the composite fractions composite promote direct backbone PMMA hydrolysis to PMAA. A dual-phase recycling method is optimal: the first heating stage at 300 °C releases water to minimize hydrolysis, followed by a second stage at 400 °C to maximize MMA production. This method achieved a 66% g/g MMA recovery and converted the inorganic fraction to boehmite, a γ-alumina precursor. Additionally,

the process produced enough coke to render the calcination of the inorganic fraction energy self-sufficient.

The three sub-objectives, when combined, advance the state of knowledge in PMMA recycling:

- Post-industrial PMMA recycling to MMA is already an established industrial practice. Recyclers now have access to data-driven scenarios to inform their business decisions, and to expand recycling to a broader kind of waste. Interestingly, higher-cost technologies producing higher-quality outputs are more economically viable in the long term than cheaper plants processing highly contaminated PMMA waste, even when the waste is available at no cost.
- A reliable and universal method for estimating the capital costs of chemical recycling plants is now available, offering plant owners and recyclers a dependable tool for early-stage investment decisions
- Artificial marble (ATH-filled) is a difficult-to recycle PMMA-based composite. A dual-stage process recover both MMA and valuable by-products like boehmite, demonstrating that chemical recycling methods must be tuned on the material to preserve its full value.
- PMMA-to-MAA recycling proves advantageous over PMMA-to-MMA recycling for specific low-or negative-cost waste streams, particularly when local demand for "green" MAA is high. Otherwise, MMA remains the preferable option.

1.4.2 Summary of contributions

This study contributes to the research on PMMA recycling in the following ways:

1. Provides a comprehensive analysis of the technical and economic factors influencing PMMA recycling, with particular focus on high-value outputs and detailed capital cost estimation models.
2. Expands the scope of PMMA recycling research to include difficult-to-recycle waste streams, such as post-consumer composite PMMA materials, with a special focus on artificial marble.
3. Offers practical tools for engineers, plant owners, and decision-makers to evaluate (PMMA) recycling technologies based on economic viability, particularly in terms of capital cost and process efficiency.

During my PhD program I published 4 papers on topics related to my doctoral program and 1 book chapter, and 6 on different topics within the research group. In the order:

- *Risk analysis on PMMA recycling economics* J De Tommaso, JL Dubois. Polymers 13 (16), 2724, 2021
- *Total Capital Investment of plastic recycling plants correlates with energy losses and capacity* J De Tommaso, F Galli, R Weber, JL Dubois, GS Patience. ChemSusChem, 17(5), e202301172, 2024
- *Waste Artificial Marble hydrolysis and pyrolysis* J De Tommaso, F Galli, JL Dubois, GS Patience. Waste Management, 2024 (under review)
- *Upcycling Polymethyl methacrylate to Methacrylic acid* Y Zhuang, N Saadatkhah, T Nguyen, J De Tommaso, C Wang, A Ajji, GS Patience, reaction chemistry & engineering, 2024 (accepted)
- *Recycling of Artificial Marble - Chapter 16* J De Tommaso, GS Patience, JL Dubois, Polymer Circularity Roadmap - 2nd edition, De Gruyter, 2025 (in print)
- *Experimental methods in chemical engineering: Pressure* K Wu, F Galli, J de Tommaso, GS Patience, JR van Ommen. The Canadian Journal of Chemical Engineering 101 (1), 41-58, 2023
- *Experimental methods in chemical engineering: Hazard and operability analysis: HAZOP* P Mocellin, J De Tommaso, Chiara Vianello, Giuseppe Maschio, Thomas Saulnier Bellemare, Luis D Virla, Gregory S Patience. The Canadian Journal of Chemical Engineering 100 (12), 3450-3469, 2022
- *Gas to liquids techno-economics of associated natural gas, bio gas, and landfill gas* F Galli, JJ Lai, J De Tommaso, G Pauletto, GS Patience. Processes 9 (9), 1568, 2021
- *Experimental methods in chemical engineering: Process simulation* J De Tommaso, F Rossi, N Moradi, C Pirola, GS Patience, F Galli. The Canadian Journal of Chemical Engineering 98 (11), 2301-2320, 2020
- *Experimental methods in chemical engineering: Zeta potential* CN Lunardi, AJ Gomes, FS Rocha, J De Tommaso, GS Patience. The Canadian Journal of Chemical Engineering 99 (3), 627-639, 2021
- *Review on Alternative Route to Acrolein through Oxidative Coupling of Alcohols* V Folliard, J Tommaso, JL Dubois. Catalysts 11 (2), 229, 2021

1.5 Thesis structure

Chapter 2 continues the literature review, and contains a bibliometrics map-driven review on chemical recycling of PMMA, with a focus on the techniques of recycling, and the gap in the state of the art.
Chapter 3 is the first sub-objective (or first paper) "Risk analysis on PMMA recycling economics". Chapter 4 is the second sub-objective "Total Capital Investment of plastic recycling plants correlates with energy losses and capacity", and Chapter 5 the third, "Waste Artificial Marble Pyrolysis and Hydrolysis". Chapter 6 resumes the main findings, conclusions, limitations, and the future work.
The book chapter "Recycling of Artificial Marble - Chapter 16" is in the annex. At the beginning of each chapter there are introductory paragraphs to connect the upcoming chapter with the literature review or the results from previous chapters, as a way to guide the reader through the manuscript.

CHAPTER 2 LITERATURE REVIEW

The history of PMMA recycling demonstrates how, since the 1950s, PMMA recycling and depolymerization processes have cyclically risen and faded in response to market demand and feedstock availability. However, the focus of academia and industry has not always been aligned. Most depolymerization processes, in fact, originated directly from industrial practice. To investigate this, I queried both academic and industrial (patent) literature using the following search algorithm: *(((PMMA OR Polymethylmethacrylate OR (poly)methylmethacrylate) AND (Recycling OR Depolymerization) AND (Process OR Method)) AND NOT (Patient OR nano*))*. The exclusion of "Patient" and "nano*" terms was necessary to filter out a large number of medical-related results, where PMMA is either used in chromatographic techniques or as a composite material in drug nano-carriers.

2.1 Academic and Industrial investigation 1950 - 2020

Initially, I focused on academic research via the Web of Science (WoS) database. I generated a bibliometric map based on keywords from 192 articles resulting from my query (Figure 2.1). The software identified 62 of the most frequently cited keywords in the titles and abstracts, which were grouped into five clusters. The most cited term was plastic (134 occurrences), followed by separation (78 occurrences), both part of the largest, green cluster. Other significant terms in this cluster include density (39), flotation (16), and mixture (50).

The red cluster contained terms related to depolymerization (58), temperature (74), MMA (78), and degradation (42). Additionally, there were clusters focused on recycling (70) and more application-oriented topics such as blade (26) and copolymer (36). The reviewed articles span from 1950 to September 2020, coinciding with the start of this project. In general, the main trend we see is that researchers in academia are investigating ways to separate PMMA from other plastic, before or after mechanically or chemically recycle it.

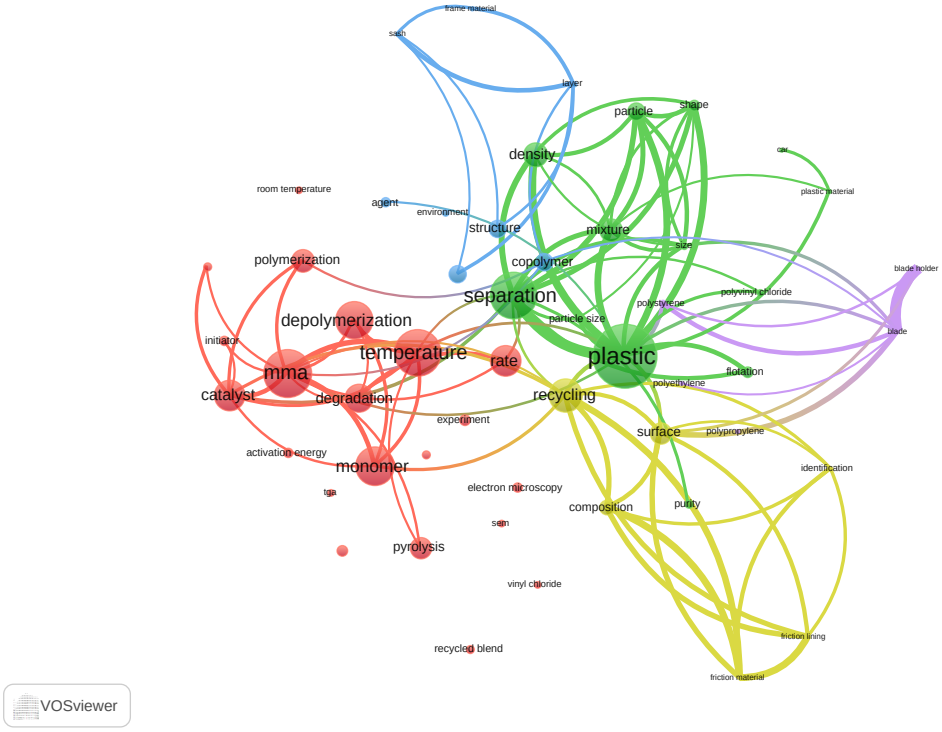

Figure (2.1) VOSViewer keyword bibliometric map based on the query: *(((PMMA OR Polymethylmethacrylate OR (poly)methylmethacrylate) AND (Recycling OR Depolymerization) AND (Process OR Method)) AND NOT (Patient OR nano*))* derived from articles indexed by Web of Science from 1950 to September 2020 [87,88]. The text font size and circle diameter are proportional to the keyword occurrences in the articles indexed during this period.

A major challenge in PMMA recycling is the availability of a relatively clean feedstock, especially from complex mixtures such as e-waste [89]. As a result, separation methods such as flotation [90–92], magnetic separation [93], electrostatic separation [94], cyclones [95], infrared NIR [96], and triboelectric separation [97] emerged in the analysis.

When sorting is possible, or for homogeneous streams, thermolysis is the most explored recycling route, with [98], or without a catalyst [99]. r-MMA composition is also important. For instance, Godiya demonstrated PMMA depolymerization through thermal degradation, followed by purification via re-dissolution and re-precipitation [66]. Impurities, even in high-grade PMMA, significantly affect both the re-polymerization process and the resulting PMMA properties [64]. These impurities also influence the depolymerization process itself, particularly during pyrolysis [100–102]. Similarly, copolymer formulations affects mechanisms and kinetics of PMMA degradation and depolymerization [103], as well as and recycling efforts [104]. With few exceptions, academic research focused on the fundamentals of PMMA

recycling, rather then the technologies.

For this reason, I queried over 6,000 patents from WIPO (6589) [105] and 3,000 patents from Lens (3305) [106], two open-source patent databases, and combined these results with the academic query (Figure 2.2). The top inventors in PMMA recycling include:

1. 3M (274 patents)
2. BASF (151 patents)
3. ARKEMA (92 patents)
4. Toray (52 patents)
5. DuPont (50 patents)
6. GE (50 patents)
7. P&G (36 patents)
8. LG (30 patents)
9. Sony (29 patents)
10. Dow (27 patents)

VosViewer identified 116 frequently cited keywords from the patent search, which were grouped into four clusters. Due to the technical nature of patent language, I excluded terms such as *num, respect, amount, mol, iii, portion, preparation, device, presence, formula, element, and apparatus.*

Despite the significantly higher number of patents compared to academic articles, the clusters remained similar (Figure 2.1). The red cluster now includes terms such as polymethylmethacrylate (478), polymer (3353), reaction (368), reactor (259), heating (166), blend (447), PVC (117), and hydrogen (167). However, this time, the results focus more on the meso-scale of recycling–addressing practical processes and reactor technologies–rather than molecular mechanisms, The main PMMA recycling technologies are:

2.1.1 Molten Bath

Operators feed re-ground PMMA (or mixed waste [107]) into a metal or salt molten bath, with or without pre-heating [108]. The temperature depends on the bath type, ranging

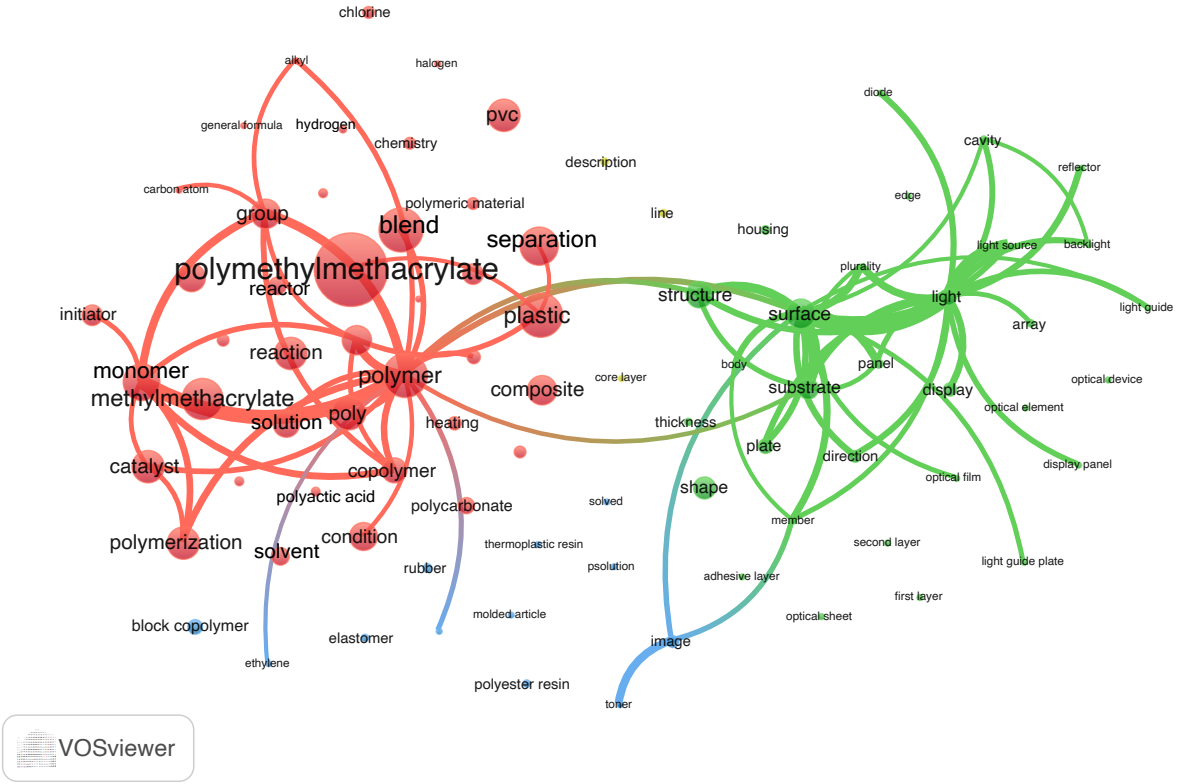

Figure (2.2) VOSViewer keyword bibliometric map based on the query: *(((PMMA OR Polymethylmethacrylate OR (poly)methylmethacrylate) AND (Recycling OR Depolymerization) AND (Process OR Method)) AND NOT (Patient OR nano*))* derived from articles indexed by WoS and WIPO from 1950 to September 2020 [87, 88, 105]. The text font size and circle diameter represent the number of keyword occurrences during this period.

from 500 °C for lead [53] to 1300 °C for iron-copper [107], as well as the required residence time [109]. The gas products exit the bath, pass through a condenser, and are then collected. Typically, PMMA recycling employs a lead bath (e.g., [110] by Rohm & Haas), yielding MMA at rates of 70-90% [111]. Some countries in Europe, such as Italy, still utilize this World War II-era setup, originally patented by Domingo [112], to recover MMA from acrylic aircraft components. The main advantage of this technology is the separation of solid impurities and residues during the reaction due to the density gradient in the medium. In case of a molten-lead bath, for instance, lead is much more dense of the residues so they float on the surface of the bed. However, although its vapour pressure is small, some lead inevitably vaporizes and contaminates r-MMA. Similarly, The impurities concentrate on the bath's surface and

must be continuously scrubbed off, resulting in carbonaceous residues with high lead content that are difficult to dispose of [35, 79].

Other suitable metals are tin or zinc, but tin is more expensive than lead, and zinc poses even more contamination and operative problems then lead due to a higher partial pressure [35]. Alternatively, some processes use salt baths, such as $KCl/MgCl_2$ [113] or LiCl/KCl, though these methods tend to underperform compared to metal baths [114].

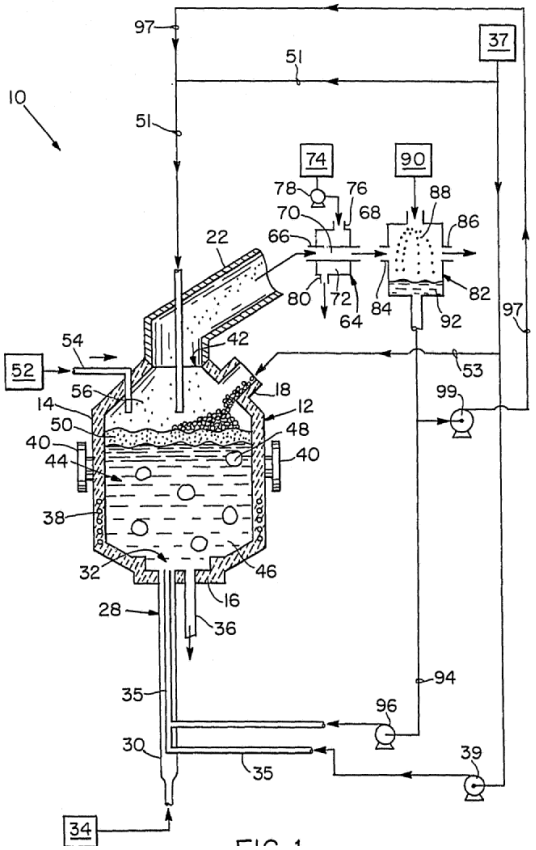

Figure (2.3) Molten bath setup [109]. The reactor (12) is externally heated with an induction coil (38), and the plastic is pumped via a concentric cooled tube (28) from the bottom of the reactor, from the side (53), or the top (51). The molten metal is periodically purged via a bottom spout (36), and the gas leaves from the top of the bed passing through a ceramic layer (50), if the chosen metal is prone to surface oxidation.

2.1.2 Dry-Distillation and its variations

In 1936 DuPont patented a process "For depolymerizing alpha substituted acrylic acid esters" [115], that followed a similar patent of 1935 by Rohm [116]. The process is basically a batch distillation where "the polymeric ester is heated (by contact) at substantially atmospheric pressure to a temperature substantially above its decomposition point", and the

produced vapours are condensed and distilled with 80% yield in r-MMA. Because of the low capital costs, dry distillation is nowadays the state-of-the art in eastern countries such as China [117, 118] or India (Figure2.4). However, the daily cycles of heating and cooling decrease the lifespan of the unit. Char builds overtime due to the uneven batch heating, promoting hydrogen transfer reaction like MMA to methyl isobutyrate, an odorous molecule with the same boiling point of MMA. Dry-distillation is also more appropriate for homogeneous PMMA waste streams, that volatilize completely during the reaction. In case of PMMA composites, the inorganic fractions accumulate over the reaction time (several hours to one day), which complicates the reactor cleaning [35]. In those particular cases where PMMA represents a very small fraction of the composite or mixed stream, for instance vehicles, sometimes is more economically viable to dry distillate the whole shredded residue to fuel, than separate PMMA (0.1-0.4 %) and come back to the monomer [119, 120].

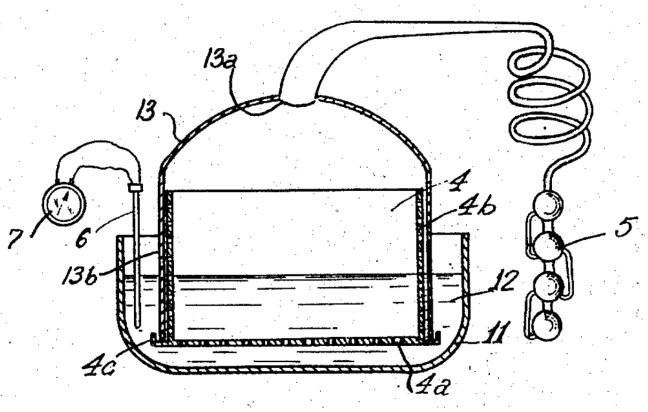

Figure (2.4) Dry Distillation setup [112].

Rotating drum is an agitated batch variation of the dry-distillation, and commonly seen in Asia for tyre pyrolysis. Agitation introduces a more homogeneous heat exchange, but it limits the dimensions of the unit. To treat more plastic and keeping the same heating input, the unit develops horizontally. This means that during the heating and cooling cycles the thermal expansion increases for bigger units, to a point where the seal around the mobile part of the machine is more prone to fail [35].

A **stirred-tank** reactor functions as a continuous variation of dry distillation [35]. The system continuously feeds plastic in either solid or molten form, with external heating and mechanical agitation. Agitation improves heat and mass transfer and reduces the reaction time, though the high viscosity of molten PMMA increase the operative costs – up to ten-fold compared to HDPE [121, 122]). In the 1980s, Röhm employed stirred-tank reactors for PMMA thermolysis [123]. Today, companies prefer this technology for mixed plastic

waste streams [124], as seen with Plastic Energy [125]. For PMMA-based waste, stirred-tank reactors offer the advantage of continuously expelling solids and gases, making them ideal for processing high-residue materials like composites. One example is the Korean company R&E, which produces r-MMA and α-Alumina from waste artificial marble (ATH-filled PMMA) (Annex A). Another example, still in very small scale, is the Canadian company Pyrovac [126]. However, the combination of high temperatures and moving parts increases the risk of mechanical failure, making this technology more capital-intensive.
Modifications of the stirrer-tank include the **auger-screw** and the **rotating paddle process**. In the auger-screw reactor, an Archimedes screw pushes the polymer through the reactor, where it depolymerizes [127]. The single screw is not self cleaning, and this limits the auger reactor to "clean" feedstocks [35]. In the rotating paddle process, heat-sensitizing particles (such as metallic balls or sand) are introduced into the reactor to improve heat transfer and reduce reaction time [128]. However, the constant friction of the sensitizers produces fine dust particles, which are are effectively pyrophoric particles in a semi-confined space [129].

2.1.3 Fluidized bed and its variation

Fluidized bed is the most investigated technique for PMMA thermolysis. This technology has a success-track in the industry for heavy duty applications like fluid catalytic cracking, combustion or gasification, but also in chemical or miner industry [130]. Superior heat transfer along with high mixing rate, and short contact times, are the main advantages of the fluidized bed. Here, PMMA scraps are suspended in a medium of inert or catalytic particles, fluidized with a gas free of oxygen, for instance nitrogen or part of the same produced MMA. The solid bed behaves like a liquid, hence the superior heat and mass transfer (e.g. $400\,\mathrm{W/m^2K}$ to $500\,\mathrm{W/m^2K}$ [53]).
Laboratory tests in the 1980s demonstrated that fluidized beds could achieve high MMA yields and purity [53, 113]. Kaminsky, for example, reached a 97% MMA yield by feeding 1.5 mm PMMA pellets into a bed of sand-like particles using a screw extruder [131]. However, processing real PMMA waste presents challenges. Reducing particle sizes below 5 mm requires expensive methods such as high-energy mechanical milling [132] or cryogenic milling [133].

Bigger particles disrupt the fluidization process and extend depolymerization times. Particles smaller than 5 mm flow well but demand too much energy to crush, while those larger than 15 mm don't fully depolymerize within the typical residence time of 0.8 s to 60 s [49,102,131]. Larger particles also tend to foam before devolatilizing, leading to bed segregation [134].

This foam accumulates at the top, where heat transfer is less efficient, and eventually causes defluidization [135–137].

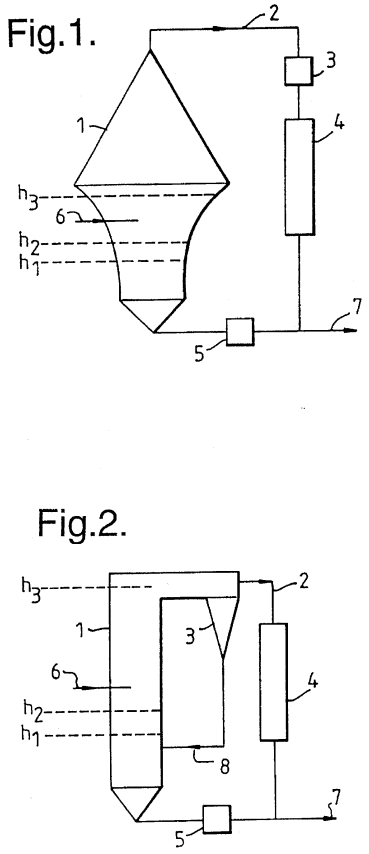

Figure (2.5) Example of PMMA recycling by a fluidized bed process [53].

To overcome these issues, companies have developed more advanced fluidized bed designs. Vaughan depolymerized PMMA in a circulating sand particle bed or a variable-area throat bed to improve self-regulation (Figure 2.5) [53]. In these systems, the r-MMA vapors drive the fluidization, and controlling the vapor condensing temperature allows throughput regulation. These designs maintain agitation in the bed, preventing segregation and reducing foaming. At startup, nitrogen stabilizes the bed until depolymerization begins, at which point the system becomes self-regulating. While this process addresses fluidization issues, problems caused by impurities, remaining plastic on the sand, or char formation remains. Recirculating sand containing char is then burned for energy recovery [137]. High amounts of char and residue can make the process uneconomical. In cases where the feedstock contains materials with varying melting points, such as composites or PMMA with fillers, the polymer surface softens as bed temperatures rise, causing sand particles to stick to the polymer [135]. As the polymer volatilizes, sand embeds into the surface, forming aggregates. These can

either grow or crumble [135, 136, 138, 139]. Raising the bed temperature above 500 °C helps prevent this, but reduces monomer yield [131]. In some cases, adding mechanical agitation to the fluidized bed [56, 140, 141] helps mitigate this issue.

The **Mitsubishi process** of 1998-2008 starts from these premises, with continuous regeneration and recirculation of the sand as heating vector [56, 57]. A rotating agitator, a paddle or an anchor blade, improves the flowability of the bed and a separate heating chamber burns off the "unpyrolyzed material" (e.g. plastic, coke, residues) from the sand. The original US20100121097 patent also foresee the possibility to fill the bed with materials other than the sand, like ceramic or metal particles, alone or in combination, inert or catalysts to the pyrolysis. Compared to the other technologies, this version of the fluidized bed offers high heat exchange coefficients, along with a stable flowability for industrial end-of-life resins due to the circulating nature. However, Mitsubishi aborted the process after pilot-scale tests. The system only managed to process the 2 kt/y equivalent feed for a maximum of 30 minutes under stable conditions before defluidization occurred [142]. In September 15, 2020, I participated to a virtual workshop on *polymer recycling* held by the MMAtwo consortium. Incidentally, Andre Bragg, Downstream Technology Manager first, and Business Project manager later of Lucite, who worked on the PMMA depolymerization joint Lucite-Mitsubishi project was there, and when I asked why the project was halted, and what were the technical difficulties they encountered that undermined the fluidized bed stability, he replied:

" *The problem with fluidized bed is long time bed stability. It is very easy to get dead spots and non-uniform areas. Have an homogeneous flow across the bed is very challenging. In addition, gas volumes to sustain the fluidization were much higher than expected. The combination of these two (issues), made the process uneconomical. Theoretically, the technology ([56]) would work, but economically it wasn't viable at that time. ... ... Fluidized beds control the temperature accurately, so you don't degrade the monomer, but operating it remains a challenge.* "

The technology also struggled to treat composite-like and filled PMMA waste due to the high energy required to maintain fluidization (e.g., high sand turnover ratio) and prevent agglomeration, bed channeling, and eventual defluidization.

Spouted beds are an alternative to address defluidization issues in plastics pyrolysis, benefiting from the cyclic movement of solids in the conical section of the bed [143]. Lopez et al. achieved an 80% MMA yield from commercial PMMA resin using this method [144]. Despite their advantages of lower pressure drops and simpler designs [145], spouted beds remain under-utilized, especially at the industrial scale [146, 147].

Nevertheless, new fluidized bed processes for PMMA depolymerization continue to emerge.

In 2019, Arkema patented a process to hydrolyze PMMA resin into MAA [148], in presence of acidic catalysts like alumina, FCC, tungsten on TiO_2, or MgO. They also proposed coupling this hydrolysis catalyst with depolymerization initiators such as inorganic peroxides (H_2O_2, percarbonate, perborate, or persulfate) to accelerate the unzipping process.

In the fluidized bed embodiment of the patent (Figure 2.6), Arkema's process depolymerizes PMMA composites into MAA, with fillers or reinforcements (e.g., fiberglass) recovered downstream via a cyclone. One advantage of this method is that impurities difficult to separate from MMA (like ethyl acrylate), become compounds easy to separate from MAA. To address the longstanding issue of bed defluidization, Arkema incorporates a swirling flow through a toroidal distributor featuring fixed inclined blades, similar to the TORBED technology [149, 150]. The solids are forced into a rotating flow by a cone positioned above the distributor.

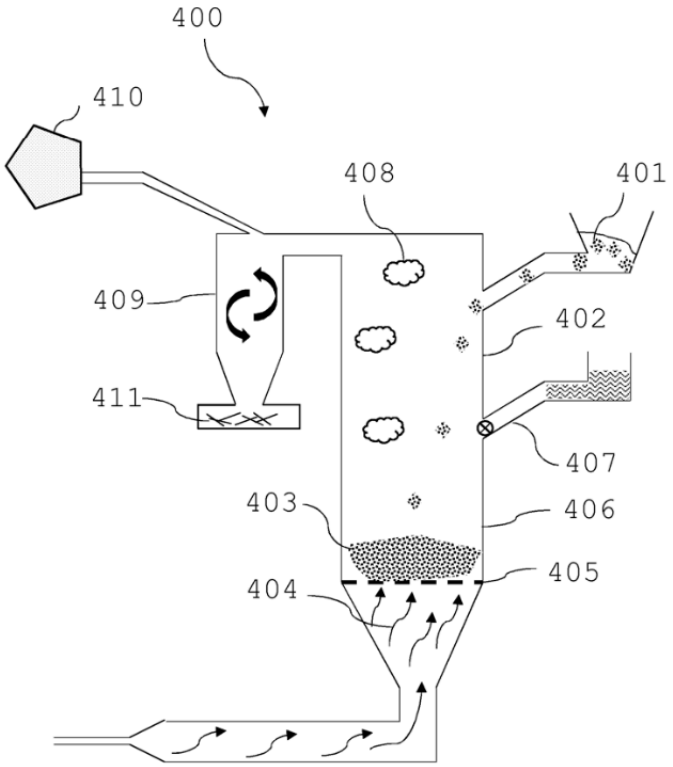

Figure (2.6) Fluidized bed configuration from [148]. PMMA (401) and water (407) are fed to the reactor, and fluidized together with a mixture of hydrolysis catalyst and/or inert (403), through an hot gas (404) coming downward (through grid 405). A cyclone (409) separates fillers and/or residues through the product vapour, that in turn passes through a cooler (410) before the purification step (not shown).

They demonstrated the process at the bench scale using high-grade commercial PMMA resin

(V-826), but with no long-term operational stability guarantees. Moreover, the details of the bed's hydrodynamics remain unclear. They fluidize a 30 cm diameter reactor with 4.2 kg/hr of flue gas at 575 °C, but with a central cone of 24 cm, the actual annular diameter is just 6 cm, giving an annular area of 0.029 m^2. For toroidal distributors, the open area to be around 15% of the total [151]. With the blades angled at 23 deg, and the flue gas density at 575 °C around 0.4 kg/m^3, the vertical component of the superficial velocity (U_v) is $U_v = U * \sin(23)$, equating to 15.7 m/s. Swirling fluidized beds with annular distribution behave differently from typical fluidized beds, particularly in operational regimes and elutriation limits [152], as the swirling flow affects fines suspension within the bed [153]. However, 15.7 m/s seems unusually high for this setup, and the system's stability, particularly concerning fines elutriation and catalyst regeneration, warrants further investigation.
Currently, no operating facility recycles PMMA in fluidized beds, or at least none advertise it. Pryme has constructed a 40 kt/y catalytic fluidized bed to recycle a mixture of PS (the closest thermoplastic to PMMA), PE, and PP into naphtha oil. However, other fluidized bed pyrolysis projects for mixed plastics, such as those by Recycling Technologies in the UK, have been divested.

2.1.4 Twin-screw extruder and other electrified processes

The twin-screw extruder belongs to the screw reactor family, which also includes screw tubular reactors, single-screw, and auger reactors [154,155]. Essentially, it functions as a plug-flow stirred reactor with optimized heat transfer [35]. This design minimizes the residence time to seconds and ensures that the amount of polymer/monomer in the system is minimal at any given time, making it intrinsically safe in case of a sudden shutdown. The intertwined screws are self-cleaning, so that the solid residues move along the reactor without accumulating. Polymer depolymerization occurs through external heating and shear forces from the mixing screw, with the option of electrifying the screw itself [156]. PMMA melts in the first barrel and creates a plug that avoids back-flush, and the products are expelled at the end of the unit for cooling and condensation. However, like the rotating drum, the twin-screw is limited by its size, as most heat transfer occurs through the reactor walls, capping capacity at 2 kt/y to 5 kt/y [35]. Despite this, its fully electrified operation and familiarity among recyclers–who use extruders in mechanical recycling and polymer processing–have gained interest in chemical industry over the last 20 years. Already in 1998, Michaeli and Breyer described a degradative extrusion process using a co-rotating, intermeshing twin-screw extruder to depolymerize PMMA [157]. However, it is only with the European project MMAtwo that twin-screw became a standard in PMMA recycling. In this project, Arkema, JSW, and several other companies along the PMMA value chain, adapted JSW's patented twin-screw

system for PMMA depolymerization [158, 159] (Figure 2.7), leveraging on another JSW's earlier patent from 1976 [160]. Arkema also patented a twin-screw process to produce up to 73% yield of MAA from PMMA [148]. More recently, Lucite partnered with Agylix to adapt their proprietary PS depolymerization technology [161,162] for PMMA recycling [163], likely using a self-cleaning dual-screw reactor. Sumitomo Chemical, or Renov8, two PMMA producers, also recently started to recycle PMMA in a twin-screw extruder [164, 165].

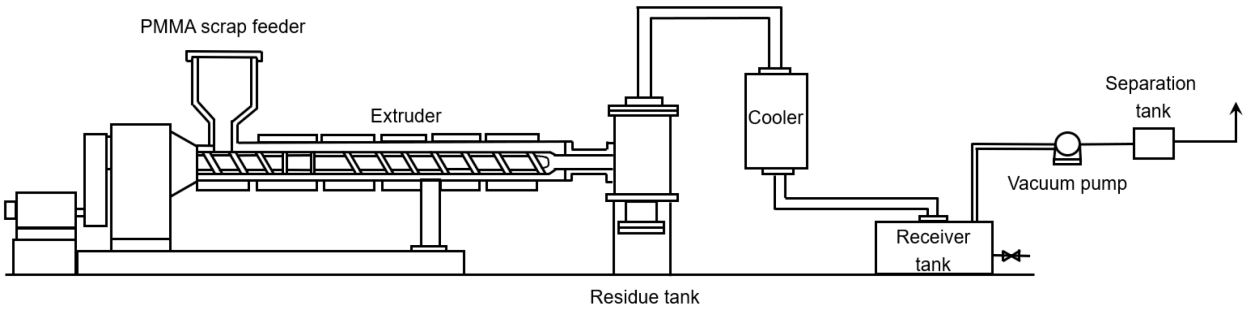

Figure (2.7) 1997 Extruder depolymerization setup by JSW [159].

Plastic producers also investigated microwave and Inductive heating to recycle PMMA. Both improve the heating transfer, and can rely on electricity from renewable sources. However, PMMA does not directly adsorbs the microwave, so it necessitates a susceptor, i.e. a material with "a high dielectric loss factor" [54]. In the best scenario, microwaves increase the energy efficiency up to ten fold compared to fluidized bed (2 MJ/kgMMA versus 25 MJ/kgMMA [166], similar to what the MMAtwo extruder achieved [167]). The chemical group AECI (South Africa) depolymerized PMMA with a microwave-heated reactor. At a temperature of 300 °C to 400 °C, 90 % to 99 % of the polymer decomposed, with a monomer yield of 90 % to 95 %. The gas was then condensed and distilled to achieve a 98 % to 99 % pure product. They produced 2 kt/y but then stopped the process to screen alternative technologies, and because microwave had no effect on reaction per se, and it was an expensive way to heat the polymer [54]. The company now disappeared after an acquisition from LUCITE in 2008. Nowadays, microwave generators evolved, and companies like Gr3n for PET, Pyrowave for PS, or Enval for mixed plastics, have been investigating it.

Inductive heating shares advantages and limitations of microwave, in terms of heat transfer, penetration depth and the need for thermal sensitizers, respectively. Again, metal balls are the preferred heating medium, [168] but in this case the reactor is static, which minimizes the attrition and the formation of dust.

2.2 Where is the research going?

To identify the most recent focus of both academia and industry, I narrowed down the bibliometrics search to the last five years (2019-2024), or the timeline of this work. The program VosViewer generated an occurence based bibliometric map of keyword on the articles (70), and patents (436 on WIPO and 445 on LENS) resulting from the query (Figure 2.8). Parsing title and abstract, VosViewer retained 115 of the most cited keywords, and it grouped them into 5 clusters (4 main plus 1). Again, I had to exclude several words due to the patent wording: *present disclosure, mol, moles, embodiment, minute, hour, total weight, opening, mass, range, iii, amount, disclosure, mean, advantage, plurality, apparatus, end, element, device, example, product, portion, direction.* For the first time, we now have fiber (68), light (33) (including light source), residue (96), adhesive (58), and bio (58).

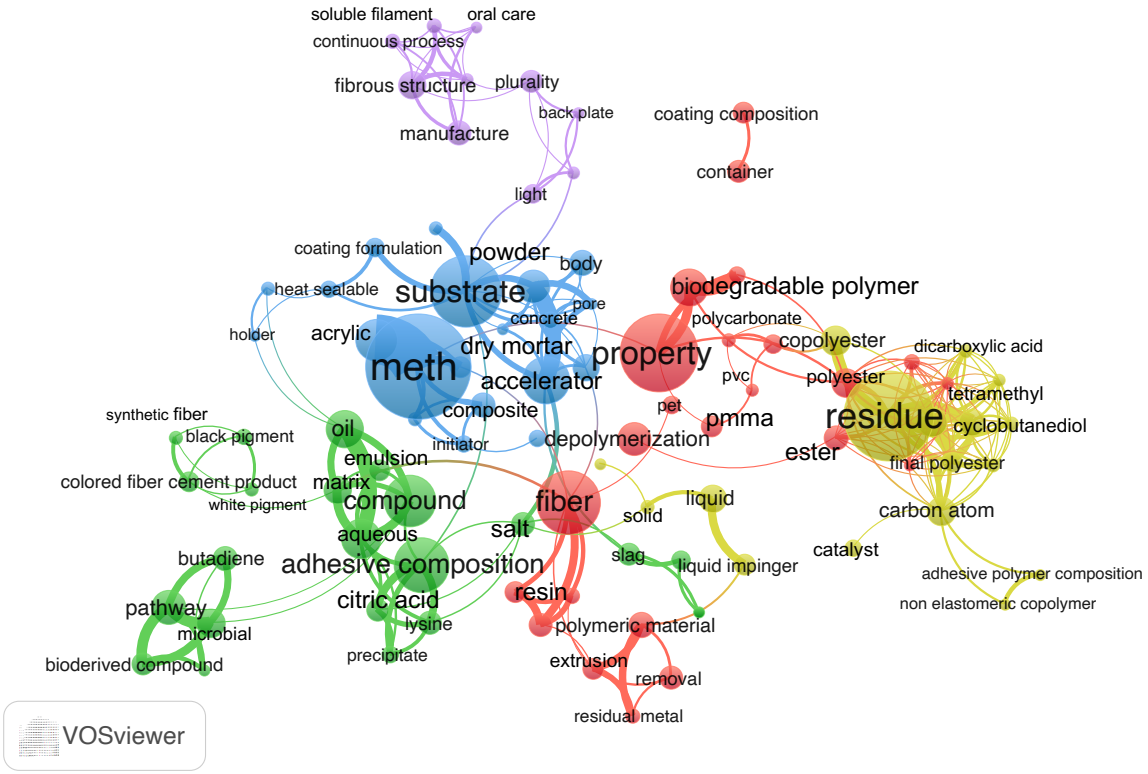

Figure (2.8) VOSViewer keyword bibliometric map based on the query: *(((PMMA OR Polymethylmethacrylate OR (poly)methylmethacrylate) AND (Recycling OR Depolymerization) AND (Process OR Method)) ANDNOT (Patient OR nano*))* derived from articles that WoS and WIPO indexed from 2019 to 2024 [87, 88, 105]. The text font size and diameter of the circles are proportional to the number of occurrences in the articles indexed during this time.

In the last five years, the most active companies in terms of patents were [105]:

1. Procter & Gamble (43);
2. Sika Tech AG (40);
3. Eastman chemical company (27);
4. Arkema France (13);
5. Andersen Co (12);
6. CJ Cheiljedang (12);
7. Genomatica (10);
8. Arlanxeo (8)
9. Lubrizol (8)
10. Tundra composites (8)

with LENS also indexing:

- Swimc Llc (11);
- Total Res & Technology Felui (9);
- Ifp Energies Now (9) and
- Entegris Inc (8), and BASF (7)

The general attention has shifted towards recovery [90,169,170], reuse [171–173], and recycling [72, 174], as well as the production of bio-sourced [175], recycled [176], or recyclable PMMA polymers [177]. The industry focuses more on immediate needs, such as how to incorporate recycled streams into existing objects (e.g., composites [178] or resin panels [179]), while academia focuses on more open-ended problems such as recycling processes and economics [68, 180, 181]. At the same time, companies are still interested in new PMMA applications in conventional markets: lighting [182], automotive [183], or electronics [184]. This suggests that research and development regard PMMA as both a commodity plastic and a component of the circular economy model. Some of these applications select PMMA purposely because of its recyclability [185–187], and research is ongoing on r-MMA polymerization [176], as well as on novel routes to produce PMMA [188].

2.2.1 Knowledge Gap

At the outset of this project in 2019-2020, PMMA was predominantly landfilled or poorly managed globally. Contrary to conventional wisdom, recycling technologies for PMMA were not lacking. What was absent were the practical tools to move from theoretical understanding, such as the micro-scale unzipping of PMMA, to the complexities of mixed end-of-life recycling streams. Knowledge about PMMA depolymerization was fragmented, with much of it confined to patent literature. The state of the art revealed a disconnect: those involved in PMMA recycling were neither sharing nor publicizing their practices, while researchers focused on peripheral issues.

This disconnect is evident in the continued academic promotion of fluidized bed-based technologies as promising, despite multiple project failures. In contrast, technologies like dry distillation and molten lead, which are employed by the few operational recycling plants, were virtually absent from academic discussions. A long-standing divide between academic research and patent literature contributes to this gap, though it does not fully explain the challenges in the field.
Recyclers, for their part, overlooked the broader techno-economic risks associated with PMMA depolymerization, and instead relied on established practices. Much of the research focused on generic "PMMA recycling", without considering the diverse forms and grades of PMMA– whether post-consumer or post-industrial, containing inhibitors, copolymers, or used as part of composites. For instance, the idealized Sigma Aldrich laboratory-grade PMMAs is a far cry from real-world materials, especially PMMA-based composites, which pose more complex recycling challenges.

Polymethylmethacrylate (PMMA) is one of the easiest polymers to depolymerize, yet only around 10% of it is recycled globally. This stark discrepancy between recyclability potential and actual recycling rates reflects not only technical challenges but also economic and logistical hurdles. The industry has long struggled to balance technical feasibility with cost-effectiveness, particularly when dealing with highly contaminated or composite PMMA waste streams. Furthermore, the recycling industry has been slow to adopt new technologies due to uncertainty in profitability, technical challenges with sorting and processing, and a lack of robust, scalable solutions.
The goal of this work was to bridge the existing knowledge gap, by providing tools that will promote widespread PMMA recycling. This work addresses both the technical challenges of recycling diverse PMMA waste streams and the economic uncertainties surrounding chemical recycling plants. In the next chapters, we demonstrate:

1. **The structure and operation of a typical PMMA thermolysis plant, identifying the key factors that most significantly affect its economic viability (Chapter 3);**
2. **A (more) reliable method for estimating the capital cost of a chemical recycling plant in its early stages of development (Chapter 4)**; and
3. **The valorization of a real-world waste PMMA-based composite, and the broader implications for PMMA recycling as a whole (Chapter 5).**

By integrating practical, data-driven approaches with a focus on real-life waste streams, this work provides the necessary framework for an economically viable and environmentally sustainable PMMA recycling.

CHAPTER 3 ARTICLE 1 – RISK ANALYSIS ON PMMA RECYCLING ECONOMICS

In Chapters 1 and 2 we proved that PMMA recycling is underexploited: researchers focus on difficult to scale technologies, while recyclers rely on experience rather than facts. In this chapter we analyze current PMMA thermolysis technologies, and we propose the layout of a typical state-of-the art plant. Then we analyze the economic risks associated with such a plant through a Monte-Carlo simulation accounting for all the process variables: capital investment, product and feedstock price, energy price, type of feedstock, and plant global mass yield. However, these variables vary with time, and are often interdependent. To increase the accuracy of the stochastic analysis, we correlated the variables' distributions via a matrix, based on historical data and expert judgement. Finally, we evaluate multiple business scenarios to offer data-driven guidance to researchers–highlighting areas to reduce uncertainty–and recyclers–suggesting when and how to invest effectively.

Jacopo De Tommaso, Jean-Luc Dubois

Published in: Polymers, 13 (16), 2724, August 15, 2021

Abstract

Poly(methyl methacrylate) (PMMA) is a versatile polymer with a forecast market of 4 Mton/y by 2025, and 6 USD billion by 2027. Each year, 10% of the produced cast sheets, extrusion sheets, or granules PMMA end up as post-production waste, accounting for approximately 30 000 ton/y in Europe only. To guide the future recycling efforts, we investigated the risks of depolymerization process economics for different PMMA scraps feedstock, capital expenditure (CAPEX), and regenerated MMA (r-MMA) prices via a Monte-Carlo simulation. An analysis of plastic recycling plants operating with similar technologies confirmed how a maximum 10 M USD plant (median cost) is what a company should aim for, based on our hypothesis. The capital investment and the r-MMA quality have the main impacts on the profitability. Depending on the pursued outcome, we identified three most suitable scenarios. Lower capital-intensive plants (Scenarios 4 and 8) provide the fastest payback time, but this generates a lower quality monomer, and therefore lower appeal on the long term. On 10 or 20 years of operation, companies should target the very best r-MMA quality, to achieve the highest net present value (Scenario 6). Product quality comes from the feedstock choice, depolymerization, and purification technologies. Counterintuitively, a plant processing low quality scraps available for free (Scenario 7), and therefore producing low purity r-MMA,

has the highest probability of negative net present value after 10 years of operation, making it a high-risk scenario. Western countries (especially Europe), call for more and more pure r-MMA, hopefully comparable to the virgin material. With legislations on recycled products becoming more stringent, low quality product might not find a market in the future. To convince shareholders and government bodies, companies should demonstrate how funds and subsidies directly translate into higher quality products (more attractive to costumers), more economically viable, and with a wider market.

Keywords: methyl methacrylate, PMMA recycling, Monte Carlo, economic analysis, regenerated MMA, depolymerization, scenario, net present value (NPV), payback period, risk analysis

3.1 Introduction

Poly(methyl methacrylate) (PMMA), known as acrylic or acrylic glass, as well as Perspex, Plexiglas, and Altuglas, is a transparent thermoplastic and an alternative to glass due to its UV resistance and transparency. The methyl methacrylate (MMA) global market was valued 7.8 billion US dollars in 2018 [189], and the production volume assessed around 3.9 Million ton in 2019/2020 [190, 191]. These figures are foreseen to increase steadily in the next years, to reach 5.7 Mil-lion ton of MMA worldwide produced by 2028 [190], and an estimated worth of 4.8 USD billion for MMA by 2028 in Europe only. Similarly, the PMMA market volume passed from 2 Million ton/y in 2017 [192], to 2.6 Million ton in 2019 [193], and it is estimated to reach a market value of 6 USD billions by 2027 [194].

The Covid 2019 pandemic had a significant effect on the PMMA market. On one side, the global crisis put a strain on the automotive and construction industry, that ac-counts for more than 60% of the PMMA application [191, 195]. At the same time, sheets production boomed, along with demand for medical diagnostic equipment such as incubators, or medical cabinets, among others. For this reason, although the production of PMMA incidentally decreased in the first two quarters of 2020, spot prices and requests for PMMA increased by 25% in 2020 [195], making it the most sought-after polymer in the world. In particular, the protective sheet market made the feedstock price (MMA) bouncing back after 27 months of pricing decline [196], and therefore ICIS foresees a "strong (+10%) rebound in 2021" (of PMMA market), "to be completed in 2022 returning to pre-crisis demand levels" [191].

Concurrent with the increasing market and production volume trend of the last years, the End-of-Life and post-production waste ramped up as well. The MMAtwo consortium estimated that, in Europe only, out of the 300,000 ton/y produced, only 8000 are recycled in Europe, most of which (70%) coming from post-production streams such as PMMA offcuts,

saw dust, production scraps, or off-grades [37].

The market demands of PMMA and MMA represent a relatively small volume compared to other plastics (10 – 100 times less [52, 197]). Therefore, the general public often oversees strength and opportunities of PMMA recycling. Nevertheless, already back in 1945, only 17 years after Otto Röhm first synthesized PMMA, Gem Participations patented a "heat transfer bath process" to depolymerize "Lucite" scrap back to the monomer [44]. Due to its higher price (compared to large volume plastics like polyolefins for instance), several companies and academic groups investigated PMMA chemical recycling to MMA. PMMA thermally depolymerizes to MMA by radical unzipping starting at 350 °C, and pure PMMA fully depolymerizes to MMA at 450 °C [198]. Thermochemical technologies emerged in time, with the main being dry distillation, molten metal bath, fluidized beds, and extruders [46, 52]. Regardless the technology, the economic viability has always hurdled the large-scale industrialization of any recycling process [199]. To guide the future recycling efforts, we investigate the economics of PMMA recycling, detailing the effect of feedstock type, product quality, and capital investment.

The "Dry-distillation" is commonly practiced in several countries, including India, China, or Brazil. In this process, PMMA scraps are loaded in a tank, which is heated with a direct burner most of the time, and when no more cracked products are emitted, the unit is cooled to be reloaded. Crude MMA is condensed, and purified, most often with a rough distillation. The "Rotating-drum" process is a variation of the dry-distillation, which is also popular in Asia. It can be operated continuously, but most of the time it is a batch process. The PMMA scraps are loaded in the rotating cylinder, which provides a kind of mixing of the material, and avoids one of the drawbacks of the dry distillation (the heat transfer limitation through the char layer which forms in the unit). The "Molten Metal" process, uses most often molten lead, but can also use tin or zinc. The molten metal has a high specific heat which is efficiently transferred to the PMMA. When these units are operated properly there is no contamination of the product nor the environment. However, when low quality scraps are processed, a high amount of solid residues are produced, contaminated with the metal used. This generates additional cost to dispose them of properly. This technology is still in operation in several countries, including Italy, Spain, Egypt, and in South East Asia for example. The "Fluid-Bed" process involves a twin fluid bed circulating reactor system. Hot sand is circulated between a depolymerization reactor and a regenerator where carbon de-posits are burned and sand is reheated. This process has been piloted at rather large scale, but was not industrialized yet, although several variations have been investigated. Other technologies are under development like the use of microwaves, Joule effect (ohmic heating), and inductive heating. "Stirred-Tank" process is also a variation of the dry distillation, in which a stirrer

is used in the reactor for better heat and mass transfer. That requires a molten polymer base to be able to stir the scraps. To the best of our knowledge, a few units are using this type of technology. The technology investigated in the MMAtwo research project is based on a "Twin-screw extruder". This process was used at industrial scale on high-quality cast PMMA scraps, and is investigated in the project for all kinds of PMMA wastes, including post-industrial and post-consumer wastes. In this process, the scraps are continuously fed in the extruder where the residence time is very short, and the crude MMA vapors are condensed, and further purified.

All the processes, in use today, include a scrap pretreatment (crushing, separation of the polyethylene films and PVC parts), a condensation, and a purification section. The level of purification varies greatly between the sites, with product as low as 91 wt% MMA content seen and up to 98.5 wt% seen on the market, or 99.8 wt% achieved in the MMAtwo project. The sequence of purification steps depends on the usual impurities and the target for the regenerated MMA producer. The distillation can be operated in a batch mode with a single column or in a continuous mode with two distillation units, and in some cases with extra purification steps such as washing steps and dehydration steps. So, the capital cost and operating cost are strongly affected by the level of purity expected for the r-MMA. At the same time, the quality of the scraps has also a strong impact on the final r-MMA purity: a clean cast PMMA will give better r-MMA quality as it does not contain co-monomers unlike the injection and extrusion grades PMMA. Therefore, not all the scraps have the same market value.

3.2 Materials and Methods

3.2.1 Depolymerization Process

At a first glance typical PMMA recycling processes have a common backbone (Figure 3.1):

1. Pre-treatment in or off-site (1000);
2. Depolymerization section (2000);
3. Purification section (3000).

The nature of each process step varies based on the interdependence of feedstock source the target product quality and the available technological know-how. Combination of different steps gives the full spectrum of process technologies (dry distillation molten bath fluidized bed extruder etc.).

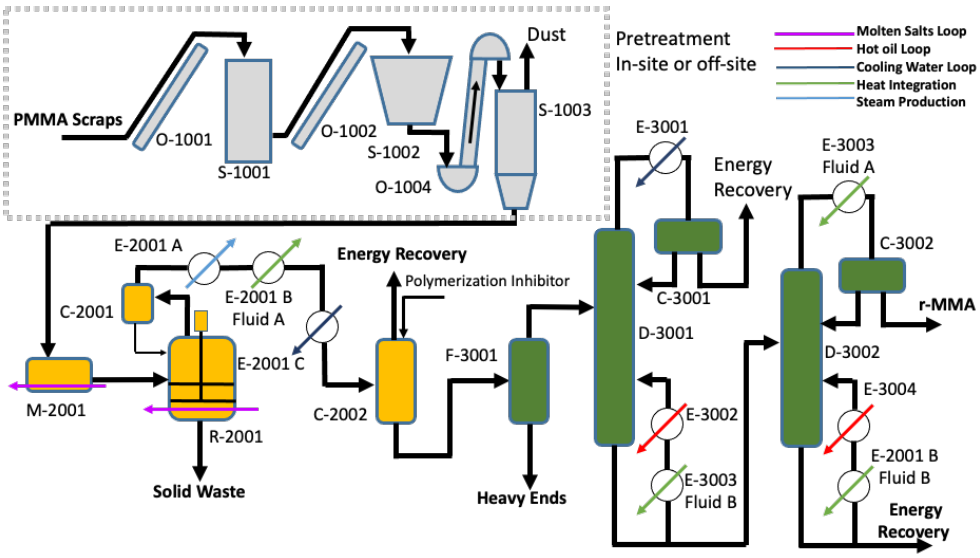

Section	*Unit*	*Name*	*Details*
1000-Pretreatment	*S-1001*	*Impactor*	
	S-1002	*Granulator*	
	S-1003	*Bag filter*	
	O-1001/1002	*Conveyers*	
	O-1003/1009	*Screw Conveyers*	*Not shown*
	O-1004	*Bucket Elevator*	
2000-Depolymerization	*M-2001*	*Melter*	*Extruder premelter*
	C-2001	*Deduster*	
	C-2002	*Liquid gas separator*	
	V-2001	*Skimmer separator*	*Not shown*
	R-2001	*Depolymerization Reactor*	*Stirring tank*
	E-2001 A	*Cracking gas cooler*	*Steam generator*
	E-2001 B	*Cracking gas condenser*	*Fluid A*
	E-2001 C	*Cracking gas subcooler*	
	F-2001	*Molten salts Furnace*	*Not shown*
3000-Purification	*F-3001*	*Evaporator Heavies*	*Thin-film evaporator*
	C-3001	*D-3001 Reflux drum*	
	C-3002	*D-3002 Reflux drum*	
	E-3001	*D-3001 overhead condenser*	
	E-3002	*D-3001 reboiler*	
	E-3003	*Condenser/reboiler Heat integration*	*C-3001 reboiler/C-3002 Condenser*
	E-3004	*C-3002 reboiler*	
	E-3005	*r-MMA air cooler*	*Not shown*
	D-3001	*Lights Column*	*70°C, 0.5 atm*
	D-3002	*Monomer Column*	*80°C, 0.5 atm*
	F-3001	*Hot-oil Furnace*	*Not shown*
	T-2001	*Monomer storage tank*	*Not shown*

Figure (3.1) Simplified flowsheet for our design of a PMMA depolymerization process.

Although no process route is dominating worldwide [52], some are preferred when lower quality r-MMA is acceptable, or less capital-intensive plants are required. For in-stance, dry distillation plants have a low capex, but produce a lower quality monomer (<98% wt.), nevertheless accepted in the local markets (e.g., India, China, Brazil) [52, 200, 201]. Molten lead

baths, instead, are very sensitive to PMMA scraps quality, and have a proven track record with high-quality waste [52, 202]. The MMAtwo twin-screw extruder technology depolymerized several post-industrial, and end-of-Life PMMA grades, into a r-MMA as pure as 99.8% wt. (after distillation) [203]. However, this comes with a higher capital investment, compared to dry distillation, for instance. Theoretically, the ideal technology not only produces the best product from the worst waste, at the lowest capital investment, but it also eases as much as possible its environmental foot-print. For this reason, we report the flowsheet of our own PMMA design of recycling process, organized here to be a compromise or average representative of the existing technologies and heavily energy integrated (Figures 3.1 and 3.2).

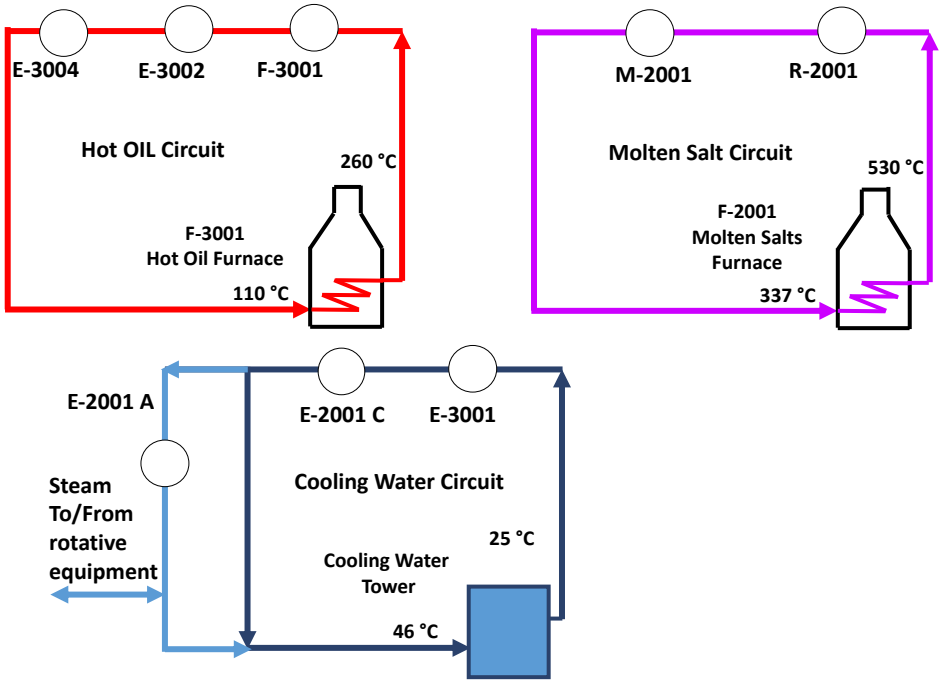

Figure (3.2) Utilities loop for a typical PMMA depolymerization process.

The PMMA scraps are pre-treated in or off site (section 1000), crushed, granulated, and then conveyed to the reaction section (2000). Because it is nowadays seen more and more often in mixed waste plastic recycling technologies, and because it was explored in the past by Mitsubishi Rayon, [204] we considered a stirred tank reactor for the depolymerization. The PMMA granules are pre-melt (M-2001), for instance in a single screw extruder, and then depolymerized in a stirred tank reactor R-2001 (Figure 3.1). This combination of melter/reactor is similar to what we see in Agilyx, or plastic energy [205, 206]] recycling technologies. Compared to a "typical" PMMA process, we minimized the capital and operating expenses (Capex/Opex) at the pre-treatment by not including a washing step.

The depolymerization vapors condense and are then purified to r-MMA in a series of columns. First, the crude is pre-purified from the very heavy ends in the evaporator F-3001, and then two distillation columns fix the purity of the monomer. The plant pro-duces by-products, burnt on site for energy recovery (section 4000 – not shown), r-MMA, and solid and liquid waste (heavy ends), which are disposed of outside the battery limits. The pigments, fillers, charred polymer, and other polymer residues tend to accumulate in the solid residue, which might also contain some substances of very high concern, therefore requiring proper disposal protocols. The heavy ends contain dimers and oligomers, but also some other cracked polymers that contaminated the PMMA.

Reaction and purification sections are technology-neutral, meaning that any other reactor or purification choice are valid in lieu of our design, since our goal is to explore the economics of PMMA recycling at large. Same applies for the heating medium choice (molten salt or hot oil), that are interchangeable with any other heating carrier (e.g., steam, flue gases, or direct heating) as long as we assume the same heating energy demand. Other purification technologies are sometimes used by operators such as a washing step with sodium hydroxide solution, but that introduces water in the MMA, and increases the complexity of the distillation due to an azeotrope between water and acrylates and methacrylates. In absence of added water washing step, the losses due to the azeotropes can be minimized.

The by-products combustion provides heat energy and steam for the rotative equipment. Natural gas complements the heating duty required. Natural gas and by-products fuel a molten salt, and a hot oil circuit. The molten salt loop supplies the heat to the reaction section, while a hot oil circuit supplies the purification section. Because of the high energy content of the by-products (comparable to that of MMA – 26.2 MJ/kg [207]), the energy recovered from their combustion is high enough to satisfy almost all the energy requirements of the process, with only a little natural gas contribution. In general, the cast scraps have a better yield in r-MMA, with a lower production of waste, and they require a proportionally higher natural gas consumption compared to the mixed PMMA scraps (Table 3.1).

Table (3.1) Mass balance for 5000 PMMA scraps ton/year plant in case of Cast and Mixed PMMA scraps.

Feedstock/Product/Waste	**Cast PMMA Scraps (90 wt % yield)**	**Mixed PMMA Scraps (78 wt % yield)**
PMMA scraps (ton/y)	5000	5000
Natural Gas (ton/y)	106	80
Heavy Ends (ton/y)	119	411
Solid Waste (ton/y)	100	200
r-MMA (ton/y)	4512	3889

The quality of the feedstock affects the energy requirement of the process. High-quality waste, such as clean cast PMMA scraps, are more expensive, require less energy for the purification, and produce less by-products. Regarding the net energy recovery, cast scraps will require slightly more external energy source than mixed PMMA waste scraps. Although the MMAtwo consortium alone has committed to collect and treat up to 27,000 ton/y of PMMA by 2023, the current European plant size is around 5000 ton/y, as the experience of Madreperla, Monomeros del Valles, and in the past Evonik, Arkema, or Du Vergier [37, 208] suggests. While sorting and collection volumes ramp up, especially for end-of-life waste, highly industrialized and densely populated areas can easily have access to similar volumes. Therefore, we believe that 5000 ton/year of scraps is what any new plant should realistically aim to start with, especially while establishing a sound market.

3.2.2 PMMA – Case Study

Since the nature of scraps affects the mass and energy balance of the process to investigate the PMMA recycling options we benchmarked cast and mixed scraps on a common final r-MMA purity. In general for any given r-MMA grade mixed scraps present a lower global (depolymerization + purification) r-MMA yield compared to cast (78% wt. vs 90% wt. respectively – Table 3.1). At the same time mixed scraps produce proportionally more waste but require less external source of energy. In Table 3.1 we report the mass balance for both cast and mixed scraps processes.

3.2.3 Economic Analysis

When a portfolio of potential projects is available, companies or public investors need to evaluate the potential profitability of each project, to assess when and if to take a risk. The profitability of a project can be assessed by different methodologies, such as the payout period plus interest (POP), the net present value (NPV), the discounted cash flow rate of return (DCFROR), and the uniform annual cost (UAC), among others citePerry2019. The NPV, also known as net present worth (NPW), is the most common quantitative methodology to assess the profitability, since it considers the effect of the time value of money on the profitability [209], and the annual variation in expenses and revenues [210]. The NPV of a project is the sum of the present values of future cash flows [210]:

$$\mathrm{NPV} = \sum_{n=1}^{t} \frac{CF_n}{(1+i)^n} \tag{3.1}$$

where CF_n represents the annual operational cash flow for year n i is the interest rate and t

the project life in years.
When the NPV is positive the project earns more than the interest (discount) rate selected or the best alternative project [209]. The annual operational cash flow CF_n is the sum of the annual net profit after taxes (ANP) and the depreciation D:

$$CF_n = \text{ANP} + \text{D} \tag{3.2}$$

With ANP being the annual gross profit minus the taxes (TR). The annual gross profit (AP) is the sum of sales (S) minus expenses (E) minus depreciation (D) so that the annual operational cash flow CF_n becomes:

$$CF_n = \text{S} - \text{E} - \text{D} \times (1 - \text{TR}) + \text{D} \tag{3.3}$$

The sales are the revenue generated from the r-MMA, the expenses are the total expenses of the plant, the tax rate is set at 35% as for France, and the depreciation follows the straight line depreciation on 10 years [209]. In our assessment, we divided the expenses in Fixed, and Variable. The Fixed expenses are:

- Direct labor;
- Operating supervision assumed as 18% of the direct labor;
- Laboratory charges assumed as 18% of the direct labor;
- Plant overhead assumed as 60% of direct labor;
- Administration assumed as 20% of direct labor;
- Maintenance and repairs assumed as 2% of the total investment but which could be higher for a cheap equipment;
- Operating supplies assumed as 1% of the total investment;
- Financial interests assumed as 2% of the total investment;
- Property taxes assumed as 2% of the total investment; and
- Insurance assumed as 2% of the total investment.

The Variable expenses are:

- Raw Materials (PMMA scraps natural gas);
- Waste disposal (Solid waste heavy ends);
- Other utilities (water electricity etc.) assumed as 3% of total raw material and waste disposal because we did not go into that level of details;
- Distribution and selling as 5% of the sales because we assumed here to have a limited pool of customers that therefore minimizes the distribution related costs;
- R&D and Royalties as 3% of the sales in total. This way R&D budget depends on the sales but remains in the range of what is seen for commodity chemicals.

We also made the additional general assumptions for the plant:

- Plant life is 20 years;
- The plant is located in France;
- Operating time is 8000 h or 330 days;
- Depreciation is in 10 years;
- Internal rate of return (IRR) is 10%;
- Labor cost is calculated for 5 shifts per day continuous process;
- The plant needs 2 operators per shift at a cost of 60 000 USD/y per operator;
- The capital investment is spread over two years (year 0 and year 1) where 2/3 of the capital is invested in the first year and 1/3 in the second;
- The plant starts to operate in the third year at 50% production capacity then it ramps up to 75% in the fourth year 90% in the fifth and finally 100% starting from the sixth year (year 5 in following tables and figures).

At this early stage the capital investment can be estimated in different ways. In 2017 Tsagkari et al. reviewed cost estimation methods for biomass conversion processes at class 4 – 5 AACE (Association for the Advancement of Cost Engineering) [84, 211], pointing out that there are several methods for early stage estimation. In our case, we can rely on the Petley [212], and Lange methods [213]. The Petley method estimates the ISBL of the plant starting from the number of functional units, the capacity of the plant, the maximum pressure and

temperature. In 2001, Lange proposed two capital cost estimation methods, one based on the plant energy losses, and one on the plant energy transfer. Both methods are appropriate for highly exothermic, or endothermic processes and start to be reliable for energy transfer/losses higher than 10 MW.
The original Petley's correlation (from 1988) updated to 2019 and relocated to France is:

$$\text{ISBL}_{2019} = 55882 Q^{0.44} N^{0.486} T_{max}^{0.038} P_{max}^{-0.22} F_m^{0.341} \frac{\text{CEPCI}_{2019}}{\text{CEPCI}_{1988}} \cdot F_l \tag{3.4}$$

where ISBL is the Inside Battery Limit investment Q is the plant capacity in ton/y of scraps N the number of process steps (4 here) T_{max} the maximum process temperature in K (723 K) P_{max} the maximum pressure in bar (1.5 bar) and F_m the material construction factor (1.5). The Chemical Engineering Plant Cost Index (CEPCI) updates the plant cost from 1988 to 2019 and the relocation factor (F_l) relocate it to France. In 1988 the CEPCI was 342.5 while in 2019 it was 607.5 [214, 215]. The Peters and Timmerhaus handbook suggests that the Outside Battery Limit (OSBL) investment is 25 – 40% of the ISBL [216] so we selected 40% to be conservative.
Lange correlated the ISBL with the energy losses in the plant calculated as $\text{LHV}_{(\text{feed+fuel})}$-$\text{LHV}_{(\text{product})}$:

$$(\text{ISBL} + \text{OSBL})_{2019} = 3.0 \cdot (\text{energy} \quad \text{losses}[MW])^{0.84} \cdot \frac{\text{CEPCI}_{2019}}{\text{CEPCI}_{1993}} \cdot F_l \tag{3.5}$$

Again we updated the investment with the CEPCI of 1993 (343.5) and the relocation factor for France.
Alternatively he correlated the ISBL with the energy transferred in within the process as:

$$\text{ISBL}_{2019} = 2.9 \cdot (\text{energy} \quad \text{transfer}[MW])^{0.55} \cdot \frac{\text{CEPCI}_{2019}}{\text{CEPCI}_{1993}} \cdot F_l \tag{3.6}$$

A fourth method is by expert judgment adjusted on existing plant capital costs. We know that the PMMA recycling process does not differ that much from a plastic to oil pyrolysis plant, some pyrolysis-based plastic to fuel, or some existing plastic to plastic recycling plants. In the last 10 years, several plants suitable for comparison have been built, in Europe or US, and even more have been announced in the near future (Table 2). Reviewing such plants, along with process reviews from expert companies (e.g., HIS [58], or Nexant [217]), we gave a best educated guess on the capital cost of the plant.
In Figure 3.3, we report the capital cost vs capacity of some selected projects scaled to 2019 in France, as well as the estimated capital cost. For a 5000 ton/y plant, the two Lange

methods reach their validity limit, (under)estimating a capex of 3.3 M USD, and 7.2 M USD respectively. The Petley method probably overestimates the capex at 18 M USD. Both methods are indeed "Class V" for process engineers, or technology readiness level "TRL 3 – 4" for chemists, and they carry significant uncertainties. For comparison, for similar plant sizes, announced investments for recycling plant were between 11 M USD, and 25 M USD for the first of a kind (FOAK) Plastic energy Plastic to Oil plant [218]. Obviously, FOAK plant are more expensive than nth of a kind (NOAK) for the same technology/company, because of learning and technology maturity [219]. For instance, this is the case of Plastic Energy, Quantafuel, or QM Recycled Energy, in Table 3.2.

Table (3.2) Historical data of first of a kind (FOAK) or nth of a kind (NOAK) plastic to liquid plants.

Company	**Capacity (kton/year)**	**Investment (M US$)**	**Year**	**Project Type**	**Process Type**
Cyclix [220]	33	80	2020	NOAK	Plastic to Oil
Plastic Energy [218, 221]	5	20	2014/15	FOAK	Plastic to Oil
Plastic Energy [218]	20 – 25	35	2019	NOAK	Plastic to Oil
Renewlogy [222]	3.3	4	2018	NOAK	Plastic to Fuel
Renew Phoenix [223, 224]	3.3	5.5	2019	NOAK	Plastic to Fuel
QM Recycled Energy [225]	10	9	2018	FOAK	Plastic to Oil
QM R.E. Biofabric [226]	1.6	2	2020	FOAK	Plastic to Oil
Quantafuel [227]	20	17.5	2018	FOAK	Plastic to Fuel
Quantafuel [228]	25	18	2020	NOAK	Plastic to Fuel
Quantafuel/Vitol [227, 229]	100	75	2020	NOAK	Plastic to Fuel
Recycling Technologies [230]	7	7.7	2018	FOAK	Plastic to Oil
Carbo Hydro Transformation	8	2	2018	FOAK	Plastic to Fuel

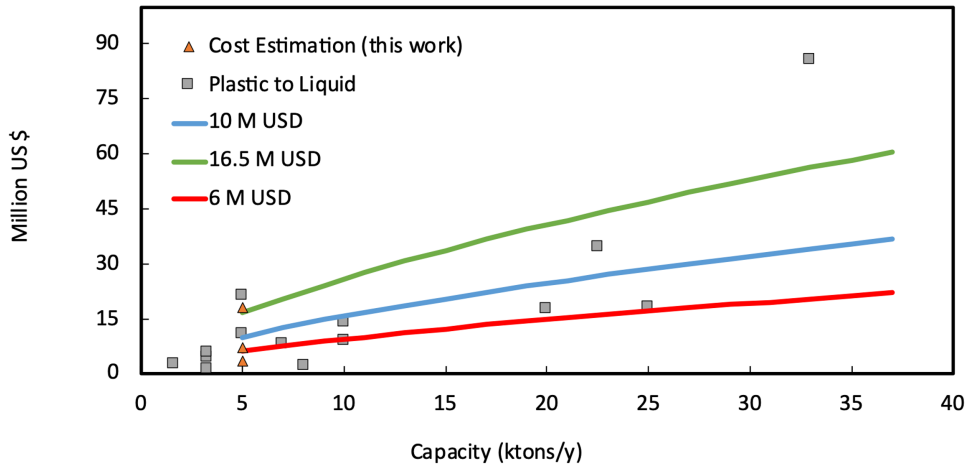

Figure (3.3) Scaled Investment (2019 France) versus original plant capacity. Historical data of plastic to liquid (oil or fuel) plants (grey squared marks) and early estimation methods (triangular marks) for a 5 kton/year scraps Mixed or Cast scraps PMMA depolymerization plant. The blue line represents the power-law with a reference investment of 10 M USD while the green and the red with 16.5 M USD and 6 M USD respectively.

To select the most appropriate investment at this early stage we extrapolated the data of (Figure 3.3) with the power law method scaling everything to 5000 ton/y:

$$\frac{C1}{C2} = \left(\frac{S1}{S2}\right)^{0.65} \tag{3.7}$$

where C is the Cost (ISBL or OSBL etc.) and S the plant size the scaled 5000 ton/y would therefore be in the 6 to 16.5 M USD range. On the basis of different evaluation methods we assumed a reference capital investment of 7.5 M USD that translates into a median (p50) CAPEX of 10 M USD (p10 at – 20% reference Capex (i.e. 6 M USD); and p90 at +120% (i.e. 16.5 M USD) – Figure 3.3) and which also includes working capital and start-up costs. When a plant starts it always needs raw material/product stocks and some budget allocated for unforeseen contingencies.

3.2.4 Monte-Carlo Simulation

To factor in all the variables uncertainties at once, as opposed to inspect only one variable at the time (sensitivity analysis), we performed a probability risk analysis, also known as Monte-Carlo simulations. The way we described it so far, the NPV method is a deterministic method, meaning that we obtain a single output when plugging in a fixed input. However, if we input probabilistic distributions instead, we obtain an output with its own probabilistic

distribution. In the Monte-Carlo simulation technique, each input has its own statistical distribution (normal, log-normal, gaussian, gamma, etc.,), from which the calculator selects one random value. From the random input series, the simulation calculates the output variable, for instance the NPV. The process is then repeated a high enough number of times so that the output becomes reliable, for instance in the order of thousands. Eventually, out of the frequency of recurring of each outcome, we can calculate the probability of happening of a certain outcome (e.g., NPV on a certain year). The Perry's Handbook, or our previous paper on Risk assessment using Monte-Carlo simulation is a good starting reference on this technique [209, 231, 232].
In layman's terms, the risk assessment analysis consists in:

1. Based on production price index-adjusted historical data, set a statistical distribution for the future price of raw materials (PMMA, natural gas), waste (solid wastes and heavy ends), and product (r-MMA);
2. Based on the combination of cost estimation techniques, plant historical investments, future announced investments, and expert judgement, set a statistical distribution for the capital cost;
3. Based on the inflation adjusted historical prices, find the historical correlation between raw materials, waste, and product price;
4. Based on the expert judgment, give the best educated guess on the raw materials, waste, and product future prices correlation;
5. For each input (capital cost, raw materials, waste, and product prices) adjust the random variables for the correlation matrix. In this way, the inputs do not vary independently, but we force their variation according to the correlation matrix;
6. Determine the profitability (i.e., NPV, production cost);
7. Repeat the last steps 3000 times;
8. Evaluate the probability of each occurrence to happen, and look at the median probability, the p10 and p90 (10% and 90% probability) for the variables of interest.

The Monte Carlo simulation copes with the uncertainties on raw material price, waste price, product price, and investment. This approach is very appropriate, as a risk analysis, in this very early stage evaluation of processes, to identify the most viable scenario leading to a successful project. We kept all the other values as a fixed deterministic variable (labor cost, other utilities cost, depreciation, taxes, all the other fixed costs).

Raw Materials

The main raw materials are the PMMA scraps, and the natural gas to compensate for the extra heat needed.

The MMAtwo consortium estimates that before the Chinese trade ban, Europe was exporting between 15,000 ton/y and 30,000 ton/y to India and China [52], with around 8000 traded within Europe [37,52]. Hence, we collected some market prices for PMMA scraps for the 2013 – 2016 period in the major ports of India (Figure 3.4) from Zauba [233], and Eximpulse [234]. What we see here are relatively good quality scraps, most likely cast materials, traded as "Acrylic scraps HS39159030". Lower quality scraps are difficult to trace, also because they might be sourced from the local market. For this reason, we assumed two different statistical distributions for the PMMA scraps (Figure 3.5):

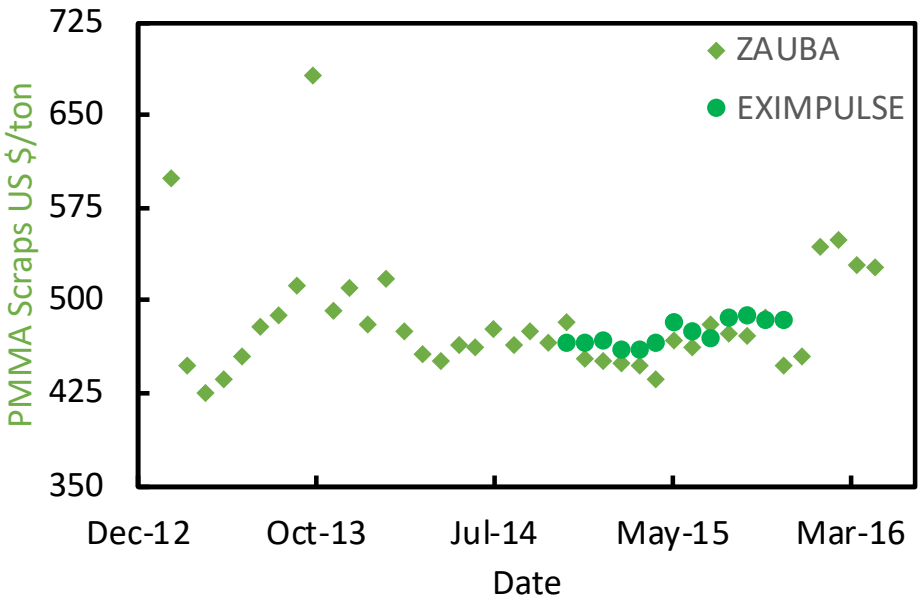

Figure (3.4) PMMA scraps import prices in India between 2013 and 2016 from Zauba [233] and Eximpulse [234].

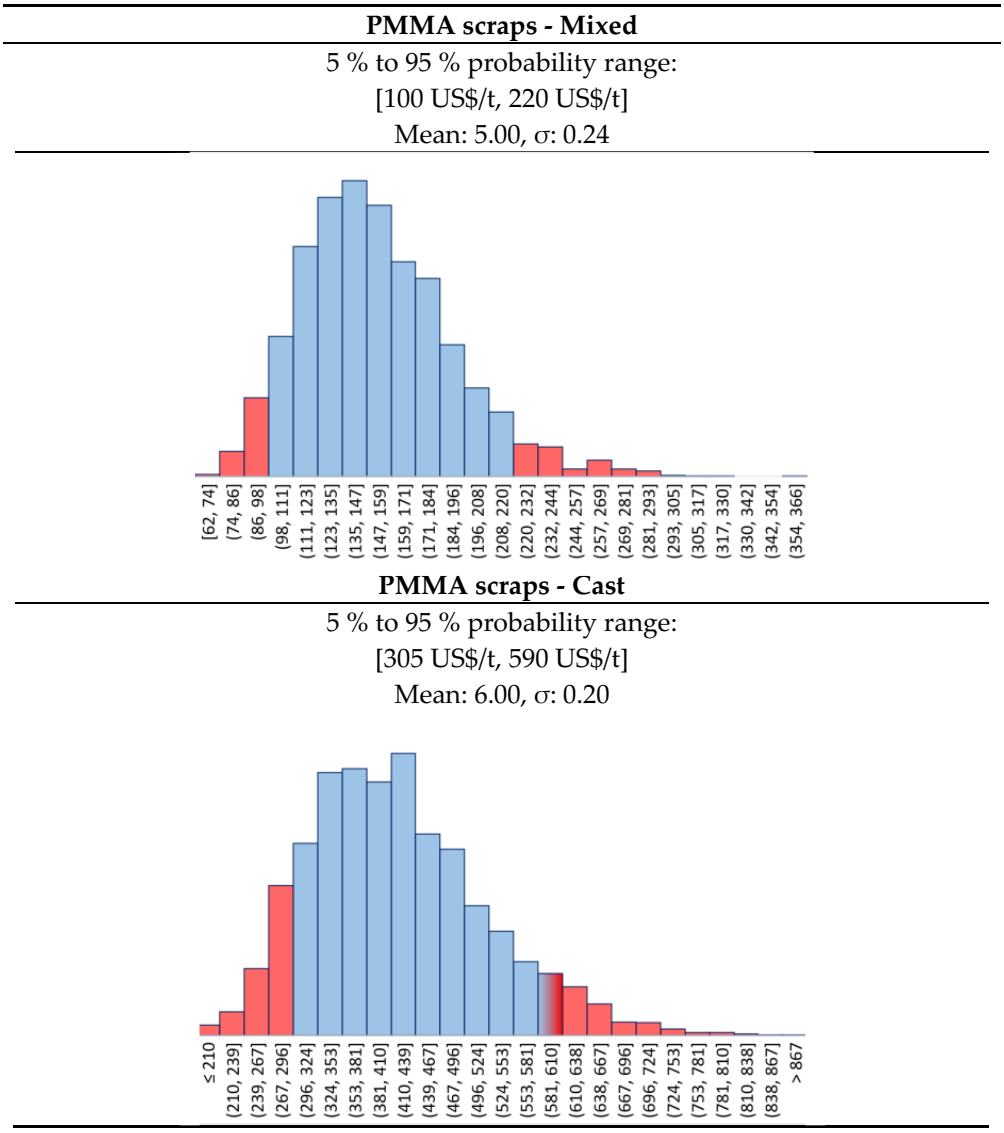

Figure (3.5) Log-Normal distribution for Mixed and Cast PMMA scraps prices.

- The "Cast" PMMA scraps, more expensive because they are a higher purity kind of scrap; and
- The "Mixed" PMMA scraps, a lower quality, cheaper feedstock.

In both cases, we assumed a log-normal distribution for the future price of the scraps. The "Cast" scraps have a [p10, p90] interval in between [305, 590] USD/t, while for the "Mixed" we selected [100, 220] USD/t. There is also a **third**, extreme **scenario**, where the scraps quality is so low, that they become available at zero price. For the European Natural, gas we collected the monthly price in USD between 2000 and 2020 from FRED (Federal Reserve

Economic Data) [235] (Figure 3.6). Then, we adjusted for inflation, and we found out that the prices can be fitted best with a log-normal distribution.

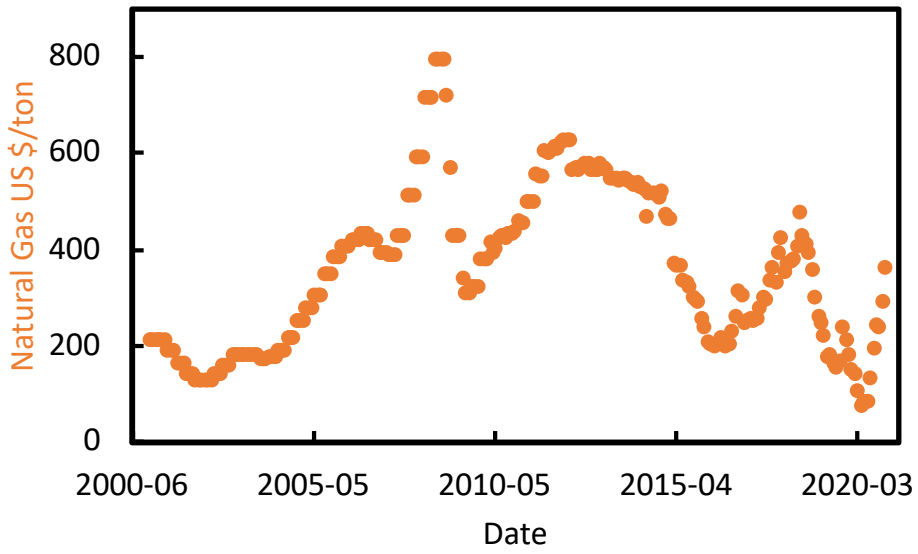

Figure (3.6) Historical natural gas prices in EU from [235].

We do not see any reason why natural gas should change its statistical distribution over time in the near future, nor we think that its value should deviate much from last years' trend. Therefore, we assumed a log-normal distribution for the natural gas price, with a [p10, p90] interval of [190, 705] USD/t, with the mean lying around 300 USD/t (Figure 3.7).

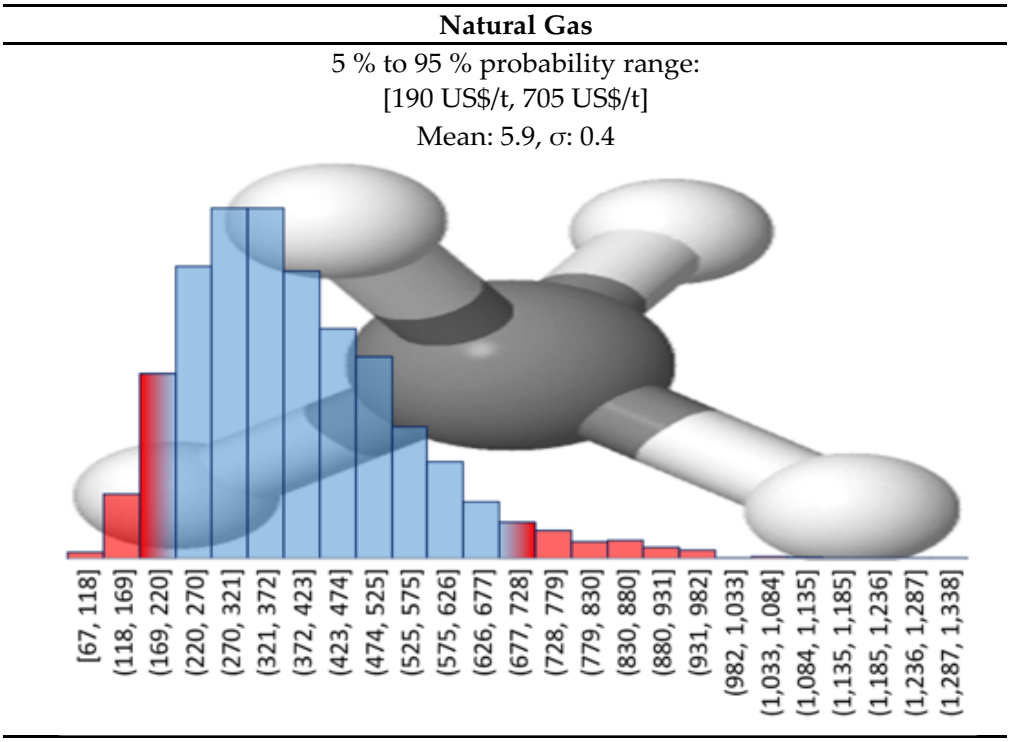

Figure (3.7) Log-normal distribution for natural gas prices.

Products – r-MMA

The recycled MMA (r-MMA) price depends strongly on the product quality. PMMA producers aim at the very best monomer quality that satisfies their needs, which could be up to that of the virgin material (>99.8% wt. purity [236]). At the same time, the western world, and in particularly Europe, is pushing toward sustainable development, and promoting circular economy models. For instance, Europe recently updated its circular economy action plan (March 2020 [237]), toughening the policy on waste export outside Europe, and it imposed a contribution of about 1000 USD/t for non-recycled plastic packaging to curb plastic waste [238]. In this framework, we foresee how recycled MMA will play an even bigger role hereafter. We collected the virgin MMA spot historical prices in EU (Figure 3.8), and we adjusted them for inflation with the PPI (producers price indices) index. The PPI index, available online on the organization for economic co-operation and development (OECD), is an "advanced indicator of price changes throughout the economy" that measures the average price change over time in selling price from the sellers' perspective [239]. In this way, the only factor playing a role in the historical prices' trends is geo/political. Virgin MMA price is highly correlated to crude oil price (Figure 3.8) and we believe that this will not change in the near future.

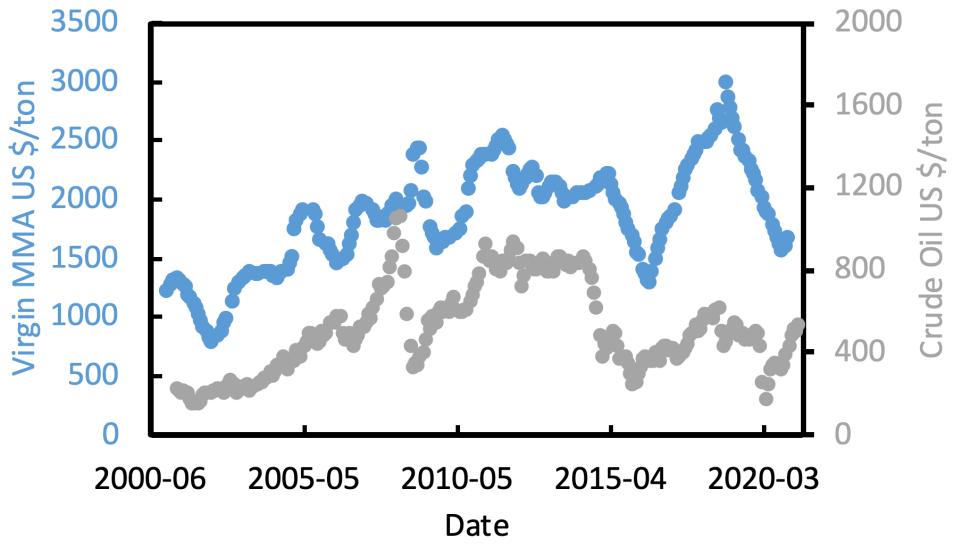

Figure (3.8) Virgin MMA spot prices from [196, 240, 241] and crude oil [242].

We also collected some prices for exported "regenerated black MMA" HS 29161400 in the ports of India between 2013 and 2016 [243] (Figure 3.9), a period during which crude oil prices varied a lot. All shipments were destined to Asia (e.g., China, Bangladesh, or Pakistan), for an average tonnage of 400 ton/y. In the period of interest, this lower quality crude MMA product was selling at an average of 30% discount over the virgin material.

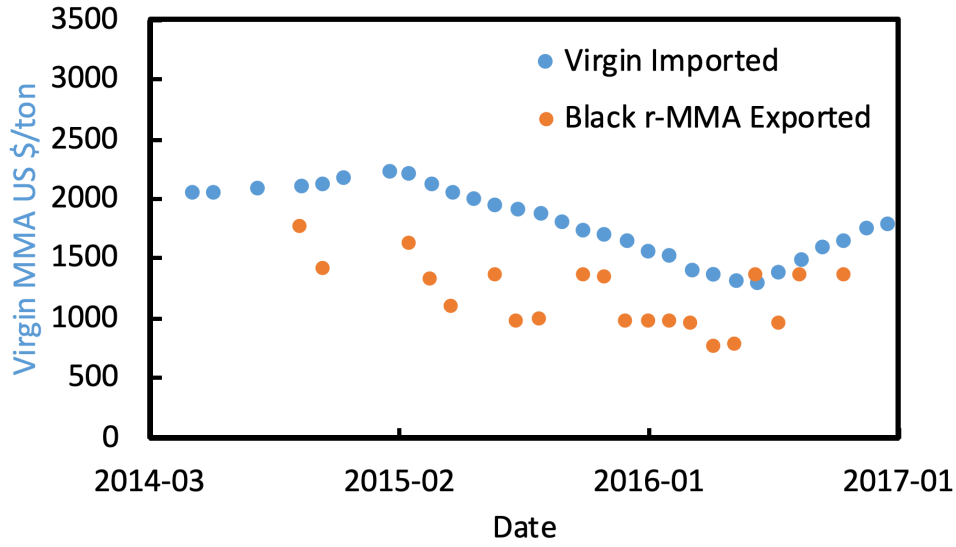

Figure (3.9) Crude exported MMA price [243] and virgin imported spot price between 2014 and 2017 in India.

Again, the best fit for the PPI adjusted historical prices of virgin MMA was the log-normal distribution. For our future prediction, we imagined different r-MMA prices, for three different product's qualities, each with a log-normal distribution (Figure 3.10):

- **Virgin-like MMA** price;
- **20% discount MMA** price. In western markets it will be very unlikely to see very low-quality products. Requests for r-MMA will increase due to stricter policies and increasing environmental awareness of the final customers. Therefore, we expect that recycling companies and PMMA producers will settle midway for a fairly good enough "low-quality" r-MMA;
- **20% premium MMA** price. Either for increasing requests, superior quality, or market fluctuations, we believe that a scenario where PMMA (or other MMA derivatives) producers will pay a premium for their r-MMA is plausible. It could also correspond to subsidies given to recycled products based on their quality.

r-MMA Virgin Price

5 % to 95 % probability range:
[1655 US$/t, 2665 US$/t]
Mean: 7.65, σ: 0.14

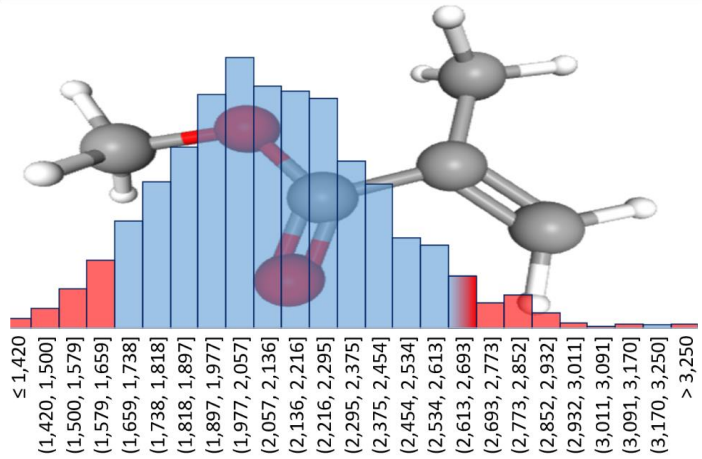

r-MMA 20% Premium

5 % to 95 % probability range:
[2000 US$/t, 3225 US$/t]
Mean: 7.86, σ: 0.14

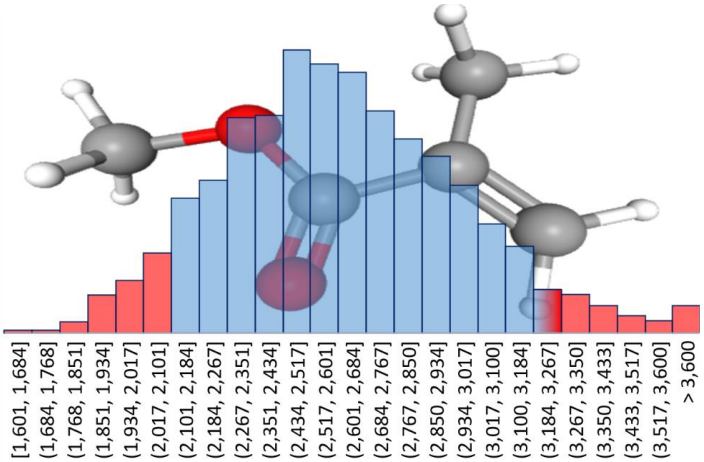

r-MMA 20% Discount

5 % to 95 % probability range:
[1290 US$/t, 2080 US$/t]
Mean: 7.40, σ: 0.14

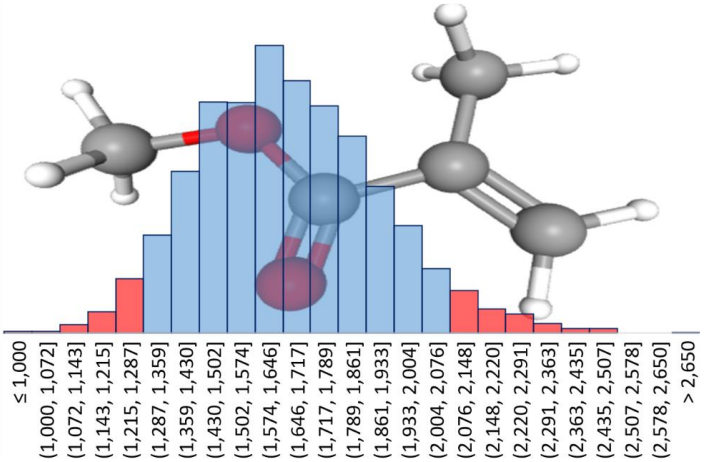

Figure (3.10) Log-normal distribution for r-MMA at virgin price 20% premium and 20% discount.

Waste – Heavy Ends and Solid Waste

The depolymerization step produces char and dust as cracking by-product, while the purification train separates the heavy ends from the recycled monomer. Carbonaceous waste from the depolymerization is collected and either sold as charcoal to heavy industries (e.g., steel), or landfilled. Heavy ends can be either burnt on site for heat recovery, or if their quality as combustible is too low, they must be disposed of. In our case, we assume to remove the very heavy ends in the evaporator V-3001 (Figure 3.1), in form of a syrup-like fluid. Then, the distillation fixes the purification and removes some slightly lighter heavy cuts that are burnt on site for energy. In the mass balance (Table 3.1), we assumed the very heavy ends to leave the plant as by-product. In the economic assessment, this oil could either be sold as a heating oil equivalent or disposed of. To be conservative, we assumed that there is no market for these very heavy ends, and they must be disposed of.
Same applies for the solid wastes. Because of the increasing public awareness, landfill taxes and gate fees have been swiftly increased in Europe in the last 20 years, as shown for instance by ADEME (French government agency) in a comparative report of 2017 [244]. As a reference, Finland had a landfill tax of 25 USD/ton in 2003 [245], which rose to 85 USD/ton in 2020 [246]. As per 2020, 23 EU members have a landfill tax, that varies from 10 (Latvia) to 150 USD/ton (Belgium) [247], as well as Switzerland and UK (150 USD/ton) [246].
To this tax, we still need to add the gate (or tipping) fee, at the entrance of the landfill. Gate fees depends again on the country, but they roughly are comparable to landfill taxes [64]. We believe that henceforward, landfill taxes will keep increasing in EU, leaning toward the highest rates in the continent (i.e., central and northern Europe countries such as Belgium, Luxemburg, Denmark, Sweden, etc.,).
For both heavy ends and solid wastes, we assumed a gaussian distribution. For solid wastes we assumed a median cost (landfill tax + gate fee) of 250 USD/t and a deviation of 50 USD/t, and for the heavy ends a median cost of 150 USD/t (Figure 3.11) and a deviation of 50 USD/t. In this way, we assume to treat the plant by-products according to the highest European standards in terms of waste disposal, as opposed of what happens in existing lower quality PMMA recycling plant in developing countries (e.g., India, Brazil, etc.,).

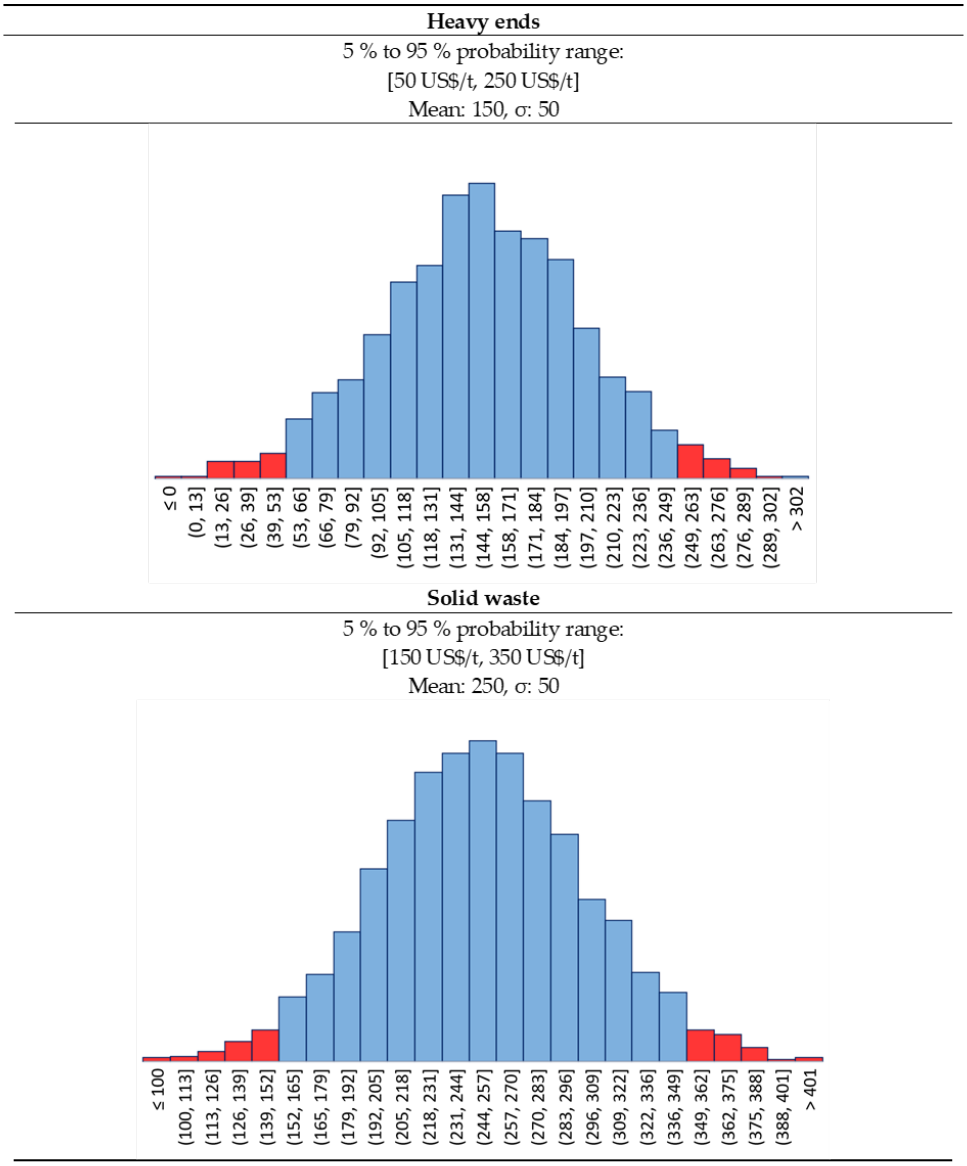

Figure (3.11) Solid waste and heavy ends statistical distribution.

Investment

In a study of 2012, J.K. Hollmann queried over 1000 projects in different industries, and demonstrated how the p10/p90 accuracy range of the capital investment, is close to -20%/+120%, in a log-normal statistical fashion [85]. Thus, in our Monte Carlo simulation, we assumed a log-normal distribution for the capital investment, where p10 corresponds to -20% of the capital cost, and p90 to the + 120%.

For the analysis, we selected four conditions:

1. **Full CAPEX at 10 M USD** (Figure 3.12), for a higher capital-intensive plant. This is the case when we have lower quality scraps (MIXED or 0 price scraps);

2. **30% subsidies on Full CAPEX** for a final CAPEX of 7 M USD (Figure 3.13). It is again a higher capital-intensive plant treating lower quality scraps. Local authorities are more willing to provide subsidies when they see the benefit of the money they spent. In this case, lower quality scraps might need higher cost at pre-treatment or purification, and subsidies could cover that;

3. **Full CAPEX at 7 M USD** (Figure 3.13), for a slightly lower capital-intensive plant. We imagine this to be the case when treating only Cast scraps. The feedstock is relatively "clean", and a cheaper plant is expected; and

4. **Full Capex at 1.3 M USD**. This is the case of a cheap technology, or a plant made of second-hand equipment. In both cases, the lower capital expenditure is likely to be accompanied by a shorter plant life (e.g., 10 years instead of 20), an overall lower quality of the final product, and so a lower price.

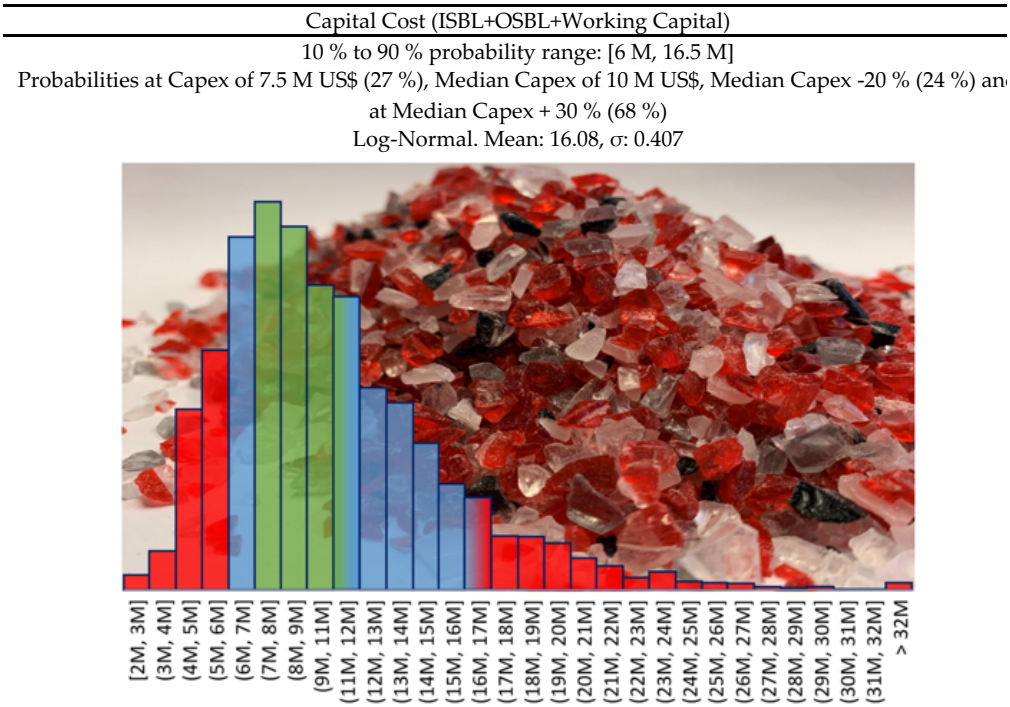

Figure (3.12) Capital cost distribution for 5000 ton/year PMMA scraps plant, at 10 M USD CAPEX – Capital Cost -20%/+ 30 % (Green Area) corresponds to Class 3 confidence interval of the Association for the Advancement of Cost Engineering (AACE) [211].

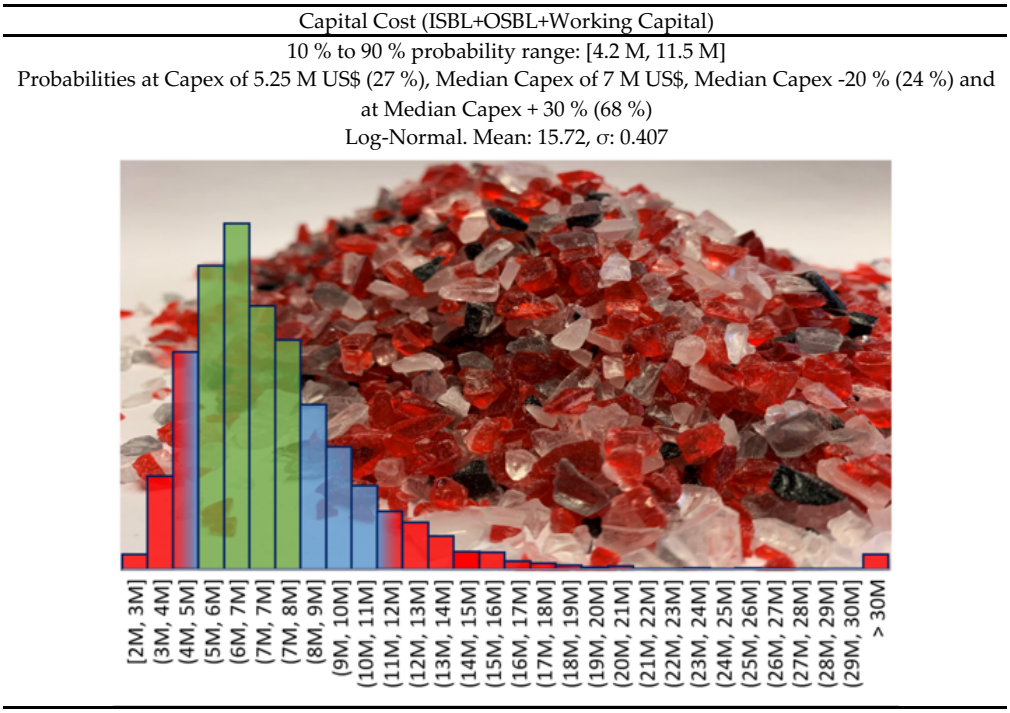

Figure (3.13) Capital cost distribution for 5000 ton/year PMMA scraps plant, at 7 M USD CAPEX – Capital cost -20%/+ 30 % (Green Area) corresponds to Class 3 confidence interval of the Association for the Advancement of Cost Engineering (AACE) [211].

3.3 Results

3.3.1 Scenarios

To study the challenges and possibilities of the recycling industry at large, we compared the profitability for different scenarios (Table 3.3). The scenarios differ for kind of feedstock (Mixed or Cast), final product quality and selling price (20% discount, virgin or 20% premium price), or CAPEX. In Table 3, we summarize the scenarios, and the prices distribution for raw materials, waste/by-products, and products. We ended up outlining nine different scenarios (Table 3.3):

- **Scenario 1** – The plant treats mixed scraps, with a full Capex at 10 M USD, and the r-MMA sells at virgin price. This is our base case. Processing mixed scraps needs a relatively higher capital-intensive plant to reach an acceptable purity for the EU market.
- **Scenario 2** – Like Scenario 1, but the project obtains external funding as grants or subsidies (30% is an accessible value for a European plant);

- **Scenario 3** – Like Scenario 1, but the r-MMA purity requested is higher, and it sells with a premium of 20%. This is more representative of what could happen in the long-term;

- **Scenarios 4 and 8** – The plant treats mixed scraps, with a second-hand, or a cheap process technology (e.g., dry distillation). Therefore, the r-MMA produced is of a lower quality and sells at 20% discount compared to the virgin. In Scenario 4, the plant life is still 20 years, while in Scenario 8 the plant is replaced after 10 years.

- **Scenarios 5 and 6** – The plant processes Cast scraps, more expensive than the mixed, but requiring less/cheaper equipment. The r-MMA sells at virgin or premium price, in Scenarios 5 and 6, respectively;

- **Scenarios 7 and 9** – PMMA scraps are very low quality, and therefore available for free. However, the plant still needs a relatively high investment (10 M USD) to purify the MMA to a grade pure enough to at least enter the market. Nonetheless, r-MMA sells at a 20% discount price. This scenario is representative of very polluted end-of-life streams, where sorting is difficult due to poor infrastructure. For instance, it could apply to the automotive or the construction industry; Scenario 7 is at full capex (10 M USD), while Scenario 9 is with 30% subsidies. Because the project repurposes waste that would otherwise inevitably end in landfill, local bodies grant subsidies for environmental reasons rather than economic reasons only. Our guess is that for the most part, these two scenarios are probable to be transient. The public opinion calls for more sustainable materials, and the government agencies legislate accordingly. Hence, the collecting and sorting infrastructure will eventually keep up with the demands for scraps. When that will happen, PMMA producers in EU will not easily settle for a poor-quality monomer.

Table (3.3) Scenarios and prices overview.

Scenario	**1**	**2**	**3**	**4**	**5**	**6**	**7**	**8**	**9**
Scraps	Mixed	Mixed	Mixed	Mixed	Cast	Cast	Mixed 0 price	Mixed	Mixed 0 price
r-MMA (price)	Virgin	Virgin	20% premium	20% discount	Virgin	20% premium	20% discount	20% discount	20% discount
CAPEX	10 M $	7 M $ (30% subsidies)	10 M $	1.3 M $ 20 y lifetime	7 M $	7 M $	10 M $	1.3 M $ 10 y lifetime	7 M $ (30% subsidies)

Feedstock/Product/Waste	**Distribution Law**	**Mean, Deviation**	**[5%, 95%] Probability ($/ton)**
PMMA Mixed	Log-Normal	[5.00, 0.24]	[100, 220]
PMMA Cast	Log-Normal	[6.00, 0.20]	[305, 590]
Natural Gas	Log-Normal	[5.90, 0.40]	[190, 705]
Heavy Ends	Gaussian	[150, 50]	[70, 240]
Solid Waste	Gaussian	[250, 50]	[165, 300]
r-MMA 20% discount	Log-Normal	[7.40, 0.14]	[1290, 2080]
r-MMA Virgin	Log-Normal	[7.65, 0.14]	[1655, 2670]
r-MMA 20% premium	Log-Normal	[7.84, 0.14]	[2000, 3225]

3.3.2 Correlation Matrix

In 2019, the OECD (Organization for Economic Co-operation and Development) demonstrates that, with few exceptions, waste generation "is still very much linked to economic growth" [248]. Therefore, although prices for feedstock and products/waste vary with time, such variations are not completely random. When the economy is booming, people get better salaries, eat more (or better food), and their purchasing power increases. The downside is that energy and food prices increase too, as well as waste production, especially plastic waste [249]. For instance, Germany has a GDP per capita of around 40,000 USD, and produces 0.5 kg of plastic waste per capita, same applies for the Netherlands (Figure 3.14). On the contrary, Albania has a GDP per capita of 10,000 USD, and produces less than 0.1 kg plastic per person (Figure 3.14).

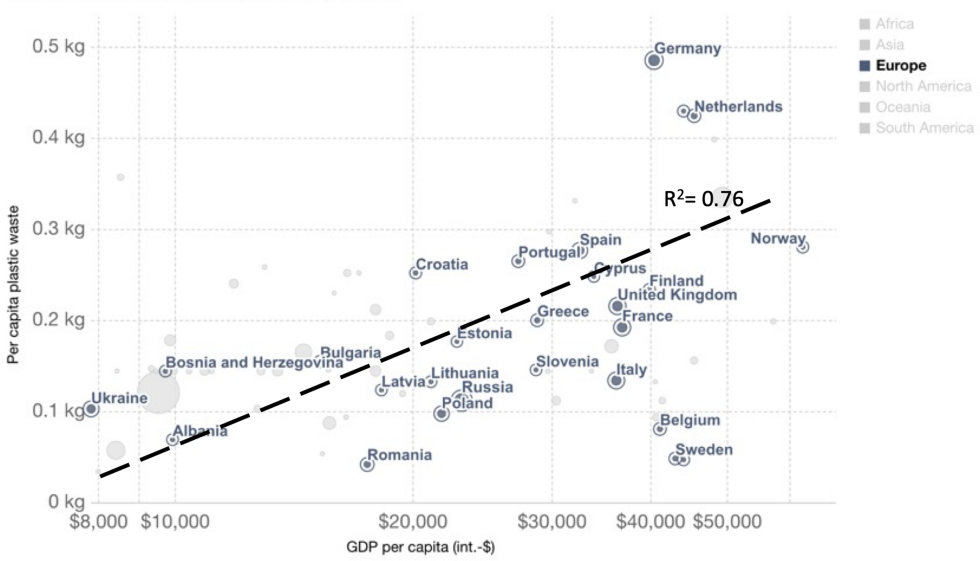

Figure (3.14) Per capita plastic waste vs. GDP per capita (2017), measured in 2011 international USD – From Our World in Data [249] – World Bank [250] and Jambeck et al. [251]

Moreover, in our case, PMMA scraps price is highly correlated to r-MMA price, and r-MMA price is correlated to price of energy (Natural Gas for us). Same applies to the price of waste disposal that are expected to be linked. To be conservative, we decided to consider the heavy ends as a waste. However, we know that its properties are like those of a heating oil [252], so historically it has been correlated to natural gas, as well as MMA. For PMMA scraps very scarce historical data are available, or in a very narrow timespan (e.g., Zauba imports 2013 – 2017). Based on the historical data (if any), and our expert judgment, we represented our vision of the future in a correlation matrix, that mimic prices trends fluctuations at the best of our knowledge (Table 3.4). Once correlated, the prices for the 3000 Monte-Carlo cases appear as in 3.15.

	PMMA Scraps	**Natural Gas**	**Heavy ends**	**Solid Waste**	**r-MMA**
PMMA Scraps	1				
Natural Gas	0.2	1			
Heavy ends	0.05	0.5	1		
Solid Waste	0.05	0.05	0.8	1	
r-MMA	0.8	0.4	0.4	0.05	1

Table (3.4) Proposed correlation matrix for the future, based on historical data and expert judgement. Green stands for highly correlated, while red for lowly correlated.

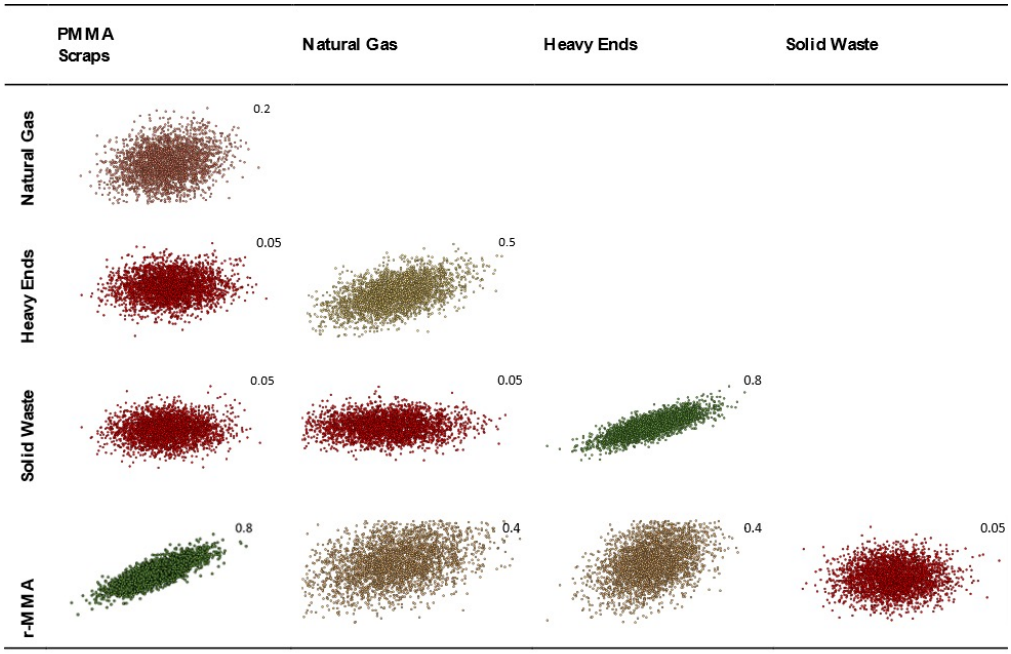

Figure (3.15) Visualization of the correlated prices of raw materials and products based on our vision of the future.

3.3.3 Profitability Analysis by Monte Carlo Simulation

Under our assumptions, the base case (Scenario 1), where the plant is built without subsidies, treating 5000 ton/y of mixed scraps to produce 3889 ton/y of r-MMA selling at virgin price is not very appealing. Over 3000 simulations, the project has a (median) payback time of 8 years (Figure 3.16) with 30% probability to make no money after 10 years of production (Figure 3.17). To understand where assumptions improvements would be most effective, we studied the impact of the individual uncertainties of feedstock, waste, product, and investment, on the median NPV. In Scenario 1, when the parameters vary in between their 10% and 90% probability of their statistical distribution, the NPV changes accordingly to the impact that the single uncertainty has on it. The r-MMA price has the largest influence on the NPV, comparable to that of the investment cost (Figure 3.18). This means that improving the assumptions on the statistical distribution of either, should improve the uncertainties on the NPV, and lower the risk of losing money. For instance, if the investment uncertainties reduce as low as the equivalent of a Class 3 AACE (extreme values of the tornado at p29 and p75), the investment has an impact on the NPV comparable to that of PMMA scraps (Figure 3.19). To reach the confidence of a AACE class 3, we need a well identified list of equipment. After class 3, the improvement is marginal (at this stage) (Figure 3.19). In the Tornado graph (Figure 3.18), the investment varies in between -20% and +120% (p10, p90), of the

selected investment (7.5 M USD), whose median is 10 M USD. Instead, the tornado capex plot (Figure 3.19) varies from the median. For instance, Class 5 in Figure 19 corresponds to a [p10, p90] of -50% and + 100% of the median, while the [p10, p90] in Figure 3.18 are the 10th and 90th percentile of that log-normal distribution having 10 M USD as median. The Tornado graph was generated to illustrate the impact of the definition of the project (Capex) on the dispersion of the NPV values.

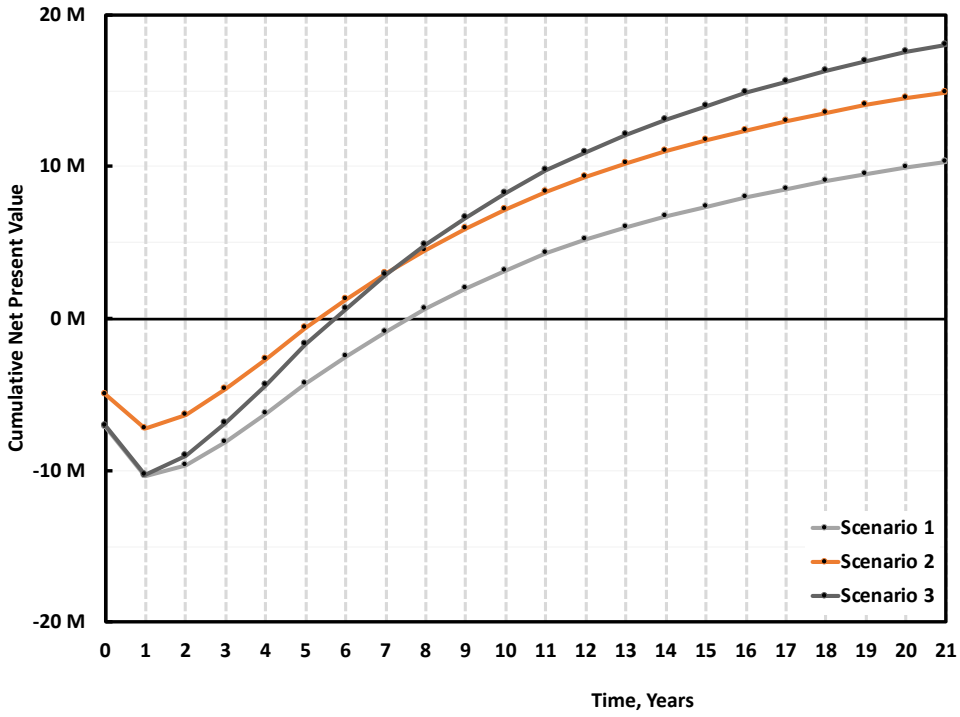

Figure (3.16) Median cumulative cash flow (NPV) over 20 years of production for 5000 ton/y plant, Scenario 1, 2, and 3 (Table 3.3). Scenario 1 is the base case, mixed scraps, Full 10 M USD Capex, and r-MMA sold at virgin price. Scenario 2 is when such a project gets 30% subsidies on the Capex, while Scenario 3 is when the r-MMA sells at 20% premium price.

When Scenario 1 gets either 30% subsidies on the Capex (Scenario 2), or sells r-MMA at 20% premium price (Scenario 3), the project becomes much more viable (Figure 3.16). Both solutions reduce the median payback period to 5/6 years; while the 20% premium solution (Scenario 3) becomes more profitable on the long-term (Figure 3.16). Both Scenarios (2 and 3) are equally attractive, but they still have a 10 – 15% probability of not earning any money after 10 years of production (i.e., probability at 0 NPV) (Figure 3.17).

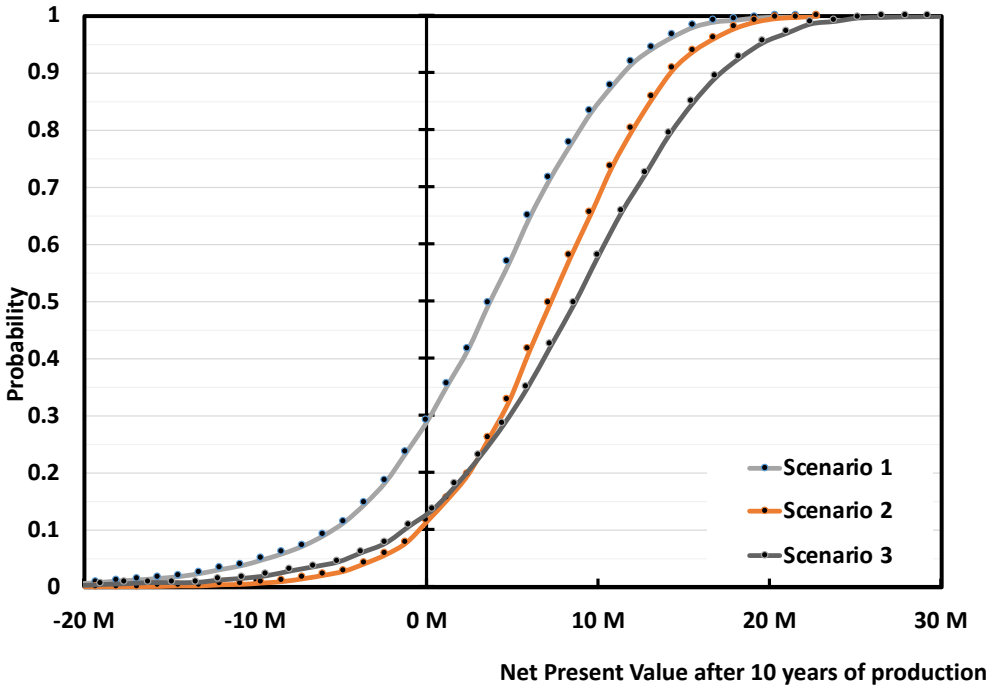

Figure (3.17) Probability vs Cumulative NPV over 10 years of production 5 000 ton/y plant. Scenario 1, 3 and 3. Scenario 1 is the base case, mixed scraps, Full 10 M USD Capex, and r-MMA sold at virgin price. Scenario 2 is when such a project gets 30% subsidies on the Capex, while Scenario 3 is when the r-MMA sells at 20% premium price.

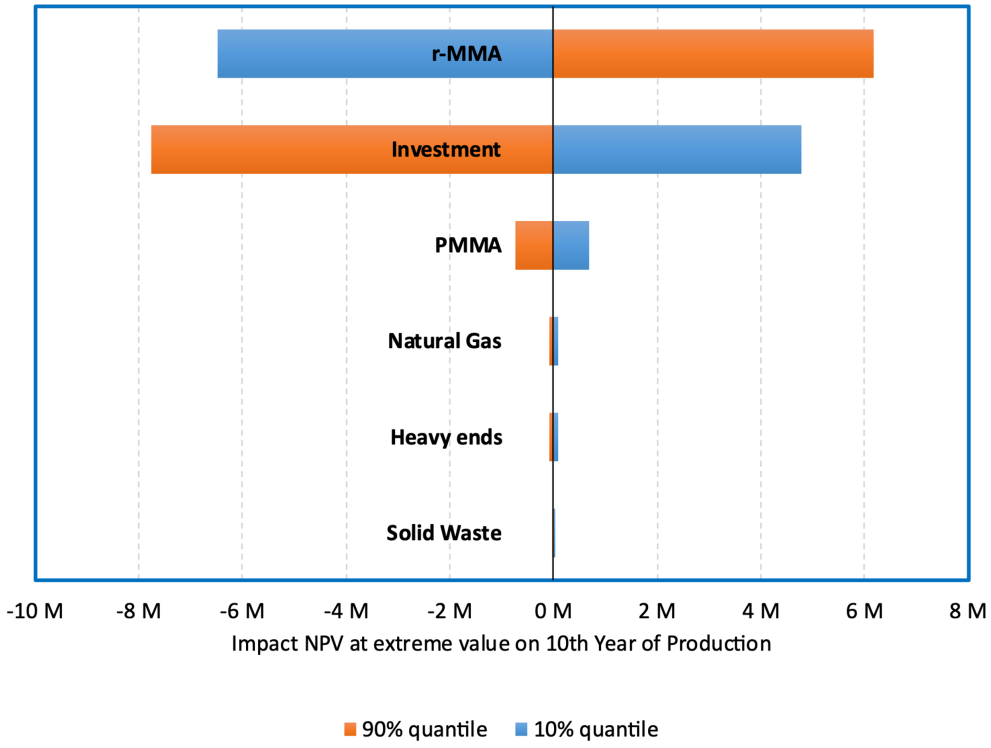

Figure (3.18) Tornado Plot for 5000 ton/y plant, **Scenario 1**. Effect of Raw-materials, waste, products, and investment variation (10% and 90% quantile), on the median NPV.

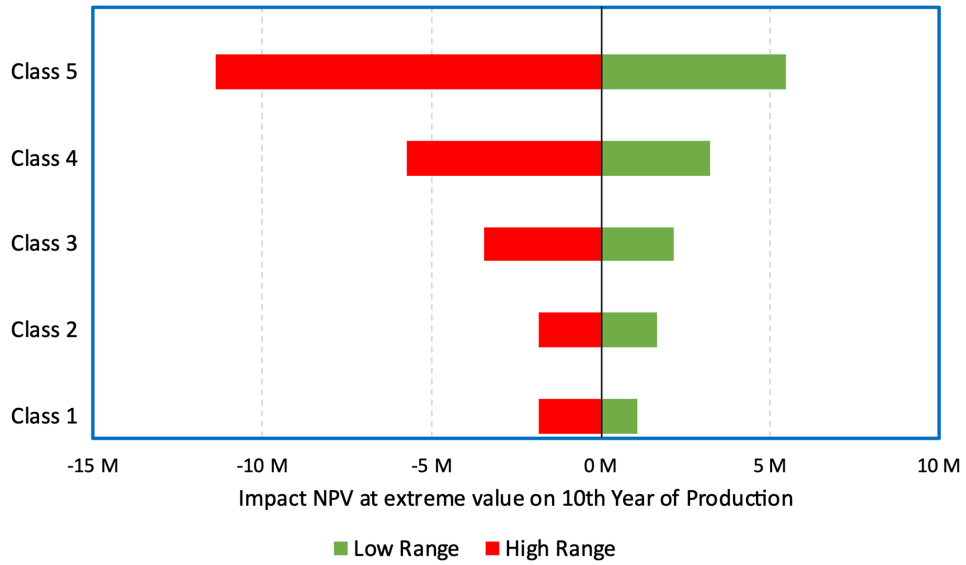

Figure (3.19) Scenario 1, impact of Capex class on the median NPV. Class 5 AACE corresponds to extremes at p4 – p96 (or -50%, +100% of the median); Class 4 AACE corresponds to extremes at p85 – p19 (or -30%, +50% of the median); Class 3 AACE corresponds to extremes at p29 – p75 (or -20%, +30% of the median); Class 2 AACE corresponds to extremes at p34 – p64 (or -15%, +15% of the median); Class 1 AACE corresponds to extremes at p40 – p64 (or -10%, +15% of the median).

In the current political climate, we cannot really give an excessive premium on the r-MMA price, but we do have a good case to present to local authorities when asking for subsidies. Scenarios 4 and 8 are representative of a second-hand plant, or a very cheap technology (Capex 1.3 M USD), that treats mixed scraps to produce low-quality r-MMA selling at 20% discount price. When operating a low capital-intensive plant, provided that the r-MMA quality is still acceptable to enter the market, we cover the plant cost after a little more than 1 year of production (Figure 3.20). The fast payback time makes this a low-risk alternative. However, with time, the higher r-MMA selling price overcomes the effect that a low depreciation has on the expenses. At the end of the plant life Scenario 2 has the same NPV as Scenario 4. Moreover, if we expect to replace the second-hand equipment/low-quality plant after 10 years, eventually Scenario 8 has a lower NPV than Scenario 2, almost comparable to that of Scenario 1. With the difference that while Scenario 1 has still room for improvement (subsidies, higher r-MMA price due to EU policies), Scenario 8 has limited growing potential. This suggests that public or private investors should look at solid technologies, which are able to provide a good quality product, rather than very cheap plants, even if the former are more expensive upfront.

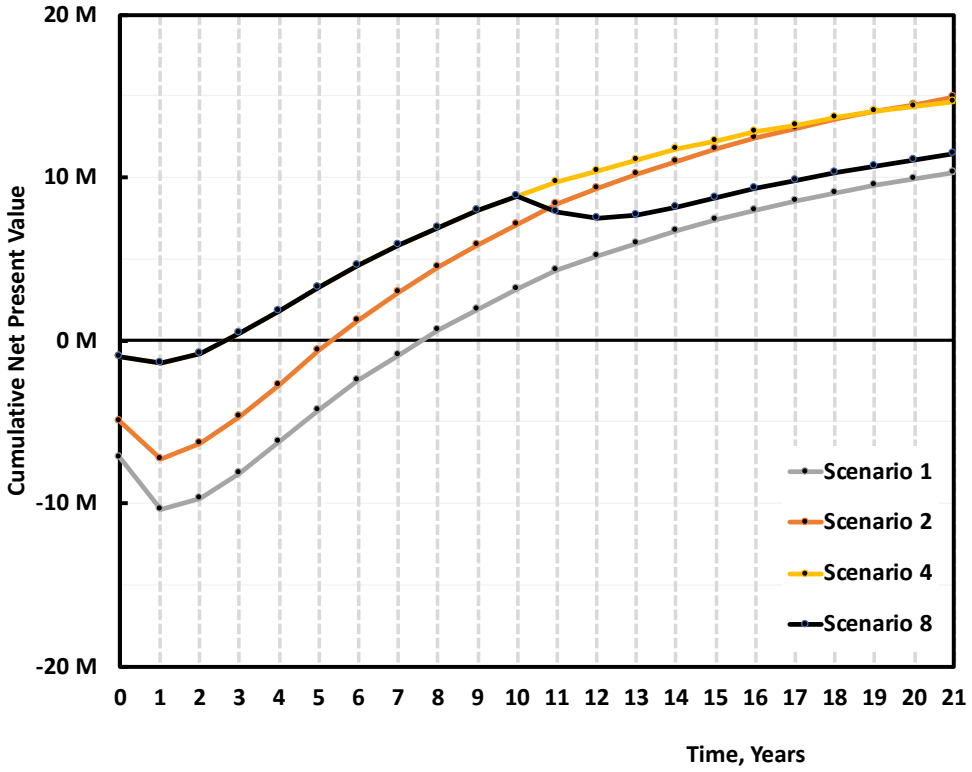

Figure (3.20) Median cumulative Cash Flow (NPV) over 20 years of production for 5000 ton/y plant, Scenario 1, 2 and 4, 8 (Table 3.3). Scenario 1 is the base case, mixed scraps, Full 10 M USD Capex, and r-MMA sold at virgin price. Scenario 2 is when such a project gets 30% subsidies on the Capex. Scenarios 4 and 8 are the case of a low-quality plant (1.3 M USD Capex), treating mixed scraps and selling r-MMA at 20% discount price. In Scenario 4 we operate the plant for the full 21 years, while in Scenario 8 we must replace it after 10 years.

When comparing Cast and Mixed scraps, Cast scraps makes for an overall better case. Cast scraps are more expensive, but they can be used in a cheaper plant, and have less carbon losses along the process, making for a better r-MMA global yield. We compared the base case (Scenario 1), with the case of a 5000 ton/y cast scrap 7 M USD plant, producing 4512 ton/y of r-MMA selling at virgin price (Scenario 5), or 20% premium price (Scenario 6) (Figure 3.21). At full investment cost, selling at virgin price, the mixed scrap plant (Scenario 1), falls short compared to its Cast equivalent (Scenario 5). Over the plant life, the cumulative NPV plot slope is the same in these two cases (Scenario 1 and 5). Namely, the better r-MMA cast global yield compensates for the higher feedstock price, with respect to the Mixed scrap case. Similarly, Scenario 5 and Scenario 2, i.e., the case where we get 30% subsidies on the mixed scrap plant, have NPVs which basically overlap. This means that the investment plays

here a fundamental role. At parity of investment and selling price, the economic viability is not influenced by the kind of scraps. However, mixed scraps consist in post-production, but end-of life PMMA as well. Should PMMA producers be willing to pay a premium for r-MMA from end-of-life products only (the only ones that have made a full cycle in the economy), for instance to better advertise their product, the mixed plant would have a more positive case than the cast (Scenario 3 vs 5), even at a higher Capex.

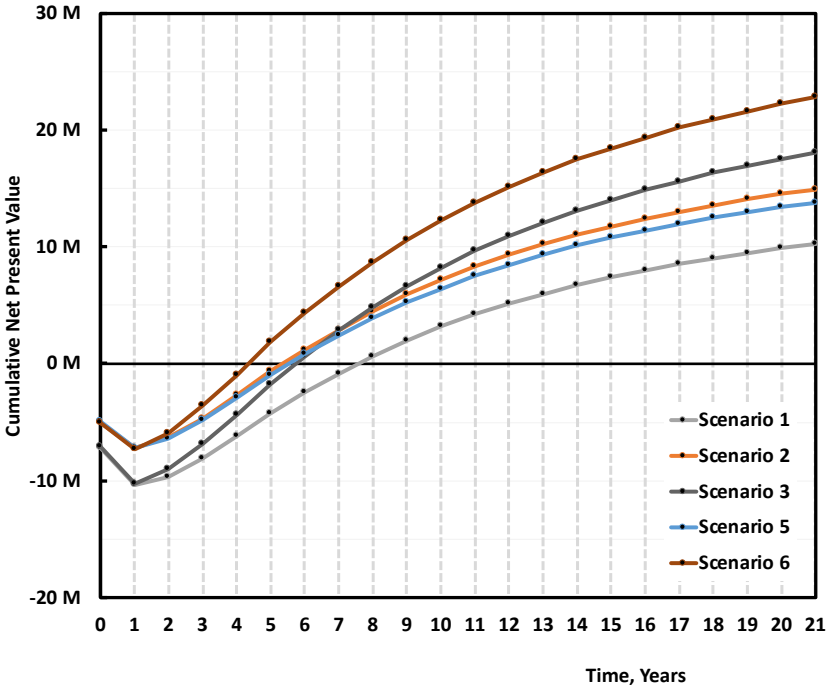

Figure (3.21) Median cumulative NPV over 20 years of production for 5000 ton/y plant, Scenario 1, 2, 3 and 5, 6 (Table 3.3). Scenario 1 is the base case, mixed scraps, Full 10 M USD Capex, and r-MMA sold at virgin price. Scenario 2 is when such a project gets 30% subsidies on the Capex, and Scenario 3 when r-MMA is sold at 20% premium price. Scenarios 5 and 6 are the case of a Cast scrap plant, that sells at either virgin (Scenario 5), or 20% price (Scenario 6).

The overall superiority of the cast over the mixed scenarios appears also on the NPV probability curve at the 10th year of production (Figure 3.22). Scenarios 5 and 6 have a probability of making zero money of 15% and 5% respectively, while Scenario 1 lost money around 30% of the times. Again, Scenarios 2 and 3 are equivalent to Scenario 5 in terms of cumulative NPV equal to zero at year 12 (10th year of production).

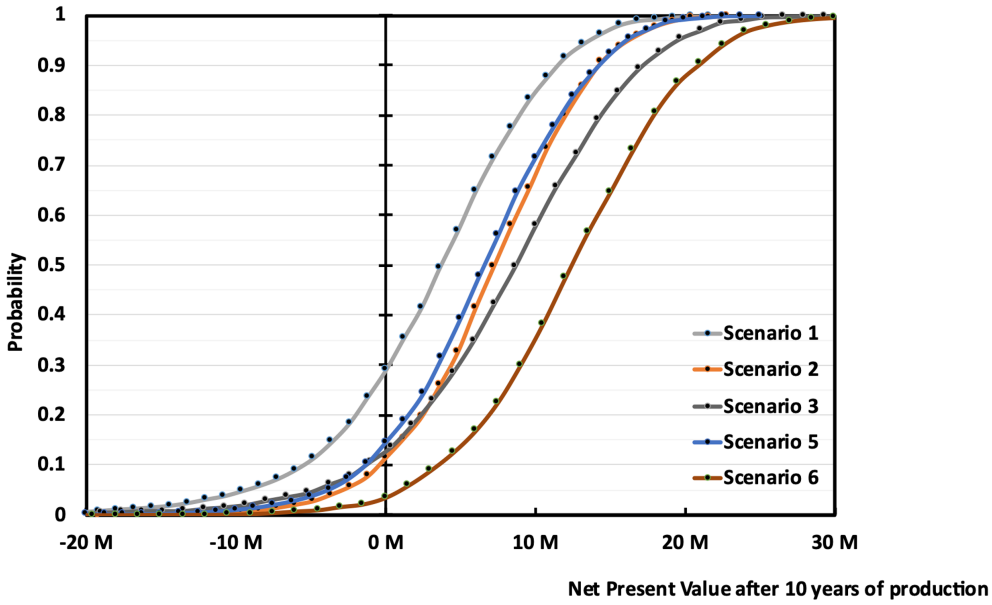

Figure (3.22) Probability vs Cumulative NPV over 10 years of production 5000 ton/y plant, Scenario 1, 2, 3 and 5, 6 (Table 3.3). Scenario 1 is the base case, mixed scraps, Full 10 M USD Capex, and r-MMA sold at virgin price. Scenario 2 is when such a project gets 30% subsidies on the Capex, and Scenario 3 when r-MMA is sold at 20% premium price. Scenarios 5 and 6 are the case of a Cast scrap plant, that sells at either virgin (Scenario 5), or 20% price (Scenario 6).

Nowadays, we see more and more techno-economic assessment on plastic recycling setting the feedstock price at zero [253], or even at a negative value [254]. PMMA is a relatively expensive plastic, compared to higher volume materials like PP, PVC, or PE. Therefore, as demonstrated by the few available historical import data, PMMA scraps have a market, nonetheless. However, the socio-political climate around the plastic recycling world is mercurial. Therefore, we wanted to investigate what would happen if our scraps were of such a low quality (e.g., end-of-life not completely sorted) to be available free of charge.
In this case, we can expect to either pay an extra for the pre-treatment (e.g., additional sorting, crushing, washing, and drying), lose in global yield to reach the target quality, or accept a lower quality monomer but with the same global r-MMA yield. We decided for this last option, and assessed the economics of a mixed scrap plant, treating unsorted scraps at 0 cost, selling low quality (e.g., 97 - 98 wt.% pure or less) r-MMA at 20% discount. We assumed such a plant to require the same capital expenditure of our base case (Scenario 1 at 10 M USD), and we evaluated it with (Scenario 9) and without (Scenario 7) subsidies (Figure 3.23). The raw materials contribution to the total expenses is now (Scenarios 7 and 9) much lower. In the global model, the other utilities are expressed in terms of a percentage

of raw materials cost. In the case of the scrap at 0 price, with the mass yield of the mixed feedstock, we expressed the utility cost as a fixed value, equal to that of the base case.

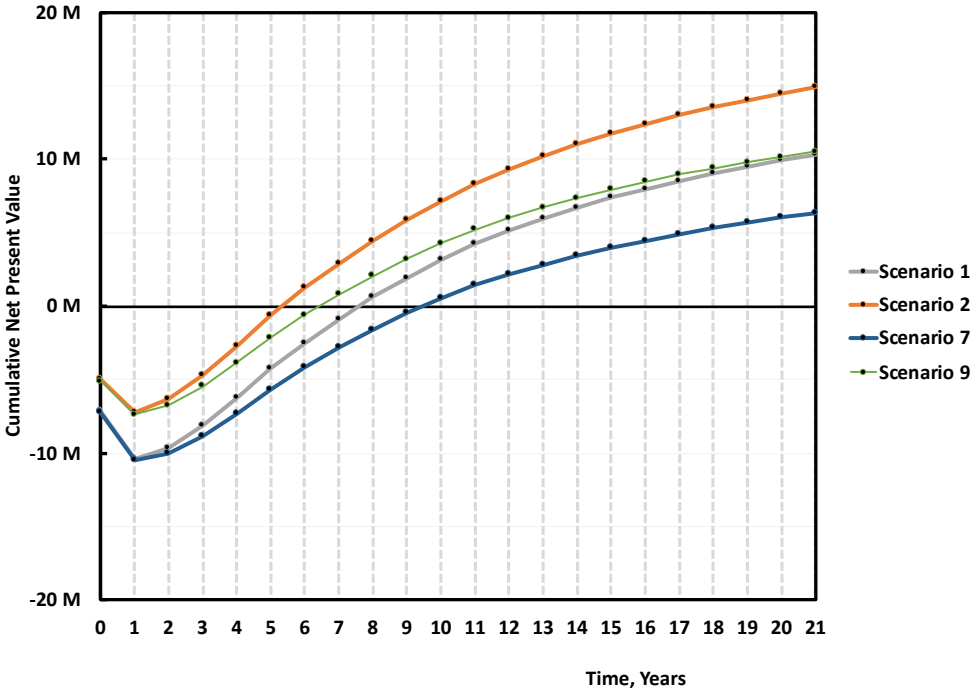

Figure (3.23) Median cumulative NPV over 20 years of production for 5000 ton/y plant, Scenario 1, 2, and 7, 9 (Table 3.3). Scenario 1 is the base case, mixed scraps, Full 10 M USD Capex, and r-MMA sold at virgin price. Scenario 2 is when such a project gets 30% subsidies on the Capex. Scenarios 7 and 9 are the case of a mixed scrap plant, with (Scenario 9) or without (Scenario 7) 30% subsidies, processing 0 cost low, quality PMMA, and selling r-MMA at 20% discount price.

Once more, the r-MMA quality differentiates between positive and negative cases. At first glance, scraps at zero cost may seem more attractive, but it is not correct. Scenario 7, the equivalent of Scenario 1, has a 40% probability of nullifying the NPV at the tenth year of production, as opposed to 30% in Scenario 1 (Figure 3.24). Besides, Scenario 7 cumulative NPV turns positive only after 9/10 years, 2 years later than Scenario 1 (Figure 3.23). The subsidized Scenarios 2 and 9, follow the same trend, with Scenario 2 being more profitable (Figures 3.23 and 3.24). Even if, for environmental reasons, public bodies granted funds to the 0 scrap price plant only, this case (Scenario 9) gains the same profits (in median) than Scenario 1 at the end of the plant life, with the risk that a zero cost feedstock may see an increase of its price when alternatives develop (such as fuel users). To target high-quality product is just overall more viable.

Ideally, the best process technology can process all the scraps grade, yielding to the top quality r-MMA product, regardless the nature of the scrap itself. In the MMAtwo experience we found out how, on some extent, all the technologies tend to be feedstock sensitive (some more than others). These results suggest that any new player in the PMMA recycling field must demonstrate the maturity of their process, to produce high-quality r-MMA. Getting low quality scraps as cheap as possible, is not only difficult, but can be negative for the profitability of the plant. The only case where this could make sense, is if these scraps come with an important negative price.

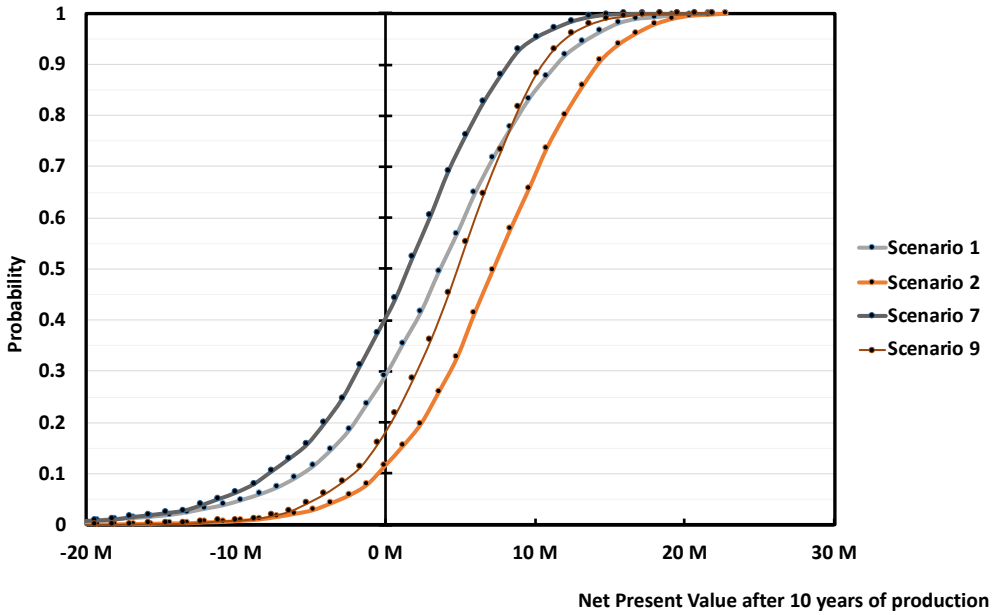

Figure (3.24) Probability vs Cumulative NPV over 10 years of production 5 000 ton/y plant, Scenario 1, 2, and 7, 9 (Table 3.3). Scenario 1 is the base case, mixed scraps, Full 10 M USD Capex, and r-MMA sold at virgin price. Scenario 2 is when such a project gets 30% subsidies on the Capex. Scenarios 7 and 9 are the case of a mixed scrap plant, with (Scenario 9) or without (Scenario 7) 30% subsidies, processing 0 cost, low quality PMMA, and selling r-MMA at 20% discount price.

3.3.4 Cost of Production

When the input variables are probabilistic functions, the cost of production is a probabilistic function as well. For all the cases, the cost of production before depreciation distribution fits well a normal, or log-normal distribution. For instance (Figure 3.25), Scenario 1 has a cost of production before depreciation between 784 and 1176 USD/ton for the interval of probability p5 – p95 (green interval – Figure 3.25). Labor cost, the "other fixed", and "other variable" costs are the most important contributors to the cost of production (Figure 3.26).

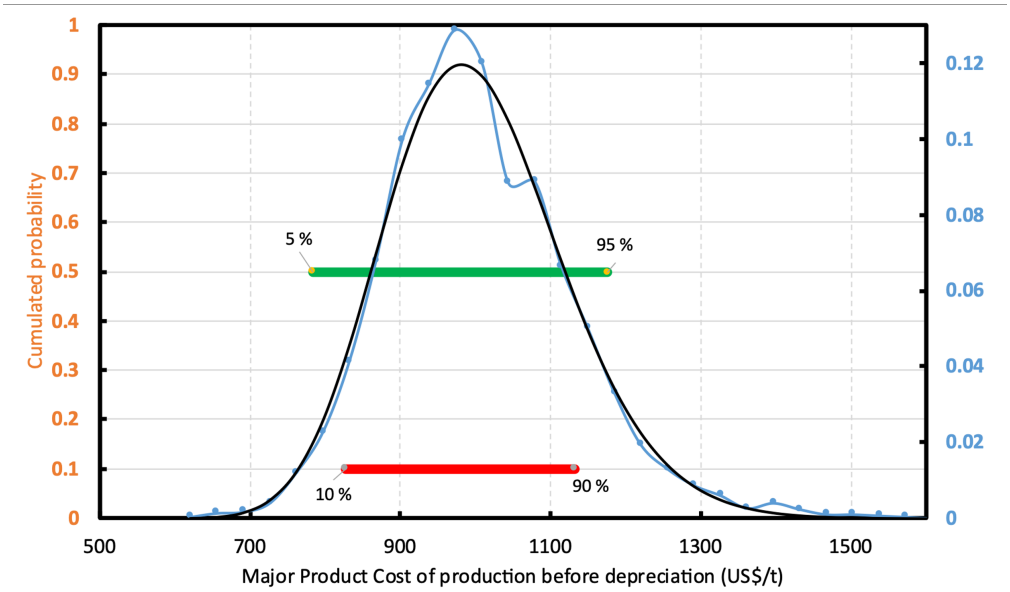

Figure (3.25) r-MMA cost of production before taxes and depreciation. Distribution for Scenario 1. The Blue line is the simulated distribution that fits a log-normal distribution (black line).

The "other fixed" costs comprehend (Section 2.2) maintenance and repairs, operating supplies, property taxes, financing interests, and insurance. The "other variable" costs are instead (Section 3.2.3) expressed as a % of the sales, includes R&D and Royalties, and distribution and selling.

We already assumed to run a lean plant, with only two operators per shift, which is the minimum for safety reasons. The only way to improve that, would be erecting the plant as a brownfield. In this way, we could run the plant with only 1 operator per shift, while there would still be somebody else on the industrial site.

The other fixed costs (as well as the depreciation) are linked to the investment. The only way to reduce that is to keep the plant layout as simple as possible. An idea could be to reduce number of spare equipment, or minimize the side streams that have to be treated on-site.

Classically, savings are made on the other variable cost, but not much can be done in our case. With only a total of 8% of the sales, there is a small room for improvement. Since the plant is in the middle of Europe, close to PMMA producers and scrap collectors, we already imagined keeping the distribution and selling costs quite low. Moreover, because there are numerous running technologies, we also assumed a low R&D and royalty contribution. Most of the processes have already demonstrated to be mature enough to produce sellable r-MMA. R&D should focus on tuning the right technology with the right feedstock available, or target product, rather than finding novel routes.

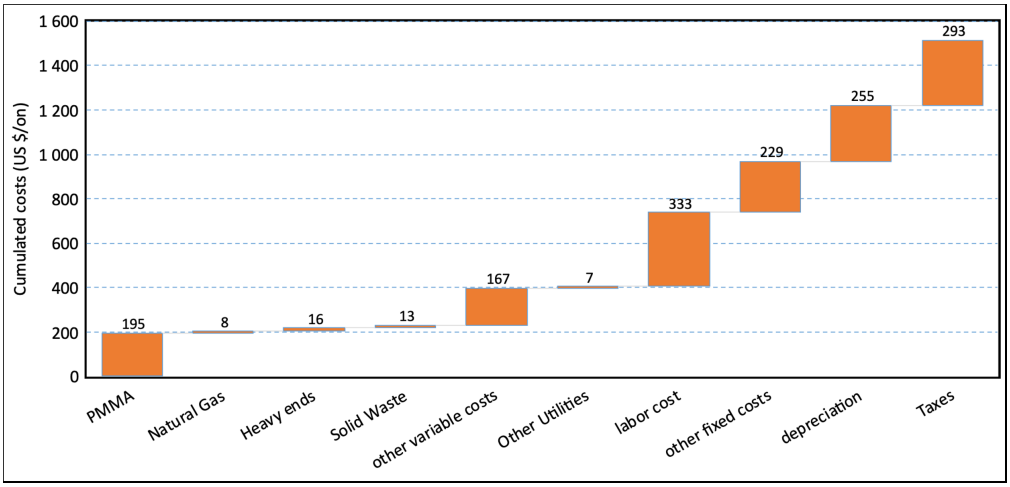

Figure (3.26) Median production cost cascade for Scenario 1.

3.4 Discussion and Conclusions

To highlight challenges and opportunities of PMMA recycling we performed a Monte Carlo simulation with a total of 3000 iterations. The risk analysis debunks some preconceptions, and it is a support for any future work in the field.
Based on the results of our simulation, we ranked the Scenarios according to different selected outcomes: (i) Pay-back time; (ii) NPV after 10 y of operation; (iii) probability of losing money after 10 y of operation (Table 3.5).

The 5000 ton/y, 10 USD M plant of Mixed PMMA scraps, producing 3889 ton/y of r-MMA selling at virgin price, is the most representative case, and acts as baseline for comparison. We demonstrated how:

- A highly energy integrated process minimizes waste streams, utility consumptions, and environmental burden, as well as contributing to make a positive economic case;
- A median Capex of 10 M USD (or lower) is what companies should aim at for a 5000 ton/y PMMA depolymerization plant;
- NPV is most sensitive to the uncertainties on r-MMA price and investment. Expert judgment, experience on similar plants, subsidies, reduce the risk on the investment. Securing a deal with the r-MMA final buyers narrows down the r-MMA statistical distributions and improves the reliability of the business plan;
- New players should not compromise on product quality, even if this means higher capital plants, or "cleaner" and more expensive scraps. Whenever capital cost (Scenarios 4 and

Table (3.5) Ranking of Scenarios according to different criteria/expected outcomes.

Criteria	Ranking (Scenarios)	Conclusions
Pay-back time (from short to long)	1. **Scenarios 8/4** 2. Scenario 6 3. Scenarios 2/3/5 4. Scenario 9 5. Scenario 1	Cheap technology/second-hand equipment plant pay back in the shortest time.
NPV after 10 y of operation (highest first)	1. **Scenarios 3** 2. Scenario 2/5 3. Scenarios 8 4. Scenario 9 5. Scenario 1	After 10 y of operation, high-quality r-MMA, coupled with expensive technology pays off more than cheap plants, or low-quality scraps at zero price. If the market can accept both high and low purity product, companies should target high-quality r-MMA.
Probability of losing money after 10 y of operation (from low to high)	1. **Scenario 6** 2. Scenario 2/3/5 3. Scenario 9 4. Scenario 1 5. Scenario 7	Despite feedstock available for free, Scenario 7 has more probability of losses than the base case Scenario 1. The better the quality of the scraps/product, the lower the probability to lose money becomes.

8) and scrap composition (Scenarios 7 and 9) diminish the product quality, the overall economics worsens. Cheap plants allow for a faster pay-back time but are less profitable overall compared to the base case. The lower profits in the zero price waste scraps plant outweigh the reduced cost of operation.

- If we are in a market with a sufficiently high demand for low quality product (e.g., India, or Brazil), there is no need to over-purify the regenerated monomer, the plant is already economic as it is. However, the evolving EU legislation might hurdle the entrance of low quality r-MMA in the European market;
- Currently, Cast scraps plants are more viable than Mixed scrap plants, under the hypothesis that the first are less capital-intensive. However, when a plant is designed and built to treat both, it can switch with no effect on the cumulative NPV. The better global yield of Cast scraps counterbalances the lower feedstock price of Mixed scraps;
- The r-MMA cost of production follows a log-normal distribution, and labor cost, investment, and "other variable cost" are the main contributors.

Therefore, regardless the process technology, we outlined what are the minimum requirements that a plant should check in terms of mass balance, capital investment, feedstock and product prices, feedstock quality, and economic figures, in order to be competitive.

A first improvement for the model could be to investigate further waste streams. For instance, PMMA/fiber glass composites that might be employed in boats and wind blades, PMMA/ATH (aluminum trihydroxide), or solid surface materials, which are sold as a marble substitute. Future research is needed to understand how to best valorize each part of the composite, while still having a positive case.

An equally interesting scenario to investigate, would be when local governments grant subsidies on the product made, rather than the plant. This would be a variation of the 20% premium scenario we analyzed. Because of the volatile nature of the plastic recycling world, it would be wise for governmental agencies to subsidize only the winning horse, i.e., only when a company has already demonstrated production. At the beginning, the company takes all the risk, because they put money up-front. However, if the plant works, and it demonstrates production, subsidies on the product should guarantee a higher return than subsidies on the Capex.

Furthermore, r-MMA is currently sold in Europe under Reach registration exemption for recycled materials. In the framework of this study, it means that the regenerated monomer can directly enter the market. This might change in the future. As pointed out, r-MMA quality is feedstock sensitive and process sensitive, to some extent. Standards to select properly the PMMA scraps are then needed, in order to assign them the best value and address them to the different depolymerization technologies

CHAPTER 4 ARTICLE 2 – TOTAL CAPITAL INVESTMENT OF PLASTIC RECYCLING PLANTS CORRELATES WITH ENERGY LOSSES AND CAPACITY

In Chapter 3 we established that the most representative potential PMMA recycling plant has a capital investment of 10 M USD, processes mixed PMMA waste scraps, and sells r-MMA at a price comparable to virgin. In this scenario, capital cost is the factor affecting the most the plant viability, together with r-MMA cost. Methyl Methacrylate market depends factors outside of one's control. However, we can reduce the plant capital cost uncertainty. In this Chapter we demonstrate how conventional early-stage cost estimation models are inapt for chemical recycling plants, based on a database of 167 existing or planned plants. From the extrapolated plants' heat and mass balances, we propose novel reliable and accurate estimation models.

Jacopo De Tommaso, Federico Galli, Robert Weber, Jean-Luc Dubois, Gregory S. Patience

Published in: ChemSusChem, 17(5), e202301172, 12 January, 2024

Abstract

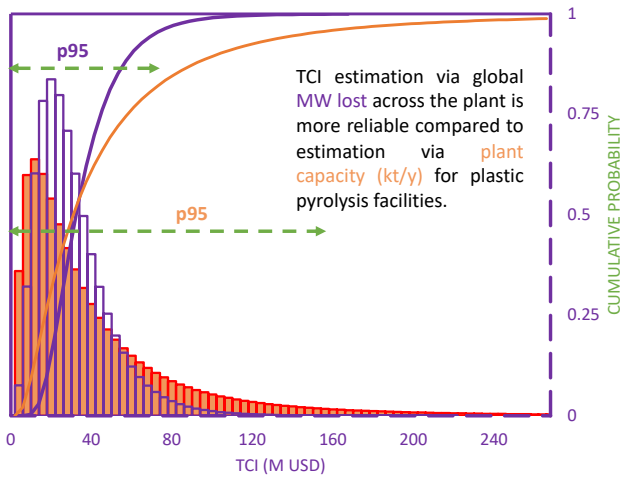

Plastic pollution is a generational problem, and stakeholders are turning to chemical recycling as a potential solution. However, decision-makers necessitate quick and reliable capital investment estimations to evaluate innovative technologies, especially in the early project stage, when limited historical data are available. To address this need, we built a database of 160+ chemical recycling plants, querying for nominal capacity, year and place of construction, total

capital investment (TCI), number of long-term jobs and opportunity of subsidies. Then, we compared conventional association of the advancement of cost engineering AACE class 5 estimation methods, with literature estimates, and commercial capital expenditure confidence intervals for pyrolysis, gasification, solvolysis, and selective dissolution. We demonstrate the unreliability of classic methods, and we propose ballpark correlations based on the plant capacity, or the energy loss. Chemical recycling plants suffer from poor economy of scale (with current technologies), and capacity is not always the best indicator for TCI estimation. Pyrolysis and gasification are energy-driven technologies, and their TCI correlates very well (R^2=0.91-0.92) with the total energy losses. Solvolysis and selective dissolution, instead, are at an earlier development stage, so cost engineers or researchers will have to accept less certain TCI vs capacity (R^2 = 0.60).
Keywords: Plastic recycling, Total Capital Investment, Pyrolysis, Gasification, Cost estimation

4.1 Introduction

Plastics are valuable and versatile materials, with more than 450 millions of tons produced worldwide in 2019, and applications in packaging, construction, textiles, transportations and electronics. [255] The European circular economy action plan, [256] Canada's zero plastic waste strategy, [257] and finally the UN 2022 resolution to a "internationally legally binding instrument", [258] demonstrates national and international commitments to curb plastic pollution and improve its end-of-life.

However, the OECD (Organization for Economic Co-operation and Development) reports that in 2019 only 9 wt% of the world plastic was collected for recycling, with the rest landfilled (49 wt%), littered or mismanaged (22 wt%), or incinerated (19 wt%).[1] In the same series of reports, the OECD states that the amount of waste generated is still "very much linked to economic growth". [248] When the GDP (Gross domestic product) of a country increases, people have higher salaries, access to better food, and they spend more. This turns into a higher per capita waste produced, especially plastic waste. [249]

GDP is not the sole (or the best) predictor for plastic waste. Additional soft and hard indicators such as level of education, [259] density of population, [260] land use, level of infrastructures and even nightlight population concentration in a certain area, factor in when predicting the plastic waste management and production. [261] Nevertheless, more developed economies (i. e., higher GDP per capita), have access to more advanced and effective waste treatment processes. [262]

When not littered, countries manage plastic waste in 4 ways: landfilling, incineration, me-

chanical recycling, and chemical recycling. Landfilling is still the preferred handling method for waste in the majority of the world, excluding OECD Asian and EU members. [255] However, it breaks the carbon cycle, poses threats for areas and wildlife, and it is ultimately unsustainable. [263] Incineration is the preferred method in large urban areas where land is lacking and landfilling is publicly opposed, because it reduces the volume of solid waste up to 90 wt%.. [264] Incineration (for energy recovery) has been consistently replacing landfilling in the last 10 years in EU, [11] but in July 2022 the European Commission included waste-to-energy plants in the list of activities "considered to do significant harm to the circular economy, including waste prevention and recycling". [12] Therefore they are now excluded from subsidies and financial support. [265] Mechanical recycling is the preferred recycling choice for most plastic (all thermoplastic in theory [266]), and it is the most convenient recycling method in terms of time, economic viability, [267] and environmental footprint. [268] However, mechanical recycling affects mechanical and optical properties of the material over the cycles, it is susceptible to additives and inhibitors, as well as polymer blends, [268] and it is for this reason prone to downcycling with time (e. g. the Sprite's case [269]). On the other hand, chemical recycling (reversion to monomer) is more versatile because it is not bound to a limited number of cycles, and degradation of plastic properties, [270] therefore being the ideal solution for "difficult to (mechanically) recycle" plastic waste. Pyrolysis, gasification, solvolysis break down plastic on a molecular level to produce (depending on the technology-feedstock coupling) monomers, syngas, a broad range of liquids (from waxes to diesel substitutes), or char.

Selective dissolution bridges chemical and mechanical recycling, because it requires the use of solvents, but does not break the chemical bonds of the material (which would classify it as a mechanical recycling solution).

A comprehensive review of the chemistry and engineering of pyrolysis, gasification, solvolysis and selective dissolution is outside the scope of this work, and we note recent detailed reviews. [270–272]

Despite the advantages and the government commitments, chemical recycling contributes still marginally (e. g. < 1 wt.% in EU) [273] to the total recycled volumes. There are several reasons including but not limited to, from a macro to micro scale:

- conflict between government policies and directives; [273–275]
- fragmented or nonexistent literature on regulatory issues on the recycling chain (e. g. US does not have a federal mandate to ban brominated flame retardants that are banned in EU);[[273, 276] and

- scattered (and weak) quantitative analysis of the most common technologies (what can be treated, how much investment is required, where plants be located).

These factors reinforce a limited interest from the chemical industry to take risks and be the first to invest. Here we analyze chemical recycling technologies and provide early-stage capital investment estimation correlations for pyrolysis, gasification, solvolysis, and selective dissolution. Our goal is to reply to the research question: "How much does it cost to build a chemical recycling plant?", and in doing so offer policy makers, public bodies, private investors, and researchers, a tool to assess with high(er) accuracy total capital investments (TCI) of new recycling plants, based on individual technologies, type of feedstocks, products and utilities. The estimated CAPEX is essential to feed a first economic evaluation of the cost of production.
First, we benchmarked representative early-stage capital cost estimation correlations from selected academic publications on chemical recycling. Then, we compared the results of the benchmarks with a database of 169 chemical recycling plants (built or planned) to draw probabilistic conclusions. From this analysis, we propose new plug-in correlations to estimate the total capital investment of a new plant for a given technology starting from plant capacity, or total energy losses, demonstrating how the latter is statistically more significant for selected technologies. Finally, we show how researchers and cost engineers can use the database and the correlations drawn from it.

4.2 Methods

To address the research question, we consider:

1. What are the essential elements of total capital investment?
2. How does we attribute a cost to each of these elements and their uncertainty
3. How to validate established estimation methods versus historical data?

In this section, we provide the tools to navigate through these questions: what is the TCI, which families of estimation methods exist, and which of those are more pertinent in the framework of chemical recycling of plastic.

Then, we explain how the database for this work was constructed, how how the models compare with the published data on plant cost, and finally how to leverage on the database benchmark to develop novel regression models and draw conclusions on chemical recycling at large.

4.2.1 Definition of Capital Cost

The top 10 chemical companies by sales represent around 10% of the total revenue of the chemical industry (360 billion USD in 2019 out of 3.6 trillion USD). [277] All of these companies made claims or commitment to sustainability. However, only three (Ineos, Exxon-Mobil, with Mitsubishi ranked 11th) own chemical recycling plants, while the others outsourced the risk and are either external investors or final users. Capital cost in the chemical industry in general, [84] and in particular in chemical recycling, [181, 253, 255, 278–280] is among the variables with highest impact on net present value (NPV). Chemical recycling is capital-intensive (especially compared to mechanical recycling), and economic viability is often the reason why projects fail, [281, 282] or disappear altogether. [283] Although the technologies date back to 1980 (Figure 4.1), commercial interest has only picked up in the last 10–20 years.

Relying on start-up or early stage companies to develop technologies and prove it, it is beneficial on the short term for the individual investor but it is shortsighted for the ecosystem. Start-ups rely mostly on external funds to survive, pay high insurance fees due to the frequency of accidents in the field, [284] and they have higher failure rates (for multiple reasons not necessarily related to the technology itself) so that it is hard even for governments to rationalize the investment.

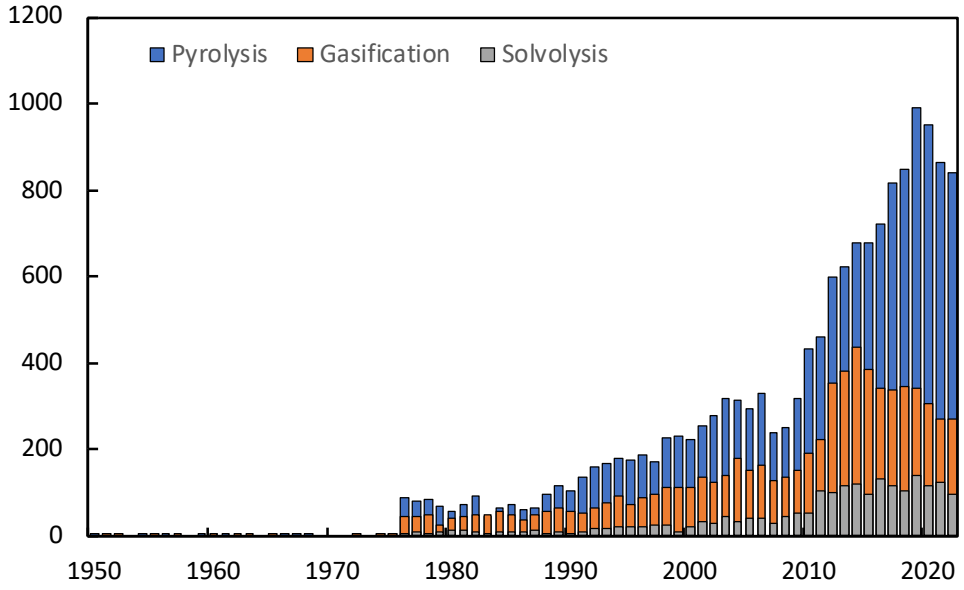

Figure (4.1) Granted patents for pyrolysis, gasification and solvolysis of plastic, from the Lens database [285]

The Total Capital investment of a plant (TCI) is comprised of:[28]

$$\text{TCI} = \text{Startup} + \text{WC} + \text{DCC} + \text{ICC} \tag{4.1}$$

That is:

- Start-Up costs such as raw material and products inventory, spare parts inventory, cash in hands and so on.
- Working Capital (WC), that is the money to meet short-term obligations (e.g., temporary jobs for construction); and
- Direct Capital Cost (DCC) (Inside and Outside battery limit ISBL+ OSBL), including everything that is physically built onsite;
- Indirect Capital Cost (ICC) (Engineering, Procurement and Construction);

In layman's terms, the Total Capital Investment (TCI) of a plant is what companies have to spend before any operation commences. This is what the management must justify to investors or shareholders. On average, large plant projects in the process industry (oil, gas, chemicals, metal, etc.) overrun their budget estimate by 20%, with a 10% probability of 70% overrun. [85] The spread between plan and reality increases when the capital cost estimation maturity level is below 30%. [85] A scope definition maturity of 30% is equivalent to something as detailed as a preliminary engineering design for budget authorization. The AACE (Association for the Advancement of Cost Engineering) divides capital cost estimation into 5 categories, corresponding to different maturity levels of a project, and the expected accuracy of different estimation methods (Table 4.1). [286] While other classifications are common in the process industry as well, like the TRL concept, [287] or the UK association of cost engineers ACostE, we will refer only to the AACE to avoid confusion.

Once a project passes the AACE class 3 equivalent milestone, any modification on the design, such as reactor type or purification strategies, has a huge impact on the capital cost. [288,289]

When a project is still at class 4 or 5 level, it is still possible to investigate a lot of possible alternative processes, catalysts, feedstocks, purifications... and it is wise to spend money in research to pick the best alternative. But there might be a lot of possible options. So, at this time, a ranking of all the alternatives should be done, in order to prioritize the R&D activities.

When chemical companies, local bodies, governments, or supranational unions want to finance new programs, or erect new plants, they will look at the highest return on investment,

the shortest payback period, and overall, the lowest probability to lose money over time. This translates into the necessity to provide the most reliable estimate at the earliest stage possible, i.e., an AACE Class 5 or 4 estimate. AACE Class 5 or 4 methods encompass: [84]

- Power law or exponential estimating;
- Factorial estimating;
- Process steps or parametric estimating; and
- Thermodynamic estimating.

These approximate methods rely on one or more of the following:

- Historical data of similar plants (e.g., Power law);
- A preliminary block or process flow diagram (e.g., process step);
- Some preliminary process data such as maximum pressure, temperature, yield, etc. (e.g., process step methods);
- Preliminary list of process equipment and their cost information – either as a vendor quote, or from similar plants built in the past (e.g., factorial methods); and
- Expert judgment (process step methods).

Still considered AACE class 5, but under a different approach, are the thermodynamic methods for example adopted by Jean-Paul Lange in 2001, [213] that builds on the idea that the TCI is correlated with the energy lost or exchanged in a plant. For a more detailed review of each family of methods we suggest Tsagkari, [84] Chauvel, [290] or Gerrard. [291] Here we briefly explain the rationale of each group, and its pros and cons in the framework of capital estimation for chemical recycling plants.

4.2.2 Capital cost estimation: Power law methods

Power law methods adjust the cost (TCI in our case) of a new plant (or piece of equipment) based on an empirical statistical similarity with a similar kind of plant but processing different capacities, as:

$$\frac{\mathrm{TCI}_1}{\mathrm{TCI}_2} = \left(\frac{\mathrm{S}_1}{\mathrm{S}_2}\right)^f \cdot \mathrm{F_l F_t} \tag{2}$$

Where TCI are the total capital investments of the two plants, S are the sizes or scale of the two plants, f is the scaling factor, and F_t and F_l are actualization factors for time and location respectively. Traditionally, in the chemical industry f varies on average to 0.6 (0.7 for a piece of equipment), so this equation is referred to as the "six-tenths rule".

Time actualization factors adjust the cost based on: [292]

- inflation and deflation over time;
- state of technological and industrial progress; and
- relative level of wages and work conditions.

Table (4.1) Engineering Milestone Classes and Method Accuracy

Class	**Project Maturity Level**	**Engineering Milestone Reached**	**Method Accuracy**	**Method Cost as % of TCI [291]**
Class 5	0 to 2%	Block Flow Diagram	L: -20 to 50% H: 30 to 100%	0 to 0.1
Class 4	1 to 15%	Process Flow Diagram	L: -15 to -30% H: 20 to 50%	0.1 to 0.2
Class 3	10 to 40%	Piping and Instrumentation Diagram Issued for Design	L: -10 to -20% H: 20 to 50%	0.4 to 0.8
Class 2	30 to 75%	Engineering Deliverables Issued for Construction	L: -15 to -5% H: 5 to 20%	1 to 3
Class 1	65 to 100%	All Deliverables Complete	L: -3 to -10% H: 4 to 15%	4 to 10

There are multiple time actualization factors: some are regional, like the R. Boulitrop's index (Techniques de l'ingenieur) in France, the WEBCI index in the Netherlands, [293] or the NAPPCI, the PEP published by IHS; others are specific for a branch of the process industry (e.g. Oil and petrochemical [294]). In general, the chemical industry relies mostly on the M&S (Marshall and Swift), and the CEPCI (Chemical Engineering plant cost index) published by the Chemical Engineering online journal. [295] These factors are compounded factor with mechanical, electrical, civil, site, overhead, and labor contributions. For instance, the CEPCI comes from the compounding of :

- equipment;
- construction labor;
- buildings; and
- engineering and supervision indexes.

It is good practice to choose an index aligned with the purpose and location of the cost study. [296] Because more US-centered indexes like CEPCI or NAPCCI have up to a 20% spread compared to EU-based factors (e.g., WEBCI). Although time adjustment factors differ among different contractors and service operators in the world, globalization is shrinking this difference.

Location adjustment factors quantify how much it would cost to build a plant with similar (but not necessarily identical) function and envelope, in a different region/country, at a given time and a given currency exchange rate. [291] They are only pertinent in AACE class 4 and 5 estimations, when quotes for labor, material and equipment are nonexistent or cumbersome to obtain. [297] Within a country, a rule of thumb is to add 10% to the cost for every 1000 miles to the nearest industrial center. [298] When comparing different countries, location factors account for currency exchange rates, materials and labor, productivity, contingency costs, feedstocks and consumable prices, and ambient conditions. [296] The most reliable source for location factors to/from US is Richardson International Construction Factors, that is now inside a paywall at `http://www.costdataonline.com` (after being for several years part of the Aspen capital cost estimator suite). In this work, we adopted the last available open access version of the data from 2007, [299] that we then updated to today as: [258]

$$\mathrm{F_{l,a,2}} = \mathrm{F_{l,a,1}} \cdot \frac{USD/\$_{\mathrm{a,2}}}{USD/\$_{\mathrm{a,1}}} \tag{4.2}$$

That is basically multiplying the location factor of 2007 (1) of a given country (a) to the ratio of the currency exchange ratio of that country in 2020 (2) to 2007 (1) compared to US dollars.

4.2.3 Capital cost estimation: Factorial Methods

Factorial methods build on equipment costs, factoring in one (Lang-like) or multiple factors (Hand-like). [286] Lang-derived factorial methods originate from the series of papers by Lang in 1947, [300–302] where the TCI is equal to the sum of all the equipment cost E_k times a

factor F depending on the nature of the process (solid, liquid, solid-liquid), plus the working capital WC (Eq. 7).

$$\mathrm{TCI} = \mathrm{F} \cdot \sum \mathrm{E}_k + \mathrm{WC} \tag{4.3}$$

Instead, in 1958 Hand assigned factors for equipment type, [303] rather than process type, to construct a correlation for the inside battery limits investment ISBL (Eq. 8):

$$\mathrm{ISBL} = \sum \mathrm{F}_k \cdot \mathrm{E}_k \tag{4.4}$$

More recent correlations are from Peter and Timmerhaus, or Sinnot and Towel, built on Lang's and Hand's hypothesis.

Factorial methods highly rely on the accuracy and the scope of the database, which are rarely specified. [286] These methods can be used for Class 5 estimations, but they usually require equipment list and specifications, that are unavailable at the early stage of the project.

4.2.4 Capital cost estimation: Process step methods

Process step methods postulate the Total Capital Investment (TCI) as a function of the main process steps and parameters, such as temperature, pressure, capacity, and construction materials. [84] They follow the general formula: [286]

$$\mathrm{TCI} = \mathrm{K} \cdot C \cdot B \tag{4.5}$$

Where K is a numerical constant, C is one or more factors accounting for the main process parameters, and N is the number of process steps (or units).

Tsagkari pointed out how the main disadvantage is the loose definition of "process step," which can vary by author, and the "lack of historical data for regression analysis." For this reason, Gerrard suggests that "collect[ing] data ... for the process of interest" is more reliable than "us[ing] the standard correlations" (i.e., those from the literature), because, once again, the scope of the published equations is limited to the database from which they are drawn. [291]

Compared to the factorial methods, here the cost engineer only needs the number of units

and some general information about the plant, which are available at the maturity level equivalent to a Class 4 or 5 AACE. This approach, in theory, makes the process step methods appropriate for an early-stage estimation. The IFP's Functional modules method and Petley's [290, 304] correlation are the most recent examples of this group, although their application increased only after Tsagari's review of 2016.

4.2.5 Capital cost estimation: Thermodynamic methods

Thermodynamic methods take a different, indirect approach. In 2001, Lange demonstrated that for fully optimized (design-wise) chemical and petrochemical plants, the Direct Capital Cost (DCC), or sum of ISBL and OSBL, of a plant correlates with the energy lost, and the ISBL with the energy transferred in the process. [213] This is based on the underlying assumption that the energy lost or exchanged is proportional to the area of the heat exchangers, which is in turn a component of the DCC. To test his hypothesis, he compiled a database made of internal Shell data of fuel plants, and an overall review data of representative technologies between 1960-1986 calculated by Chauvel and Lefebvre. [292] In his formulation:

$$\text{DCC} = 3 \cdot (\text{Energy losses/MW})^{0.84} \tag{4.6}$$

With the DCC expressed in million USD of 1993. The energy losses are calculated by multiplying the global inlet and outlet of a plant's streams for their lower heating values (LHV), as:

$$\text{Energy losses/MW} = \sum LHV_{in} - \sum LHV_{out} \tag{4.7}$$

Where LHV_i is the flowrate multiplied by the LHV. Similarly, the ISBL cost (in 1993 million USD) correlates with the global energy transferred as:

$$\text{ISBL} = 2.9 \cdot (\text{Energy losses/MW})^{0.55} \tag{4.8}$$

Both equations are valid for energy (lost or transferred) higher than 10 MW, because they deviate for small or energy-neutral plants.

Moreover, the original dataset comprises data from large (compared to plastic recycling) industrial-scale facilities, built by the same company with similar standards as nth of a kind (NOAK). Conversely, chemical recycling plants are mostly at the pilot or demo scale (sole-

of-a-kind or first-of-a-kind at best), with expected fully operational industrial plants with a capacity of 40–50 kt/year. We postulate that this scale involves smaller energy loss, and therefore the original model (Eq. 9) was valid in form, but not in substance.

More recently, [305] Lange revised the heat transfer equation when applied to the estimation of a distillation train, and he found, conveniently, that the exponent of the energy transfer-cost correlation became 0.65, which is what is usually encountered in capacity-cost scale-up curves.

Lange's models claim an accuracy equivalent to an AACE class 5 (-50, +100%), but in fact, only the energy loss model (Eq. 9) is suitable for an AACE class 5 estimation. To calculate the energy losses, we would only need a block flow diagram knowing "what comes in" and "what goes out" of the plant, or the energy content of feed, products, waste, fuel, as well as the global electricity input, which are available at the very early stage (Table 1) of a project. To calculate the energy transfer, namely as heat (reactors, heat exchangers network) or mechanical (rotative equipment or electricity) transfer duty, one would need a detailed process flow diagram, which is something available later on (AACE3 or 4 equivalent). This correlation, when based on full-scale plants, also integrates all the energy recovery options which would have been put in place at higher Capex, and which might not be justified for a pilot or demonstration unit.

4.2.6 Capital cost estimation: Process build-up method

The "process build-up" estimation rationale, an early estimation (AACE Class 5) method for biorefineries beyond the state of the art, [306] combines power-law and process step estimation in a probabilistic fashion assisted by a database of 300 existing or announced plants. Although this method requires low-maturity level project information, it is specific for biorefineries projects, and it is only appropriate to estimate similar projects. [306] The authors identified common "process blocks" across the biorefinery technologies, so that new projects (within or beyond the state of the art) are series of process blocks. Then, one can calculate the cost of each block, adjusting the block reference cost from the database by an efficiency factor that varies by the kind of block. The efficiencies are the process variables available at a 0–2% maturity level: yields, product purity, flowrates, etc.
The process build-up method is a useful approach, but it is based on a database unfit for chemical recycling plants of plastic, so outside the scope of this work.

subsectionDatabase construction and statistical analysis

Several techno-economic assessments in the academic literature indirectly already address the research question "How much does it cost to build a chemical recycling plant?". Some of them rely on process simulators (e.g., APEA –Aspen Process Economic Analyzer [253]), others on vendor quotes, [307,308] estimation methods, [309] or follow a hybrid approach. [181,310] In 2011, Feng tested 5 process simulators on the same set of equipment and found that there is up to a 200% variability between costs estimated by different simulators. Estimation of the cost of power machines is consistent among software, but the estimate of the cost of shell equipment is not.

When testing Class 3 or Class 4 factorial methods, a more detailed scope than the one proposed here (Class 5), Van Amsterdam [286] demonstrated that half the time the methods he selected were wrong, that is, they yielded a 43% absolute average error instead of the " - 25% + 35%" he was targeting. Class 3 or 4 methods already require up to 10 times more preparation effort than class 5 methods, and more advanced process deliverables. He also pointed out how the database on which the models relied has the biggest impact on the difference among methods, rather than the structure of the equations itself.

Similarly, cost estimation accuracies decrease by 20 to 30% if they are not backed by pre-commercial or commercial demonstrations, or if they do not include any site-specific data. [311] This is even more relevant when paired with upper management requests for reduced estimates, which results in technologies pushed too fast, with minimal process validation. Additionally, process estimates come in ranges (e.g., Table 1), but experience teaches how ultimately the final figures are always close to the maximum amount allocated in the budget, [311] i.e., the upper range of the estimation, in a sort of "self-fulfilling prophecy".

We then concluded that to answer the question we needed to build a database tailored to chemical recycling, then test conventional methods, and finally decide which approach (exponential, thermodynamical, etc.) is the most appropriate for our scope.

In more detail, in this work we:

- Queried the open literature for press releases, white papers, newspaper articles, journal articles, government grants, environmental assessments, technical reports, companies' websites, investor presentations, conference presentations, academic literature, congress hearings or any other governmental required interaction or document, in over 15 languages;
- Mined the sources for information on plant technology, capacity (intended as waste

fed to the plant), year of real or expected construction, geographical site, total capital investment;

- Updated the plants' TCI to pre-COVID 2020 US with a CEPCI factor for the time, and Richardson International Construction Factor for the location;
- Divided the data per technology clusters, and correlated the total plant capacity in terms of feedstock (or treated plastic), with the TCI;
- Regressed a linear, log-log fit, and calculated confidence and prediction intervals of the sets; and
- Fit TCI probabilities with a statistical distribution to validate the collected data relevance, because we know that total capital investment probability generally follows a log-normal distribution. [85, 311–313]

At this point, we had a database of over 169 chemical recycling plants (Annex B):

- Pyrolysis (107);
- Gasification plants (32);
- Solvolysis plants (18); and
- Selective dissolution (10).

On this set, we adopted a three step approach first (**i**) we tested some "conventional" capital estimation methods to see how they would compare with the real data and their confidence interval. To compare conventional AACE class 5 estimation models we selected representative projects from highly cited papers in the literature where the capital cost was claimed to come from either engineering detailed designs by third parties, internal references, or directly from vendor quotes on the detailed flowsheet (Table 4.2).

We selected those projects to represent pyrolysis and gasification state-of-the-art plants. For selective dissolution and solvolysis, the database is so sparse, and the technologies so diverse, that we decided not to benchmark those two families for capital cost estimation models.

Among pyrolysis plants, there are facilities producing a diesel-like fuel (PtF), and ones aiming at naphtha-like oil (PtO) to be sold as a feedstock for steam crackers in the petrochemical industry (to ultimately produce virgin plastic). We therefore had two subclusters for pyrolysis, and one for gasification.

Then, (**ii**) we verified the accuracy of the reference projects selected with the total plant database, to draw capacity vs TCI linear regressions with statistical significance. Here we verified whether or not the plant capacity is an appropriate indicator for TCI, and what is the probabilistic distribution of TCI based on the interval of prediction built on the historical plant database.

Table (4.2) Selected project for benchmark (PtF is plastic to diesel fuel; PtO to naphtha oil).

Technology	**Capacity (kt/year)**	**TCI (M USD, 2020 US)**	**Capital Cost Source**	**Base of Reference**
Pyrolysis–PtF (Fivga [213])	80	16	Vendor quotes + power law estimation	UK, 2013
Pyrolysis–PtF (Ghodrat [308])	13	6	Vendor quotes + Factorial methods	Australia, 2017
Pyrolysis–PtF (Riedewald [307])	40	28	Vendor quotes on detailed design	Belgium, 2020
Pyrolysis–PtO (Gouzhan [310])	16	6	Hybrid: - Vendor quotes - Simulators - Technical reports	UK, 2018
Pyrolysis –PtO (Volk [314])	65	70	Technical report	Germany, 2021
Gasification– NREL [315]	79	111	Internal Reference	US, 2021
Gasification– Lan [316]	655	980	Hybrid: - Vendor quotes - Technical reports	US, 2021

After that, (**iii**) when possible, we regressed the heat and mass balance of each pyrolysis and gasification plant, under the hypothesis that energy lost is a better indicator than capacity for TCI. In fact, when we calculate the theoretical energy of pyrolysis for selected plastics as a contribution of sensible heat, depolymerization, heat of fusion (in the case of crystalline

polymers), and vaporization, we realize that even assuming a 100% wt. polymer to monomer yield, polyolefins are the most energy-intensive plastics to depolymerize (Figure 4.2). And yet, they are the preferred feedstock for these technologies, which suggests that capital investment has to be related with the way energy is input or withdrawn in the process, especially if such a process is highly exothermic or endothermic.

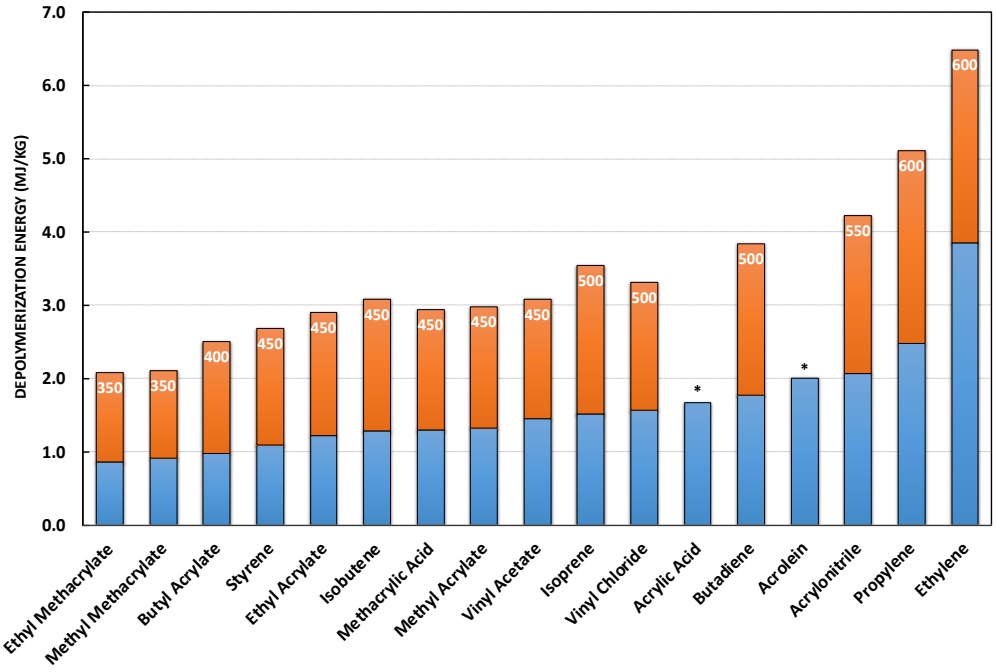

Figure (4.2) Energy Intensity (MJ/kg) in Pyrolysis - Polymer to Monomer (assuming 100% yield, depolymerization). Depolymerization in MJ/kg is expressed as sensitive heat (orange) + heat of depolymerization and vaporization (blue), at its temperature (°C) of depolymerization (white). The sensitive heat is calculated as $c_p \Delta T$ with data from, [317] and the depolymerization and vaporization values are taken from the literature and the NIST WebBook. [318, 319]

Adopting a black box perspective, we computed the overall energy loss across the plant using Equation 4.7. This calculation involves the sum of the product of flow rate and lower heating value (LHV) of all input streams (inclusive of fuel and electricity), subtracted by the equivalent sum of all output streams. Essentially, if by-products are combusted on-site for energy recovery (a common practice for light incondensable fractions in pyrolysis), they aren't included in the output streams, as they technically do not exit the plant.

4.2.7 Selected estimation methods for benchmark

Power-law, process step, and thermodynamic methods are the most suited for the benchmark. They require minimal effort and low-level detail project deliverables. We selected Petley's, Wilson's, Bridgwater's, Lange's, and Zvenik & Buchanan methods (Table 3). The original equations are for ISBL, OSBL, or their sum; for the sake of clarity, we directly report the correlations for the TCI, in million USD of 2020 in US dollars. Chemical engineering handbooks like Sinnot & Towel and Perry's suggest (at least) the following compounding to transform ISBL into TCI: [320]

- OSBL + ISBL = 1.4 * ISBL = DCC;
- ICC + DCC = 1.3 * DCC; and
- TCI = WC + Start-Up + DCC = 1.15 * DCC;

Which means that the TCI is roughly twice the ISBL. The manuals suggest these factors as the lower-end for "a typical petrochemical plant," which would not be representative for our case studies. One approach would be to analyze the projects (Table 4.2) case by case and select the compounding factors on a "best-educated guess" rationale. However, given that we know the real TCI, this approach could be biased, because the criteria for the selection of the factors are "large and small projects," or "technological uncertainty," which are hard to quantify.

Ideally, estimation methods would benchmark selected projects in a database built on TCI values. The key hypothesis in the TCI collected is that companies release the best figures they have at the time. Whenever possible, we considered the most recent communications to reflect any possible cost increase over time. However, companies are both reluctant to divulge details, and their TCI figures follow a log-normal distribution with a p50 of +30%. [85] Nevertheless, at the time of release, most of the work has already been done, and quotations from key suppliers have been obtained, so that a database built on this information cannot be more accurate than that.

At the same time, detailed estimations like the ones released to the investors often include some contingencies, which we cannot access. Moreover, the investment data are primarily disseminated to attract funding, which may result in a tendency towards over-optimism, as well as the simplification of the plant design and dependence on existing assets. We assumed that these two aspects ultimately even out, which substantiates the hypothesis that the cost

announced is as close as it gets to the real TCI.

For the deterministic analysis, when available, we directly compared the methods' outputs (ISBL) to avoid introducing extra factors. For the probabilistic analysis, we decided to adopt a fixed factor of 1.4 to convert ISBL into TCI when needed in the estimation methods, assuming that because we are looking at AACE class 5 estimation methods, they come with a [-20%, +100%] accuracy (Table 4.1), so we do not want to introduce new uncertainties. In this way, we infer that whatever mismatch there is between what we calculate from 1.4xISBL and the TCI of the dataset, it is within the expected range of the estimation methods. The scope of our analysis is not to find the perfect method, but to see whether the methods fall within the interval of prediction of our dataset, or namely if they could be a good first educated guess for researchers and technology owners at the early stage of a project.

Table (4.3) Selected methods for deterministic and probabilistic benchmark.

Method	**Ref**	**Relation for TCI/M USD**	**Description**
Petley	[62]	$\text{TCI} = 1.4 \cdot 55882 \cdot P^{0.44} \cdot N^{0.486} \cdot T_{\max}^{0.038} \cdot P_{\max}^{-0.02} \cdot F_m^{0.341} \cdot \frac{\text{CEPCI}_{2020}}{\text{CEPCI}_{1998}}$	$T_{\max}$ is the maximum temperature in the process $P_{\max}$ is the maximum pressure in the process P is the plant capacity expressed as "what is leaving the plant" F_m is the material factor N is the number of functional units
Wilson	[80]	$\text{TCI} = 1.4 \cdot f_I \cdot N \cdot (\text{AUC}) \cdot F_m \cdot F_p \cdot F_t \cdot \frac{\text{CEPCI}_{2020}}{\text{CEPCI}_{1971}}$ $\text{AUC} = V^{0.675}$	AUC is average unit cost of main plant items, proportional to the plant capacity V (what is fed to the process) f_I is the investment factor, a tabulated value depending on AUC and the kind of process (Fluid, liquid, gas) F_m is the material factor, from 1 (mild steel) to 2 (titanium) F_p is the design pressure factor F_t is the design temperature factor N is the number of functional units
Bridgwater A	[81]	$\text{TCI} = 1.4 \cdot 0.000489 \cdot N \cdot \left(\frac{Q}{s^{0.5}}\right)^{0.85} \cdot \left(\frac{n \cdot T_{\max}}{N}\right)^{-0.17} \cdot \left(\frac{n' \cdot P_{\max}}{N}\right)^{0.14} \cdot \frac{\text{CEPCI}_{2020}}{\text{CEPCI}_{1976}}$	N is the number of functional units s conversion Q the capacity in ton/y, expressed as what is fed to the process n number of units whose temperature is higher than $T_{\max}/2$ n' number of units whose pressure is higher than $P_{\max}/2$ 1.4 is to transpose the original ISBL correlation to TCI Reported accuracy is [-20%, + 20%]
Bridgwater B	[82]	$\text{TCI} = 1.4 \cdot 0.001 \cdot N \cdot \left(\frac{Q}{s}\right)^{0.675} \cdot \frac{\text{CEPCI}_{2020}}{\text{CEPCI}_{1981}}$ if $\left(\frac{Q}{s}\right) > 60000$ $\text{TCI} = 1.4 \cdot 0.103 \cdot N \cdot \left(\frac{Q}{s}\right)^{0.3} \cdot \frac{\text{CEPCI}_{2020}}{\text{CEPCI}_{1981}}$ if $\left(\frac{Q}{s}\right) < 60000$	
Bridgwater C	[82]	$\text{TCI} = 1.4 \cdot \left[3 + 9.7 \cdot 10^{-6} \cdot \frac{Q}{s}\right] \cdot N \cdot \frac{\text{CEPCI}_{2020}}{\text{CEPCI}_{1981}}$	
Bridgwater D	[82]	$\text{TCI} = 1.4 \cdot 0.0014 \cdot \left(\frac{Q}{s}\right)^{0.655} \cdot e^{Q \cdot 2.58 \cdot 10^{-7}} \cdot T_{\max}^{-0.022} \cdot P_{\max}^{-0.064} \cdot \frac{\text{CEPCI}_{2020}}{\text{CEPCI}_{1981}}$	
Taylor	[83]	$\text{TCI} = 1.4 \cdot k_T \cdot \sum_1^N (1.3)^{CS} \cdot Q^{0.39} \cdot \frac{\text{CEPCI}_{2020}}{\text{CEPCI}_{1977}}$	k_T is a constant CS is the complexity index for each functional unit N Q the capacity in ton/y, expressed as what is fed to the process
Lange A	[45]	$\text{TCI} = 3 \cdot (\text{Energy losses MW})^{0.84} \cdot \frac{\text{CEPCI}_{2020}}{\text{CEPCI}_{2001}}$	Details in Eq. 4.6
Lange B	[45]	$\text{TCI} = 1.4 \cdot 2.9 \cdot (\text{Energy transfer MW})^{0.55} \cdot \frac{\text{CEPCI}_{2020}}{\text{CEPCI}_{2001}}$	Details in Eq. 4.8
Zevnik & Buchanan	[84]	$\text{TCI} = 1.4 \cdot 7470 \cdot Q^{0.6} \cdot 10^{\left((0.1 \cdot \log P_{\max}) + \left(1.8 \cdot 10^{-4} \cdot (T_{\max} - 300)\right) + F_m\right)} \cdot \frac{\text{CEPCI}_{2020}}{\text{CEPCI}_{2000}}$	$T_{\max}$ is the maximum temperature in the process (K) $P_{\max}$ is the maximum pressure in the process (atm) Q the capacity in ton/y, expressed as what is fed to the process F_m the material factor (0.1 aluminum to 0.4 for precious metals) N is the number of functional units log is in base 10

4.3 Results and Discussion

The research query identified plants mainly in three macro-regions (Figure 4.3):

- Australia and North America;
- Europe; and
- Eastern and South-Eastern Asia.

These areas share different views on recycling, and they are at different stages of their zero-waste journey. Europe and the US are the most fertile ecosystems for new plants, with most plants in our database based there. South Korea and Japan lead the effort in Asia. The plastic waste control plan in South Korea aims to reduce the plastic content of total waste to 50% and increase plastic waste recycling to 70%. [317] Japan's Resource Circulation Strategy for Plastics, instead, targets 100% of used plastic for reuse or recycling. [318] A smaller cluster of plants (mainly pyrolysis to road fuel) is in Australia, where the National Waste Policy promotes circular economy initiatives, albeit later than "other jurisdictions". [319]
The authors know by direct experience that areas not represented in the map, such as Latin America, northern Africa, or India, have recycling plants as well. For cultural reasons, and the absence of coordinated regulations, plant owners often prefer to trade in the local market, or they do not advertise the recycling content of their products, especially if the quality is comparable to the virgin (monomer, road fuel, naphtha oil). In fact, if the end-user does not see the difference in the final product, recyclers do not want to disclose their feedstock (i.e., plastic waste) source. With some geographical exceptions, consumers still value price and quality over environmental impact, [321] and they expect to pay a discount if the goods are made with recycled material because they believe it to be of lower quality. [322]

Figure (4.3) Map of chemical recycling plants, [323] divided into gasification (yellow), pyrolysis to fuel (blue), pyrolysis to naphtha oil (red), solvolysis (light grey), and selective dissolution (dark grey).

4.3.1 Deterministic and Probabilistic Benchmark for Pyrolysis

We divided pyrolysis into two sub-technological clusters: Plastic to Fuel and Plastic to Naphtha oil with, respectively, three and two reference projects. Although each estimation model has its own accuracy, in general, 5 AACE methods are supposed to estimate with a [-50%, +100%] accuracy on the median value (Table 4.1). From a deterministic point of view (a fixed value for the estimation), Wilson's and Bridgewater's (A and D) are the best performers for pyrolysis overall (Table 4.4), because their errors are within the AACE accuracy range. However, when we benchmark the methods on the historical database of plants, the majority of reference projects underestimate the TCI compared to the historical database. This underestimation suggests that techno-economic assessments require a more analytical approach, and researchers in academia need guidelines and references when estimating TCI of plastic recycling plants. At the same time, Wilson's method falls within the 95% (or 2σ) confidence interval (Figure 4.4) of the best-fit line only for two projects, while Bridgewater (A,D) only one (Figures 4.4 and 4.5). Overall, the family of methods that show that the thermodynamic group (Lange A, B) are the most accurate; they estimate within the 95% confidence interval four out of five times. However, Lange B models rely on the energy exchanged in a process, which we calculated from the detailed process flowsheets in the academic papers. At the

very early stage, we may have partial access to this information, for instance we might be able to roughly estimate the heat of reaction and/or purification, but not the energy for rotary equipment. For this reason, Lange B, which is the top performer among the ones we tested, is not always usable. If we consider the other best methods, Petley, Wilson, Lange A, no method is clearly better than the others. Wilson and Bridgewater (A and D), the top methods in the deterministic analysis, fall within the 95% confidence interval 0 and 1 times respectively.

Table (4.4) Deterministic comparison for pyrolysis, with absolute errors

Method	**Pyrolysis PtF [213]**	**Pyrolysis PtF [308]**	**Pyrolysis PtF [307]**	**Pyrolysis PtO [310]**	**Pyrolysis PtO [314]**
Capacity/kton year^{-1}	80.0	13.2	40.0	16.0	64.0
Original (ISBL / TCI) M USD	**16 (TCI)**	**6 (TCI)**	**28 (TCI)**	**4 (ISBL)**	**15 (ISBL)**
Petley	49 (+199%)	17 (+201%)	34 (+23%)	20 (+437%)	42 (+103%)
Wilson	29 (+75%)	9 (+56%)	19 (-32%)	6 (+61%)	23 (+11%)
Lange A	55 (+233%)	6 (-2%)	66 (+138%)	7 (+105%)	34 (+67%)
Lange B	20 (+24%)	15 (+161%)	15 (-46%)	11 (+196%)	19 (-8%)
Bridgwater A	27 (+68%)	9 (+49%)	15 (-46%)	7 (+102%)	34 (+65%)
Bridgwater B	13 (-21%)	18 (+217%)	15 (-46%)	12 (+235%)	20 (-5%)
Bridgwater C	22 (+36%)	28 (+375%)	20 (-29%)	19 (+430%)	33 (+63%)
Bridgwater D	15 (-10%)	9 (+58%)	10 (-65%)	7 (+86%)	25 (+20%)
Zevnik & Buchanan	178 (+992%)	76 (+1209%)	92 (+229%)	75 (+1956%)	175 (+1094%)
Taylor	22 (+34%)	9 (+56%)	5 (-80%)	9 (+160%)	13 (-36%)

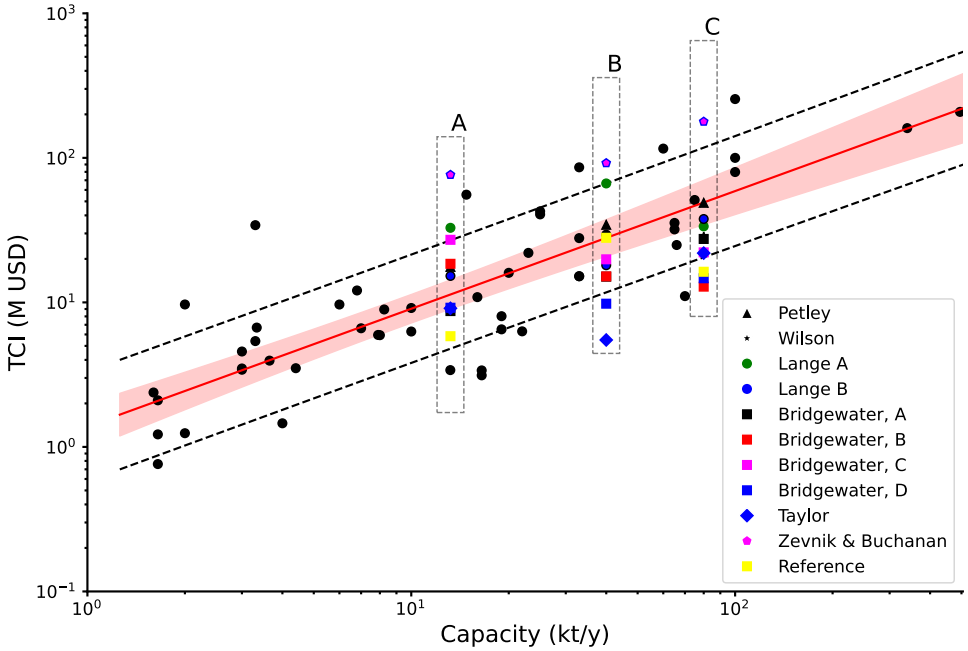

Figure (4.4) Pyrolysis - Plastic to Road Fuel - Probabilistic Analysis. References (in yellow) A: *Ghodrat 2017*; B: *Riedewald 2020*; C: *Figva 2013*. The capacity correlates with the TCI: $\mathbf{\log(TCI) = 0.81 \log(Capacity) + 0.14}$ with a $R^2 = 0.75$. Dashed black lines represent 1σ prediction interval, while the red region represents the 2σ confidence interval around the best fit (red line). The black dots are the plants part of our database. Confidence interval is the one where to expect the best regression line, while prediction is the interval to be used for future observations.

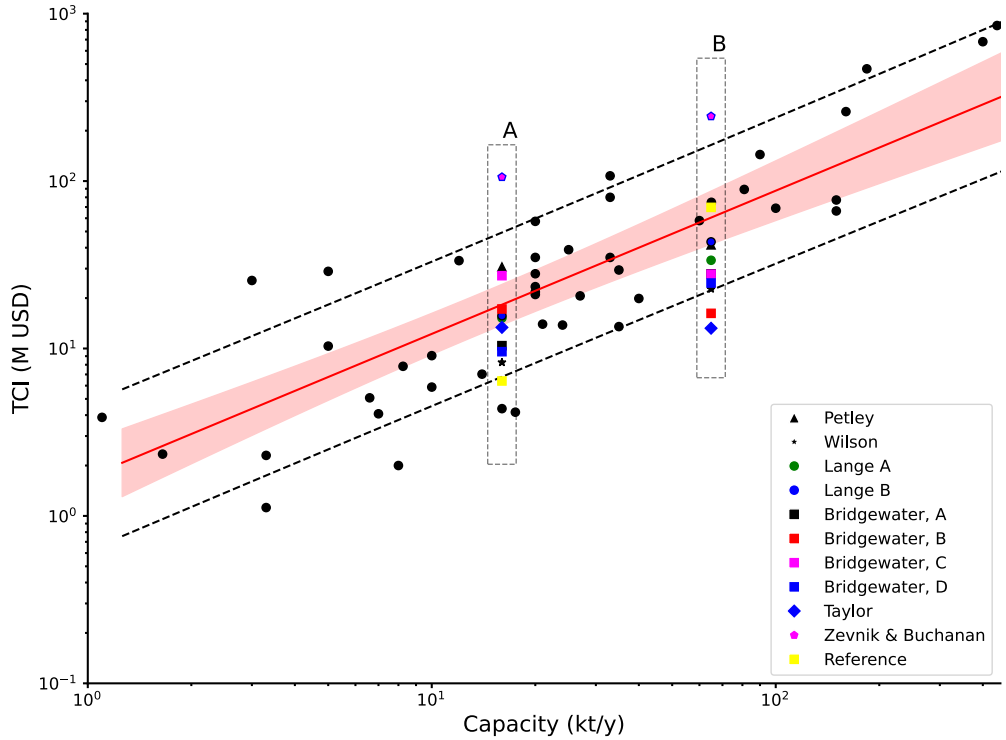

Figure (4.5) Pyrolysis - Plastic to Naphtha Oil - Probabilistic Analysis. References (in yellow) A: *Volk 2021*; B: *Gouzhan 2018*. The capacity correlates with the TCI: $\mathbf{\log(TCI) = 0.86 \log(Capacity) + 0.24}$ with an $R^2 = 0.72$. Dashed black lines represent 1σ prediction interval, while the red region represents the 2σ confidence interval around the best fit (red line). The black dots are the plants part of our database. Confidence interval is the one where to expect the best regression line, while prediction is the interval to be used for future observations.

The probabilistic analysis also gives insights on plastic pyrolysis as a whole:

- Recyclers are migrating from a business model that converts waste plastic to diesel fuel to one that converts waste plastic to naphtha oil.
- The technology suffers from a poor economy of scale, because TCI scales up with capacity$^{0.81}$ to capacity$^{0.86}$ for PtF and PtO respectively, which hints that they are based on unit parallelization principles rather than size scale up. However, capacity is not the ideal indicator to estimate TCI, given that the $R^2 = 0.71 - 0.75$ for the predictions.
- Recyclers choose a standard plant size, on the order of 35–45 kton/year of capacity.
- The TCI for the plants follows a log-normal distribution for a given capacity.

These results find practical implications with what we observe in the industry. Theoretically, the main contributor to the TCI (on the equipment side) is the reactor. We note that the most common reactor designs are stirred tank (Plastic Energy), an auger reactor (Agylix), and a microwave reactor (Pyrowave). The first two have in common a limited wall surface to transfer heat to the plastic, so that the energy fed depends on the transfer area. This geometry suggests (on the basis of surface area per unit volume) a scaling factor of 0.5. [324] However, reactors are size-limited because in pyrolysis the heat has to be transferred through the walls, so that increasing the plant capacity necessitates numbering up rather than scaling up (which explains why there is limited economy of scale). [323] Of course, the temperature at which the process is carried out is also important, and it should not compromise the product quality. If additional reagents are used in the process, such as steam, hydrogen, or catalysts, they would affect the product quality and might give a better value to the product.

Microwave reactors are limited in the penetration depth of the irradiation and by the volume to be irradiated. Finally, pyrolysis in general is impeded by feedstock (waste plastic) collection. Plastic is a low-density material, which means high transport volume (i.e., trucks). Moreover, mixed waste sorting is better effected by individual households rather than in more highly populated areas, but collection volumes trend in the opposite direction. [325, 326]

In addition, the wastes to be processed are not "uniform" nor standardized. Numbering up rationales are therefore preferred to cope with the heterogeneity of the feedstocks from batch to batch.

The dispersion in CAPEX, whatever the correlation selected, illustrates the diversity of technologies that are possible for pyrolysis. Some technologies cannot be easily scaled up and so require reactor numbering up. Other technologies are more appropriate for scaling up and would have a lower "power law" factor for the pyrolysis reactor. For these reasons, for plastic pyrolysis, there is an optimum plant size (35–45 kton/y range) where companies can save on engineering costs by building a "standard" kind of reactor, while allowing for the practicalities of feedstock sourcing. In the future, we foresee companies will look at a hub and spoke model to incorporate the pyrolysis plants in an existing refinery center. Here, small, delocalized pyrolysis plants surrounding a bigger existing refinery will receive low-density plastic waste and liquefy it into naphtha-like oil that feeds the central facility to refine or crack the output, to ultimately produce new plastics.

Where possible (40 out of 106 plants), we calculated the global mass balance and the energy loss across the plant, for the whole pyrolysis database (PtF + PtO).

The energy loss (MW) correlates linearly with the TCI (Figure 4.6) better than the plant capacity does ($R^2 = 0.92$, versus $R^2 = 0.76$ for capacity). This also supports the hypothesis that factors that correlate with energy input are the main contributors to the pyrolysis

economics.

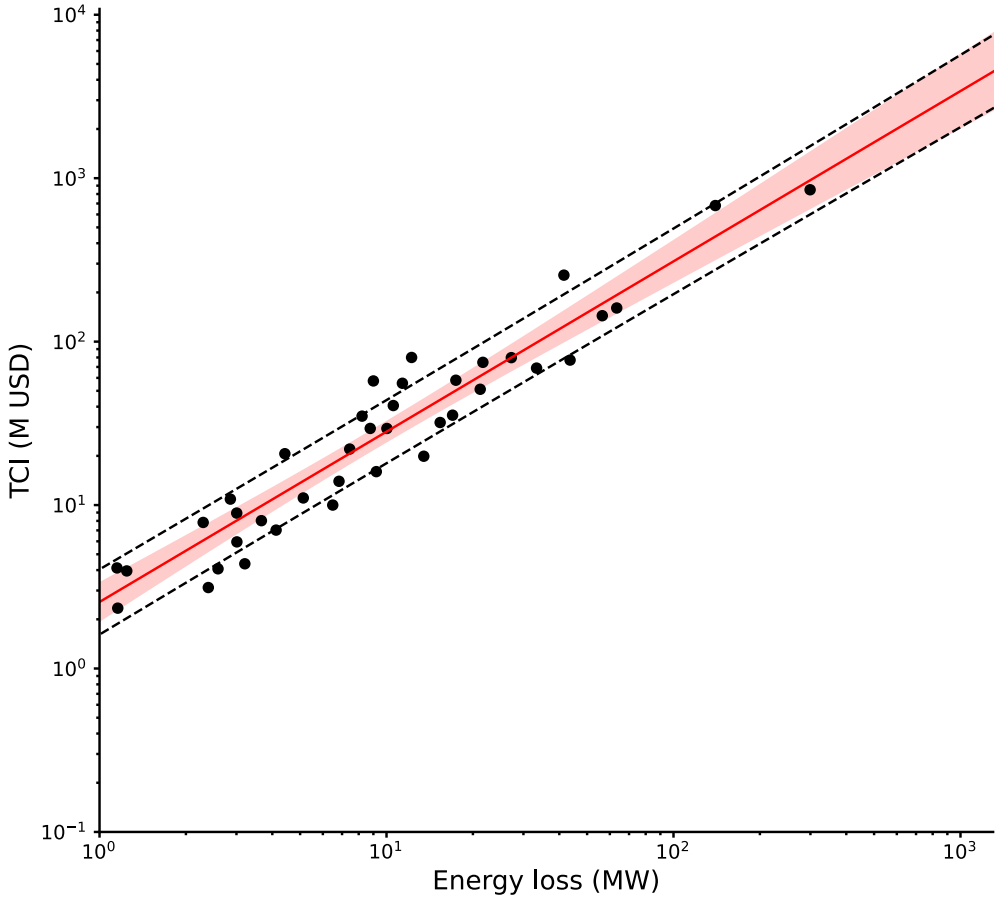

Figure (4.6) **Pyrolysis – Probabilistic Analysis Energy loss vs TCI.** The energy loss in MW correlates with the TCI: $\mathbf{\log(TCI) = 1.04 \log(MW_{loss}) + 0.41}$ with an $R^2 = 0.92$. Dashed black lines represent the 1σ prediction interval, while the red region represents the 2σ confidence interval around the best fit (red line). The black dots represent the plants that are part of our database. The confidence interval is where to expect the best regression line, while the prediction interval is for future observations.

At low project maturity levels, with this correlation (Figure 4.6), one can directly estimate the plant TCI with a very high confidence and screen different technologies based on estimated capital cost. To do so, researchers need to know (or calculate):

- Global plant mass balance; and
- Nature of feedstock and products, which are available at the beginning of the project.

When possible, the MW loss is not just a better indicator for the TCI nominally, but also probabilistically (Figure 4.7). However, similar to Lange A, when a project is non-thermal

or highly energy integrated, the correlation would not be as reliable. In the special case of plastic pyrolysis, it is common practice to use part of the products as fuel to make the process energy self-sufficient, which makes the calculation easier because one only needs to know (or set) the total mass yield for the process (as opposed to the utility balance). Generally, uncondensable off-gases are targets for energy recovery, and a rule of thumb for a quick estimation is to assume them as 15–30% wt. of the products.

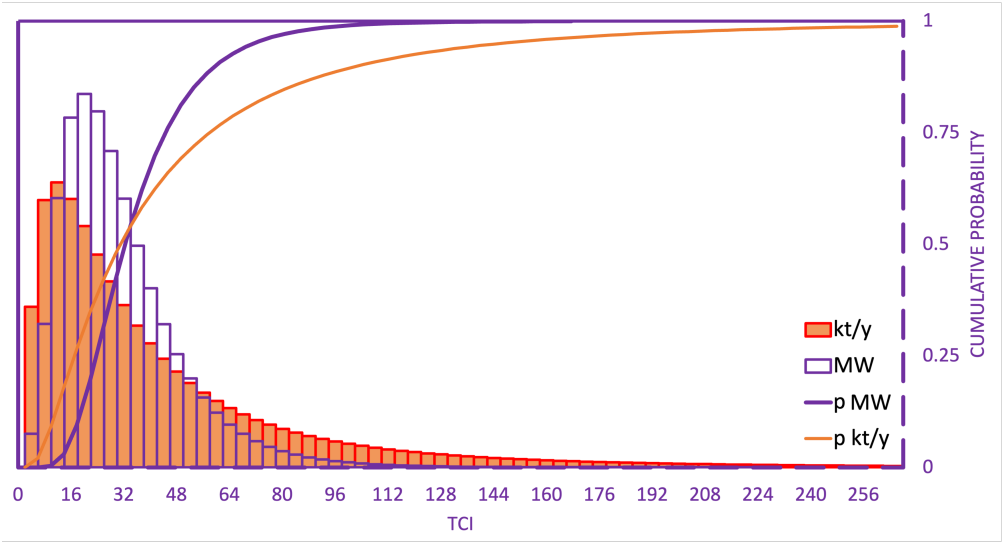

Figure (4.7) TCI log-normal distribution for a representative plant using the capacity (kton/y) or the energy losses (MW), and their cumulative probabilities (p).

For a typical pyrolysis plant from the database, the log-normal distribution of TCI is sharper when estimated from the MW lost compared to the capacity in kton/y, which leads to a higher level of confidence in the overall estimation.

4.3.2 Deterministic and Probabilistic Benchmark for Gasification

We selected two reference plants for gasification, one to produce H_2, and the other to produce methanol, which are representative of the technologies seen in the industry presently. Again, Wilson, Lange A, and Bridgewater (A, B, C, D) perform the best in the deterministic analysis, because they estimate with errors within the AACE class 5 boundaries in both case studies, with Lange and Bridgwater A and C being the most accurate of all (Table 4.5).
One reference (NREL 2020) falls in the 95% confidence interval for the probabilistic analysis, and in this case, Bridgewater (A, C) are actually the best methods overall. The other reference (Lan 2021) falls outside the 95% confidence interval, and Bridgewater C and D are the best performers when comparing with the database (Figure 4.8). Bridgewater C is

overall the best estimation method. However, once again one should not rely too much on the performance of the methods, because they were developed for different types of plants, and for larger-scale applications. For instance, Bridgwater developed his first method (A) using 24 plants from 16 hydrometallurgical processes, [84] and even he stopped using his methods (A–D) in favor of more specific correlations for the process at hand. [327]
Once again, the problem of using methods based on process steps is that they are highly dependent on the definition of the "process steps" (N-Table 4.3), which are not unequivocal in the literature. Unlike with pyrolysis, gasification capacity correlates very well with TCI ($R^2 = 0.91$), and regressing energy and mass balances (when possible) did not improve the correlation taking the total plant energy losses as basis (Figure 4.9).

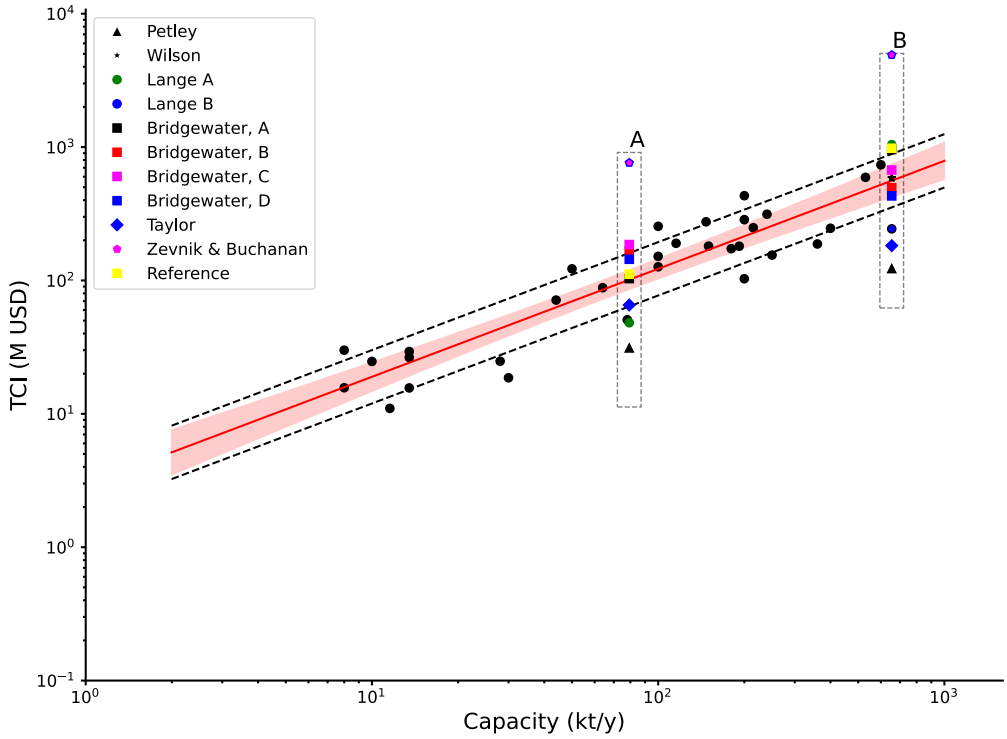

Figure (4.8) Gasification - Probabilistic Analysis. References (in yellow) A: NREL 2021; B: Lan 2021. The capacity correlates with the TCI: $\mathbf{\log(TCI) = 0.81 \log(Capacity) + 0.47}$ with an $R^2 = 0.91$. Dashed black lines represent 1σ prediction interval, while the red region represents the 2σ confidence interval around the best fit (red line). The black dots are the plants part of our database. Confidence interval is the one where to expect the best regression line, while prediction is the interval to be used for future observations.

For a typical pyrolysis plant from the database, the log-normal distribution of TCI is sharper when estimated from the MW lost compared to the capacity in kton/y, which leads to a higher level of confidence in the overall estimation. Additionally, gasification facilities can

run with a "flexible feed" or "clean feed" approach. Process gas or fuels in the gasifier are less problematic (i.e., cheaper) than processing waste (biomass or plastic), because the latter need additional Capex for waste residue sorting, pelletizing or pre-treatment (for plastic), additional operative costs to dispose of the residues, and present technical challenges during operation due to the presence of sticky ash prone to agglomeration in the reactor. Conversely, plants designed to use clean fuel and handle only pre-sorted plastics would incur costs for their feedstocks. Although the projects populating the database claim to be plastic gasifiers, we can assume that this is completely true only for new or under-construction projects; existing projects are likely to operate in flexible feed mode, [328] which was more attractive in the recent past.

Table (4.5) Deterministic comparison for gasification, with absolute errors.

Method	**Gasification H_2 [316]**	**Gasification MeOH [315]**
Capacity (kton/year)	656	79
Original (ISBL / TCI) M USD	**580 (ISBL)**	**75 (ISBL)**
Petley	88 (-85%)	49 (-35%)
Wilson	419 (-28%)	131 (+74%)
Lange A	744 (+28%)	63 (-16%)
Lange B	174 (-70%)	Insufficient data
Bridgwater A	686 (+18%)	86 (+15%)
Bridgwater B	354 (-39%)	46 (-38%)
Bridgwater C	480 (-17%)	65 (-14%)
Bridgwater D	307 (-47%)	41 (-45%)
Zevnik & Buchanan	3607 (+505%)	800 (+987%)
Taylor	130 (-78%)	47 (-38%)

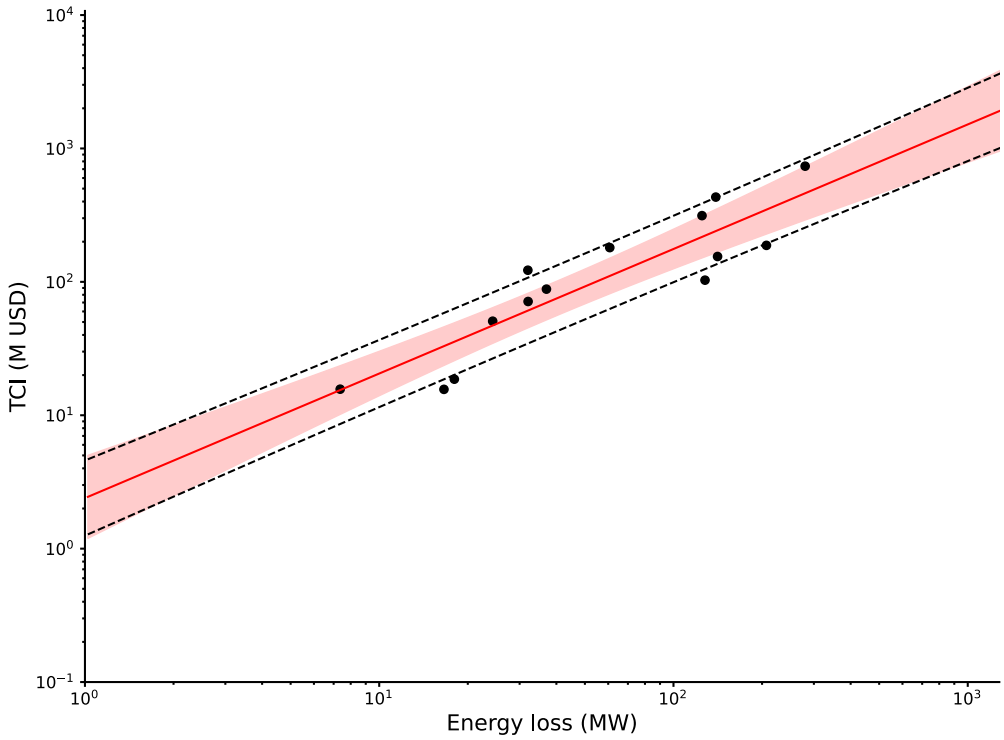

Figure (4.9) Gasification - Probabilistic Analysis Energy loss vs TCI. The energy loss in MW correlates with the TCI: $\mathbf{log(TCI) = 0.93\,log(MW_{loss}) + 0.37}$ with an $R^2 = 0.91$. Dashed black lines represent 1σ prediction interval, while the red region represents the 2σ confidence interval around the best fit (red line). The black dots are the plants part of our database. Confidence interval is the one where to expect the best regression line, while prediction is the interval to be used for future observations.

Because the plants are not so well defined, we therefore must accept an uncertainty in TCI, and also contend with a variability in the feedstocks and products.

The probabilistic analysis for gasification suggests that:

- Capacity (expressed in terms of kton/year) is a sufficient basis for estimating the TCI. It is as accurate as total energy loss through the plant;
- Gasification, like pyrolysis, suffers from poor economy of scale, and it scales up with as capacity$^{0.81}$;
- The average plant size of the database is 145 kton/year, and 2016 is the average year of construction, similar to pyrolysis to diesel fuel. This observation supports the hypothesis that some of the bigger size plants might be multipurpose facilities.

Additionally, because of its multipurpose nature, gasification may be better suited for municipalities, because the sorting and/or waste pretreatment can be outsourced, as suggested

by the early experience of Enerkem. [329]

4.3.3 Deterministic and Probabilistic Benchmark for Solvolysis and Selective Dissolution

Solvolysis and selective dissolution are similar in many ways; for instance, both employ a solvent and must be tuned for the specific polymer (depolymerized or dissolved, respectively). The difference is that selective dissolution is more flexible in terms of waste feedstock. Both technologies are newer compared to pyrolysis or gasification, and data are mostly limited to pilot or demo scale, with few industrial-scale plants. Solvolysis projects mainly target PET (in different alternatives – Glycolysis, methanolysis, hydrolysis), polycarbonate, and foam polyurethanes (more recently). Selective dissolution is appropriate for polyolefins, polystyrene, polycarbonate, and mixed plastics which are difficult to recycle mechanically, such as multilayer films.

Patent and academic literature is ample, but the low maturity level of existing projects increases the uncertainties in the estimation. Similarly, the variability (chemical or technical) of the process within this cluster is an additional source of dispersion in the data. For instance, in hydrolysis, methanolysis, or glycolysis, PET depolymerizes respectively to terephthalic acid, dimethyl terephthalate, or PET glycolates (e.g., bis-2-hydroxyethyl terephthalate). Hydrolysis produces an easier-to-sell but difficult-to-purify product; dimethyl terephthalate is, in turn, easier to purify but has a smaller market; and glycolysis requires a catalyst for a real plastic-to-plastic (PET) recycling. [270]

The database includes diverse processes, such as Gr3n, which uses a microwave reactor, Carbios, which uses enzymatic hydrolysis, or Ioniqua's catalytic glycolysis with magnetic separation for catalyst recovery. The technology spread causes the total capital cost to be only poorly related to feedstock capacity (Figure 4.10, and 4.11), with selective dissolution having a better economy of scale compared to solvolysis. Theoretically, scale-up for solvolysis and selective dissolution is correlated to the volume and is limited by the productivity. Dissolution and solvolysis require several hours (if not days) of residence time, so that when one wants to increase the capacity, numbering-up rationales are employed on the reactors to increase flexibility.

However, estimation for new plants relies on scarce full-scale data and therefore must accept higher uncertainties. At the same time, the investor should not be lured with promises of low capex and production costs, so it is especially important to be able to estimate as early as possible the full production cost.

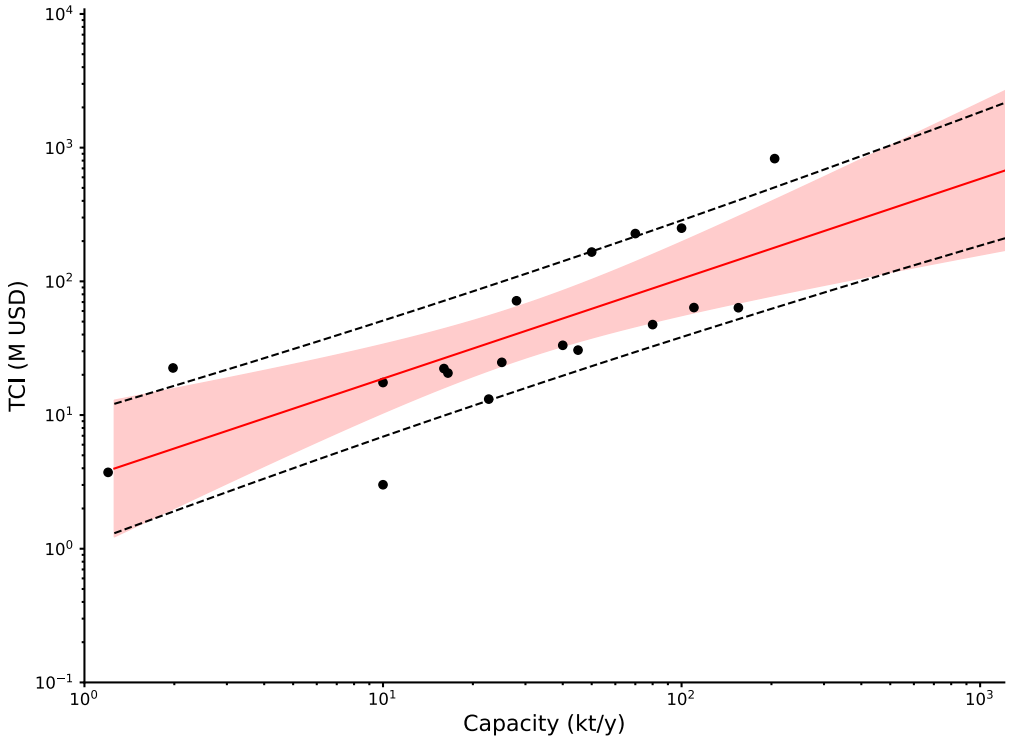

Figure (4.10) Solvolysis - Probabilistic Analysis. The capacity correlates with the TCI: $\mathbf{\log(TCI) = 0.75 \log(Capacity) + 0.52}$ with an $R^2 = 0.61$. Dashed black lines represent 1σ prediction interval, while the red region represents the 2σ confidence interval around the best fit (red line). The black dots are the plants part of our database. Confidence interval is the one where to expect the best regression line, while prediction is the interval to be used for future observations.

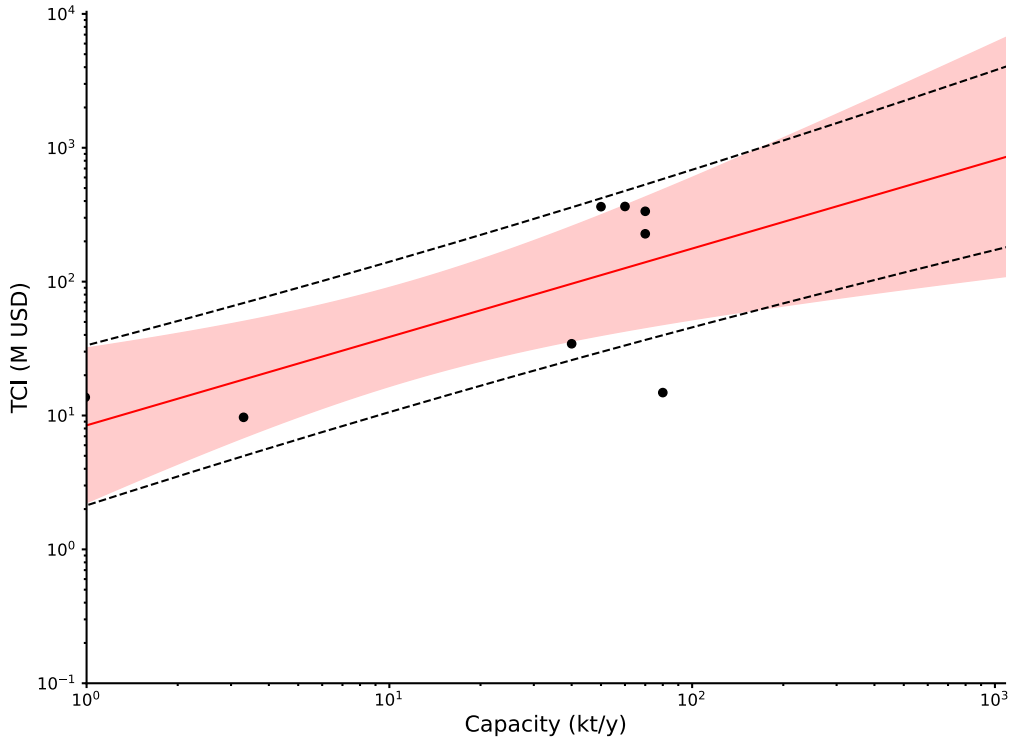

Figure (4.11) Selective Dissolution - Probabilistic Analysis. The capacity correlates with the TCI: $\mathbf{\log(TCI) = 0.66 \log(Capacity) + 0.93}$ with an $R^2 = 0.63$. Dashed black lines represent 1σ prediction interval, while the red region represents the 2σ confidence interval around the best fit (red line). The black dots are the plants part of our database. Confidence interval is the one where to expect the best regression line, while prediction is the interval to be used for future observations.

4.3.4 How to Use the Database

Researchers have to convince either their company, investors, or funding agency that the technology they promote is the future "blockbuster". To do so, they must demonstrate that the technology will have superior economic and technological advantages to compensate for the risk of investing in a new (unproven) technology. This must be done at a time when little to no pilot results are available. At best, one has to convince the funding agencies when a Technology Readiness Level (TRL) of 3–4 has been reached, and within the companies even at lower TRL to get the money to start the preliminary research. It is then particularly important to be able to provide some numbers at low TRL levels when many issues are not yet solved. Of course, these numbers come with a lot of uncertainty or dispersion. But as we have seen earlier, even a Class 5 estimate is given at +100%/-50% level. For that level of precision, process engineers need already a good definition of how the plant would look like, and it might take them several months and a few 100 kUSD to provide a value. Therefore,

what is needed is a method which might have a larger dispersion, but is faster and cheaper. Once a capital cost has been calculated, it would be fed into the production cost model. It has multiple impacts: as depreciation cost first, but also on maintenance, insurance, property taxes which are factored from the capital cost. There is also a correlation between the capital cost and the labor cost. Here also it can be related to the number of processing steps, whether the process is operated in batch or continuous mode, the plant capacity, and the wages. Indeed, in countries with low labor costs, it might be better to reduce the Capital cost and increase the labor cost.

For the investor, the Capital cost is where the risk is taken. The world is full of plants that have been built but never operated as expected. In the capital cost, there are contingencies and start-up costs included to compensate for those risks, but nevertheless plants can finally cost twice as much as initially planned or never operate as expected. Especially for a completely new technology, the investor needs to see much better economics than with alternative processes, and requests to have lower capex and production costs by 30% are not uncommon.

As explained previously, the capex (TCI) feeds into the fixed cost and labor cost. There are other costs such as R&D, Laboratory (quality control), sales, and distribution that have to be added but which are usually proportional to the sales, and so to the plant capacity and product price. The variable costs will include mostly the feedstocks and utilities (gas, electricity, water, etc.) needed for the plant. It might also be difficult to assess the variable costs initially, but again a fair percentage of the sales can give a good estimate.

What is interesting with the correlation between the TCI and the energy loss, is that it could also work in the opposite direction. If we have a fair estimate of a plant cost (TCI), we can derive a fair estimate of the energy consumption (knowing the mass balance).

All those data come with uncertainties or dispersions, and Monte Carlo type simulations can be used to get a dispersion on production prices. [181,231] It might then be easier to convince management, shareholders, investors, and funding agencies on a probability to reach a given production price. What those data usually demonstrate is where the focus should be for the improvement of the technology.

One key question that one might have at an early stage of the process is: should I focus on reducing the Capex, but then buy a more expensive feedstock, or make a lower purity product (sold at a lower price), or should I try to make the highest purity product, with the cheapest feedstock at the expense of the plant complexity? The answers to these questions are going to determine how the experimental work should be conducted. It would not be at all the same type of experiments if the feedstock is already very pure (for example, post-production plastic waste), or if one has to use a dirty waste (for example, post-consumer, 30-year-old

plastic with additives and ingredients which are no longer allowed on the market). Also, the type of purification technologies to be validated strongly depends on these assumptions. Upper management pressures researchers and cost engineers to have the most precise estimation possible on the capital cost (at the earliest possible stage). However, Monte Carlo simulations demonstrate that the TCI is only one of the three main contributors to economic feasibility, together with product selling price, and purchasing price of feedstock (if any). [181, 253, 330] Let's now assume that upper management wants to build a plant to recycle 100 kt/y of waste, with no precise technology in mind yet, and they need to estimate its TCI to ultimately decide whether or not to move on with the investment. Our database demonstrates that it is not the detail of the technology that makes the difference (Figure 12), because within the early-stage estimation uncertainties, all the technologies yield similar TCIs (e.g., between 55 and 215 M USD for 100 kt/y). This is why in the early-stage development it is not essential to pursue higher precision on the capital investment beyond what we suggest in this study, as we would lack precision on the other two factors – purchasing and selling cost anyway.

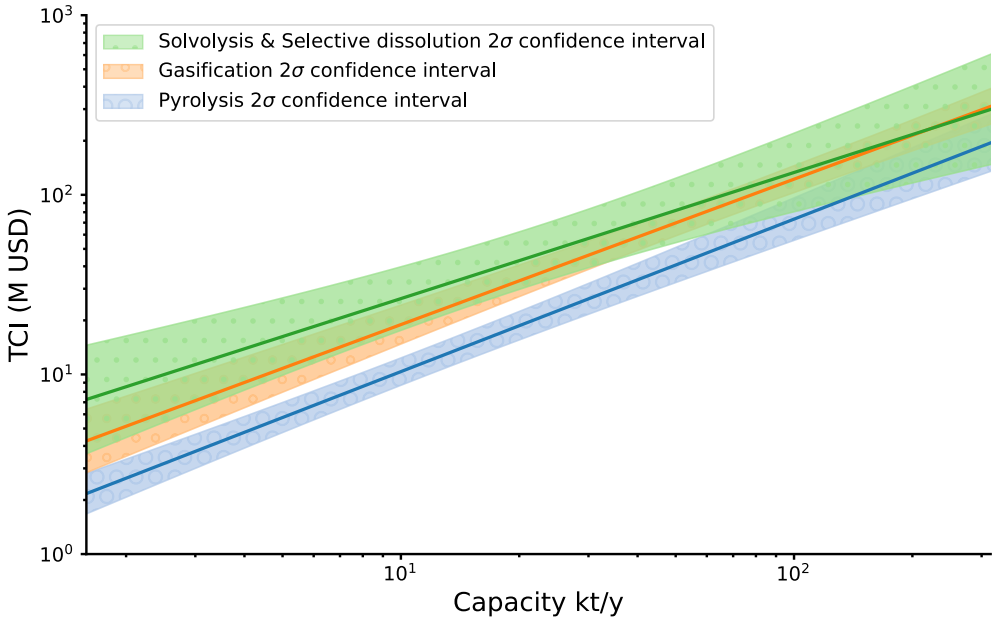

Figure (4.12) 2σ confidence interval around the best fit for Pyrolysis (PtF + PtO) – in blue, Gasification – in orange, and Solvolysis + Selective Dissolution – in green.

Instead, special attention should also be given to the mass yield of the recycling processes, especially when considering closed-loop recycling. This would justify classifying the processes based on the number of cycles the carbon can make while retaining 50% in the economy. When the polymer-to-product mass yield is 90%, it is possible to keep 50% of the carbon in the economy after $0.5 = (0.9)^6$, 6 recycling operations. Mixed plastics (polyolefins) pyrolysis

would give 70% mass yield to liquid products, and only 70% of it would be directed to a steam cracker. Then, the usual yield of a steam cracker is 50% ethylene + propylene. So, only 25% of the initial mass can return to the polymer economy. Other plastics have much better mass yields, such as PMMA (polymethylmethacrylate) with more than 90% with the best quality scraps, and PS (polystyrene) with about 70%, with depolymerization via pyrolysis. [35] Therefore, from an environmental point of view, one should favor the technologies that keep the carbon longer in the economy. In that sense, mechanical recycling has a high mass yield, but suffers from down-cycling (the product often does not return to the same application in the economy). For instance, waste PVC window frames are recycled mechanically in the same market but are diluted with virgin PVC in a sandwich layout where recycled PVC containing harmful additives like Pb is at the core, and virgin PVC is on the external surface. So, the yield is high, but it is not completely closed-loop. If we project ourselves into the future, the carbon source should come from biomass, recycling, and as little as possible from fossil sources. The only way to achieve this target is to have a high recycling yield because the amount of biomass available is limited.

An additional factor often overlooked by researchers is the use of existing assets. Again, we can take a real-world example. PET recyclers have multiple options: mechanical recycling; solvolysis via glycolysis, methanolysis, hydrolysis, or ammonolysis; selective dissolution; and even (albeit more technically and economically challenging) pyrolysis or gasification. A company like SABIC tried to make a new material with added value, so they selected a type of glycolysis. Toray, which is a PET producer, also selected glycolysis. Eastman, which is a PET producer, selected methanolysis. Carbios, which develops an enzymatic hydrolysis, partnered with Indorama to adapt their process to PET. An even more self-explaining scenario is the one of mixed plastics. With exactly the same waste, Enerkem selected gasification while others chose pyrolysis. In the first case, Enerkem gasifies to methanol or ethanol, while in the second case, the target is to make a stream that can feed a steam cracker and use that existing asset. The mass yield is poor in the case of the steam cracker and will always be low because of the high energy and temperature needed to depolymerize PE and PP back to the olefins (Figure 2). The mass yield could be much higher with gasification, especially with added hydrogen from electrolysis. But the assets of a steam cracker are so expensive that petrochemical companies want to fill them as much as possible. They could have selected, with the same TCI, to invest more in waste pretreatment, sorting, washing, and mechanical recycling/selective dissolution. But that does not use the steam cracker assets and would be considered as a form of cannibalization. Similarly, smaller plants have a larger uncertainty in the TCI vs. capacity (Figure 4.12), also because in some cases the product can be diluted in a bigger stream (like pyrolysis oil in a steam cracker), and the hydrothermal section of the

plant to remove heteroatoms (e.g., N, O, or S) can be omitted. At the same time, however, smaller plants are more prone to reuse existing assets compared to bigger plants, so that albeit not always the best choice, executives are more inclined to give them the green light. What ultimately the correlations derived in this paper teach us is that there can be a large dispersion of capital cost for the same capacity, but that for the same feedstock and same product, the energy is independent of the route. The correlation is independent here of the details of the process. The guideline for the technology developer is then to select a process that would minimize the energy losses.

For the selective dissolution and solvolysis processes, which are closer to chemical plants, there is a wide diversity of processes. That's also where it would be important to be able to select the right one as early as possible. But there is also a wide diversity of feedstocks and targeted products. For example, in the case of PET, one would not build the same plant to depolymerize bottle-grade PET (transparent clear) and unsorted PET textile. In such a case, it will be necessary to have a more complete definition of the process blocks that have to be combined.

4.4 Conclusions

To guide decision makers and researchers who are tasked with screening among different chemical recycling technologies, we built a database of over 160 existing industrial facilities from several countries. The majority of our projects are in Europe and North America, with some in Eastern Asia and Australia. We demonstrated that conventional AACE class 5 capital cost estimation methods are deterministically and/or probabilistically unreliable for chemical recycling projects. In fact, no class of method estimates correctly (and consistently) pyrolysis and gasification projects, while solvolysis and selective dissolution are so early in their technology development journey that it is currently impossible to fully validate the existing correlations.

Starting from as simple as a global plant mass balance, the new empirical equations we propose can estimate the TCI of plastic waste pyrolysis and gasification facilities both easily and accurately.

Convention wisdom not withstanding, [331] we found that plastic recycling plants do not benefit much from economies of scale.

When available, energy losses estimate the TCI way better than the plant capacity, but they are not always possible to calculate. Moreover, one-size fits all scaling factors are not appropriate, especially when the TCI accuracy plays a key role in determining whether or not a project will be profitable. Future work should focus on expanding the database for solvent

based technologies and understanding (similar to what we did for energy-based processes) which variables can correlate directly with the TCI of those processes. Similarly, continuous updates and refinements of the empirical equations proposed in this study will also contribute to improving the accuracy of TCI estimation for different chemical recycling technologies as the industry matures.

CHAPTER 5 ARTICLE 3 – WASTE ARTIFICIAL MARBLE PYROLYSIS AND HYDROLYSIS

In Chapters 3 and 4, we illustrated the design and operation of a typical PMMA thermolysis plant, explored the conditions under which such a plant can maximize investment returns, and provided a reliable method for estimating chemical recycling plants cost (including PMMA) using a database of existing or planned facilities. To expand PMMA recycling to real-world post-consumer waste, this chapter focuses on artificial marble waste, a PMMA-$Al(OH)_3$ composite that dominates the artificial stone market. Artificial marble exemplifies the challenges of recycling composites, as during thermolysis, $Al(OH)_3$ releases water, which hydrolyzes the volatilizing MMA into MAA (Annex A). Since MAA is also a valuable compound, we explored thermolysis and hydrolysis of artificial marble to understand the hydrolysis mechanisms and optimize the yield of either MMA or MAA, alongside the recovery of the inorganic fraction, which is crucial for ensuring economic viability. In the annex A we analyze from a technical and environmental point of view, the industrial standard of artificial marble thermolysis, the R&E process in Korea. R&E currently recycles several tons of waste artificial marble to low quality (i.e. 96.5 % pure) MMA and Alumina. We back-engineer their process layout, as well as heat, mass, water and CO_2 balance, to serve as benchmark for the results of this upcoming chapter.

Jacopo De Tommaso, Federico Galli, Tien Dat Nguyen, Yanfa Zhuang, Jean-Luc Dubois, Gregory S. Patience

in: Waste Management, 9 August 2024

Abstract

Artificial marble, a composite material consisting of 40 % (g g^{-1}) Poly Methyl Methacrylate (PMMA) and 60 % (g g^{-1}) aluminium hydroxide $Al(OH)_3$, combines the durability and aesthetics of real marble with the lightweight and moldability of plastic. It is the most sought-after synthetic stone in the world, with a production volume of over 1 million t in 2021. However, due to a high level of cross-linking, mechanical recycling of the composite is impossible, while chemical recycling is achievable, yet unprofitable. The only economically viable recycling solution is to retain the value of both the organic and inorganic fraction of the composite. We investigated the pyrolysis and hydrolysis of post-consumer end-of-life artificial marble to identify possible valorization routes, examining the effects of tempera-

ture, water content, catalyst presence, and heating style. Temperature directly accelerates thermolysis, and indirectly hydrolysis. The water inherently present in $Al(OH)_3$ drives initial hydrolysis, and temperature expedites inorganic fraction dehydration, increasing local water partial pressure near polymer ester sites. Above 350 °C, PMMAeq depolymerizes faster than it hydrolyses, balancing the effects of temperature on water dehydration with the depletion of available ester sites for hydrolysis. Contrary to intuition, PMMA does not depolymerize to its monomer MMA and then hydrolyze its acid (methacrylic acid); instead, PMMA partially hydrolyzes to poly methacrylic acid (PMAA) while also depolymerizing to MMA. PMAA then dehydrates and degrades, releasing CO and CO_2. The optimal method involves a heating ramp that first releases water at 300 °C, minimizing hydrolysis, and then favors MMA production at 400 °C, achieving a 66 % (g g^{-1}) MMA yield. Regardless of the operative conditions, the inorganic fraction transforms from $Al(OH)_3$ to a γ-alumina precursor, boehmite. Additionally, the remaining polymer in the residue, about 9 % (g g^{-1}), has the required heat capacity for an energy-self sufficient calcination to γ-alumina. This dual-phase process not only maximizes MMA recovery but also retains the value of the inorganic fraction, providing a sustainable and economically viable recycling method for artificial marble.

5.1 Introduction

PMMA, poly methyl methacrylate, also known as acrylic glass, ® Plexiglas, Persplex ®, or Altuglas ™ is a versatile thermoplastic that gained prominence during the pandemic as a protective barrier in public spaces. Its properties, including tensile and flexural strength, UV resistance, and clarity, make it essential in automotive, construction, electronics, signage, and coatings sectors [65, 332, 333].

The global PMMA market exceeded 4.5 billion USD in 2021 and is expected to surpass 3 million tonnes annually by 2028 [24, 25]. However, approximately 800 000 t to 1 000 000 t of PMMA waste remains unaddressed annually [334]. Despite initiatives by major companies like Trinseo (MMAtwo [35]) and Mitsubishi, along with smaller recyclers [24, 335–337], comprehensive sorting, collection, and recycling are imperative. Among commodity plastic, PMMA is one of the best candidates for high yielding plastic-to-plastic recycling. Mmechanical recycling of PMMA is suitable for clear and transparent injection and extrusion grade scraps, yet the resultant product necessitates blending with fresh plastic due to the degradation in mechanical and optical properties [40, 46, 65]. Over cycles, molecular weight declines [46], and yellowing or colour changes occur, leading to downcycling [35, 46]. Besides, some PMMA grades, for instance those with cross-linkers, are unsuitable for molding and reshaping because they behave more like thermoset than a thermoplastic [338].

PMMA pyrolyzes to methyl methacrylate (MMA) at 350 °C to 450 °C with yields over 90% [46, 339]. PMMA has a lower ceiling temperature (the equilibrium temperature corresponding to an equal polymerization and depolymerization's Gibbs energy) compared to other polymers, making it more likely to depolymerize to its monomer during pyrolysis [83]. PMMA is more suitable to a real polymer-to-polymer recycling than other thermoplastics, with a ceiling temperature of 192 °C [39, 40], which is approximately 150 °C to 200 °C below its standard thermolysis operating temperature. For comparison, polyethylene has a ceiling temperature of 610 °C and an industry-standard pyrolysis temperature of 400 °C to 500 °C [340, 341], while polystyrene is at 395 °C [342] and 450 °C to 550 °C [343, 344], respectively.

Industrially, PMMA conversion to MMA has moved from theory to practice. The MMAtwo initiative, a European collaborative effort, successfully depolymerized selected cast, injection, and extrusion grade scraps, achieving a plastic-to-monomer yield of 80 (% g g^{-1}) to 90 (% g g^{-1}) and MMA purity up to 99.80% [345]. However, at parity of capital investment, subpar PMMA waste results in lower-quality MMA with impurities like acrylates, acids, or esters, which have similar structures and boiling points as MMA [35, 66, 131]. This poses distribution challenges, especially in the EU or US markets [24]. The depolymerization process can also produce impurities like methyl isobutyrate through hydrogen transfer reactions, especially in reactor configurations that promote static contact with charred surfaces and molten polymer [35] (e.g. dry distillation). Optimal conditions are when the cleanest scraps (e.g. post industrial, pre-sorted) depolymerize in the best reactor configuration (the one introducing the least external impurities), so to produce a regenerated MMA (r-MMA) that necessitate the least purification [24]. This typically excludes a large portion of PMMA waste, including post-consumer contaminated scraps and PMMA-based composites, which require case-by-case approaches based on the quantity and nature of co-composites (often inorganic) [35].

PMMA hydrolysis to methacrylic acid (MAA) offers technical, economical, and market benefits [81, 82, 346]. PMMA hydrolyses to MAA in the presence of zeolite, with up to 60 % (g g^{-1}) yields in small laboratory scale fixed or fluidized beds [82, 347]. MAA purification is simpler than MMA, allowing for a broader range of waste materials as feedstocks [82, 346]. While PMMA recycling to MMA is industrially established, feedstocks unsuitable for r-MMA are good candidates to be recycled to MAA. Acrylic artificial marble is one of those. This composite, composed of 35 % to 45 % (g g^{-1}) cross-linked PMMA and 45 % to 65 % (g g^{-1}) aluminium trihydroxide (ATH - $Al(OH)_3$), predominantly in gibbsite form [348], is the main

type of artificial marble in circulation, and the leading world synthetic stone in terms of volume [349]. In 2021, production reached 1 million t - with Korea and US, the principal markets, contributing 40% each [350, 351]. This translates to a 1.8 billion USD market value in 2021, with an estimated CAGR of 6% [349, 350].
The construction industry employs artificial marble for its moldability, mechanical strength, lightweight nature, and thermal resilience, in applications like countertops, tables, sinks, and shelves [338, 348]. It is also favoured in public spaces like hospitals because its non-porous surface offers better hygiene than natural marble [352]. Polishing, cutting, and grinding generate post-industrial scrap and dust, amounting to about 20% of the processed material [348]. Because of its thermoset-like behaviour, mechanical recycling of artificial marble would downcycle it to fillers or partial replacements in other composites [353]. The flame retardants in the organic fraction hinder incineration, and landfilling contaminates soil and water because the waste is not biodegradable [354].

Artificial marble pyrolyzes to MMA and alumina at 350 °C to 500 °C in a multiple stages [86, 348, 355]. In Korea, Veolia's subsidiary R&E operates three pyrolysis facilities, recycling 35 000 t of waste artificial marble annually [356]. They collaborate with domestic artificial marble producers (Dupont, Lotte, LG Hausys) to recycle their post-industrial waste artificial marble and supply the local market with low-quality (97 % (g g^{-1}) pure) α-alumina as fire proof material, and 96.5 % (g g^{-1}) pure) r-MMA [357, 358]. However, this r-MMA purity is lower than required in equivalent markets like the EU and even less stringent markets in Southeast Asia [24]. Korea's K-REACH, unlike the EU's REACH, does not exempt recycled or regenerated monomers from registration, posing additional challenges [359, 360].

While regulations surrounding recycled chemicals are still in transition, trading r-MMA with higher contamination levels across regions will become more difficult. One of the reasons for the inferior purity of r-MMA from artificial marble is the higher acidity and water content compared to similar regenerated monomers [49, 352]. When heated in an inert atmosphere (i.e. pyrolyzed) PMMA and ATH degrade at similar temperatures. Commercial ATH start to degrade above 200 °C (Table 5.1a) to AlOOH and/or Al_2O_3 as (Figure 5.1b:

$$Al(OH)_3 \xrightarrow{dH} AlOOH + H_2O \tag{5.1}$$

$$2Al(OH)_3 \xrightarrow{dH} Al_2O_3 + 3H_2O \tag{5.2}$$

PMMA undergoes depolymerization to its monomer through a radical unzipping mecha-

nism [46, 72]. Below 270 °C, the process is driven by head-to-head fission, whereas above 350 °C, head-to-tail radical initiations [47] dominate. PMMA depolymerizes to its monomer (primarily), oligomers, and cracking gases such as CO_2/CH_4 and CO/CH_3OH (in molar ratio). However, both water and hydroxyl surface groups of the AlOOH / Al_2O_3 system promote the hydrolysis of the ester site either at a monomer [49, 86, 348], or at a carbonyl group on the polymer chain level [361–364].

(a)

Supplier or Consultant	$T_{\text{start degradation}}$ (°C)	$dH_{\text{decomposition}}$ (kJ/kg)
Alteo [365]	≈ 200	Undisclosed
Huber [366]	200 to 230	1050
Nabaltec [367]	>200	1075
Martin Marietta [368]	230	1170
Roskill Information Service [369]	180	1300

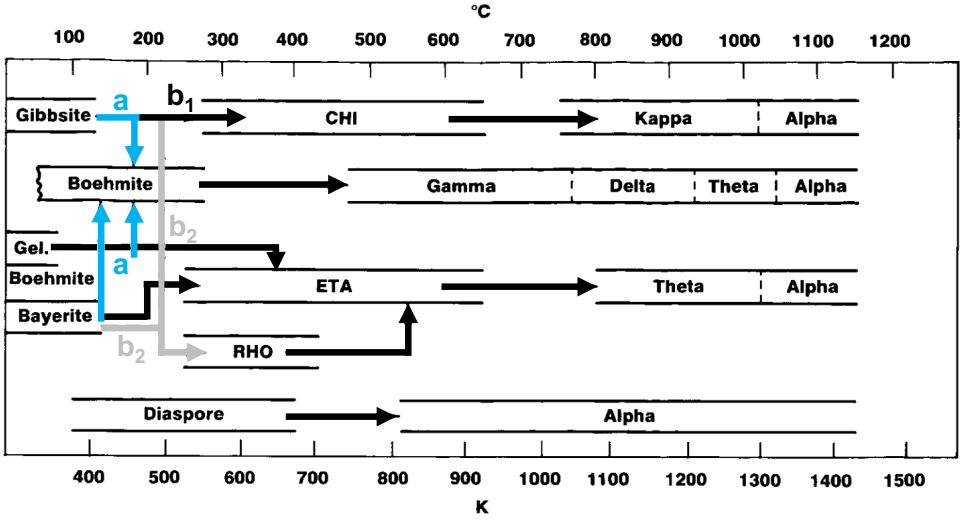

(b)

Figure (5.1) **a**) Thermal degradation properties of selected commercial ATH. **b**) $Al(OH)_3$ - gibbsite, bayerite; Al_2O_3 - alpha, gamma, delta, eta, theta, kappa, rho; and AlO(OH) - bohemite, diaspore thermal evolution. The black arrows represent heating in air at atmospheric pressure, the blue arrows hydrothermal transformations, the grey arrow heating in dry air under vacuum. Gibbsite transforms to either boehmite (**path a**), chi-alumina (**path b1**), or rho-alumina (**path b2**). When the water cannot easily vacate the crystal matrix during the thermal treatment (because grain size or humidity in the air), the pressure inside the particle increases, and gibbsite transforms to boehmite (**path a**). As a rule of thumb, path a corresponds to: heating ramp >1 °C/min; particle diameter >100 μm; moist air, and/or P >1 atm [370–372]. When the water can evaporate freely from between the grains, gibbsite dehydrates to chi-alumina (**path b1**), or rho-alumina (**path b2**) if the heating happens under vacuum [371, 372]. Path b corresponds to: heating ramp <1 °C/min; particle diameter <10 μm; dry air, and/or P atm [370–372]. Bayerite transforms boehmite in hydrothermal conditions, which is an usually undesired side-formation for large bayerite particles [371]. When bayerite is heated in intergranular dry conditions, transforms to co-existing eta, theta and alpha alumina [372, 373], at P >1 atm, and rho-alumina if under vacuum. Gelatinous boehmite, the amorphous form of boehmite, develops area and transitions aluminas similar to bayerite [371, 372]. Modified image from [371].

Due to the inherent presence of surface hydroxyl groups and water (released or adsorbed) in inorganic part of the artificial marble (regardless of its polymorphous phase) [362, 374], pyrolysis of the composite is prone to parasite hydrolysis reactions. Furthermore, commercial artificial marbles contain some butyl acrylate as a copolymer [375]. Even without water, these butyl groups can facilitate H-transfer reactions to carbonyl groups, competing with PMMA's unzipping and generating byproducts such as acids (e.g., MAA) and gases [376]. These side reactions either reduce profits or necessitate more capital for purification. R-MMA facilities for PMMA scraps (not artificial marble) typically employ rough short-cut batch distillation or continuous two-column setups, based on desired purity, target market, or scrap nature [24]. The introduction of water and methanol complicates purification due to azeotropes (Annex Table C.3) and liquid-liquid partial miscibility (e.g., Water/MMA/Methanol [377, 378], or Water/MMA/Butanol [379]).

To mitigate these issues, industrial plants recycling artificial marble adopt preventive at the composite feeding, pretreatment stages, or during the r-MMA separation phase. For instance, R&E claims to employ (in one of their many patents) a semi-batch reactor with multiple heating ramps. The first ramp (25 °C to 250 °C), maximizes water release from ATH dehydration. Subsequently, in the 250 °C to 450 °C range, product collection occurs, with the majority of the composite's polymer depolymerizing in this interval [380,381]. The pyrolysis gases condense and undergo a series of tri-phase separators, distillation columns (3 to 4), chemical washing trains, and filters.

Separation is as important as reaction and pretreatment for pure PMMA recycling [35], and, even more so for artificial marble, where increased capital navigates the liquid-liquid and liquid-vapor equilibria of the involved species, ensuring the maximum removal of water and acids.

Similarly, in a continuous process, reducing the composite feed rate and the residence time in the reactor minimizes the partial pressure of MMA and water in the reactor, thus reducing the hydrolysis rate [49].

For these reasons, we conclude that existing recycling techniques converting artificial marble to low-qualitiy r-MMA and α-Alumina are ill-suited for this feedstock. Instead of tailoring the process to the composite's nature, they adopt a one-size-fits-all approach common in chemical recycling. Capital investment, selling price, and product yield impacts the most the overall economic viability of PMMA chemical recycling [24]. We hypothesize a similar trend for artificial marble pyrolysis. This clarifies why one must first understand the interplay between $Al(OH)_3$ dehydration, PMMA depolymerization, and hydrolysis to target the best liquid product (MMA or MAA) and high-value Alumina for a viable business case.

In fact, when PMMA or MMA undergo hydrolysis, they yield MAA or PMAA (poly methacrylic acid) respectively, producing methanol stoichiometrically. At temperatures exceeding 200 °C, PMAA exists in equilibrium with its depolymerization products, MAA and its anhydride, anhydropolymethacrylic acid, along with water [382, 383]. At those temperatures, the anhydride then degrades to CO and CO_2. At the same time, when PMMA and PMAA co-exist as copolymers, neighbouring acid groups of PMAA "auto-catalyze" the hydrolysis of the ester groups of PMMA [384]. Optimizing artificial marble recycling processes -be it hydrolysis or pyrolysis- requires to determine whether, under PMMA depolymerization conditions (above 250 °C) and in the presence of water, hydrolysis predominantly involves MMA or PMMA. If MMA primarily hydrolyzes to form MAA, methanol and MAA would be in the gas phase and collected in liquid form in a stoichiometric ratio. Conversely, if PMMA hydrolyses directly, there is a mismatch between methanol and MAA in the collected liquids, because neighbouring MAA in PMAA blocks dehydrate to anhydride, then degrade to CO_2. CO, and a backbone.

Our primary aim is to recover the most valuable product possible from composite's organic fraction and convert the $Al(OH)_3$ to γ-alumina.

We assume that: **(i)** PMMA first depolymerize to MMA and then, with maximized water partial pressure, MMA hydrolyze to MAA; and **(ii)** $Al(OH)_3$ dehydrates to AlO(OH) or a transition alumina, that we can further calcine to γ-alumina. The water released in the alumina dehydration promotes hydrolysis, which must be controlled based on the desired liquid product.

To validate our hypothesis we hydrolyzed end-of-life post-consumer waste artificial marble in a 5 L bench-scale stirred-tank reactor in batch and semi-batch modes. We continuously monitored the condensed liquid products to track MMA, methanol, MAA, and water concentrations over time, along with the overall liquid weight and the CO, CO_2, and CH_4 in the gas phase. Variations is temperature, water-to-PMMA ratio, and agitation demonstrated that higher water partial pressure in the reactor promotes direct direct PMMA hydrolysis to PMAA, followed by depolymerization.

5.2 Materials and Methods

5.2.1 Materials

Waste artificial marble comes from an end-of-life post-user kitchen counter from a local atelier dealing with artificial stone furniture. Virgin pure PMAA polymer was purchased from Scientific Polymer Products (MW 40,000), and virgin PMMA polymer powder (MW 400,000) from Sigma Aldrich (Sigma-Aldrich 182265). We characterized the material with thermo-

gravimetric analysis (TGA), 1-D X-ray diffraction (XRD), and gel permeation chromatography (GCP). HPLC grade methanol, ethanol, acetone, butanol, propionic acid, ultrapure water, and isobutyric acid from Sigma Aldrich are used to calibrate the Gas chromatography, as well as MMA ($\geq$ 99.6%, stabilized with 6-tert-butyl-2,4-xylenol, TCI America), and MAA (99%, with 250ppm MEHQ as inhibitor, Sigma-Aldrich). Zeolite YH80 were purchased from Zeolyst. Distilled water is injected for the hydrolysis test, along with 99.999 mol% nitrogen from Air Liquid.

5.2.2 Solid analysis - Thermogravimetric analysis (TGA)

A TGA 550 from TAinstruments decomposed the waste artificial marble, the solid residue after reaction, and the PMAA polymer. 25 mg of material thermally degrades under 40 mL/min of nitrogen, with a 10 °C/min ramp from 25 °C to 600 °C, followed by a 30 min isotherm. Air then replaces nitrogen at a 10 °C/min ramp up to 800 °C. The TGA determines the decomposition rate and composition of the waste artificial marble. At 600 °C the polymer fraction is fully degraded, and $Al(OH)_3$ lost its water to convert to Al_2O_3. The mass loss during the switch from nitrogen to air equated to carbon char. This carbon char includes what was originally present in the solid residue and what is produced in the TGA. To be conservative, we attribute it all to the TGA. The remaining mass after the TGA test is alumina, from which we can back-calculate the polymer amount (PMMAeq) of the composite [348, 355].

5.2.3 Solid analysis - X-Ray diffraction

X-ray diffraction (XRD, D MAX-2500H, RIGAKU, Japan) equipped with Cu radiation operating at 200 mA and 50 kV in 1D mode, scanned the inorganic fraction of the feedstock composite, as well as the solid residues after the reaction, and after calcination. The machine investigates diffraction angles 2θ 10° to 90° at a rate of 1 °/min, and it compares the resulting diffraction data with the Powder Diffraction File Database (PDF) references. The XRD can distinguish $Al(OH)_3$ polymorphous phases (Gibbsite, Bayerite), AlO(OH), and the α-Alumina, as well as the other transition aluminas, but these latter are more challenging [372]. Transition aluminas differ only for the type of packing of the Al ions, octahedral or tetrahedral, with the latter having a higher acidity. Albeit possible with XRD, Al^{27} NMR (Nuclear Magnetic Resonance) is more appropriate to identify univocally the different alumina phases [371, 372]. However, for our application, diffraction analysis is capable to distinguish between Al hydroxides and oxides.

5.2.4 Solid analysis - ATR FT-IR

We investigated the functional groups of PMMA and PMAA by a PerkinElmer Spectrum 65 ATR FTIR Spectrometer. Acetone (7 mL) dissolved 0.5 g of polymer in a vial at room temperature overnight. One drop of the supernate dropped on the surface of spectrometer's sample chamber and evaporated at room temperature for 10 min. The spectrometer scanned the polymer film formed after acetone evaporation from $4000\,\mathrm{cm}^{-1}$ to $600\,\mathrm{cm}^{-1}$ at a $4\,\mathrm{cm}^{-1}$ resolution and 32 scans. The main bands of interests for are 1730, 1700 and 1800/1755 cm^{-1} for PMMA, PMAA and methacrylic acid anhydride, respectively (Annex Table C.4). Other important bands for PMMA are 1150/1190 cm^{-1} (C-O-C vibration), and 2850 to 3100 cm^{-1} (C-H stretching vibration).

5.2.5 Liquid analysis: gas chromatography with mass spectrometer detector

An Agilent 7890A GC-MS system analyzed the liquid products qualitatively and quantitatively [82]. The selected ion monitoring (SIM) mode targeted specific m/z values: acetone (m/z 43 & 58), methanol (m/z 31), MMA (m/z 41, 69 & 100), MAA (m/z 41 & 86), isobutyric acid (m/z 43 & 73), and butanol (m/z 31, 41, 43, & 56). External standards are in ppm (mg/l), and liquid density calculation with a Mettler Toledo ME54TE analytical balance reconciled the measurements to mass basis. The concentration (C) as well as yield (Y) of each molecule are therefore expressed in mass basis, as:

$$C_i = \frac{\text{mass of } i}{\text{mass of liquid}} \times 100 \tag{5.3}$$

$$Y_{\text{MAA}} = \frac{\text{mass of MAA liquid} \times (g/mol \text{ MMA})}{(g/mol \text{ MAA}) \times \text{mass of PMMA}_{\text{eq}}} \tag{5.4}$$

$$Y_{\text{MMA}} = \frac{\text{mass of MMA liquid}}{\text{mass of PMMA}_{\text{eq}}} \times 100 \tag{5.5}$$

$$Y_{\text{Hydrolysis}} = \frac{\text{mass of methanol liquid} \times (g/mol \text{ MMA})}{(g/mol \text{ methanol}) \times \text{mass of PMMA}_{\text{eq}}} \times 100 \tag{5.6}$$

$$\widetilde{Y}_{\text{CO+CO}_2} = \frac{\text{mass of CO+ mass of CO2}}{\text{mass of PMMA}_{\text{eq}}} \times 100 \tag{5.7}$$

$$\widetilde{Y}_{\text{Char}} = \frac{\text{mass of Char (TGA)}}{\text{mass of PMMA}_{\text{eq}}} \times 100 \tag{5.8}$$

$$Y_{\text{Polymer in solid residue}} = \frac{\text{mass of Polymer (TGA)}}{\text{mass of PMMA}_{\text{eq}}} \times 100 + \widetilde{Y}_{\text{Char}} \tag{5.9}$$

$$\widetilde{Y}_{\text{Gas+other}} = Y_{\text{CO+CO}_2} + \frac{\text{mass of other-unquantified}}{\text{mass PMMA}_{\text{eq}}} \times 100 \tag{5.10}$$

where the mass of $PMMA_{eq}$ is the polymer part (in mass) calculated from TGA in the artificial marble, and i the liquid component (MMA, MAA, methanol, etc.). $\widetilde{Y}_{\text{Gas + other}}$ is a fictitious Yield to represent the amount of gas and unquantified molecules (e.g. MMA oligomers) based on the initial PMMAeq, which cannot be added to Y because the gases also come from PMAA degradation. Similarly, $\widetilde{Y}$char is attributed to YPolymer in solid residue as part of it might come from the TGA itself. The hydrolysis yield is calculated based on methanol rather than MAA, with MAA yield confirming the pathway (depolymerization or hydrolysis first). . For instance, if $Y_{\text{Hydrolysis}} = 0.3$, and $Y_{\text{MAA}} = 0.15$, it means that 30 % (g g^{-1}) of the initial PMMAeq hydrolyzed, but only half of it hydrolyzed to MAA (via MMA). The other-quantified aliquot includes: (i) Butyl acrylate hydrolysis to butanol. Quantified with the concept of effective carbon number (ECN) for GC-MS. Butyl Acrylate can hydrolyze to Butanol, or it can decompose to acrylic acid and 1-butene (which can further isomerize), but we decided only to check the first route (the one producing butanol); and (ii) Propanoic acid, 2-methyl-, 1-(1,1-dimethylethyl)-2-methyl-1,3-propanediyl ester production. Quantified with the concept of effective carbon number (ECN) for GC-MS using MMA as reference product [385]. The calculated ECN for this product is 13.2, and MMA is 3.5, and the calculated molecular weight is 286.4 g/mol.
Non-quantified yield includes all gases other than CO and CO_2, MMA-oligomers, higher molecular weight acids, and everything else unquantified. We express the product yields in % (g g^{-1}) terms of initial PMMA-eq present in the feedstock. The main assumption is here that the other-unquantified are mostly in gas phase, as we collect every condensable compound.

5.2.6 Material pretreatment: Crushing and grinding

We chopped the artificial marble counter into pieces of roughly 5 cm in diameter. A Fritch Jaw crusher "Pulverisette 1" with Zirconia mobile parts then crushed these chunks to 3 mm in diameter at a feed rate of approximately 50 kg/hr. An MPE Chicago 6F roller grinder with stainless steel internals further pulverized the material to the 250 μm to 1500 μm range (ASTM U.S.A standard 8" full height test sievers). Artificial marble, with a hardness comparable to natural marble ($\approx$ 85 on the Rockwell "M" Scale, or $\approx$ 55 on the Barcol Scale), is "soft" compared to stones but "hard" in the realm of plastics. Mechanical grinding heats the material, which can eventually cause it to fuse [386]. Particles that are too large face mass and heat transfer limitation during hydrolysis (or depolymerization). For industrial application,the optimal grinding size for PMMA is between 5 mm to 15 mm [35]. From our experience, artificial marble is harder but more brittle than PMMA, so that shredding to 3 mm is feasible, and grinding to 1 mm is possible if necessary.

5.2.7 Hydrolysis in the stirred tank reactor

The system consists of an Inconel 5 L stirred tank reactor with a single flight helix impeller, a Bronkhorst CEM 202 producing 5 barg superheated steam at reaction temperature with nitrogen as carrier gas, a manual particle feed port, a Chemtech DEWAR type lower reservoir for condensing reaction gases and collecting samples online, and a cold trap with a 1:1 ice and ice melter mixture (NaCl, $MgCl_2$, $CaCl_2$) from a hardware store (Annex Figure C.1). Once the reactor reaches the selected reaction temperature under a 400 mL/min nitrogen flow, we feed the solid surface particles (artificial marble) in batch or semi-batch fashion, 300 g or 20 g in two shots respectively, and start to feed water to the steam generator. Reaction gases are condensed, sampled, and collected with about 0.02 g of hydroquinone per aliquot as a polymerization inhibitor. The gases from the Dewar condenser are further cooled at −20 °C in a cold trap for maximum product collection. Nitrogen and the incondensable gases are sampled in 5 or 10 L gas bags and immediately analyzed in a GC-FID to quantify CO, CO_2, and CH_4.

After the reaction, the reactor cools overnight under reduced flow of nitrogen (100 mL/min), and the following day we collect the solid residue as a fine powder. The objective is to determine the conditions and mechanisms that yield the highest amount of MMA or MAA from artificial marble chemical recycling. We conducted a series of OFAT (one factor at the time) tests on temperature (T), agitation rate (A) and H_2O/PMMAeq molar ratio (R), along with additional test without steam, introducing dehydration ramps to study the effect of water naturally contained in the composite ($Al(OH)_3$) on the process (**Table** 5.1). Additionally, we investigated the effect of zeolite Y, an heterogenous catalyst, on PMMA and/or MMA hydrolysis to MAA [81, 82, 347, 387](Annex Figure C.1).

5.2.8 Hydrolysis of PMMA to PMAA

As a FTIR reference for hydrolyzed PMMA, we partially hydrolyzed some of the ester sites of virgin PMMA in a 150 mL stainless steel autoclave reactor at 240 °C for 40 hrs, with a wt. PMMA to DI water ratio of 1:2.5 (30 g of polymer and 75 g of water per batch). The resulting polymer dries at 65 °C under vacuum to remove the excess water. To confirm the polymer nature and grade of hydrolysis we analyzed thermo gravimetrically, with FTIR, and with potentiometric titration in acetone with aqueous 0.1 NaOH M as titrant. The partially hydrolyzed PMMA is used here as reference FTIR, and is part of a pyrolysis study on PMMA/PMAA copolymer whose results will be part of a future paper.

Table (5.1) Single-factor-at-a-time (OFAT) tests + additional tests.

Test	**Factor or Test Type (Hydrolysis H, Dehydration D, Pyrolysis P)**	**Temperature (T), Agitation rate (A), H_2O:PMMA mol. (R)**
0	P	350 °C, 100 rpm, No Steam 1.6
1	(T) - H	300 °C, 100 rpm, 8.5
2	(T) - H	460 °C, 100 rpm, 8.5
3	(T) - H	350 °C, 100 rpm, 8.5
3C	3 catalytic 10:1 (g g^{-1}) PMMAeq - H	350 °C, 100 rpm, 8.5
4	(T) - Additional - H	420 °C, 100 rpm, 8.5
5	(A) - H	350 °C, 150 rpm, 8.5
7	(R) - H	350 °C, 100 rpm, 18.9
7C	7 catalytic 10:1 (g g^{-1}) PMMAeq - H	350 °C, 100 rpm, 18.9
10	Additional - D 300 °C, H 400 °C	D then H, 100 rpm, 18.9
12	Additional - (T) and (R) H	400 °C, 100 rpm, 18.9
16	Additional - D and P	D 250 °C P 350 °C, 100 rpm, No Steam 1.6
18	Additional - D and P	D 300 °C P 400 °C, 100 rpm, No Steam 1.6

5.3 Results

5.3.1 Characterization of waste artificial marble

ATR FT-IR spectroscopy (Fig. 5.2a) confirms the PMMA nature of the polymer part of the artificial marble. The supernatant of a suspension of composite powder in acetone sharply absorbs at 1730 cm^{-1}, corresponding to the ester carbonyl peak, 1150 cm^{-1} and 1190 cm^{-1} , the C-O-C ether symmetric and asymmetric vibrations, and at 2850 cm^{-1} and 2950 cm^{-1}, the methyl stretches (Annex Table C.4).

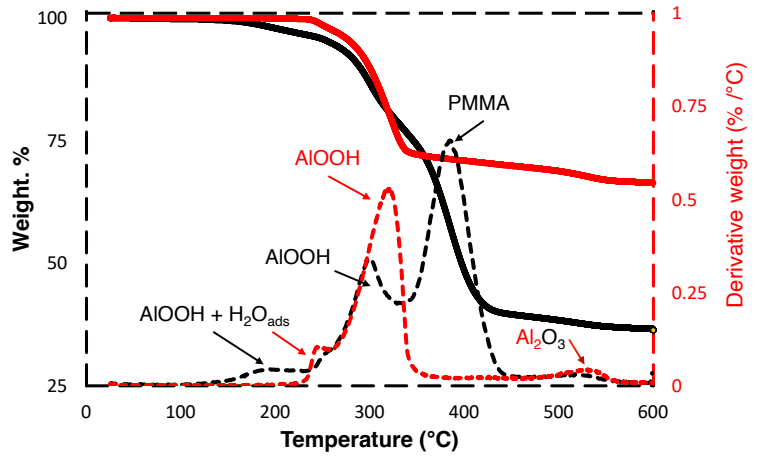

(a)

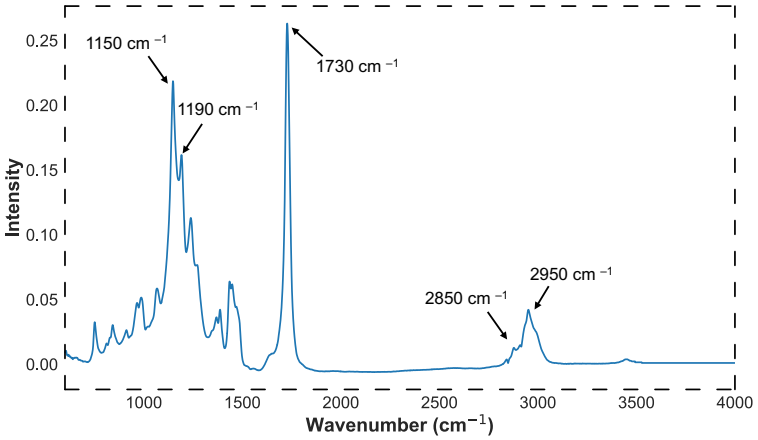

(b)

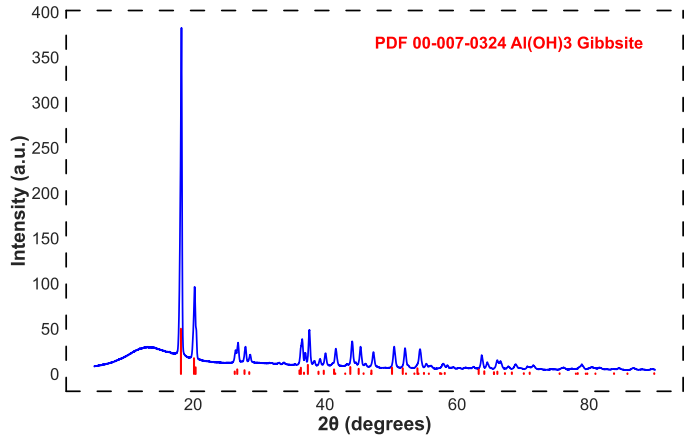

(c)

Figure (5.2) Characterization of the end-of-life artificial marble through: **a)** TGA in 40 mL/min Nitrogen, at 10 °C/min up to 600 °C, and **b)** ATR FT-IR spectrum in the 600 cm^{-1} to 4000 cm^{-1} range. **c)** Artificial marble X-Ray diffraction spectrum, with Gibbsite diffraction patterns from the PDF database of the International Centre for Diffraction Data [388].

Similarly, XRD spectra of artificial marble suggests that $Al(OH)_3$ is present in gibbsite form (Fig. 5.2c), which aligns with Dupont's claims for their "Corian" artificial marble [389]. TGA of artificial marble versus pure gibbsite differentiate the thermal degradation of organic and inorganic fractions (Fig. 5.2a). Gibbsite ($Al(OH)_3$) has two theoretical weight losses within 25 °C to 600 °C [390]: **(i)** $Al(OH)_3$ to AlO(OH) for a theoretical weight loss of 23.08 % around 300 °C, with concurrent parasite further dehydration to χ - Alumina (few (g g^{-1}) [391,392]); and **(ii)** AlO(OH) to Al_2O_3 (usually γ - Alumina) for a theoretical weight loss of additional 11.54 % around 525 °C.
These are confirmed by our analysis, which also shows a small additional weight loss starting at 180 °C, representing the release of adsorbed water and the start of gibbsite dehydroxylation to boehmite [390, 393]. TGA of pure boehmite versus artificial marble reveals one additional peak corresponding to PMMA degradation weight loss at 400 °C [348]. This temperature is slightly higher than the 360 °C to 380 °C found for pure PMMA [394], which depends on molecular weight and polymer grade, affecting the thermal degradation route (i.e. initiation, propagation, termination) [35]. The higher peak degradation temperature in artificial marble is reasonable due to its enhanced thermal and flame resistance necessary for the final application. PMMA is degrades completely past 500 °C, and the alumina weight loss at 525 °C overlaps in the TG of artificial marble and gibbsite. From the composite TG curve we estimate the polymer and inorganic (ceAl(OH)3) weight percentage in our artificial marble to be 44 % (g g^{-1}) and 56 % (g g^{-1}), respectively.

5.3.2 Artificial Marble Pyrolysis

Artificial marble pyrolyses at 350 °C in batch, [49, 86, 348, 380], and we selected it as benchmark test (Test 0) (Fig. 5.3). The composite pyrolysis produces up to two liquids, one solid and one gas product. The liquids are: an oil rich phase with MMA, the organic by-products, and part of the methanol; and an aqueous rich phase with water, most methanol (70 % to 90 % at any given liquid aliquot), and acids. Initially, the reaction produces both liquid fractions, with aqueous phase collection faster than the oil counterpart (Fig. 5.3b), due to the lower temperature of gibbsite dehydration compared to PMMA depolymerization. As $Al(OH)_3$ dehydration to AlO(OH) decelerates, the aqueous phase yield decreases, favouring the oil-rich liquid phase, containing MMA, but also methanol. MMA fragmentation to methanol is possible [395], yet negligible at 350 °C [131], because this phenomenon usually emerges above 450 °C. The only other route of methanol production is therefore through hydrolysis of either MMA or PMMA, which supports its choice as hydrolysis indicator.
Solid residues contain the inorganic fraction, the char resulting from pyrolysis, and unreacted polymer depending on the conditions (Fig. 5.3c). Even without additional steam,

water released during $Al(OH)_3$ dehydration promotes PMMA hydrolysis, with up to 17 % of PMMAeq hydrolyzed, and only 39 % of PMMAeq depolymerized to MMA. At 350 °C solid residues contain 18 % unreacted PMMAeq, 3 % char, and 20 % of the starting PMMAeq converted to gases.

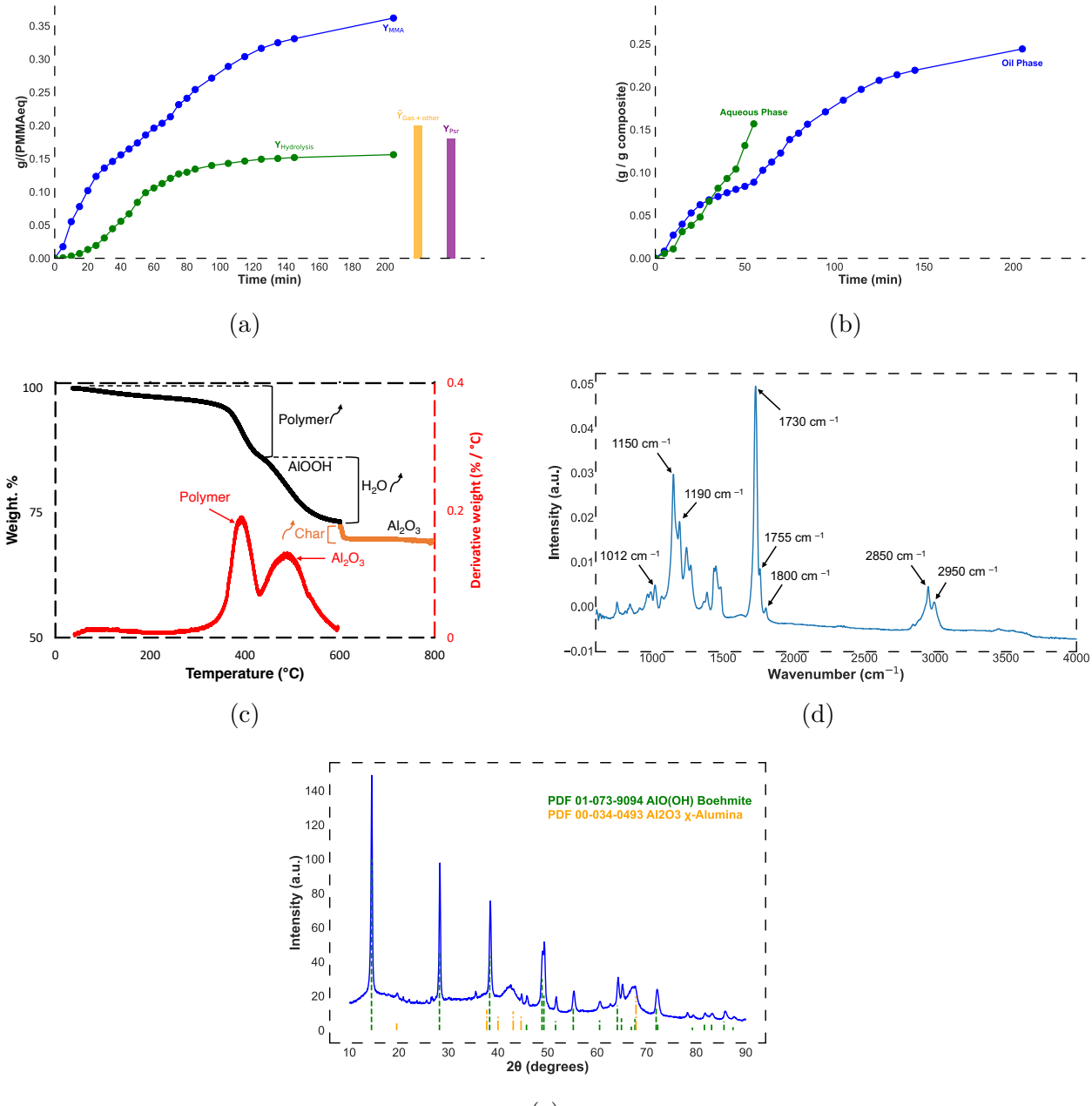

Figure (5.3) Pyrolysis of artificial marble (**Test 0** Table 5.1) **a)** and **b)**, and Solid residue Test 0 characterization **c)**, **d)**, **e)**. n=2 repetitions. **a** – cumulative MMA and Hydrolysis (Methanol) yields over time in terms of g of initial PMMAeq (eq. 5.5 and 5.6), and integral yields of gas and polymer in the solid residue. **b** – collected g of each phase (oil or aqueous) over time, divided by the starting mass of composite. **c)** Test 0 TGA in 40 mL/min of nitrogen gas, with a 10 °C min^{-1} ramp from 25 °C to 600 °C, followed by a 30 min isotherm (black curve for weight and red for derivative weight). Then, air replaces nitrogen at a 10 °C min^{-1} ramp up to 800 °C (orange curve for mass). **d)** FT-IR spectrum of the polymer fraction of the solid residue in Test 0 – Artificial marble pyrolysis at 350 °C, in the 600 cm^{-1} to 4000 cm^{-1} range. **e)** Test 0 solid residue X-Ray diffraction spectrum, with boehmite and χ-Alumina diffraction patterns from the PDF database of the International Centre for Diffraction Data [388].

The polymer in the solid residue of Test 0 absorbs at the characteristic peaks of PMMA (1730, 1150, 1190 (cm^{-1})), but also PMAA anhydride (1800 and 1755 (cm^{-1})) indicating PMMA hydrolysis to PMAA, which then dehydrates to its anhydride form (Fig. 5.3d). Pyrolysis also introduced a C-O-C peak at 1012 (cm^{-1}), characteristic of degraded PMAA [395]. The presence of PMAA anhydride also explains the absence of the typical broad hydroxyl hump at 3500 cm^{-1} and the carbonyl peak split at 1700 cm^{-1} due to MAA.

Similarly, the XRD spectrum of the residue confirms that at 350 °C all gibbsite transforms to less hydrated forms (Fig. 5.3e), predominantly boehmite, with traces of χ-Alumina, releasing water in a 1:1 stoichiometric ratio to $Al(OH)_3$ (eq. 5.11).

However, despite that up to 17 % (g g^{-1}) of PMMAeq in the marble hydrolyzes in Test 0, we only registered a Y_{MAA} (Eq. 5.4) of 1% (g g^{-1}), that confirms direct polymer hydrolysis rather than depolymerization to MMA followed by gas-phase ester hydrolysis. To further investigate the hydrolysis mechanism and rate, we added steam and varied the reaction temperature.

5.3.3 Artificial Marble Hydrolysis

Effect of temperature

At a fixed agitation rate of 100 rpm, and a given water:PMMAeq molar ratio of 8.6(including inherent water from $Al(OH)_3$ and external steam), we hydrolyzed 300g of composite from 300 °C to 460 °C over 250 min (Fig. 5.4a and Table 5.4c). Both MMA and hydrolysis yields increase with the temperature, with MMA being more temperature-dependant. Chub et Al. demonstrated that "thermolysis (of virgin PMMA powder to MMA) reaction operates best above 350 °C, while hydrolysis is best at lower (below 290 °C) temperature" [81]. Our results indicate that both processes benefit from higher temperatures, though hydrolysis shows a less pronounced trend. Initially the hydrolysis is driven by the water inherently present in the composite, as suggests the overlapping of Test 3 and Test 0, which are conducted at the same temperature but differs in steam addition (in Test 3). Artificial marble is produced via kneading, molding and pressing of an homogeneously mixed dough, [396] which maximizes the phase contact, justifying this trend.

Then, once $Al(OH)_3$ transforms to AlOOH, external water starts reacting with MMA in both solid (ester site on the polymer) or gas phase. Above (350 °C) the hydrolysis is independent of the temperature, as Test 3 (350 °C), Test 4 (420 °C) and Test 2 (460 °C) yielded virtually the same amount of methanol. Again, the water released from the marble has the most influence on the hydrolysis rate. Hydrolysis yield curves of Test 2 and 4 plateau faster

than the one of Test 3, but then reach the same final value. The higher heating gradient on the composite drives the dehydration of $Al(OH)_3$, and dominates the hydrolysis.
The concentration of ester sites has a larger influence on the hydrolysis than the temperature. PMMAeq converts fully at temperatures above 420 °C (Table 5.4c). Higher temperatures favour thermolysis over hydrolysis, thus reducing available ester sites for hydrolysis. That is, only sites in close contact with $Al(OH)_3$ experience high local water partial pressure, which facilitates hydrolysis.. When hydrolyzing PMMA-PMAA copolymers in an aqueous medium at 110 °C, Loecker found that acid-ester pairs act as kinetic entities, and that ABA (acid-ester-acid) structures control the hydrolysis initially, catalyzed by unassociated carbonyl and carboxylate (COO-) groups [384].

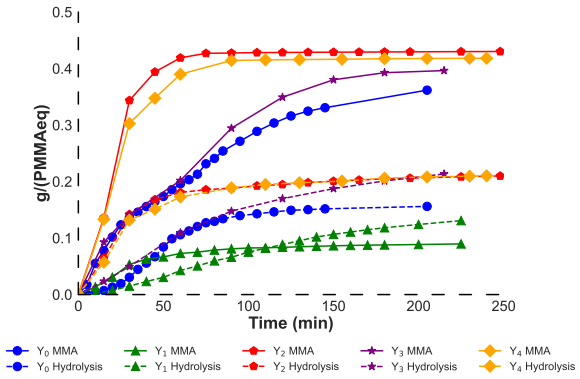

(a)

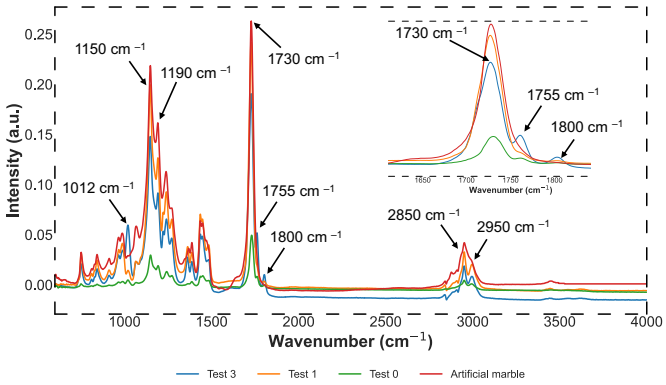

(b)

(c)

Test	T (°C)	**Water:PMMAeq mol.**	$Y_{\mathbf{MMA}}$ (g g^{-1})	$Y_{\mathbf{Hydrolysis}}$ (g g^{-1})	$Y_{\mathbf{MAA}}$ (g g^{-1})	**Polymer in residue** (g g^{-1})	$\tilde{Y}_{\mathbf{Char}}$ (g g^{-1})	$\tilde{Y}_{\mathbf{Gas+other}}$ (g g^{-1})
0	350	1.6	0.39	0.17	0.01	0.18	0.03	0.20
1	300	8.6	0.09	0.13	0.01	0.72	0.01	0.05
2	460	8.6	0.44	0.22	0.04	0.00	0.03	0.27
3	350	8.6	0.39	0.24	0.02	0.20	0.02	0.10
4	420	8.6	0.42	0.22	0.04	0.00	0.03	0.30

Figure (5.4) Hydrolysis tests results (Test 1 to 4) and Pyrolysis benchmark (Test 0) (Table 5.4c) for 300 g artificial marble in a stirred tank at 100 rpm. – Effect of Temperature. **a)** Cumulative MMA (solid line) and Hydrolysis (Methanol - dashed line) yields over time in terms of g of initial PMMAeq (eq. 5.5 and 5.6). **b)**FT-IR spectra of the polymer fraction of the solid residue in Test 0, 1, 3 and Artificial marble before reaction, in the 600 cm^{-1} to 4000 cm^{-1} range. Tests 2 and 4 contain only traces of polymer in the residue. Not shown for reason of scale, their spectra are qualitatively similar to Test 3. **c)** Overall integral results. The values appear (1 % to 2 %) higher than the final points of Fig. 5.4a due to liquid collected in the cold trap, counted in the final value but not shown in the profile over time.

Higher temperature runs maximize MMA yields and convert all PMMAeq, leaving no polymer in the solid residue (Table 5.4c). The maximum MMA yield is 0.44 (g g^{-1}) PMMAeq for run 4, comparable to [86], and 10 % to 20 % higher than [348], both performing anhydrous pyrolysis of artificial marble in similar batch reactors and temperatures. Similarly, higher temperature runs produce more gases, due to the cracking of MMA (e.g. CO_2 + CH_4, or CO + CH_3OH) [397], or decarboxylation of the (PMAA) anhydride ring structure (releasing CO_2 and CO in two steps) [395,398]. Methane was absent in Tests 0, 1, 3, and only around 1 mol % in Tests 2 and 4. Instead, for instance in Test 4, 88 % (g g^{-1}) of gases were CO_2, and 10 % (g g^{-1}) CO. The abnormal presence of carbon oxides in aluminium tri-hydroxide filled PMMA pyrolysis had already been noted by [49], which had assigned it to (parasitic) "saponification reactions". We argue that due to the high temperatures, PMMA first hydrolyses to PMAA, which then degrades. The second degradation step of PMAA anhydride (producing CO), starts around 400 °C to 420 °C, within operative T of Test 4.

The polymer in the solid residue absorbs, for all tests, at characteristic PMMA and PMAA anhydride wavelengths (Fig. 5.4b), and its amount correlates with the temperature. Similar to Test 0, there is a mismatch between the Y_{MAA} and the hydrolysis yield. Tests 2, 3, and 4 produced a slightly more MAA than the pyrolysis benchmark, but still not enough to justify MAA as target product from artificial marble recycling. Higher temperature tests produce more MAA, but we argue that is due to the PMAA anhydride degradation more than the gas phase hydrolysis.

The inorganic fraction of the residue transformed from gibbsite to boehmite completely in Test 3, but only partially in Test 1. In Tests 2 and 4, the temperature promotes the second dehydration step of the hydroxide. From the TGA plot, we calculate that in Test 2, 8 % (g g^{-1}) of boehmite started to lose its second molecule of water, and in Test 4, 1 % (g g^{-1}). The XRD confirms the presence of Alumina peaks in the solids.

5.3.4 Effect of water and agitation

We assumed the agitation rate had a negligible effect compared to temperature and water:PMMAeq ratio. To validate tthis, we repeated Test 3 at 150 rpm instead of 100 rpm (Test 5) (Table 5.1). The Y_{MMA} are identical, same for the polymer in the solid residue, which confirms that temperature controls the thermolysis (Annex Figure C.2). $Y_{\mathrm{Hydrolysis}}$ is slightly higher (0.27 vs 0.24) in Test 5, hinting that the stirring rate, correlated with the internal mixing, affects both the steam-composite contact, and the $Al(OH)_3$ dehydration rate. However, we continued our design of experiment with an agitation rate of 100 rpm, because we believed that the maximum output agitation rate (150 rpm), would not have substantially affect results. Future work optimize mixing conditions (type of stirrer and agitation rate)

to maximize the steam/composite contact, or minimize the pyrolysis time, similar to what Berruti et Al.'s "mechanically agitated fluidized bed" for biomass [399]. Both organic and inorganic residue fractions are also virtually identical in nature (Annex Figure C.3C.4).

Increasing the vapour rate more than twofold (from 40 to 100 mL/hr) promote hydrolysis, and, as a side-effect, MAA production (Table 5.6c). At 350 °C, compared to Test 0 and 3, in Test 7 the same amount of polymer remains in the solid residues, but almost no gas at all is produced. Concurrently,The polymer in Test 7's solid residue has both anhydrous (glutaric 1755 and 1800 cm^{-1}) and "hydrated" features of PMAA (O-H stretching around 3500 cm^{-1}), along with the characteristic 1730 cm^{-1} PMMA peak. This validates Grant's assumption that the PMAA decomposition is a reversible process [382]:

$$\text{two neighbouring acids} \longleftrightarrow \text{anhydride} + \text{trapped water} \longrightarrow \text{anhydride} + \text{free water} \tag{5.11}$$

whose equilibrium would usually favour the products as water continuously leaves the system. In our case, due to a local large excess of water during the reaction (18.9 water:PMMAeq mol), the equilibrium shifts back to the reagents, which the FT-IR of the remaining polymer residue confirms too (Fig. 5.5b).

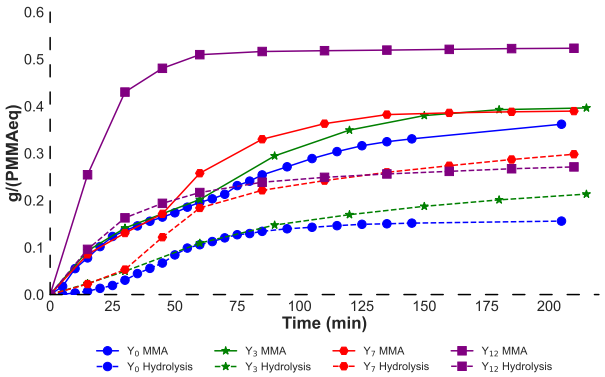

(a)

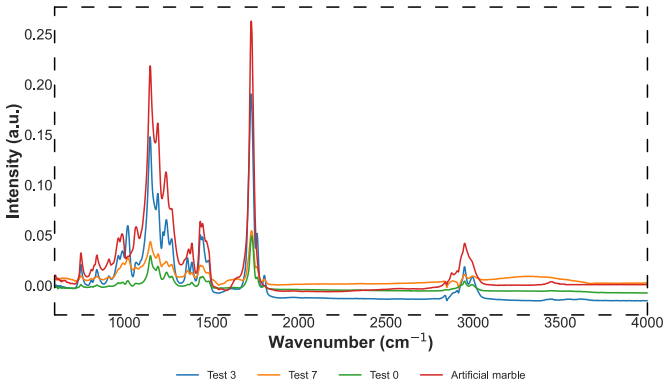

(b)

(c)

Test	T (°C)	Water:PMMAeq mol.	Y_{MMA} (g g^{-1})	$Y_{\mathrm{Hydrolysis}}$ (g g^{-1})	Y_{MAA} (g g^{-1})	Polymer in residue (g g^{-1})	$\tilde{Y}_{\mathrm{Char}}$ (g g^{-1})	$\tilde{Y}_{\mathrm{Gas+other}}$ (g g^{-1})
0	350	1.6	0.39	0.17	0.01	0.18	0.03	0.20
3	350	8.6	0.42	0.24	0.02	0.20	0.02	0.10
7	350	18.9	0.41	0.32	0.04	0.19	0.03	0.02
12	400	18.9	0.53	0.29	0.05	0.00	0.03	0.14

Figure (5.5) Hydrolysis of artificial marble (**Test 3, 7, 12**) and pyrolysis benchmark (**Test 0**) for 300 g artificial marble in a stirred tank at 100 rpm, over two repetitions. - Effect of water. **a)** Cumulative MMA (solid line) and hydrolysis (methanol - dashed line) yields over time in terms of g of PMMAeq in the initial sample (eq. 5.5 and 5.6). **b)** FT-IR spectrum of the polymer fraction of the solid residue in Test 0, 7, 3 and artificial marble before reaction, in the 600 cm^{-1} to 4000 cm^{-1} range. Tests 7 presents both peaks of PMAA and PMAA anhydride. Test 12 has close to no polymer in the residue. **c)** Overall integral results. The values appear slightly (1 % to 2 %) higher than the final points of Fig. 5.5a due to liquid collected in the cold trap that is counted in the final value but not shown in the discrete measurements over time. Symbol size represents the standard deviation over n=2.

At an equal water:PMMAeq ratio, but higher temperature (400 °C vs 350 °C), Test 12 yields roughly the same methanol amount as Test 7 (Table 5.6c), which confirms that local water content, rather than temperature, controls the hydrolysis rate (Fig. 5.5a). Test 7 and Test 12 $Y_{\text{Hydrolysis}}$ curves have different initial slopes, but similar plateau trends. Test 3 (350 °C and water:PMMAeq mol. 8.6) and Test 7 have overlapping initial $Y_{\text{Hydrolysis}}$ trends, but reach different final values. This reinforces that the water inherently present in the polymer drives the initial hydrolysis, and that above (350 °C), the overall hydrolysis becomes temperature-independent. Similarly to Test 2/4 vs Test 3, in Test 12 PMMA thermolysis is faster than hydrolysis compared to Test 7 because of the higher reaction temperature, and this reduces the availability of ester sites, or more in general ester-acid kinetic pairs, thus limiting the hydrolysis and maximizing the Y_{MMA}.
Local water content has limited effect on the global Y_{MMA}, with Test 7 and Test 3 producing similar MMA amount, comparable to regular pyrolysis at the same temperature (Test 0). Surprisingly, Test 12 reports the highest Y_{MMA} so far, despite higher water content compared to, for instance, Test 4 (420 °C for Test 4 vs 400 °C for Test 12). We attribute this behaviour to the absence of mist in the condenser while PMMA hydrolyses under a higher steam flow. Mist formation during PMMA pyrolysis inhibits MMA recovery. Laboratory-scale setups do not experience this phenomenon because they operate in a large excess of cooling, but recyclers report it in both academic and patent literature [57, 400]. In our case, the steam traps the mist and maximizes collected MMA.
The water content has a negligible effect on $Al(OH)_3$ transformation, which fully dehydrates to boehmite (with alumina traces) regardless of steam flowrate. We postulate this is due to a limited water partial pressure.

5.3.5 Effect of Zeolite Y

Despite the large water excess and the intimate contact between the supposedly catalytic alluminium hydroxide (in gibbsite or boehmite form) and PMMAeq, hydrolysis of PMMA to MAA through PMAA degradation overshadowed hydrolysis through MMA monomer. To nullify our initial hypothesis that:

"PMMA first depolymerize to MMA and then, if we maximize the water partial pressure in the system, MMA hydrolyze to MAA.

we hydrolyzed artificial marble mixed with 10:1 (g to g) PMMAeq:Zeolite Y, under the same conditions of Test 3 and Test 7, in what are now Test 3C and 7C (C stands for catalyzed) (Fig. 5.6). The catalyst has no effect on the methanol production ($Y_{\text{Hydrolysis}}$), but

affects both Y_{MAA} and Y_{MMA} (Fig. 5.6a), as well as the by-products (Annex Table C.1).

In presence of Zeolite Y, Y_{MAA} increases at the expense of Y_{MMA}, compared to equivalent runs without the catalyst. Concurrently, Tests 3C and 7C yielded a higher amount of gas and polymer in the solid residue. Since $Y_{Hydrolysis}$ remains unvaried with or without the catalyst, we conclude that the missing Y_{MMA} remains as solid in the residue, and the extra Y_{MAA} comes from MMA hydrolysis in gas phase within the zeolite as opposed to PMAA degradation. The gas phase composition of the two tests confirms that Zeolite Y promotes hydrolysis of the ester sites of the polymer. In fact, Test 3 only yields CO_2, while Test 3C both CO_2 and CO (75/25 wt. %). This suggests that in Test 3C the anhydride undergoes the second decomposition step, unlike Test 3. We argue that in presence of zeolite, there is an additional consumption of water to hydrolyze MMA in the gas phase, leaving less water available to rehydrate the anhydride in the acid pair.

For Tests 3 and 3C, despite the different quantity, the polymer in the residue remains of the same nature (Fig. 5.6b). Instead, in Test 7C, compared to Test 7, the small broad shoulder at 3500 $^{-1}$ disappears, and the anhydrous peaks are more intense compared to the ester peak. An alternative explanation is that zeolite adsorbs a significant amount of water (internal and external). This would reduce the hydrolysis in the polymer but increase the one of MMA vapour reacting on the zeolite. Hence, unchanged methanol production.

Many other catalysts and different PMMAeq:Zeolite Y proportions could be investigated. However, the results of Test 3C and 7C demonstrate that artificial marble will be difficult to convert one-pot to MAA, because part of PMMAeq inevitably converts to PMAA. A better approach would be to first maximize MMA production by minimizing the internal partial pressure of water as much as possible, and only then convert catalytically MMA (in gas form) to MAA by adding the released water in a separate reactor.

The catalyst addition does not change the nature of inorganic fraction, which remains mostly boehmite with some χ-alumina (Annex Figure C.5). However, since zeolite contains SiO_2 and Al_2O_3, its addition complicates the inorganic residue analysis and potential downstream recovery.

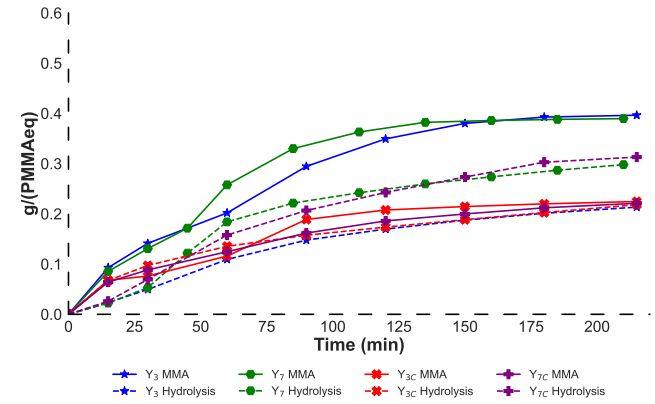

(a)

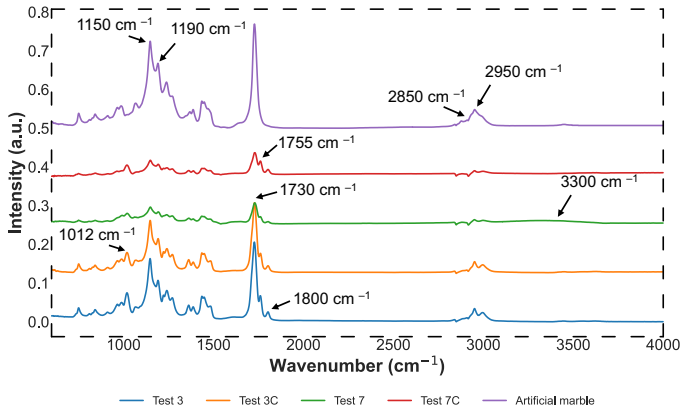

(b)

(c)

Test	T (°C)	Water:PMMAeq mol.	Y_{MMA} (g g^{-1})	$Y_{\mathrm{Hydrolysis}}$ (g g^{-1})	Y_{MAA} (g g^{-1})	Polymer in residue	Y_{Char} (g g^{-1})	Y_{Gas} (g g^{-1})
3C	350	8.6	0.24	0.24	0.09	0.27	0.05	0.20
3	350	8.6	0.42	0.24	0.02	0.20	0.02	0.10
7	350	18.9	0.41	0.32	0.04	0.19	0.03	0.02
7C	350	18.9	0.25	0.35	0.08	0.26	0.00	0.14

Figure (5.6) Hydrolysis of artificial marble with (**Test 3C, 7C**) and without (**Test 3, 7**) 10:1 wt. PMMAeq:Zeolite Y (13.3 g of zeolite Y) for 300 g artificial marble in a stirred tank at 100 rpm, over two repetitions – Effect of catalyst. **a)** Cumulative MMA (solid line) and Hydrolysis (Methanol - dashed line) yields over time in terms of g of PMMAeq in the initial sample (eq. 5.5 and 5.6). **b)** FT-IR spectrum of the polymer fraction of the solid residue in Test 3C, 7C, 7, 3 and Artificial marble before reaction, in the 600 cm^{-1} to 4000 cm^{-1} range. **c)** Overall integral results. The values appear slightly (1 % to 2 %) higher than the final points of Fig. 5.6a due to liquid collected in the cold trap that is counted in the final value but not shown in the discrete measurements over time. Symbol size represents the standard deviation over n=2.

5.3.6 Heating Ramp effect

We demonstrated that the water released from $Al(OH)_3$ promotes the solid hydrolysis of PMMA, regardless of the temperature, external water local partial pressure, or catalyst presence. However, this process impedes the valorization of the polymer component of the composite, whether it is MMA or MAA. Therefore, we investigated the effect of a heating ramp during hydrolysis or pyrolysis to enhance the economic viability of artificial marble recycling as a whole.

In Test 10, we heated the composite, without external steam, at 300 °C until condensation ceased (150 min). removing about 98 % (g g^{-1}) of the water from gibbsite. Then, we hydrolyzed the "dehydrated polymer" at 400 °C (Fig. 5.7b) with added steam. Compared to Test 12, operating under identical hydrolysis conditions, Test 10 yields the same Y_{MAA}, but a higher $Y_{Hydrolysis}$ at the cost of Y_{MMA}, with equivalent gas amount, and no char. Additionally, while Test 12's gas products contained 1%/85%/13% $CH_4/CO_2/CO$ (by mass), Test 10 produced only CO_2 and CO, in similar concentrations as Test 12, but no methane. We conclude that dehydrating the composite before hydrolyzing the remaining PMMAeq offers minimal advantages. Despite the high temperature (400 °C), the hydrolyzed PMMAeq mostly converts to PMAA or its anhydride form.

During the dehydration, we found only CO_2 in the gas phase. When the Y_{MMA} plateaus (after 230 min Fig. 5.7b), we started to detect CO, in small amount. This corresponds to the time when MAA condensed most in our liquid, which corroborates that some (or most) of this MAA comes fromPMAA degradation.

Instead, for pyrolysis, pre-dehydration benefits MMA recovery. A first heating ramp at 250 °C for 210 min (until condensation ceased) dehydrated the composite, followed by pyrolysis (in absence of steam) at 350 °C (Test 16). Compared to Test 0, which is the composite pyrolysis at 350 °C, Test 16 yielded similar liquid products amount (Methanol, MMA, MAA), but less gas (0.09 vs 0.20), and more polymer in the solid residue (Table 5.7c). The residual polymer of Test 16 contains peaks of PMMA and PMAA, but it is qualitatively more hydrated (1600 cm^{-1} and 3500 cm^{-1}) than Test 0 (Annex Figure C.6). In fact, If the polymer only contains isolated acids, they cannot rearrange in the glutaric anhydride type ring and form an anhydride. The only gas product was CO_2, and no CO formed, and there is no gas produced during the dehydration step.

since only 15 % (g g^{-1}) of the gibbsite's water is released at 250 °C, in Test 18, we operated the reactor at 300 °C until no further condensation (150 min), and then we increased the T to 400 °C to maximize Y_{MMA}. Again, the most part of the water is released in the dehydration step, and the rest as soon as the temperature ramps up to 400 °C. This approach minimizes

$Y_{\text{Hydrolysis}}$ and Y_{MAA}, that is now a by-product. Concurrently, we maximize the Y_{MMA}, reaching 66 % (g g^{-1}), the highest among all tests. Compared to Test 12 (Table 5.7c), where during hydrolysis at 400 °C there was no polymer in the solid residue, Test 18 retained 9 % (g g^{-1}) PMMAeq in the residue.
In this case too, over 98 % (g g^{-1}) of the gas is CO_2, withCO appearing only after Y_{MMA} and $Y_{\text{Hydrolysis}}$ plateaus (around 220 min). Chein and al. demonstrated how when PMAA dehydrates to its anhydride form, 1 mol of water is released for half mol of MAA group dehydrated, and 15 moles of water are detected for each mol of CO_2 produced. In Test 18, this would mean that roughly half of the PMAA produced is PMAA anhydride [398]. More precise calculations are outside the scope of this work, but they could be part of future potential studies to study in detail the kinetics of PMMA hydrolysis and dehydration, to understand how to minimize it.

The polymer in residue in Test 18 absorbs at ester and acidic wavelength (Annex Figure C.6), but it has a small, yet visible, broad peak at 1600 cm^{-1}. Some authors assign this peak to moisture or water adsorbed [401], while others to molecular H_2O bending [402]. Surprisingly, this same hump is not present in the solid residue of Test 1 (Fig. 5.4b), that was an hydrolysis at 300 °C, where one could have expected some water to be still present. We cannot explain this peak as moisture after pyrolysis at 400 °C (Test 18). Therefore, we assume that it must be water bending due to the fraction of hydrated PMAA, in an otherwise mixture of PMMA and PMAA anhydride. This would confirm the amount of CO_2 detected in gas phase.
Some polymer in the solid residue is acceptable and even beneficial. If the solid residue undergoes further calcination to transform boehmite into γ-alumina to increase its value, the residue polymer's combustion renders the calcination energy self-sufficient. We calculated with about 10 wt. % polymer in the solid residue, with thermal properties similar to those of PMMA, its heating content is sufficient for calcination and flue gas losses in a hypothetical furnace (Annex C.1). Additionally, the char ameliorates the residue's lubricant properties, which aids the shaping prior to calcination.

We demonstrate that transforming gibbsite to boehmite, while maximizing MMA recovery, is more viable if done in two steps. First, we need to release the water in the inorganic fraction, at 300 °C, which promotes transformation but hinders PMMAeq thermolysis. Then, when all (or most) of the water is released, we increase the temperature to 400 °C to recover the most MMA with minimal carbon losses. Despite the ramp, the inorganic fraction conveniently transforms to boehmite (with some χ-alumina impurities) (Annex Figure C.7), which can be

further calcined to γ-alumina (Fig. 5.1b), ensuring the process is economically viable.

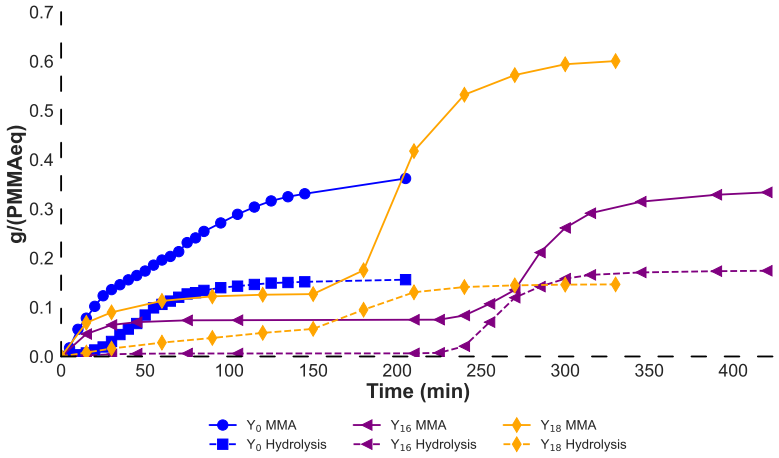

(a)

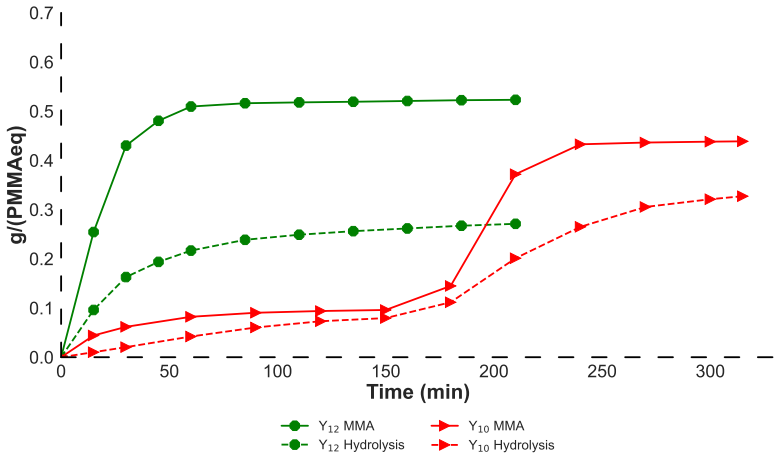

(b)

(c)

Test	T (°C)	**Water:PMMAeq mol.**	$Y_{\mathbf{MMA}}$ (g g^{-1})	$Y_{\mathbf{Hydrolysis}}$ (g g^{-1})	$Y_{\mathbf{MAA}}$ (g g^{-1})	**Polymer in residue** (g g^{-1})	$\tilde{Y}_{\mathbf{Char}}$ (g g^{-1})	$\tilde{Y}_{\mathbf{Gas+other}}$ (g g^{-1})
0	350 P	1.6	0.39	0.17	0.01	0.18	0.03	0.20
10	300 D - 400 H	18.9	0.47	0.36	0.05	0.00	0.00	0.15
12	400	18.9	0.53	0.29	0.05	0.00	0.03	0.14
16	250 D - 350 P	1.6	0.37	0.19	0.02	0.32	0.02	0.09
18	300 D - 400 P	1.6	0.66	0.16	0.01	0.09	0.00	0.08

Figure (5.7) Effect of heating ramp on pyrolysis ((**a**) Test 0, Test 16, Test 18) and hydrolysis (**b**) - Test 10, Test 12), on 300 g of artificial marble in a stirred tank at 100 rpm, over two repetitions. D stands for dehydration, H for hydrolysis, and P for pyrolysis. (**c**) Overall integral results. The values appear slightly (1 % to 2 %) higher than the final points of Fig. 5.7b and Fig. 5.7a due to liquid collected in the cold trap that is counted in the final value but not shown in the discrete measurements over time. Symbol size represents the standard deviation over n=2.

5.3.7 Semi-continuous tests

Batch tests help understand overall mass balance and reaction mechanisms but have drawbacks, especially at the bench-scale level The issue is temperature control. If we charge the composite beforehand and then heat the entire reactor, the material to start depolymerizing during the heat-up phase due to the artificial marble degradation temperature spectrum (Fig. 5.2a). Unless the heating rate is high enough to immediately bring the composite to test temperature, transient conditions will occur after we feed the sample in the reactor. To minimize these effects we repeated all tests in a semi-batch/continuous fashion where possible. At the end of the batch test, we injected two 10 g shots of artificial marble in the reactor, already containing hot, stirring "solid residue". The hot mass acts as heat transfer medium, which ensures near-immediate heating to reaction temperature on the incoming 10 g shot. For the catalyst test (C), we injected the equivalent proportional amount of catalyst (1g catalyst : 10g PMMAeq) with each 10 g composite shot.
In semi-continuous tests, the fresh solid is dispersed in a larger amount of spent residue, increasing the global water ratio but reducing the local partial pressure during hydrolysis. During the batch reactions, PMMAeq is surrounded by transforming gibbsite particles, while superheated steam sparges on it. In the semi-contionous tests, the 10g batch particle contact more external steam (from to 8.6 to 18.2 for the middle level of the DOE level), but they have less interaction with each other. In fact, the batch test, 300 g of artificial marble reacts under a 40 g/hr steam flowrate in 250 min, whereas in semi-continous test, instead, sees 10 g + 10 g of composite react under the same steam flow in 40 min.
In the semi-continuous tests, we eliminate transient regimes to directly assess the impact of external steam and intrinsic hydrolysis of individual particles, free from the interference from surrounding evaporating medium. We conduct these tests following batch tests and collect the resulting solid residues together. We assume the semi-continuous aliquot is sufficiently diluted to avoid influencing overall results. This setup allows us to sample gas and directly compare it with batch test samples.

Despite the effective higher amount of water, the semi-continuous tests have (overall) similar $Y_{\text{Hydrolysis}}$, but much lower Y_{MMA} (Fig. 5.8) compared to their batch counter parts (Fig. 5.8a, 5.8b). Gas yields are equivalent at temperatures below 350 °C, but higher at 400 °C. Exceptions are the semi-continuous catalyzed tests, 3C and 7C, with higher $Y_{\text{Hydrolysis}}$ and lower Y_{gas} (CO and CO_2 Table 5.8c) than their batch version. The Y_{MAA} remained similar, within ±3 %. Because of the low quantity, we cannot draw any definitive conclusion about it. What is interesting is how the tests within the semi-continuous series compare.
In the batch test, 7C and 7, and 3C and 3 had similar $Y_{\text{Hydrolysis}}$, respectively. However, in

the semi-continuous tests, both 7C and 3C produced significantly more methanol compared to 7 and 3, and their batch counterparts. Other pairs with comparable $Y_{\text{Hydrolysis}}$ in batch (4 and 2, and 7 and 12) maintained similar trends in the semi-continuous series. The CO_2 to CO ratios also remained consistent between continuous and batch, except for Test 10 and 12 in semi-continuous, which effectively became the same test due to the challenges of staged heating in continuous mode, yielding identical results. Test 7 in batch and Test 3 in semi-continuous run under nominally the same conditions, with a globally but not locally equivalent water ratio. Yet, Test 7 in batch hydrolyses more PMMAeq than Test 3 in semi-continuous. We attribute this to the type of contact between water and MMA sites. In Test 3 semi-continuous, 1 g of artificial marble is surrounded by about 19 grams of "spent" dehydrated AlOOH, while in Test 7 batch, 20 g of hot stirring solid dehydrate simultaneously. Therefore, surrounding particles have a much higher effect on the hydrolysis than external steam (Table 5.8c). Test 12 in batch vs Test 9 in continuous lead to similar conclusions.

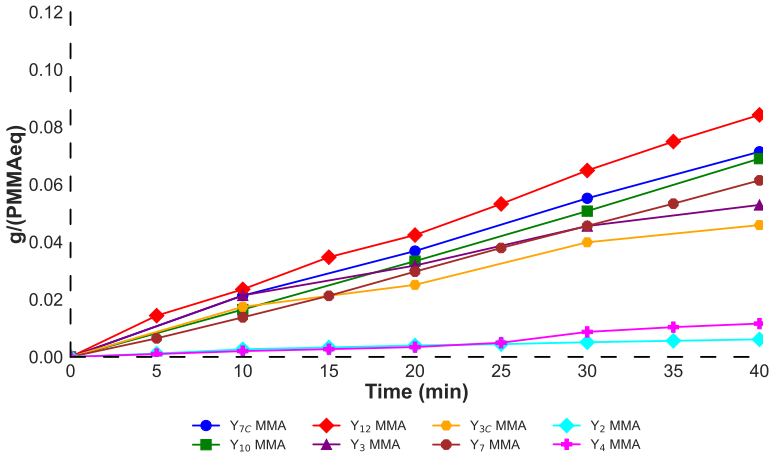

(a)

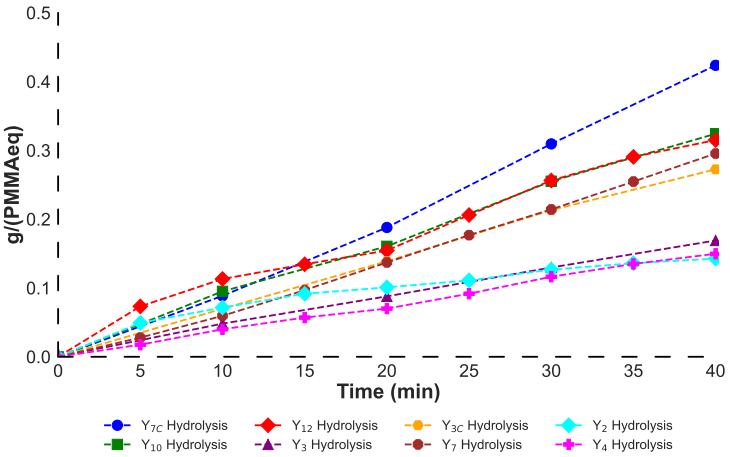

(b)

(c)

Test Batch - (Continous)	T (°C)	**Water:PMMAeq mol.**	$Y_{\mathbf{MMA}}$ (g g^{-1})	$Y_{\mathbf{Hydrolysis}}$ (g g^{-1})	$Y_{\mathbf{MAA}}$ (g g^{-1})	$Y_{\mathbf{CO2}}$ (g g^{-1})	$Y_{\mathbf{CO}}$ (g g^{-1})
7C	350	18.9 - (43.2)	0.25 - (0.07)	0.35 - (0.42)	0.08 - (0.04)	0.10 - (0.06)	0.04 - (0.02)
7	350	18.9 - (43.2)	0.41 - (0.04)	0.32 - (0.30)	0.04 - (0.06)	0.02 - (-)	0.00 - (-)
10*	300 D - 400 H	18.9 - (43.2)	0.47 - (0.07)	0.36 - (0.32)	0.05 - (0.07)	0.14 - (0.43)	0.01 - (0.05)
12*	400	18.9 - (43.2)	0.53 - (0.09)	0.29 - (0.32)	0.05 - (0.08)	0.12 - (0.49)	0.02 - (0.07)
3C	350	8.6 - (18.9)	0.24 - (0.05)	0.24 - (0.27)	0.09 - (0.04)	0.14 - (0.13)	0.06 - (0.04)
3	350	8.6 - (18.9)	0.42 - (0.05)	0.24 - (0.17)	0.02 - (0.02)	0.04 - (0.05)	0 - (0)
2	460	8.6 - (18.9)	0.42 - (0.01)	0.22 - (0.14)	0.04 - (0.01)	0.25 - (-)	0.02 - (-)
4	420	8.6 - (18.9)	0.44 - (0.01)	0.22 - (0.15)	0.04 - (0.01)	0.27 - (-)	0.03 - (-)

Figure (5.8) Y_{MMA} **a)** and $Y_{\mathrm{Hydrolysis}}$ **b)** profile over time for hydrolysis Tests, in semi-continuous mode. **c)** Overall integral results for selected tests in batch vs the equivalent semi-continuous mode test (into brackets), C stands for catalyzed, D for dehydration, and H for hydrolysis. (-) means that data is not available. * Test 12 and 10 in semi-continuous mode are effectively run under the same conditions, because the semi-continuous test starts at the end of the batch test and foresees no ramp. Symbol size represents the standard deviation over n=2.

5.4 Conclusions

To identify the most efficient and economically viable recycling route for waste artificial marble, we conducted pyrolysis and hydrolysis experiments, examining temperature effects, water content, catalyst presence, and heating styles in batch and semi-continuous modes. Artificial marble consists of organic and inorganic fractions, with the polymeric fraction potentially recyclable as MMA (ester monomer) or MAA (acid form). The inorganic fraction, similarly, has market potential as alumina in α or γ structure.
Our desired product for the polymer fraction was MAA. However, contrary to intuitive expectations, PMMAeq in the composite does not first depolymerize to MMA and then hydrolyze to MAA in the presence of water. Instead, ester sites on the polymer backbone partially hydrolyze to PMAA while undergoing thermolysis to MMA. Then, in an equilibrium reaction, PMAA dehydrates to its anhydride form, releasing H_2O, and finally PMAA anhydride degrades, releasing CO_2 and CO, indicating complete anhydride degradation. The hydrolysis reaction rate depends most on temperature and local water partial pressure.

To optimize the organic fraction's recovery, we minimize PMMAeq hydrolysis by staging thermolysis: first we release water at 300 °C, then we ramp up to 400 °C to depolymerize PMMAeq and collect maximum MMA. While this incurs additional capital costs, we can reroute the water released in the first step to a secondary hydrolysis reactor to convert the produced MMA to MAA via catalytic hydrolysis. This scenario is viable for highly contaminated post-consumer artificial marble streams, available at zero or negative cost, especially if there is a high local demand for "green" MAA. Otherwise, MMA production remains more favourable.

For instance, in Korea's dense population and localized artificial marble ecosystem, recyclers have access to both suppliers and customers, with limited logistics costs and a predisposed market and public opinion. Provided the quality of the final product is satisfactory, which staged heating achieves, MMA production is promising in this context.

The construction industry resorts to other resource-saving concrete-polymer composites: quartz or stone-filled PMMA in their many commercial declinations. Pyrolysis of such products is free of hydrolysis parasitic reaction, MMA quality is better, and the filling material can be calcined to be recycled in the same application. However, these composite have a lower % of PMMA (i.e. 20 %), and their inorganic fractions are inferior to boehmite or γ-alumina. Another example are wind blades made from PMMA, PET, PS, and fiberglass,

where the recycling requires to shorten the fiber, reducing its value (often to zero). In contrast, artificial marble is a unique case among hard-to-recycle composites. It starts with a 60/40 inorganic/organic feedstock and ends with a 25/75 organic/inorganic product. A viable business case is only possible when 100% of the product value is retained, which is achievable for artificial marble but not for many other composites.
Alongside MMA recovery, we demonstrate that the inorganic fraction of the marble transforms from $Al(OH)_3$ to a γ-alumina precursor, boehmite, regardless of the process conditions. Coke forms during the multi-step thermolysis, and it becomes a lubricant for the boehmite shaping, as well as an energy source for its calcination to γ-alumina. Coincidentally, the amount of coke formed in the two stage pyrolysis, is enough to render the calcination process energy self-sufficient, further reducing the carbon footprint of the final product.

With the overall hydrolysis mechanism now clearer, future research should focus on: (i) understanding how pyrolysis of a PMMA/PMAA composite proceeds, particularly how the MAA fraction influences the hydrolysis rate; and (ii) investigating whether the PMAA and PMAA anhydride polymer produced during hydrolysis is suitable as a rheology modifier, to instead prefer a complete polymer hydrolysis at low temperatures.

CHAPTER 6 CONCLUSION

6.1 Summary of works

PMMA is the best candidate to real plastic-to-plastic recycling. The success of MMAtwo project in Europe spurred interests in PMMA recycling projects around the world, but there is still a long way to go. Here we demonstrate how the academic and industrial research on PMMA recycling is disconnected, and that for the longest times universities have been investigating peripheral aspects. This work aims to bridge this gap, and to demonstrate valorization of post-consumer end-of-life PMMA waste, as: (before this work $\rightarrow$ after)

1. PMMA is one of the easiest polymers to depolymerize, but its global recycling rates remain low due to economic and technical challenges $\rightarrow$ Monte Carlo data-driven simulations can guide recycler's PMMA recycling techno-economic choices. For instance expensive technologies, while initially costlier, offer better economic returns and higher product quality when compared to cheaper, low-quality alternative. Similarly, cheaper technologies or lower quality waste yield sub-par r-MMA, which have a lower probability to be traded in the future.

2. Researchers and company executives rely on outdated early stage estimation methods, or have to recur to long and costly procedures $\rightarrow$ they have a quick, accurate and reliable method to screen technologies and estimate correctly (within AACE class 5) the capital cost of a new chemical recycling plant. This diminish the economic uncertainties on the capital cost, which is among the top two factors with the most impact in the viability of a PMMA recycling plant.

3. Post-industrial end-of-life PMMA is the only grade currently recycled at large scale. PMMA composites and post-consumer materials are more difficult to sort and process, and therefore overlooked. $\rightarrow$ waste artificial marble recycling, among the most challenging PMMA-based composite to treat, opens new pathways for the recovery of difficult materials. The dual-stage thermolysis of artificial marble demonstrates that successful chemical recycling must be tailored to the specific characteristics of each material–whether composite or polymer–to create sustainable and economically viable PMMA recycling approaches.

The ultimate goal of this work is to guide future researchers, plant owners, and engineers interested in PMMA recycling. Researchers will benefit transversally from chapters 2 to 5, which

demonstrate that PMMA recycling processes exist and provide insight into the challenges and opportunities surrounding them, including economic, technical, and material-specific aspects. Plant owners will benefit from data-driven scenarios and capital cost estimation methods that improve decision-making in terms of technology selection and investment strategies (Chapters 3 and 4). Engineers will gain practical tools to optimize recycling processes, especially in handling complex PMMA-based composites, ensuring that the recycling approaches are both technically viable and economically sustainable (Chapter 5).

6.2 Limitations

The conclusions drawn from Chapter 3 are reliable within the range of the Monte Carlo input functions. PMMA scrap and r-MMA distributions have the greatest impact on the analysis results, and these distributions are based on educated estimates from historical price data up to 2021. While Monte Carlo simulations account for uncertainties in raw material, product pricing, and investments, extreme market fluctuations or geopolitical events, like the recent energy crisis, fall outside the boundaries of the models. As a result, the models are more applicable to stable market conditions and may lose accuracy in highly volatile environments.

In Chapter 4, we compiled a database of total capital investment (TCI) and plant capacities of 167 planned or operational plants, and then regressed their global heat and mass balance. Similar to laboratory work, the quality of the data dictates the accuracy of the economic models. For existing plants, the data are relatively accurate. However, for planned plants, the board responds to stok and stakeholders, yet investment figures are sometimes an optimistic prospect, and it is not uncommon that projects are delayed or halted due to increased capital costs. As a result, this model's uncertainty limits its applicability to early-stage project evaluations (AACE Class 5 or 4 at best), reflecting an inherent limitation in this type of research. Similarly, these estimations are subject to further uncertainty for technologies that are still in development, as the results of solvolysis and selective dissolution teaches us.

In the second part of this study, mixing within the reactor is the main limitation. Rheological data for molten plastics, and particularly artificial marble at depolymerization temperatures, is sparse or non-existent. For the 5L stirred tank reactor, I selected a single helix agitator based on the assumption of a 10,000 cP viscosity fluid, rotating at 100-150 rpm. Ideally, a PARAVISC or SOLIDMIX VST agitator from Ekato, similar to what Plastic Energy uses, would have been more appropriate. This is a central impeller, with two baffles or feed pipes

and two blades, imposing offering axial flow and positive displacement. The reactor's steam feeding system has limitations too. While steam is sprayed on top of the molten medium, optimal contact would require steam injection from the bottom or through the agitator shaft. These factors limit our understanding of the tank's internal dynamics during the reaction, as well as the retention time of the steam, which is effectively one reagent for the hydrolysis. Additionally, we cannot confirm whether the composite behaves as a molten liquid or solid. Although increasing steam flow rate has the expected effect on hydrolysis yield, our conclusions on this are mainly qualitative. Similarly, we assume a laminar mixing regime, but there is uncertainty, which is why agitation rate was kept fixed during the design of experiments. Further research is needed to better understand the rheological properties of molten PMMA or artificial marble, optimize agitator design, and improve steam feeding techniques. During this investigation, we also discovered that PMMA tends to hydrolyze directly to PMAA rather than thermolyzing to MMA first. This insight could inform future work focused on producing PMAA directly from PMMA, although we demonstrate that MMA remains a more viable target product from depolymerization.
More in general, experimental work is focused primarily on artificial marble waste as a representative PMMA composite. This limitation restricts the generalizability of the findings to more diverse and complex real-world waste types.

6.3 Future Research

The original goal of this project was to scale-up a fluidized bed reactor for the thermocatalytic conversion of PMMA to MAA as an alternative recycling route with technical and economical benefits for highly contaminated PMMA scraps. This project was supposed to build onto laboratory scale fluidized and fixed beds experiments. However, techno-economic assessments of industrial processes indicated how fluidized beds were inadequate for PMMA thermolysis on large scale. Laboratory tests demonstrated PMMA hydrolysis with a large amount of catalyst (10 : 1 compared to PMMA), and water (1: 200) to achieve viable yields, which is neither economical nor can be translated directly. The goal of this project therefore shifted towards provide real-life tools to bridge the gap in PMMA recycling at large scale, in particular for PMMA-based composites. Future research should:

- Valorize other type of PMMA composites, specifically fiberglass based. These composite are currently employed in bath and kitchen furnitures, but are becoming the main alternative for polyester composites in wind blades and boat hulls. With the renewable energies to gain a bigger market, we can expect sizeable collection volumes in the next future. In Europe, the landfilling cost for this composite is around 200 USD/t, and

incineration around 600 USD/ton, which makes a much better case than PMMA scraps that have to be purchased as high as 600 USD/t. However, wind-blades are very long, so transportation is challenging. To thermolyse efficiently, one needs to cut and grind the composite. PMMA only represent 30/40 % of the material, and the rest is inorganic fiber. When we shorten the fiberglass we reduce its mechanical properties, and its value drops from 1700 USD/t to zero. Gees recycling, an Italian company, mix 40% ground fiberglass (< 3mm) with 60% virgin fiber to maintain its properties. Another italian company, Korec, pyrolyses fiberglass composites but after pyrolysis they assemble to fibers in non-woven mats (for fibers 3 to 25 mm), or as reinforcement material in cast articles (for fibers smaller than 0.1 mm). In both cases it is a downcycling because the fiberglass is not recycled in the same application [403].

- Investigate the properties of the PMAA/PMAA anhydrous produced by the artificial marble hydrolysis. Albeit small, PMAA has a market as super adsorbent, and there are currently no environmental friendly routes to produce it. In our artificial marble hydrolysis we wanted to depolymerize and then hydrolyze. The alternative would be to produce PMAA from PMMA, and boehmite from $Al(OH)_3$, which occurs even at 300 °C, the lowest temperature tested in our design. If depolymerization is not necessary, the reactor could operate at lower temperatures (e.g., 200 °C to 250 °C). Research is needed to optimize the conditions (water ratio, temperature, feeding, and agitation mode) and to analyze the resulting solid to fine-tune its properties. Additionally, future work should explore the pyrolysis mechanism of partially hydrolyzed PMMA at controlled PMMA/PMAA ratios. Acid units on the PMMA backbone exhibit an "autocatalytic" effect on PMMA hydrolysis in aqueous H_2SO_4 [384]. In the context of artificial marble thermolysis/hydrolysis, the influence of PMAA formation during the reaction on the overall mechanism requires investigation

- Identify a reliable (AACE 5) capital cost estimation for plants beyond the state-of-the art. The findings of Chapter 4 are based on the technical similarity of new plants, which is a reasonable approximation for established technologies like pyrolysis and gasification (TRL 6+) Conventional PMMA thermolysis shares many features with mixed plastic pyrolysis, including pretreatment, reaction, and purification stages. For reactors using established technologies (molten bath, dry distillation, fluidized bed), the results of Chapter 4 are directly applicable. However, for advanced or emerging technologies, cost engineers typically treat the results as a distribution and introduce an additional random factor based on the technology readiness level (TRL), adding another layer of uncertainty [404]. A more universal approach is the "Process Blocks Build-Up"

method [306]. Here, plants from the database in Chapter 4 would be divided into "blocks" (groups of unit operations), and the total capital investment (TCI) calculated by summing the costs of these blocks. Using a random search approach, we minimize the difference between estimated and actual plant TCIs and derive the block investment values (e.g., for sorting, washing, reaction A, reaction B, condensation, distillation, storage, utilities). The block values are probability functions (Gaussian, log-normal, etc.), which are summed to calculate the TCI of plants using technologies beyond the state of the art, where the layout is composed of blocks from existing plants. Provided enough blocks are available, this method reduces human error and the influence of user experience on the results.

What this work ultimately highlights is that the chemical industry tends to favor one-size-fits-all solutions, particularly for problems they are reluctant to address. Despite PMMA being one of the easiest polymers to depolymerize, only 10% of it is recycled globally. In practice, real materials present their own unique challenges, and more research is needed to develop methods for sorting, collecting, and recycling them in ways that are both economically viable and environmentally sustainable.

REFERENCES

[1] OECD, *Global Plastics Outlook*. Paris: Global Plastics Outlook: Economic Drivers, Environmental Impacts and Policy Options, 2022. [Online]. Available: https://www.oecd-ilibrary.org/content/publication/de747aef-en

[2] X. Yuan *et al.*, "The COVID−19 pandemic necessitates a shift to a plastic circular economy," *Nature Reviews Earth & Environment*, vol. 2, no. 10, pp. 659–660, 2021.

[3] K. S. Khoo *et al.*, "Plastic waste associated with the COVID-19 pandemic: Crisis or opportunity?" *Journal of Hazardous Materials*, vol. 417, p. 126108, 2021.

[4] A. L. P. Silva *et al.*, "Rethinking and optimising plastic waste management under covid-19 pandemic: Policy solutions based on redesign and reduction of single-use plastics and personal protective equipment," *Science of The Total Environment*, vol. 742, p. 140565, 2020.

[5] B. Joseph *et al.*, "Recycling of medical plastics," *Advanced Industrial and Engineering Polymer Research*, vol. 4, no. 3, pp. 199–208, 2021.

[6] W. Ferdous *et al.*, "Recycling of landfill wastes (tyres, plastics and glass) in construction–a review on global waste generation, performance, application and future opportunities," *Resources, Conservation and Recycling*, vol. 173, p. 105745, 2021.

[7] P. N. T. Pilapitiya and A. S. Ratnayake, "The world of plastic waste: a review," *Cleaner Materials*, p. 100220, 2024.

[8] D. C. Suyal and R. Soni, *Bioremediation of environmental pollutants*. Springer, 2022.

[9] P. Alam and K. Ahmade, "Impact of solid waste on health and the environment," *International Journal of Sustainable Development and Green Economics (IJSDGE)*, vol. 2, no. 1, pp. 165–168, 2013.

[10] European Environmental Agency, "Diverting waste from landfill effectiveness of waste?management policies in the european union – eea report no 7/2009," 2009, available at: https://www.eea.europa.eu/publications/diverting-waste-from-landfill-effectiveness-of-waste-management-policies-in-the-european-union/ (Accessed: August 27, 2024).

[11] "European environment agency," 2022, available online at https://www.eea.europa.eu/data-and-maps/daviz/ch4-emissions-from-landfills-and#tab-chart_1.

[12] European Commission, "Technical guidance on the application of 'do no significant harm' under the recovery and resilience facility regulation," 2022.

[13] E. Commission, "Scope of the EU Emissions Trading System," 2024, available at: https://climate.ec.europa.eu/eu-action/eu-emissions-trading-system-eu-ets/scope-eu-emissions-trading-system_en (Accessed: August 27, 2024).

[14] Z. O. Schyns and M. P. Shaver, "Mechanical recycling of packaging plastics: A review," *Macromolecular rapid communications*, vol. 42, no. 3, p. 2000415, 2021.

[15] J. Badia, O. Gil-Castell, and A. Ribes-Greus, "Long-term properties and end-of-life of polymers from renewable resources," *Polymer Degradation and Stability*, vol. 137, pp. 35–57, 2017.

[16] A. Dorigato, "Recycling of polymer blends," *Advanced Industrial and Engineering Polymer Research*, vol. 4, no. 2, pp. 53–69, 2021.

[17] A. Lamtai *et al.*, "Mechanical recycling of thermoplastics: A review of key issues," *Waste*, vol. 1, no. 4, pp. 860–883, October 2023.

[18] A. Rahimi and J. M. García, "Chemical recycling of waste plastics for new materials production," *Nature Reviews Chemistry*, vol. 1, no. 6, p. 0046, 2017.

[19] S. Siepen *et al.*, "How epcs and equipment suppliers can capitalize on chemical recycling," *Roland Berger*, 2024.

[20] A. Schade *et al.*, "Plastic waste recycling? a chemical recycling perspective," *ACS Sustainable Chemistry & Engineering*, 2024.

[21] I. S. Lase *et al.*, "How much can chemical recycling contribute to plastic waste recycling in europe? an assessment using material flow analysis modeling," *Resources, Conservation and Recycling*, vol. 192, p. 106916, 2023.

[22] H. H. Shah *et al.*, "A review on gasification and pyrolysis of waste plastics," *Frontiers in chemistry*, vol. 10, p. 960894, 2023.

[23] M. Bachmann *et al.*, "Towards circular plastics within planetary boundaries," *Nature Sustainability*, pp. 1–12, 2023.

[24] J. De Tommaso and J.-L. Dubois, "Risk analysis on PMMA recycling economics," *Polymers*, vol. 13, p. 2724, 2021.

[25] MarketsandMarkets, "Polymethyl methacrylate (PMMA) market," 2022, available online at https://www.marketsandmarkets.com/Market-Reports/polymethyl-methacrylate-pmma-market-715.html (accessed: August 2022).

[26] CHEMANALYST, "Decode the future of poly methyl methacrylate (PMMA)," 2023, available online at https://www.chemanalyst.com/industry-report/polymethyl-methacrylate-pmma-market-504 (accessed: August 2024).

[27] Global Market Insights, "Pmma market for construction application, by form (extruded, cell cast sheets & blocks), by application (greenhouse, doors & windows, sound barriers, facades, balustrades), regional outlook, price trend, competitive market share & forecast, 2018-2024," 2019, accessed: August 2019.

[28] ADEME, "Reemploi des materiaux de construction," 2022, available online at https://librairie.ademe.fr/urbanisme/5516-reemploi-des-materiaux-de-construction.html.

[29] Plastic Europe, "Plastics - the facts 2019," 2021, available online at https://plasticseurope.org/wp-content/uploads/2021/10/2019-Plastics-the-facts.pdf.

[30] L. Delva *et al.*, "On the role of flame retardants in mechanical recycling of solid plastic waste," *Waste Management*, vol. 82, pp. 198–206, 2018.

[31] G. Martinho *et al.*, "Composition of plastics from waste electrical and electronic equipment (weee) by direct sampling," *Waste Management*, vol. 32, pp. 1213–1217, 2012.

[32] S. R. Chandrasekaran *et al.*, "Materials and energy recovery from e-waste plastics," *ACS Sustainable Chemistry & Engineering*, vol. 6, no. 4, pp. 4594–4602, 2018.

[33] Environmental and Climate Change Canada, "Economic study of the canadian plastic industry, markets and waste: Summary report," 2019, available online at https://publications.gc.ca/collections/collection_2019/eccc/En4-366-1-2019-eng.pdfAccessed:2019.

[34] Cordis Europe, "Second generation methyl methacrylate (mmatwo) - horizon 2020 - results," 2024, available at: https://cordis.europa.eu/project/id/820687/news (Accessed: August 27, 2024).

[35] D. D'Hooge *et al.*, *Polymer Circularity Roadmap: Recycling of Poly(methyl Methacrylate) As a Case Study*, ser. De Gruyter STEM Series. Walter de Gruyter GmbH, 2022. [Online]. Available: https://books.google.ca/books?id=M3EFzwEACAAJ

[36] Statista, "Chemical industry - overview," 2024, available at: https://www.statista.com/markets/410/topic/445/chemical-industry/#overview (Accessed: August 27, 2024).

[37] S. van der Heijden, "Perspectives for pmma recycling–the relevance and societal impact of the mmatwo project," in Proceedings of the MMAtwo Virtual Workshop on Polymer Recycling, Virtual, 15 September 2020; European Union: Brussels, Belgium, 2020, doi:10.13140/RG.2.2.36739.73765.

[38] J.-L. Dubois, "Chemical recycling: A deep dive on depolymerization." *Chemical Engineering*, vol. 131, no. 8, 2024.

[39] T. Kashiwagi, T. Hirata, and J. E. Brown, "Thermal and oxidative degradation of poly (methyl methacrylate) molecular weight," *Macromolecules*, vol. 18, no. 2, pp. 131–138, 1985.

[40] M. Sponchionia and S. Altinokb, "Poly (methyl methacrylate): Market trends and recycling," *Towards Circular Economy: Closing the Loop with Chemical Recycling of Solid Plastic Waste*, p. 269, 2022.

[41] K. Ragaert, L. Delva, and K. Van Geem, "Mechanical and chemical recycling of solid plastic waste," *Waste management*, vol. 69, pp. 24–58, 2017.

[42] J. Beigbeder *et al.*, "Study of the physico-chemical properties of recycled polymers from waste electrical and electronic equipment (weee) sorted by high resolution near infrared devices," *Resources, Conservation and Recycling*, vol. 78, pp. 105–114, 2013.

[43] A. Zanetti, "The evolution of pmma recycling," 2024, available at: https://www.certech.be/files/uploads/2024/04/The-evolution-of-PMMA-recycling.pdf (Accessed: August 30, 2024).

[44] M. Isador and A. Beiser, "Art of reclaiming plastic scrap," Patent US2 470 361A, June 27, 1945.

[45] K. Albrecht, M. Stickler, and T. Rhein, *Polymethacrylates*. John Wiley & Sons, Ltd, 2013. [Online]. Available: https://onlinelibrary.wiley.com/doi/abs/10.1002/14356007.a21_473.pub2

[46] E. Moens *et al.*, "Progress in reaction mechanisms and reactor technologies for thermochemical recycling of poly(methyl methacrylate)," *Polymers*, vol. 12, no. 1667, 2020.

[47] E. K. Moens *et al.*, "Coupled matrix-based monte carlo modeling for a mechanistic understanding of poly (methyl methacrylate) thermochemical recycling kinetics," *Chemical Engineering Journal*, vol. 146105, 2023. [Online]. Available: https://doi.org/10.1016/j.cej.2023.146105

[48] K. Smolders and J. Baeyens, "Thermal degradation of pmma in fluidised beds," *Waste Management*, vol. 24, no. 8, pp. 849–857, 2004.

[49] G. Grause, M. Predel, and W. Kaminsky, "Monomer recovery from aluminium hydroxide high filled poly (methyl methacrylate) in a fluidized bed reactor," *Journal of analytical and applied pyrolysis*, vol. 75, no. 2, pp. 236–239, 2006.

[50] J.-L. Dubois, "Mmatwo workshop–guidelines for depolymerization at pilot and industrial scale," in Proceedings of the second MMAtwo Virtual Workshop on Polymer Recycling, Virtual, February 2022; European Union: Brussels, Belgium, 2022, doi:1: 10.13140/RG.2.2.31754.75202.

[51] EASECAST NEWS, "LEAD REGULATION IN THE EU (Status: March 2024)," 2024, available online at https://www.rheinmetall.com/Rheinmetall%20Group/Systeme%20und%20Produkte/KS%20Gleitlager/Datenbl%C3%A4tter/EASECAST%20NEWS%20en.pdf (accessed: August 2024).

[52] J.-L. Dubois, "Mmatwo workshop–pmma depolymerization: Scale-up and industrial implementation," in Proceedings of the MMAtwo Virtual Workshop on Polymer Recycling, Virtual, 15 September 2020; European Union: Brussels, Belgium, 2020, doi:10.13140/RG.2.2.23546.52162.

[53] P. W. Vaughan and D. J. Highgate, "Depolymerisation – us5663420a1," Patent, 1994.

[54] I. D. Poree *et al.*, "Process for decomposing a polymer to its monomer or monomers," Patent US6 160 031A, 1997.

[55] S.-P. Mannsfeld, K.-J. Paulsen, and E. Buchholz, "Production of monomeric cleavage products by thermal decomposition of polymers," Patent US3 494 958A, 1967.

[56] A. Sasaki *et al.*, "Recovery method of pyrolysis product of resin," Patent US20 100 121 097A1, 2008.

[57] A. Sasaki and T. Tsuji, "Poly (methyl methacrylate) pyrolysis by two fluidized bed process," in *The 5th symposium on feedstock and mechanical recycling of polymeric materials (ISFR2009). Chengdu (China)*, 2009, pp. 79–83.

[58] "Ici's polymethyl methacrylate tertiary recycling technology," iCI International: London, UK, 1998.

[59] "Practical closed recycling process developed for acrylic resin products," 2008, available online at https://www.m-chemical.co.jp/en/news/mrc/p08/press20080908.html(accessed: September 2024).

[60] "Mmatwo website - mmatwo aims to secure the supply of commercial plant recycling units with at least 27 000 tons feedstocks pmma scraps and end-of-life products." available online: https://www.mmatwo.eu/ (accessed on 23 July 2021).

[61] Trinseo Website, "Regenerated mma through next-gen acrylic recycling," 2024, available online at https://www.trinseo.com/Thought-Leadership/2024/July/Depolymerization-Technology-Advancing-PMMA-Circularity(accessed: September 2024).

[62] Microwave Chemical Co., Ltd, "Chemical recycling by microwave technology," 2024, available online at https://gj-eedf.org/system/files/document/15_microwave-chemical_mr.-iwata_compressed.pdf(accessed: September 2024).

[63] Mitsubishi Chemical Group, "Mitsubishi chemical increases the pace on a circular economy for pmma with agilyx corporation," 2024, available online at https://mcc-methacrylates.com/ja/press_releases/mitsubishi-chemical-increases-the-pace-on-a-circular-economy-for-pmma-with-agilyx-corporation/(a September 2024).

[64] V. Popescu *et al.*, "The characterization of recycled pmma," *Journal of Alloys and Compounds*, vol. 483, no. 1-2, pp. 432–436, 2009.

[65] S. S. Suresh, S. Mohanty, and S. K. Nayak, "Investigation into the mechanical and thermal properties of poly (methyl methacrylate) recovered from light guidance panels with a focus on future remanufacturing and sustainable waste management," *Journal of Remanufacturing*, vol. 7, pp. 217–233, 2017.

[66] C. B. Godiya *et al.*, "Depolymerization of waste poly (methyl methacrylate) scraps and purification of depolymerized products," *Journal of Environmental Management*, vol. 231, pp. 1012–1020, 2019.

[67] C. Lemenu, "Mmatwo workshop–gemissions and odours from regenerated (P)MMA," in Proceedings of the second MMAtwo Virtual Workshop on Polymer Recycling, Virtual, February 2022; European Union: Brussels, Belgium, 2022, doi:1: 10.13140/RG.2.2.10713.19040.

[68] H. J. d. S. Ribeiro *et al.*, "Depolymerization of pmma-based dental resin scraps on different production scales," *Energies*, vol. 17, no. 5, p. 1196, 2024.

[69] C.-C. Chang and S.-W. Wan, "China's motor fuels from tung oil," *Industrial & Engineering Chemistry*, vol. 39, no. 12, pp. 1543–1548, 1947.

[70] J.-L. Dubois, "RECOVERY OF (METH) ACRYLIC RESIN BY DEPOLYMERIZATION AND HY – us11739192b2," Patent, 2023.

[71] G. Smets and R. Van Gorp, "Acrylic and methacrylic acid copolymerization parameters," *European Polymer Journal*, vol. 5, no. 1, pp. 15–19, 1969.

[72] K. Gkaliou *et al.*, "Recycled pmma prepared directly from crude mma obtained from thermal depolymerization of mixed pmma waste," *Waste Management*, vol. 164, pp. 191–199, 2023.

[73] PubChem, NCBI, "Chemical properties and safety data for common compounds," 2024, available online at https://pubchem.ncbi.nlm.nih.gov (accessed: September 2024).

[74] PubChem, NCBI, "Propanoic acid: Chemical properties and safety," 2024, available online at https://www.chemeo.com/cid/55-113-5/1-4-Cyclohexanedicarboxylic-acid-dimethyl-ester (accessed: September 2024).

[75] TradeMap, "291613 methacrylic acid and its salts - trademap," 2021, available online at https://www.trademap.org/Country_SelProduct.aspx?nvpm=1%7c%7c%7c%7c%7c291613%7c%7c%7c6%7c1%7c1%7c1%7c1%7c1%7c2%7c1%7c1%7c1 (accessed: March 29, 2023).

[76] TradeMap, "291614 esters of methacrylic acid - trademap," 2021, available online at https://www.trademap.org/Country_SelProduct.aspx?nvpm=1%7c%7c%7c%7c%7c%7c291614%7c%7c%7c6%7c1%7c1%7c1%7c1%7c1%7c2%7c1%7c1%7c1 (accessed: April 31, 2023).

[77] K. Sunitha *et al.*, "Novel superabsorbent copolymers of partially neutralized methacrylic acid and acrylonitrile: synthesis, characterization and swelling

characteristics," *Designed Monomers and Polymers*, vol. 18, no. 6, pp. 512–523, 08 2015. [Online]. Available: https://doi.org/10.1080/15685551.2015.1041082

[78] G. Swift, *Acrylic (and Methacrylic) Acid Polymers*, 2023/04/02 2002. [Online]. Available: https://doi.org/10.1002/0471440264.pst009

[79] M. J. D. Mahboub *et al.*, "Catalysis for the synthesis of methacrylic acid and methyl methacrylate," *Chemical Society Reviews*, vol. 47, pp. 7703–7738, 2018.

[80] O. V. Chub, J.-L. Dubois, and G. S. Patience, "Tandem fluidized bed/milli-second fixed bed reactor produces methacrylic acid from poly(methyl methacrylate)," *Applied Catalysis A: General*, vol. 647, p. 118887, 2022. [Online]. Available: https://www.sciencedirect.com/science/article/pii/S0926860X22004100

[81] O. V. Chub, J.-L. Dubois, and G. S. Patience, "Tandem fluidized bed/milli-second fixed bed reactor produces methacrylic acid from poly (methyl methacrylate)," *Applied Catalysis A: General*, vol. 647, p. 118887, 2022.

[82] Y. Zhuang *et al.*, "Upcycling polymethyl methacrylate to methacrylic acid," May 2024, in submission.

[83] J. De Tommaso *et al.*, "Total capital investment of plastic recycling plants correlates with energy losses and capacity," *ChemSusChem*, p. e202301172, 2024.

[84] M. Tsagkari *et al.*, "Early-stage capital cost estimation of biorefinery processes: A comparative study of heuristic techniques," *ChemSusChem*, vol. 9, p. 2284, 2016.

[85] J. Hollmann, "(risk 1027) estimate accuracy: Dealing with reality," AACE International, Morgantown, WV, USA, Tech. Rep., 2012.

[86] J. Poudel *et al.*, "Methyl methacrylate (mma) and alumina recovery from waste artificial marble powder pyrolysis," *Journal of Material Cycles and Waste Management*, vol. 23, pp. 214–221, 2021.

[87] C. Analytics, "Web of science all databases," http://apps.webofknowledge.com, accessed: 15/09/2020.

[88] N. J. Van Eck and L. Waltman, "Software survey: Vosviewer, a computer program for bibliometric mapping," *Scientometrics*, vol. 84, no. 2, pp. 523–538, 2010.

[89] F. Wagner *et al.*, "Towards a more circular economy for weee plastics-part b: Assessment of the technical feasibility of recycling strategies," *Waste Management*, vol. 96, pp. 206–214, 2019.

[90] J. Wang, H. Wang, and D. Yue, "Separation of waste polymethyl methacrylate and polyvinyl chloride mixtures by flotation after fenton oxidation," *Journal of Cleaner Production*, vol. 228, pp. 1218–1228, 2019.

[91] J. Wang *et al.*, "A novel process for separation of hazardous poly (vinyl chloride) from mixed plastic wastes by froth flotation," *Waste Management*, vol. 69, pp. 59–65, 2017.

[92] L. Huang *et al.*, "Microwave-assisted surface modification for the separation of polycarbonate from polymethylmethacrylate and polyvinyl chloride waste plastics by flotation," *Waste Management & Research*, vol. 35, no. 3, pp. 294–300, 2017.

[93] X. Zhang *et al.*, "Magnetic projection: A novel separation method and its first application on separating mixed plastics," *Waste Management*, vol. 87, pp. 805–813, 2019.

[94] D. E. Fekir *et al.*, "Technicoeconomic comparison between two new triboelectric charging processes of insulating granular products and their application to the electrostatic separation of weee," in *2018 International Conference on Electrical Sciences and Technologies in Maghreb (CISTEM)*. IEEE, 2018, pp. 1–6.

[95] M. Gent *et al.*, "Evaluation of ground calcite/water heavy media cyclone suspensions for production of residual plastic concentrates," *Waste Management*, vol. 71, pp. 42–51, 2018.

[96] C. Signoret *et al.*, "Mir spectral characterization of plastic to enable discrimination in an industrial recycling context: I. specific case of styrenic polymers," *Waste Management*, vol. 95, pp. 513–525, 2019.

[97] G. Zhang *et al.*, "Removing inorganics from nonmetal fraction of waste printed circuit boards by triboelectric separation," *Waste Management*, vol. 49, pp. 230–237, 2016.

[98] Y. Sano *et al.*, "Controlled radical depolymerization of chlorine-capped pmma via reversible activation of the terminal group by ruthenium catalyst," *European Polymer Journal*, vol. 120, p. 109181, 2019.

[99] Y. Kikuchi *et al.*, "Design of recycling system for poly (methyl methacrylate)(pmma). part 1: Recycling scenario analysis," *The International Journal of Life Cycle Assessment*, vol. 19, pp. 120–129, 2014.

[100] W. Kaminsky, "Recycling of polymers by pyrolysis," *Le Journal de Physique IV*, vol. 3, no. C7, pp. C7–1543, 1993.

[101] K. S. Ryoo, "Study on recycling technology of waste artificial marble using starch," *Journal of the Korean Chemical Society*, vol. 62, no. 6, pp. 433–440, 2018, (in Korean).

[102] W. Kaminsky, M. Predel, and A. Sadiki, "Feedstock recycling of polymers by pyrolysis in a fluidised bed," *Polymer Degradation and Stability*, vol. 85, no. 3, pp. 1045–1050, 2004.

[103] J. Pavlinec, M. Lazar, and K. Csomorova, "Thermal degradation of multilayer methacrylate-acrylate particle-bead polymer powders and melts," *Polymer Degradation and Stability*, vol. 55, no. 1, pp. 65–71, 1997.

[104] K. Charmondusit and L. Seeluangsawat, "Recycling of poly (methyl methacrylate) scrap in the styrene-methyl methacrylate copolymer cast sheet process," *Resources, Conservation and Recycling*, vol. 54, no. 2, pp. 97–103, 2009.

[105] WIPO, "Patent scope," https://www.wipo.int/portal/en/index.html, accessed: 15/09/2020.

[106] The Lens - Free & Open Patent and Scholarly Search, "Lens.org," accessed: December 10, 2024.

[107] "Method and system for forming carbon dioxide from carbon-containing materials in a molten bath of immiscible metals," Patent US5 177 304A, 1991.

[108] "Method of manufacturing molding of mixed molten plastics of different types," Patent CA2 288 108, 1999.

[109] "Method for producing unsaturated organics from organic-containing feeds," Patent AU1 995 014 412, 1994.

[110] J. M. Rzonca, "De2132716a1–process for the production of monomeric esters of acrylic acid and substituted acrylic acid," Patent, 1972.

[111] M. Newborough, D. Highgate, and P. Vaughan, "Thermal depolymerisation of scrap polymers," *Applied Thermal Engineering*, vol. 22, no. 17, pp. 1875–1883, 2002.

[112] J. Domingo and D. Cabanero, "Process and device for regeneration of monomer from polymethyl methacrylate," Patent 192 909, 1949.

[113] J. Schoeters, A. Buekens, and E. Samyn, "Abstract of the dgmk symposium grundlagen und prozesse der pyrolyse und verkokung," in *DGMK Symposium, 6-8 September 1989, Essen*, 1989, p. 39.

[114] T. Tatsumi, H. Yoshihara, and G. Uesaka, "Method for depolymerizing thermoplastic resins by liquid heat transfer media," Patent US3 886 202A, 1970.

[115] "Process for depolymerizing alpha substituted acrylic acid esters," Patent US2 030 901A, 1935.

[116] Rohm and H. GmbH, "Method of producing monomeric methacrylic acid esters," Patent GB460 009A, 1935.

[117] "Dry-distillation type cracker with stirring function," Patent CN203 316 130U, 2013.

[118] "City household garbage cooking distillation comprehensive separation treatment method," Patent CN107 052 023, 2017.

[119] M. Horii and S. Iida, "Gasification and dry distillation of automobile shredder residue (asr)," *JSAE Review*, vol. 22, no. 1, pp. 63–68, 2001.

[120] B. J. Jody *et al.*, "End-of-life vehicle recycling: state of the art of resource recovery from shredder residue," 2011, no. ANL/ESD/10-8, Available online at: https://www.osti.gov/servlets/purl/1007810, accessed: September 2024.

[121] C. Abeykoon, P. Pérez, and A. L. Kelly, "The effect of materials' rheology on process energy consumption and melt thermal quality in polymer extrusion," *Polymer Engineering & Science*, vol. 60, no. 6, pp. 1244–1265, 2020.

[122] D. B. Todd, "Mixing of highly viscous fluids, polymers, and pastes," *Handbook of Industrial Mixing: Science and Practice - Chapter 16*, pp. 987–1025, 2003.

[123] M. Muller and F. Wenzel, "Process and device for the thermal depolymerisation of polymers," Patent DE3 146 194, 1981.

[124] F. Randazzo and A. Naviglio, "Process and relative plant for the depolymerization of plastic materials for the production of hydrocarbons," Patent IT201 800 009 798, 2018.

[125] D. Mcnamara *et al.*, "A reactor assembly," Patent WO2 020 065 316A1, 2018.

[126] J. Dubois *et al.*, "Process for treating a gaseous effluent from pyrolytic decomposition of a polymer," Patent EP3 866 950B1, 2019.

[127] P. Das *et al.*, "Value-added products from thermochemical treatments of contaminated e-waste plastics," *Chemosphere*, vol. 269, p. 129409, 2021.

[128] F. Sasse and G. Emig, "Chemical recycling of polymer materials," *Chemical Engineering & Technology: Industrial Chemistry-Plant Equipment-Process Engineering-Biotechnology*, vol. 21, no. 10, pp. 777–789, 1998.

[129] J. Evans, W. Borland, and P. Mardon, "Pyrophoricity of fine metal powders," *Powder Metallurgy*, vol. 19, no. 1, pp. 17–21, 1976.

[130] F. Winter and B. Schratzer, "Applications of fluidized bed technology in processes other than combustion and gasification," in *Fluidized bed technologies for near-zero emission combustion and gasification*. Elsevier, 2013, pp. 1005–1033.

[131] W. Kaminsky and J. Franck, "Monomer recovery by pyrolysis of poly (methyl methacrylate)(PMMA)," *Journal of Analytical and Applied Pyrolysis*, vol. 19, pp. 311–318, 1991.

[132] A. P. Smith *et al.*, "High-energy mechanical milling of poly (methyl methacrylate), polyisoprene and poly (ethylene-alt-propylene)," *Polymer*, vol. 41, no. 16, pp. 6271–6283, 2000.

[133] D. Bruyere *et al.*, "Cryogenic ball milling: a key for elemental analysis of plastic-rich automotive shredder residue," *Powder Technology*, vol. 294, pp. 454–462, 2016.

[134] F. Garcia-Ochoa *et al.*, "A study of segregation in a gas-solid fluidized bed: particles of different density," *Powder Technology*, vol. 58, no. 3, pp. 169–174, 1989.

[135] U. Arena, A. Cammarota, and M. L. Mastellone, "The phenomenology of comminution in the fluidized bed combustion of packaging-derived fuels," *Fuel*, vol. 77, no. 11, pp. 1185–1193, 1998.

[136] U. Arena and M. L. Mastellone, "Defluidization phenomena during the pyrolysis of two plastic wastes," *Chemical Engineering Science*, vol. 55, no. 15, pp. 2849–2860, 2000.

[137] "Process and apparatus for treating waste comprising mixed plastic waste," Patent WO2 014 128 430A1, 2013.

[138] U. Arena and M. L. Mastellone, "Fluidized bed pyrolysis of plastic wastes," in *Wiley Online Library*. Wiley, 2006, ch. 16, pp. 435–474.

[139] M. L. Mastellone and U. Arena, "Bed defluidisation during the fluidised bed pyrolysis of plastic waste mixtures," *Polymer Degradation and Stability*, vol. 85, no. 3, pp. 1051–1058, 2004.

[140] S. Yasuda *et al.*, "Recovery of oil from waste plastic and system therefor," Patent JPH09 235 563A, 1996.

[141] K. Kanamaru *et al.*, "Device for thermal decomposition of organic solid waste," Patent JPS5 483 002A, 1994.

[142] L. Mitsubishi Rayon Co., T. Ministry of Economy, and I. M. I. B. F. Division, "Acrylic resin production energy reduction technology of research and development: Evaluation materials," November 10 2008, available online in Japanese.

[143] M. Artetxe *et al.*, "Operating conditions for the pyrolysis of poly-(ethylene terephthalate) in a conical spouted-bed reactor," *Industrial & Engineering Chemistry Research*, vol. 49, no. 5, pp. 2064–2069, 2010.

[144] G. Lopez *et al.*, "Recycling poly-(methyl methacrylate) by pyrolysis in a conical spouted bed reactor," *Chemical Engineering and Processing: Process Intensification*, vol. 49, no. 10, pp. 1089–1094, 2010.

[145] M. Olazar *et al.*, "Pressure drop in conical spouted beds," *Chemical Engineering Journal*, vol. 51, pp. 53–60, 1993.

[146] "Method for converting plastics into gas, liquid fuel, and wax by cracking," Patent CN108 603 122A, 2017, chinese Patent.

[147] H.-J. Weiss *et al.*, "Method for depolymerizing polymethylmethacrylate," Patent US6 469 203B1, 2002, u.S. Patent, October 31.

[148] "Valorisation de resine (meth)acrylique par depolymerisation et hydrolyse," WO2019/207264, 2019.

[149] "Torbed compact bed reactor (cbr): Technology description," available online at http://www.torftech.com/publications.html, accessed: 22/09/2020.

[150] G. A. Wellwood, "Hydrodynamic behavior of the torbed gas-solid contactor ? a qualitative assessment," in *Proc. 7th Eng. Found. Conf. Fluid.*, Brisbane, Australia, 1992, pp. 695–702.

[151] J. Shu, V. I. Lakshmanan, and C. E. Dodson, "Hydrodynamic study of a toroidal fluidized bed reactor," *Chemical Engineering and Processing: Process Intensification*, vol. 39, no. 6, pp. 499–506, 2000.

[152] M. F. Mohideen *et al.*, "Experimental studies on a swirling fluidized bed with annular distributor," *Advanced Powder Technology*, vol. 19, no. 4, pp. 335–348, 2008.

[153] C. S. Chyang and Y. C. Lin, "A study in the swirling fluidizing pattern," *Journal of Chemical Engineering of Japan*, vol. 35, no. 6, pp. 503–512, 2002.

[154] "Solid fuel from combustible wastes and its use," Patent EP2 995 673, 2012.

[155] "Processing waste plastics for raw materials recycling," Patent DE19 505 544, 1992.

[156] "Grade-dependent depolymerization process and its use for recycling plastics," Patent EP4 155 341, 2021.

[157] W. Michaeli and K. Breyer, "Polymer recycling–status and perspectives," in *Macromolecular Symposia*. Wiley Online Library, 1998, vol. 135, pp. 83–96.

[158] Plastic Insight, "JSW providing core technology using Twin Screw Extruder for development of innovative PMMA recycling process," 2020, available online at https://www.plasticsinsight.com/jsw-providing-core-technology-using-twin-screw-extruder-for-development-of-innovative\protect\penalty-\@Mpmma-recycling-process-by-mmatwo-consortium/ (accessed: 23/09/2020).

[159] "Method and apparatus for continuous regeneration of acrylic resin," Patent JP3 410 343B2, 1997.

[160] H. Tokushige, A. Kosaki, and T. Sakai, "Method for continuously thermally decomposing synthetic macro-molecule materials," Patent US3 959 357, 1976.

[161] "Systems and methods for recycling waste plastics, including waste polystyrene," Patent US10 731 080B1, 2016.

[162] "Systems, and methods for recycling plastic," Patent US9 145 520B2, 2012.

[163] "Lucite partners with agilyx to progress pmma recycling," 2020, available online at https://www.chemengonline.com/lucite-partners-with-agilyx-to-progress-pmma-recycling/, accessed: 22/09/2020.

[164] Coperion, "Coperion supplies plant for chemical recycling of pmma to renov8," 2022, available online at https://www.coperion.com/en/news-media/newsroom/2022/pmma-recycling (accessed: 23/10/2022).

[165] Sumitomo, "Sumitomo chemical to construct chemical recycling pilot facility for acrylic resin to reduce impact on the environment," 2021, available online at https://www.sumitomo-chem.co.jp/english/news/detail/20210823e.html (accessed: 23/10/2022).

[166] J. De Wilde, "The heat of gasification of polyethylene and polymethylmethacrylate," *Delft University of Technology, Faculty of Aerospace Engineering, memorandum m-593*, 1988.

[167] M. Bossard, "MMAtwo - deliverable wp7 - communication, dissemination and academic outreach d7.4 second project newsletter," 2021, available online at https://www.mmatwo.eu/wp-content/uploads/2022/01/MMAtwo_D7.4_29112021_VF.pdf (accessed: 23/10/2022).

[168] A. T. Ural *et al.*, "Pyrolysis reactor," Patent WO2 019 226 135, 2018.

[169] I. Belyamani *et al.*, "Toward recycling "unsortable" post-consumer weee stream: Characterization and impact of electron beam irradiation on mechanical properties," *Journal of Cleaner Production*, vol. 294, p. 126300, 2021.

[170] Y. HIROTO, "Recycling device and recycling method for developing liquid, and development device," Patent EP4 009 105, 2022.

[171] D. Krishnamoorthi *et al.*, "Evaluation of the in-vitro cytotoxicity of heat cure denture base resin modified with recycled pmma-based denture base resin," *Journal of Pharmacy and Bioallied Sciences*, vol. 14, no. Suppl 1, pp. S719–S725, 2022.

[172] N. Silva de Souza Lima Cano, M. U. Hossain, and M. M. Bilec, "Environmental impacts of circularity strategies for social distancing plastic shields made of polymethyl methacrylate in the united states," *Waste Management & Research*, p. 0734242X241237102, 2024.

[173] U. Chianese, "Thermoplastic material," Patent US20 200 283 608, 2018.

[174] E. Jung *et al.*, "Depolymerization of polymethacrylates with ball-mill grinding," *Macromolecules*, vol. 57, no. 7, pp. 3131–3137, 2024.

[175] L. Macedo *et al.*, "An alternative to discarded plastic: A report of polymer optical fiber made from recycled materials for the development of biosensors," *Optical Fiber Technology*, vol. 72, p. 103001, 2022.

[176] P. GERARD *et al.*, "(meth)acrylic composition comprising recycled material, method for producing said composition and uses thereof," Patent WO2 024 115 786, 2024.

[177] C. CHAZOT, M. CREIGHTON, and A. . HART, "Methods, apparatus, compositions of matter, and articles of manufacture related to additive manufacturing of polymers," Patent WO2 023 081 467, 2023.

[178] R. Ginder *et al.*, "Hybridized recycled fiberglass and thermoplastic comingled technical yarn," Patent US20 240 052 535, 2024.

[179] C. Moore, "Architectural resin panel with incorporated scrap materials," Patent US20 210 245 400, 2021.

[180] R. Arif *et al.*, "Recycling of poly-(methyl methacrylate) waste sheets to synthesize catalyst-free bi-functional cation-exchange resin for sequestering of toxic pollutant," *Polymer Bulletin*, pp. 1–18, 2024.

[181] J. D. Tommaso and J.-L. Dubois, "Risk analysis on pmma recycling economics," *Polymer*, vol. 13, p. 2724, 2021.

[182] N. KENICHI, K. KOBAYASHI, and A. HIROKO, "Light-emitting device, display apparatus, and lighting apparatus," Patent EP3 742 042, 2020.

[183] P. Bonte *et al.*, "Vehicle components formed with epoxidized chopped glass bonded to a thermoset matrix," Patent US20 190 160 794, 2021.

[184] J. J. Ge and M. AUBART, "Optical reflectors, reflection films and sheets," Patent US20 190 249 031, 2019.

[185] C. Pirro *et al.*, "Recyclable composition for paper coating," U.S. Patent US20 230 287 627, 2021.

[186] E. Ersen, N. Basak, and M. Demiray, "Waterborne polymer composition and preparation method thereof," World Patent WO2 024 126 838, 2024.

[187] P. Gerard and P. Escale, "Liquid composition comprising a phosphorus-based additive, its use and material or composition obtained following polymerisation of composition," India Patent IN201 817 049 462, 2019.

[188] S. KRILL, M. RACZEK, and R. BURGHARDT, "Process for minimising the loss of activity in reaction steps carried out in circulation," Patent WO2 022 022 939, 2022.

[189] "Global market study on methyl methacrylate (mma) increasing application in pmma production to account for significant revenue generation opportunities," available online: http://www.persistencemarketresearch.com/market-research/methyl-methacrylate-market.asp (accessed on 24 February 2021).

[190] "Methyl methacrylate market to reach 5.7 million tons by the end of 2028 business," available online: https://ipsnews.net/business/2020/06/09/methyl-methacrylate-market-to-reach-5-7-million-tons-by-the-end-of-2028/ (accessed on 24 February 2021).

[191] "Pmma faces long road to recovery. icis interactive insight," available online: https://www.icis.com/explore/services/pmma-faces-long-road-to-recovery/ (accessed on 24 February 2021).

[192] "Pmma market to see 6.2% annual growth through 2023," available online: https://www.bccresearch.com/pressroom/chm/pmma-market-to-see-62-annual-growth-through-2023 (accessed on 24 February 2021).

[193] "Pmma market for construction application growth statistic report 2024," available online: https://www.gminsights.com/industry-analysis/pmma-market-for-construction (accessed on 24 February 2021).

[194] "Reportlinker global polymethyl methacrylate (pmma) industry," available online: http://www.globenewswire.com/news-release/2020/09/25/2099510/0/en/Global-Polymethyl-Methacrylate-PMMA-Industry.html (accessed on 24 February 2021).

[195] K. Sale, "Coronavirus pandemic creates new application for pmma sheet market," available online: https://www.icis.com/explore/resources/news/2020/05/08/10505498/coronavirus-pandemic-creates-new-application-for-pmma-sheet-market (accessed on 24 February 2021).

[196] Sale, K., "Europe mma july prices increase as oversupply eases, feedstocks firm," available online: https://www.icis.com/explore/resources/news/2020/07/31/10536612/europe-mma-july-prices-increase-as-oversupply-eases-feedstocks-firm (accessed on 24 February 2021).

[197] "Plastics the facts 2020. an analysis of european plastics production, demand and waste data," plastics Europe: Brussels, Belgium, 2020.

[198] K. Albrecht, M. Stickler, and T. Rhein, *Polymethacrylates. In Ullmann's Encyclopedia of Industrial Chemistry.* Wiley: Hoboken, NJ, USA, 2013.

[199] P. Peck, "Interest in material cycle closure? exploring evolution of industry's responses to high-grade recycling from an industrial ecology perspective: Volume ii case studies," Ph.D. dissertation, Lund University, Lund, Sweden, 2003.

[200] "How to recycle waste acrylic-baruie," available online: http://www.baruie.com/PMMA_recycle (accessed on 23 June 2021).

[201] "Acrylic recycling and pmma recycling. for acrylic scrap recycling visit shimiresearch.com," available online: http://shimiresearch.in/Acrylic-Recycling.php (accessed on 23 June 2021).

[202] *Brydson's Plastics Materials–8th Edition*, 2017, available online: https://www.elsevier.com/books/brydsons-plastics-materials/gilbert/978-0-323-35824-8 (accessed on 23 June 2021).

[203] "Mmatwo newsletter january-2021," available online: https://www.mmatwo.eu/wp-content/uploads/2021/01/MMAtwo_Newsletter_January-2021_VF.pdf (accessed on 23 July 2021).

[204] H. Anzai *et al.*, "Method for recovering monomer from waste acrylic resin," Patent JP16 360 296A, May 2, 2002.

[205] D. Mcnamara *et al.*, "A reactor assembly," Patent WO2 020 065 316A1, 2020.

[206] B. Cavinaw *et al.*, "Systems and methods for recycling waste plastics, including waste polystyrene," Patent US10 301 235B1, June 28, 2010.

[207] J. Brandrup, E. Immergut, and E. Grulke, *Polymer Handbook, 4th ed.* John Wiley & Sons: Hoboken, NJ, USA, 2003.

[208] J.-L. Dubois, "New innovative process for recycling end-of-life pmma waste. mmatwo second generation methyl methacrylate 2019," available online: https://www.researchgate.net/publication/341655536 (accessed on 22 June 2021).

[209] D. Green and M. Southard, *Section 9–Process Economics. In Perry's Chemical Engineers' Handbook, 7th ed.* McGraw-Hill Education: New York, NY, USA, 2019.

[210] G. Towler and R. E. Sinnott, *Chapter 9–Economic Evaluation of Projects. In Chemical Engineering Design, 2nd ed.* Butterworth-Heinemann: Boston, MA, USA, 2013.

[211] "18R-97: Cost Estimate Classification System–As Applied in Engineering, Procurement, and Construction for the Process Industries," aACE International: Morgantown, WV, USA, 2016; 6p.

[212] G. Petley, "A method for estimating the capital cost of chemical process plants: Fuzzy matching," Ph.D. dissertation, Loughborough University, Loughborough, UK, August 1997.

[213] J.-P. Lange, "Fuels and chemicals manufacturing; guidelines for understanding and minimizing the production costs," *Cattech*, vol. 5, pp. 82–95, 2001.

[214] W. Vatavuk, "Updating the ce plant cost index," *Chem. Eng.*, vol. 109, pp. 62–70, 2002.

[215] "Chemical engineering online," 21 April 2020 Issue.

[216] M. Peters, K. Timmerhaus, and R. West, *Plant Design and Economics for Chemical Engineers*, 5th ed., ser. McGraw-Hill Chemical Engineering Series. McGraw-Hill: New York, NY, USA, 2003.

[217] NexantECA, "Advances in depolymerization technologies for recycling (2021 program)," available online: https://www.nexanteca.com/reports/advances-depolymerization-technologies-recycling-2021-program (accessed on 25 June 2021).

[218] W. Beacham, "Plastic energy plans 10 chemical recycling plants in europe, asia by 2021," available online: https://www.icis.com/explore/resources/news/2019/03/19/10335799/plastic-energy-plans-10-chemical-recycling-plants-in-europe-asia-by-2021 (accessed on 19 February 2021).

[219] L. Boldon and P. Sabharwall, "Small modular reactor: First-of-a-kind (foak) and nth-of-a-kind (noak) economic analysis," USDOE, Washington, DC, USA, Tech. Rep. INL/EXT–14-32616, December 2014.

[220] "Agilyx," available online: https://www.agilyx.com/application/files/7516/0806/8429/Agilyx_Investor_Presentation_15Dec20_FINAL.pdf (accessed on 19 February 2021).

[221] "Congreso international tenerife + sostenible," available online: http://congresotenerifemassostenible.com/wp-content/uploads/2016/06/09_B22-5-C-Monreal.pdf (accessed on 19 February 2021).

[222] J. Boal, "Utah-based renewlogy offers solution to plastic waste problem," available online: https://www.deseret.com/2018/4/1/20642672/

utah-based-renewlogy-offers-solution-to-plastic-waste-problem (accessed on 19 February 2021).

[223] "The city of phoenix to begin turning plastics into fuel," available online: https://www.phoenix.gov:443/news/publicworks/2303 (accessed on 19 February 2021).

[224] "Phoenix awards contract to renewlogy for chemical recycling project," available online: https://www.wastedive.com/news/phoenix-awards-contract-to-renewlogy-for-chemical-recycling-project/552055/ (accessed on 19 February 2021).

[225] T. StClair-Pearce and D. Garbett, "Plastic waste thermal cracking new energy investment," available online: https://www.qmre.ltd/wp-content/uploads/2018/10/QMRE-Business-Plan-Digital.pdf (accessed on 19 February 2021).

[226] "Biofabrik wastx plastic solution," available online: https://www.qmre.ltd/wp-content/uploads/2020/09/QMRE-Introduction-doc-10-03-20.pdf (accessed on 19 February 2021).

[227] "Transforming plastic waste into valuable low-carbon fuel-quantafuel," available online: https://gwcouncil.org/wp-content/uploads/2020/06/Attachment-4-Quantafuel-introduction.pdf (accessed on 19 February 2021).

[228] "Quantafuel q3. 2020," available online: https://quantafuel.com/wp-content/uploads/2020/11/QFUEL-3Q20-REPORT.pdf (accessed on 19 February 2021).

[229] "Vitol to partner with quantafuel to market synthetic fuel made from recycled plastic," available online: https://www.vitol.com/vitol-to-partner-with-quantafuel-to-market-synthetic-fuel-made-from-recycled-plastic/ (accessed on 19 February 2021).

[230] "Recycling technologies firms up plans for scottish pyrolysis plant," available online: https://www.letsrecycle.com/news/latest-news/recycling-technologies-scottish/ (accessed on 24 February 2021).

[231] G. De Leon Izeppi *et al.*, "Economic risk assessment using monte carlo simulation for the production of azelaic acid and pelargonic acid from vegetable oils," *Ind. Crops Prod.*, vol. 150, p. 112411, 2020.

[232] V. Folliard, J. de Tommaso, and J.-L. Dubois, "Review on alternative route to acrolein through oxidative coupling of alcohols," *Catalysts*, vol. 11, no. 229, 2021.

[233] "Import data and price of acrylic plastic scrap. zauba," available online: https://www.zauba.com/import-acrylic-plastic-scrap-hs-code.html (accessed on 11 March 2021).

[234] "Eximpulse, india import data of 39159030," available online: https://www.eximpulse.com/import-hscode-39159030.htm (accessed on 11 March 2021).

[235] "International monetary fund global price of natural gas, eu," available online: https://fred.stlouisfed.org/series/PNGASEUUSDM (accessed on 11 March 2021).

[236] European Chemical Bureau, "European union risk assessment report–cas no: 80-62-6," European Commission, Luxembourg, Tech. Rep., 2002.

[237] "Eur-lex–52020dc0098–en–eur-lex–a new circular economy action plan," european Commission: Brussels, Belgium, 2020.

[238] "Plastics own resource," available online: https://ec.europa.eu/info/strategy/eu-budget/long-term-eu-budget/2021-2027/revenue/own-resources/plastics-own-resource_en (accessed on 12 July 2021).

[239] "Prices producer price indices (ppi)–oecd data," available online: https://data.oecd.org/price/producer-price-indices-ppi.htm (accessed on 28 June 2021).

[240] K. Sale, "Europe mma spot prices hit four-year low as buyers try to fulfil contract minimums," available online: https://www.icis.com/explore/resources/news/2020/04/06/10493857/europe-mma-spot-prices-hit-four-year-low-as-buyers-try-to-fulfil-contract-minimums (accessed on 11 March 2021).

[241] K. Loy, "Asia mma markets slip from record highs after 12 weeks of stability," available online: https://www.icis.com/explore/resources/news/2018/09/11/10258347/asia-mma-markets-slip-from-record-highs-after-12-weeks-of-stability (accessed on 11 March 2021).

[242] "Crude oil (petroleum)–monthly price–commodity prices–price charts, data, and news indexmundi," available online: https://www.indexmundi.com/commodities/?commodity=crude-oil (accessed on 12 January 2021).

[243] "Export data and price of regenerated methyl methacrylate hs 29161400," available online: https://www.zauba.com/export-regenerated-methyl-methacrylate-hs-code.html (accessed on 29 June 2021).

[244] Ademe, "Etude comparative de la taxation de l'elimination des dechets en europe," Ademe, France, Tech. Rep., 2017.

[245] M. Olofsson *et al.*, "Driving forces for import of waste for energy recovery in sweden," *Waste Manag. Res.*, vol. 23, pp. 3–12, 2005.

[246] "Iea–waste disposal costs and share of efw in selected countries charts data & statistics," available online: https://www.iea.org/data-and-statistics/charts/waste-disposal-costs-and-share-of-efw-in-selected-countries (accessed on 29 June 2021).

[247] "Cewep–landfill taxes and bans report," available online: https://www.cewep.eu/wp-content/uploads/2017/12/Landfill-taxes-and-bans-overview.pdf (accessed on 22 July 2021).

[248] OECD, "Waste management and the circular economy in selected oecd countries: Evidence from environmental performance reviews," Tech. Rep., 2018, available online: https://doi.org/10.1787/9789264309395-en (accessed on 22 July 2021).

[249] Our World in Data, "Per capita plastic waste vs. gdp per capita," available online: https://ourworldindata.org/grapher/per-capita-plastic-waste-vs-gdp-per-capita (accessed on 1 July 2021).

[250] "World bank. world development indicators–databank. gdp per capita, ppp (constant 2011 international $)," available online: http://data.worldbank.org/data-catalog/world-development-indicators (accessed on 22 July 2021).

[251] J. Jambeck *et al.*, "Plastic waste inputs from land into the ocean," *Science*, vol. 347, pp. 768–771, 2015.

[252] "Heating oil–daily price–commodity prices–price charts, data, and news–indexmundi," available online: https://www.indexmundi.com/commodities/?commodity=heating-oil&months=60 (accessed on 1 July 2021).

[253] A. Fivga and I. Dimitriou, "Pyrolysis of plastic waste for production of heavy fuel substitute: A techno-economic assessment," *Energy*, vol. 149, pp. 865–874, 2018.

[254] H. Thunman *et al.*, "Circular use of plastics–transformation of existing petrochemical clusters into thermochemical recycling plants with 100% plastics recovery," *Sustain. Mater. Technol.*, vol. 22, p. e00124, 2019.

[255] OECD, "Global plastics outlook: Economic drivers, environmental impacts and policy options," 2022, available online at Organisation For Economic Co-Operation And Development, Paris.

[256] Communication from the Commission to the European Parliament, the Council, the European Economic and Social Committee and the Committee of the Regions, "A new circular economy action plan for a cleaner and more competitive europe," 2020.

[257] Environment and Climate Change Canada (ECCC), "Zero plastic waste: Canada's actions," 2021, available online at https://www.canada.ca/en/environment-climate-change/services/managing-reducing-waste/reduce-plastic-waste/canada-action.html.

[258] UNITED NATIONS, "End plastic pollution: Towards an international legally binding instrument," 2022, available online at https://wedocs.unep.org/bitstream/handle/20.500.11822/38522/k2200647_-_unep-ea-5-l-23-rev-1_-_advance.pdf.

[259] M. Cordier *et al.*, "Economic drivers, environmental impacts and policy options," *Ecol. Econ.*, vol. 182, p. 106930, 2021.

[260] L. Lebreton and A. Andrady, "Future scenarios of global plastic waste generation and disposal," *Palgrave Commun.*, vol. 5, pp. 1–11, 2019.

[261] Q. Schuyler *et al.*, "Human population density is a poor predictor of debris in the environment," *Front. Environ. Sci.*, vol. 9, p. 583454, 2021.

[262] S. Kaza *et al.*, *What a Waste 2.0: A Global Snapshot of Solid Waste Management to 2050.* Washington, DC: World Bank, 2018.

[263] S. Nanda and F. Berruti, "Municipal solid waste management and landfilling technologies: a review," *Environ. Chem. Lett.*, vol. 19, pp. 1433–1456, 2021.

[264] E. Commission *et al.*, *Best Available Techniques (BAT) reference document for waste incineration – Industrial Emissions Directive 2010/75/EU (Integrated Pollution Prevention and Control).* Publications Office, 2019.

[265] European Commission, "Review report on the implementation of the recovery and resilience facility," 2022.

[266] T. O. Azeez, *Thermoplastic Recycling: Properties, Modifications, and Applications.* IntechOpen, 2019.

[267] M. Kazemi, S. F. Kabir, and E. H. Fini, "State of the art in recycling waste thermoplastics and thermosets and their applications in construction," *Resour. Conserv. Recycl.*, vol. 174, p. 105776, 2021.

[268] Z. O. G. Schyns and M. P. Shaver, "Mechanical recycling of packaging plastics: A review," *Macromol. Rapid Commun.*, vol. 42, p. 2000415, 2021.

[269] "Dasani and sprite boost sustainability packaging credentials," 2022, available online at https://www.coca-colacompany.com/news/dasani-sprite-boost-sustainability.

[270] I. Vollmer *et al.*, "Beyond mechanical recycling: Giving new life to plastic waste," *Angew. Chem. Int. Ed.*, vol. 59, pp. 15 402–15 423, 2020.

[271] H. Chen *et al.*, "Waste to wealth: Chemical recycling and chemical upcycling of waste plastics for a great futureg," *ChemSusChem*, vol. 14, pp. 4123–4136, 2021.

[272] M. Solis and S. Silveira, "Technologies for chemical recycling of household plastics," *Waste Management*, vol. 105, pp. 128–138, 2020.

[273] ECHA, "Chemical recycling of polymeric materials from waste in the circular economy," 2021.

[274] US Plastic Pact, "Roadmap to 2025," 2025, available online at https://usplasticspact.org/wp-content/uploads/2024/03/USPact_Roadmap-to-2025.pdf (Accessed on September 06 2024.

[275] House of Commons of Canada, "Committee report no. 21 – envi (42-1)," 2019.

[276] M. Sharkey *et al.*, "Phasing-out of legacy brominated flame retardants: The unep stockholm convention and other legislative action worldwide," *Environ. Int.*, vol. 144, p. 106041, 2020.

[277] ICIS, "Special report top 100 chemical companies," 2020.

[278] R. P. Lee *et al.*, "An analysis of waste gasification and its contribution to china's transition towards carbon neutrality and zero waste cities," *J. Fuel Chem. Technol.*, vol. 49, pp. 1057–1076, 2021.

[279] J. Nikiema and Z. Asiedu, "A review of the cost and effectiveness of solutions to address plastic pollution," *Environ. Sci. Pollut. Res. Int.*, vol. 29, pp. 24 547–24 573, 2022.

[280] R. Voss, R. P. Lee, and M. Frohling, "Chemical recycling of plastic waste: Comparative evaluation of environmental and economic performances of gasification- and incineration-based treatment for lightweight packaging waste," *Circ. Econ. Sustain.*, vol. 2, pp. 1369–1398, 2022.

[281] "Recycling technologies in swindon enters administration," 2022, available online at https://www.bbc.com/news/uk-england-wiltshire-63072055.

[282] V. Volcovici, "Brightmark, georgia county cancel $680 mln plastic-to-fuel project," 2022, available online at https://www.reuters.com/world/us/brightmark-georgia-county-cancel-680-mln-plastic-to-fuel-project-2022-04-11/.

[283] "The recycling myth: A plastic waste solution littered with failure," 2021, available online at https://www.reuters.com/investigates/special-report/environment-plastic-oil-recycling/.

[284] P. O'Connor, "An analysis of lithium-ion battery fires in waste management and recycling," 2021, available online at https://www.epa.gov/system/files/documents/2021-08/lithium-ion-battery-report-update-7.01_508.pdf.

[285] "The lens – free & open patent and scholarly search," available online at https://www.lens.org/.

[286] M. van Amsterdam, "Factorial techniques applied in chemical plant cost estimation," Ph.D. dissertation, tudelft, 2018.

[287] I. Tzinis, "Technology readiness level," 2015, available online at http://www.nasa.gov/directorates/heo/scan/engineering/technology/technology_readiness_level.

[288] "Demystifying construction project time – effort distribution curves: Bim and non-bim comparison," 2015, available online at https://ascelibrary.org/doi/epdf/10.1061/%28ASCE%29ME.1943-5479.0000356.

[289] P. Anticona, "Does BIM offer a better approach to guarantee a reliable, accurate, and precise cost estimate?" *PM World J*, vol. 8, pp. 1–28, 2019.

[290] A. Chauvel, G. Fournier, and C. Raimbault, *Manual of Process Economic Evaluation*. Editions Technip, 2003.

[291] A. M. Gerrard, *Guide to Capital Cost Estimating*. IChemE, 2000.

[292] A. Chauvel and G. Lefebvre, *Petrochemical Processes 1 Synthesis-Gas derivates and Major Hydrocarbons.* Editions Technip, 2001, vol. Vol. 1.

[293] D. A. of Cost Engineers, "Dace price booklet. cost information for estimation and comparison," Nijkerk: Vakmedianet, 2017.

[294] "Nelson-farrar cost index," n.d., available online at https://www.bakerrisk.com/products/nelson-farrar-cost-index/.

[295] "Try Plant Cost Index today," 2021, available online at https://www.chemengonline.com/try-plant-cost-index-today/.

[296] M. van der Spek, S. Roussanaly, and E. S. Rubin, "Best practices and recent advances in ccs cost engineering and economic analysis," *Int. J. Greenhouse Gas Control*, vol. 83, pp. 91–104, 2019.

[297] C. S. Giardinella, "Applying location factors for conceptual cost estimation," 2023, available online at https://www.chemengonline.com/location-factors/.

[298] A. V. Bridgwater, "International construction cost location factors," *Chem. Eng. (N. Y.)*, vol. 86, pp. 119–121, 1979.

[299] "Cost data on line, richardson international construction factors manual," 2008, available online at https://www.costdataonline.com/.

[300] H. J. Lang, "Cost relationships in preliminary cost estimation," *Chem. Eng.*, vol. 54, pp. 117–121, 1947.

[301] H. J. Lang, "Engineering approach to preliminary cost estimates," *Chem. Eng.*, vol. 54, pp. 130–133, 1947.

[302] H. J. Lang, "Simplified approach to preliminary cost estimates," *Chem. Eng.*, vol. 55, pp. 112–113, 1948.

[303] W. E. Hand, "From flow sheet to cost estimate," *Pet. Refin.*, vol. 37, pp. 331–337, 1958.

[304] G. J. Petley, "A method for estimating the capital cost of chemical process plants: Fuzzy matching," Ph.D. dissertation, Loughborough University, Loughborough, UK, 1997, pdf.

[305] J.-P. Lange, "Don't forget product recovery in catalysis research?check the distillation resistance," *ChemSusChem*, vol. 10, pp. 245–252, 2017.

[306] M. Tsagkari, A. Kokossis, and J.-L. Dubois, "A method for quick capital cost estimation of biorefineries beyond the state of the art," *Biofuels Bioprod. Biorefin.*, vol. 14, pp. 1061–1088, 2020.

[307] F. Riedewald *et al.*, "Economic assessment of a 40,000 t/y mixed plastic waste pyrolysis plant using direct heat treatment with molten metal: A case study of a plant located in belgium." *Waste Manage.*, vol. 120, pp. 698–707, 2021.

[308] M. Ghodrat *et al.*, "Economic feasibility of energy recovery from waste plastic using pyrolysis technology : an australian perspective," *Int. J. Environ. Sci. Technol.*, vol. 16, pp. 3721–3734, 2019.

[309] V. Chhabra *et al.*, "Techno-economic and life cycle assessment of pyrolysis of unsegregated urban municipal solid waste in india," *Ind. Eng. Chem. Res.*, vol. 60, pp. 1473–1482, 2021.

[310] G. Jiang *et al.*, "Molten solar salt pyrolysis of mixed plastic waste: process simulation and technoeconomic evaluation," *Energy Fuels*, vol. 34, pp. 7397–7409, 2020.

[311] E. W. Merrow, K. E. Phillips, and C. W. Myers, *Understanding Cost Growth and Performance Shortfalls in Pioneer Process Plants*. Santa Monica, CA: Rand Corp., 1981, available online at https://www.osti.gov/biblio/6207657.

[312] D. M. Wall, "Distributions and correlations in monte carlo simulation," *Constr. Manag. Econ.*, vol. 15, pp. 241–258, 1997.

[313] J. Bertisen and G. A. Davis, "Bias and error in mine project capital cost estimation," *Eng. Econ.*, vol. 53, pp. 118–139, 2008.

[314] R. Volk *et al.*, "Techno-economic assessment and comparison of different plastic recycling pathways: A german case study," *J. Ind. Ecol.*, vol. 25, pp. 1318–1337, 2021.

[315] A. Singh *et al.*, "Techno-economic analysis of waste plastic gasification to methanol process," Golden, CO (United States), 2022, available online at https://www.nrel.gov/docs/fy22osti/82636.pdf.

[316] K. Lan and Y. Yao, "Feasibility of gasifying mixed plastic waste for hydrogen production and carbon capture and storage," pp. 1–11, 2022.

[317] Ministry of Environment, Land & Waste –Korea, 2021, available online at https://m.me.go.kr/eng/web/index.do?menuId=466.

[318] Ministry of Environment – Japan, "Environmental regeneration and resource recycling (japanese)," 2022, available online at https://www.env.go.jp/recycle/plastic/circulation.html.

[319] C. P. P. House, "Waste and recycling report," 2018, available online at https://www.aph.gov.au/Parliamentary_Business/Committees/Senate/Environment_and_Communications/WasteandRecycling/Report.

[320] G. Towler and R. S. (Eds.), *Chemical Engineering Design, 2nd Ed.* Boston: Butterworth-Heinemann, 2013, p. i.

[321] Accenture, "More than half of consumers would pay more for sustainable products designed to be reused or recycled," 2019, available online at https://newsroom.accenture.com/news/more-than-half-of-consumers-would-pay-more-for-sustainable-products-designed-to-be-reused-or-rec htm.

[322] G. Pretner *et al.*, "Are consumers willing to pay for circular products? the role of recycled and second-hand attributes, messaging, and third-party certification," *Resour. Conserv. Recycl.*, vol. 175, p. 105888, 2021.

[323] G. S. Patience and D. C. Boffito, "Distributed production: Scale?up vs experience," *J. Adv. Manuf. Process.*, vol. 2, p. e10039, 2020.

[324] D. I. Garnett and G. S. Patience, "Why do scale-up power laws work?" *Chem. Eng. Prog.*, vol. 89, pp. 76–76, 1993.

[325] H. Reijonen *et al.*, "Factors related to recycling plastic packaging in finland's new waste management scheme," *Waste Manage.*, vol. 131, pp. 88–97, 2021.

[326] M. E. Edjabou *et al.*, "Municipal solid waste composition: Sampling methodology, statistical analyses, and case study evaluation," *Waste Manage.*, vol. 36, pp. 12–23, 2015.

[327] A. V. Bridgwater, A. J. Toft, and J. G. Brammer, "A techno-economic comparison of power production by biomass fast pyrolysis with gasification and combustion," *Renewable Sustainable Energy Rev.*, vol. 6, pp. 181–246, 2002.

[328] Y. Jafri, L. Waldheim, and J. Lundgren, "Emerging gasification technologies for waste & biomass - iea bioenergy," 2020, available online at https://www.ieabioenergy.com/wp-content/uploads/2021/02/Emerging-Gasification-Technologies_final.pdf.

[329] D. A. Tsiamis and M. J. Castaldi, "The effects of non-recycled plastic (nrp) on gasification: a quantitative assessment," 2018.

[330] S. Afzal *et al.*, "Techno-economic analysis and life cycle assessment of mixed plastic waste gasification for production of methanol and hydrogen," *Green Chem.*, vol. 25, pp. 5068–5085, 2023.

[331] T. Uekert *et al.*, "Technical, economic, and environmental comparison of closed-loop recycling technologies for common plastics," *ACS Sustain. Chem. Eng.*, vol. 11, pp. 965–978, 2023.

[332] Plastic Europe, "Plastics - the facts 2022," 2022. [Online]. Available: https://plasticseurope.org/wp-content/uploads/2022/10/PE-PLASTICS-THE-FACTS_V7-Tue_19-10-1.pdf

[333] E. Pawar, "A review article on acrylic PMMA," *IOSR J. Mech. Civ. Eng*, vol. 13, no. 2, pp. 1–4, 2016.

[334] T. C. Research and D. I. S. (CORDIS), "Innovative acrylic(PMMA polymethyl methacrylate) recycling technology complying with regulations," 2022, available online at https://cordis.europa.eu/project/id/856103/reporting (accessed: August 2022).

[335] Trinseo, "Trinseo and jsw europe announce collaboration on PMMA chemical recycling," 2022.

[336] M. C. America, "Mitsubishi chemical and Agilyx announce successful trial results for advanced recycling collaboration," 2021.

[337] J.-L. Dubois, "Guidelines for PMMA depolymerization at pilot and industrial scale," 2022, https://www.researchgate.net/ (accessed: April 2022).

[338] S. Moon *et al.*, "Introduction of reversible crosslinker into artificial marbles toward chemical recyclability," *Journal of Industrial and Engineering Chemistry*, vol. 31, pp. 86–90, 2015.

[339] E. Esmizadeh *et al.*, "Waste polymethyl methacrylate (PMMA): Recycling and high-yield monomer recovery," in *Handbook of Ecomaterials*, L. Martínez, O. Kharissova, and B. Kharisov, Eds. Cham: Springer International Publishing, 2018, pp. 1–33.

[340] Plastic Energy, "Plastic energy presentation at congreso International Tenerife + sostenible," https://www.youtube.com/watch?v=iX2dKikBka0, 2016, [Online; accessed 19- August-2023].

[341] A. Maisels, A. Hiller, and F.-G. Simon, "Chemical recycling for plastic waste: Status and perspectives," *ChemBioEng Reviews*, vol. 9, no. 6, pp. 541–555, 2022.

[342] M. P. Stevens, *Polymer chemistry*. Oxford university press New York, 1990, vol. 2.

[343] Agilyx, "Systems and methods for recycling waste plastics, including waste polystyrene, US10731080B1," 2016.

[344] A. Zayoud *et al.*, "Pyrolysis of end-of-life polystyrene in a pilot-scale reactor: Maximizing styrene production," *Waste Management*, vol. 139, pp. 85–95, 2022.

[345] MMAtwo, "Mmatwo second generation methyl methacrylate - wp7. communication, dissemination and academic outreach," 2022, last checked: 29-March-2023. [Online]. Available: https://www.mmatwo.eu/wp-content/uploads/2022/01/MMAtwo_D7.4_29112021_VF.pdf

[346] J.-L. Dubois, "Recovery of (meth)acrylic resin by depolymerization and hydrolysis - US202104028," Feb 2021.

[347] O. V. Chub *et al.*, "Fluidized bed poly (methyl methacrylate) thermolysis to methyl methacrylate followed by catalytic hydrolysis to methacrylic acid," *Applied Catalysis A: General*, vol. 638, p. 118637, 2022.

[348] G. Hong, K. Song, and Y.-W. Lee, "Recycling of waste artificial marble powder using supercritical methanol," *The Journal of Supercritical Fluids*, vol. 169, p. 105102, 2021.

[349] K. I. . S. truefriend, "(171120) - Lion Chemtech," https://file.truefriend.com/servlet/Download?file_path=research/research05/&file_name=lctkorea.pdf, 2021, [Online; accessed 19- August-2023].

[350] P. M. B. N. Korea, "Korean firms push economies of scale in artificial marble market," https://pulsenews.co.kr/view.php?year=2020&no=92195, 2020, [Online; accessed 19-September-2023].

[351] Statista, "Production volume of artificial marble in South Korea from 2006 to 2017 (in metric tons)," https://www.statista.com/statistics/732841/south-korea-artificial-marble-production-volume/, 2018, [Online; accessed 19-September-2023].

[352] K. Song, " MMA(Methyl methacrylate): MMA(Methyl methacrylate) separation from waste artificial marble using sub- and supercritical fluids (in korean)," https://s-space.

snu.ac.kr/handle/10371/166608?mode=full, 2020, [Online; accessed 19- September-2023].

[353] S. J. Pickering, "Recycling technologies for thermoset composite materials?current status," *Composites Part A: applied science and manufacturing*, vol. 37, no. 8, pp. 1206–1215, 2006.

[354] M. C. Jeon *et al.*, "Method of recycling acrylic resin, composition for acrylic artificial stone, and article of artificial stone – us patent 8048934," 2011, uS Patent 8,048,934.

[355] Y. G. S. Bok Roen Kim, Chang Woo Kim and Y. S. Lee*, "A study on recovery of aluminum oxide from artificial marble waste by pyrolysis (in korean)," *Korean Chemical Engineering Research*, vol. 50, no. 3, pp. 567–573, 2012.

[356] Veolia, "Company Website," https://www.veolia.co.kr/en/our-services/re, 2019, [Online; accessed 19- September-2023].

[357] LGCHEM, "LG Chem begins to apply recycled materials to transparent ABS production," https://www.lgcorp.com/media/release/23782, 2021, [Online; accessed 19-September-2023].

[358] Veolia, "Veolia Leaflet and r-MMA properties," https://www.veolia.co.kr/sites/g/files/dvc2646/files/document/2020/06/R%26E%20Leaflet%20English.pdf, 2019, [Online; accessed 19- September-2023].

[359] ECHA, "Guidance for monomers and polymers," https://echa.europa.eu/documents/10162/2324906/polymers_en.pdf/9a74545f-05be-4e10-8555-4d7cf051bbed, 2023, [Online; accessed 19-September-2023].

[360] ECHA, "Guidance on waste and recovered substances," 2010, https://echa.europa.eu/documents/10162/2324906/waste_recovered_en.pdf/657a2803-710c-472b-8922-f5c94642f836 Online; accessed 19-September-2023.

[361] E. Papirer *et al.*, "Adsorption of poly (methylmethacrylate) on an α alumina: evidence of formation of surface carboxylate bonds," *European polymer journal*, vol. 30, no. 8, pp. 985–991, 1994.

[362] S. Pletincx *et al.*, "Unravelling the chemical influence of water on the pmma/aluminum oxide hybrid interface in situ," *Scientific reports*, vol. 7, no. 1, p. 13341, 2017.

[363] X. Lü *et al.*, "Method for preparing polymethacrylic acid from polymethylmethacrylate through non-catalyzed hydrolysis in near-critical water - CN101735360B," 2011.

[364] W. N. Ayre, S. P. Denyer, and S. L. Evans, "Ageing and moisture uptake in polymethyl methacrylate (pmma) bone cements," *Journal of the mechanical behavior of biomedical materials*, vol. 32, pp. 76–88, 2014.

[365] Alteo, "Halogen Free – flame retardant fillers – SH950 grade," https://www.alteo-alumina.com/wp-content/uploads/2019/07/ALTEO-2023_Brochure_Flame-Retardant_web.pdf, 2023, [Online; accessed 19-September-2023].

[366] Huber Martinal website, "Martinal®aluminum hydroxide, Magnifin ®magnesium hydroxide – Halogen-Free Fire Retardants for the Cable Industry," https://www.huberadvancedmaterials.com/fileadmin/02_Solutions/_Brochures/Huber_Advanced_Materials_Martinal_Aluminum_Hydroxide_Magnifin_Magnesium_Hydroxide_Cable_Industry_v01.pdf, 2023, [Online; accessed 19-September-2023].

[367] Nabaltec, "Mineral-based flame retardancy with metal hydrates APYRAL®, APYRAL®, AOH ACTILOX®B," https://azelisamericascase.com/wp-content/uploads/2020/06/Nabaltec-Mineral-based-Flame-Retardancy-with-Metal-Hydrates-Brochure.pdf, 2020, [Online; accessed 19-September-2023].

[368] M. Walter and M. Wajer, "Overview of Flame Retardants Including Magnesium Hydroxide," https://magnesiaspecialties.com/technical-resources/MagShield-Overview-of-Flame-Retardants-Including-MgOH2.pdf, 2022, [Online; accessed 19-September-2023].

[369] J. Anderson, "Ath use in flame retardants: An overview of the industry and growth in asia," Presentation at Metal Bulletin?s 5th Asian Bauxite & Alumina Conference, 23 October 2015, 2016, [Online; accessed 19-September-2023].

[370] J. Newsome *et al.*, "Alumina properties. technical paper no. 10, second revision," Aluminum Co. of America. Alcoa Research Labs., New Kensington, Penna., Tech. Rep., 1960.

[371] K. Wefers and C. Misra, *Oxides and hydroxides of aluminum - technical report.* Alcoa Laboratories Pittsburgh, 1987, vol. 19.

[372] C. V. Chandran *et al.*, "Alumina: discriminative analysis using 3d correlation of solid-state nmr parameters," *Chemical Society Reviews*, vol. 48, no. 1, pp. 134–156, 2019.

[373] D. Freude and H.-J. Behrens, "Investigation of 27al-nmr chemical shifts in zeolites of the faujasite type," *Kristall und Technik*, vol. 16, no. 3, pp. K36–K38, 1981.

[374] A. Nair, *Effects of silica, mullite, alpha-alumina, and gamma-alumina on the nonoxidative thermal degradation of poly (vinyl butyral) and poly (butyl methacrylate) - PhD dissertation*. The University of Oklahoma, 1995.

[375] Aristech Surfaces, "Acrylic Syrup - Safety Datasheet," 2014, https://a.storyblok.com/f/146114/x/82c3f19f33/50-017-sds-acrylic-syrup.pdf, Online; accessed 19-September-2023.

[376] S. Özlem-Gundogdu, E. A. Gurel, and J. Hacaloglu, "Pyrolysis of poly (methyl methacrylate) copolymers," *Journal of Analytical and Applied Pyrolysis*, vol. 113, pp. 529–538, 2015.

[377] X. Gao, M. Chen, and T. Wang, "Design and optimization for the separation of a ternary methyl methacrylate-methanol-water mixture to save energy," *Energy Sources, Part A: Recovery, Utilization, and Environmental Effects*, pp. 1–10, 2020.

[378] J. Kooi, "The system methylmethacrylate-methanol-water," *Recueil des Travaux Chimiques des Pays-Bas*, vol. 68, no. 1, pp. 34–42, 1949.

[379] J.-T. Chen and H.-Y. Chang, "Liquid- liquid equilibria of water+ 2-butanol+(methyl methacrylate or butyl methacrylate or isobutyl methacrylate) at (288.2 and 318.2) k," *Journal of Chemical & Engineering Data*, vol. 52, no. 5, pp. 1950–1954, 2007.

[380] J. Yong-Soon and L. M.-S. Noh, "Recycling method of waste scagliola – US20130055926A1," 2010.

[381] M. C. Jeon *et al.*, "Method of recycling acrylic resin, composition for acrylic artificial stone, and article of artificial stone – US8048934B2," 2010.

[382] D. Grant and N. Grassie, "The thermal decomposition of polymethacrylic acid," *Polymer*, vol. 1, pp. 125–134, 1960.

[383] D. Davidson and P. Newman, "The occurrence of anhydrides in the pyrolysis of monocarboxylic acids," *Journal of the American Chemical Society*, vol. 74, no. 6, pp. 1515–1516, 1952.

[384] W. D. Loecker and G. Smets, "Hydrolysis of methacrylic acid–methyl methacrylate copolymers," *Journal of Polymer Science*, vol. 40, no. 136, pp. 203–216, 1959.

[385] J. E. Szulejko and K.-H. Kim, "Re-evaluation of effective carbon number (ECN) approach to predict response factors of compounds lacking authentic standards or surrogates (CLASS) by thermal desorption analysis with GC–MS," *Analytica chimica acta*, vol. 851, pp. 14–22, 2014.

[386] T. Leißner *et al.*, "High voltage fragmentation of composites from secondary raw materials–potential and limitations," *Waste management*, vol. 74, pp. 123–134, 2018.

[387] O. V. Chub, J.-L. Dubois, and G. S. Patience, "Zeolite Y hydrolyses methyl methacrylate to methacrylic acid in the gas phase," *Chemical Engineering Journal*, vol. 459, p. 141479, 2023. [Online]. Available: https://www.sciencedirect.com/science/article/pii/S1385894723002103

[388] I. C. for Diffraction Data, "The powder diffraction file 2024," 2024, https://www.icdd.com/pdfsearch/ - Accessed on 22-05-2024.

[389] O'Keeffe, "Opinion of advocate general sir gordon slynn. delivered on 8 july 1982," 2024, https://eur-lex.europa.eu/legal-content/EN/TXT/PDF/?uri=CELEX:61981CC0234 - Accessed on 22-05-2024.

[390] B. Zhu, B. Fang, and X. Li, "Dehydration reactions and kinetic parameters of gibbsite," *Ceramics International*, vol. 36, no. 8, pp. 2493–2498, 2010.

[391] B. K. Gan, "Crystallographic transformations involved in the decomposition of gibbsite to alpha-alumina," 1996, PhD dissertation, Curtin University of Technology, School of Physical Sciences.

[392] G. Paglia, "Determination of the structure of γ-alumina using empirical and first principle calculations combined with supporting experiments," 2004, PhD thesis, Curtin University.

[393] D. Redaoui *et al.*, "Mechanism and kinetic parameters of the thermal decomposition of gibbsite $\mathrm{Al\,O\,(OH)}$ by thermogravimetric analysis," *Acta Physica Polonica A*, vol. 131, no. 3, pp. 562–565, 2017.

[394] M. Ferriol *et al.*, "Thermal degradation of poly (methyl methacrylate)(PMMA): modelling of dtg and tg curves," *Polymer degradation and stability*, vol. 79, no. 2, pp. 271–281, 2003.

[395] A. Jamieson and I. McNeill, "The thermal degradation of copolymers of methyl methacrylate with methacrylic acid," *European polymer journal*, vol. 10, no. 2, pp. 217–225, 1974.

[396] P. Bera *et al.*, "Recent developments in synthetic marble processing," *Rev. Adv. Mater. Sci*, vol. 32, no. 2, pp. 94–105, 2012.

[397] S. C. Moldoveanu, *Analytical pyrolysis of synthetic organic polymers*. Elsevier, 2005.

[398] B. Ho, Y. Lee, and W. Chin, "Thermal degradation of polymethacrylic acid," *Journal of Polymer Science Part A: Polymer Chemistry*, vol. 30, pp. 2389–2397, 1992.

[399] V. Lago *et al.*, "Mixing and operability characteristics of mechanically fluidized reactors for the pyrolysis of biomass," *Powder technology*, vol. 274, pp. 205–212, 2015.

[400] J.-L. Dubois and S. J. J. V. D. Heijden, "Verfahren zum recycling von kontaminierten polymeren - EP4206267," 2023.

[401] V. Rai, C. Mukherjee, and B. Jain, "Optical properties (uv-vis and ftir) of gamma irradiated polymethyl methacrylate (PMMA)," *arXiv preprint arXiv:1611.02129*, 2016.

[402] P. Maji, R. Choudhary, and M. Majhi, "Structural, optical and dielectric properties of ZrO_2 reinforced polymeric nanocomposite films of polymethylmethacrylate (PMMA)," *Optik*, vol. 127, no. 11, pp. 4848–4853, 2016.

[403] E. Santacesaria *et al.*, "Thermochemical process for recovering fiberglass reinforced plastics waste matter," Patent US10 308 784, 2019.

[404] T. Neveux, O. Authier, and Y. Le Moullec, "Estimation technico-économique d'innovations technologiques en génie des procédés," available online: https://www.techniques-ingenieur.fr/base-documentaire/procedes-chimie-bio-agro-th2/innovations-en-genie-des-procedes-42487210/estimation-technico-economique-d-innovations-technologiques-en-genie-des-procedes-j8130/ (accessed on 03 October 2021).

APPENDIX A RECYCLING OF ARTIFICIAL MARBLE

This annex investigate the state-of-the-art of waste artificial marble thermolysis (pyrolysis), following the sole operating process by the Korean company R&E. This study is chapter 16 (in print) for the second edition of the Polymer Circularity Roadmap book, a dissemination project spurring from the MMAtwo consortium, to teach about PMMA recycling. In this contribution we analyzed the patent and open literature, recreated the R&E process, and extrapolated (taking some assumptions) its heat and mass balance, water consumption, and CO_2 footprint. The goal is to underline the peculiarity of waste artificial marble thermolysis as done in the industry, its challenging azeotropic separations, and environmental impact. In the framework of this dissertation, this annex serves as benchmark and literature review of waste artificial marble valorization.
The references are at the end of the section.

Artificial Marble, also known as Solid Surface, is a composite material of an inorganic pigment, usually about 60 wt % Aluminium Trihydroxide (or ATH) and 40 wt % of a polymeric matrix made of Methyl Methacrylate and comonomers and additives. To our knowledge the technology developed by R&E in Korea is the sole technology implemented in the world to recycle this material. The other technologies investigated so far, do not allow to process this kind of materials because a large amount of solid residue would accumulate in the reactors (Dry Distillation, Rotating Drum) or would require cleaning the heat transfer medium continuously (molten lead, or fluid bed).

The process developed by R&E is a stirred tank reactor, especially designed for solid surface products. The company operates 3 sites in Korea in a cluster of solid surface producers (Figure A.1). They produce MMA and alumina. The process is done in 2 steps: a dehydration at 200 °C to 250 °C of aluminium trihydrate followed by a PMMA depolymerization. This way, the hydrolysis of the MMA can be minimized. The coked alumina is then calcined at high temperature to produce a low surface alumina.

This process allows to treat composites. The value generated by the alumina fraction is good enough to take a share of the cost and of the CO2 emissions. If the alumina can be valorised at reasonable price, the process can be sustainable. However, the quality of the rMMA is limited by the impurities generated during the depolymerization process and by the formula of the matrix.

Acronyms

MMA: Methyl MethAcrylate
Crude MMA: Crude Methyl MethAcrylate
rMMA: regenerated Methyl MethAcrylate (Purified)
PMMA: Poly Methyl MethAcrylate
$Al(OH)_3$: Aluminium hydroxide
ATH: Aluminium hydroxide
Al_2O_3: Alumina
MAA: MethAcrylic Acid
MA: Methyl Acrylate
EA: Ethyl Acrylate
MIB: Methyl Isobutyrate
E/M Propionate: Ethyl/Methyl propionate

A.1 Introduction

In this chapter, we analyse the waste Artificial Marble recycling process, a mixture of PMMA, Aluminium trihydroxide (ATH) or Al(OH)3 and additives. The products are also known as "Solid Surface" or "CORIAN" (Dupont's Brand name). In Korea, there is a recycling cluster of this waste, with many patents filled from several companies and research institutes. We will focus on the technology developed by R&E, a Korean company which claims to recycle 35 000 t/y of waste artificial marble [35% PMMA, 1% additives and 64% $Al(OH)_3$ in three different plants [1]. On their website, they advertise that they collect scraps and dust from nearby companies such as LG Hausys, Hyundai, or Dupont. From their website, and some of their patents as well as a publication, we recreated a conceptual process design to better understand the limitation of this process. The process is using a semi-continuous stirred tank reactor, fed with an auger screw. The depolymerization is done in 2 stages, with a first dehydration around 250 °C, and a depolymerization at higher temperature.

Dehydrated alumina is semi-continuously removed from the reactor, with residual carbon, and directed to a calcination furnace where the combustion of the carbon residue provides the energy for the calcination. The crude MMA enters a complex purification process, combining decantation, chemical treatments, filtrations, and distillations. Purified MMA is produced at a yield of about 54 wt% (from initial PMMA content). The artificial marble is made from $Al(OH)_3$ and MMA syrup, itself made from MMA and PMMA beads or crushed extruded

grade PMMA containing some acrylates, because low molecular PMMA dissolves more easily in MMA. So, during depolymerization, acrylates are to be expected. Acrylates will delay the depolymerization during the heating stage at 250 °C.

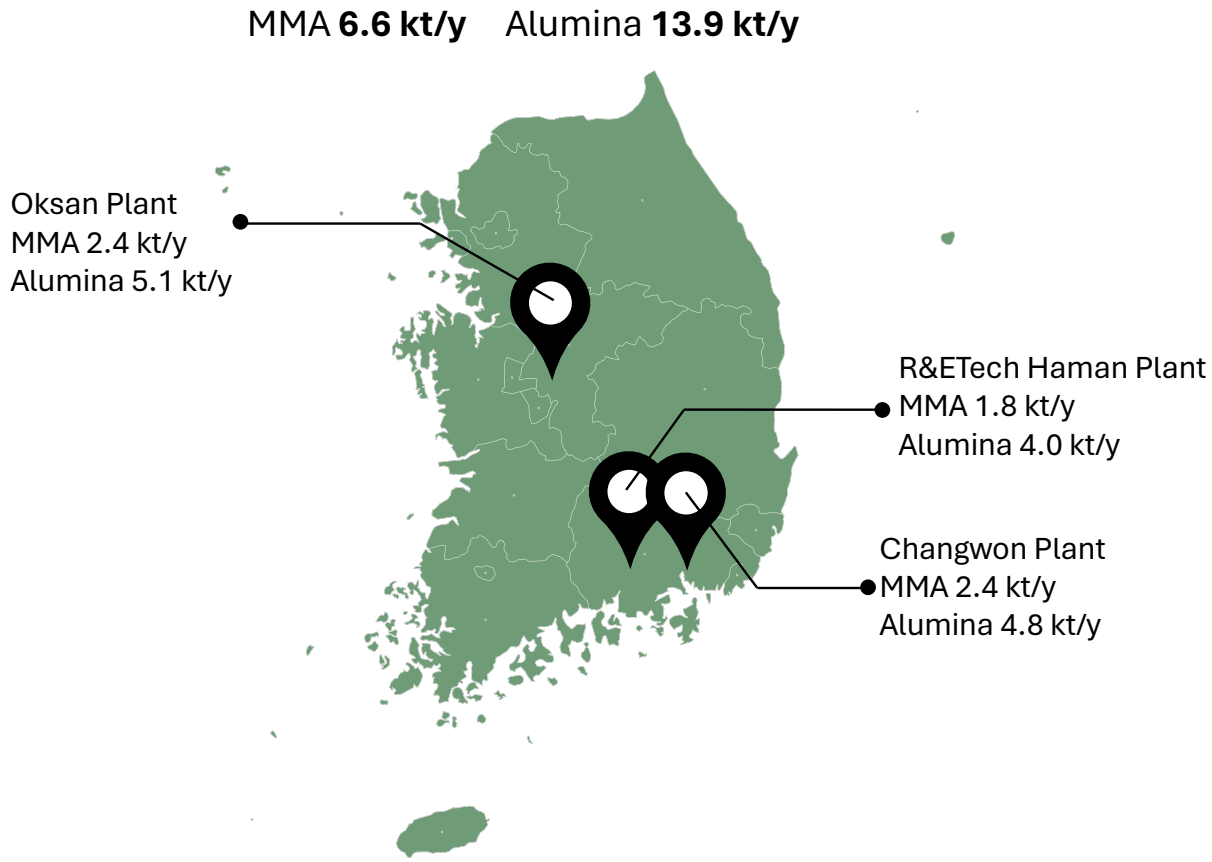

Figure (A.1) R&E solid surface chemical recycling plant in Korea [1]

A.1.1 Company presentation

R&E is a Korean recycling company, now part of Veolia (acquisition in 2019), a French multinational group that operates in water, waste management, and energy. R&E was originally established in 1999 in Korea; and since 2009 has patented several technologies for the recycling of artificial marble (or waste artificial marble). The flowsheet [1] (corresponding to US patent [2]), and the technology [3], were probably acquired by R&E in 2010 from LOTTE Advanced Materials Co. Ltd [4]. Similarly, the pre-treatment of the waste artificial marble is described in [5], the filler recovery section in [6], and the MMA purification in [7], which are all patents owned by R&E but built on, or referencing, former Lotte's patents.

A.2 Process Steps

The process is assumed to be similar to what they describe in [3], consisting of 4 sections (Figure A.2):

1. Pretreatment of the waste Artificial Marble;
2. Pyrolysis and condensation;
3. Crude Purification;
4. Filler calcination.

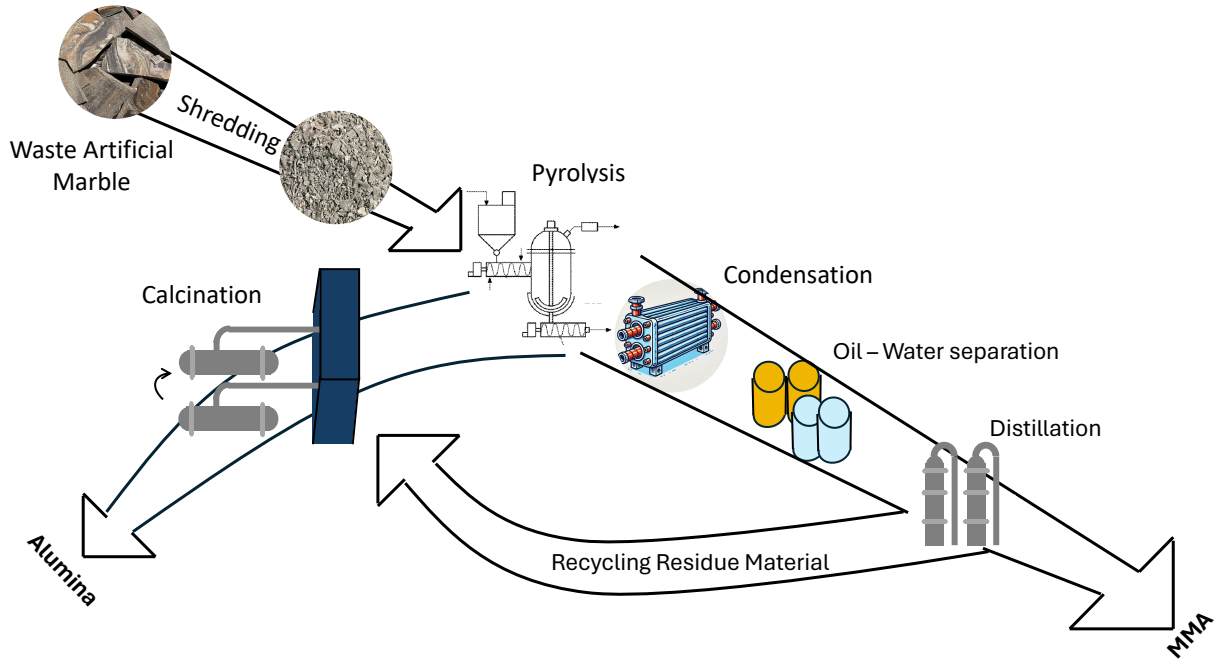

Figure (A.2) Simplified diagram of R&E process

A.2.1 Pretreatment (Section 100)

The first section (Section 100, Figure A.3) processes artificial marble waste, dry and wet dust. The artificial marble wet dust is dried in a furnace (114), and then stored in a dust storage tank along with the dry dust marble (111). The marble scraps are pulverized in a train of pulverisers (116) (120 mm to 12 mm to $2-3$ mm), sorted into dust and granules by a separator, and then stored accordingly. The dust and the granules are sent to the respective reactors (211) to be depolymerized (Section 200, Figure A.3).

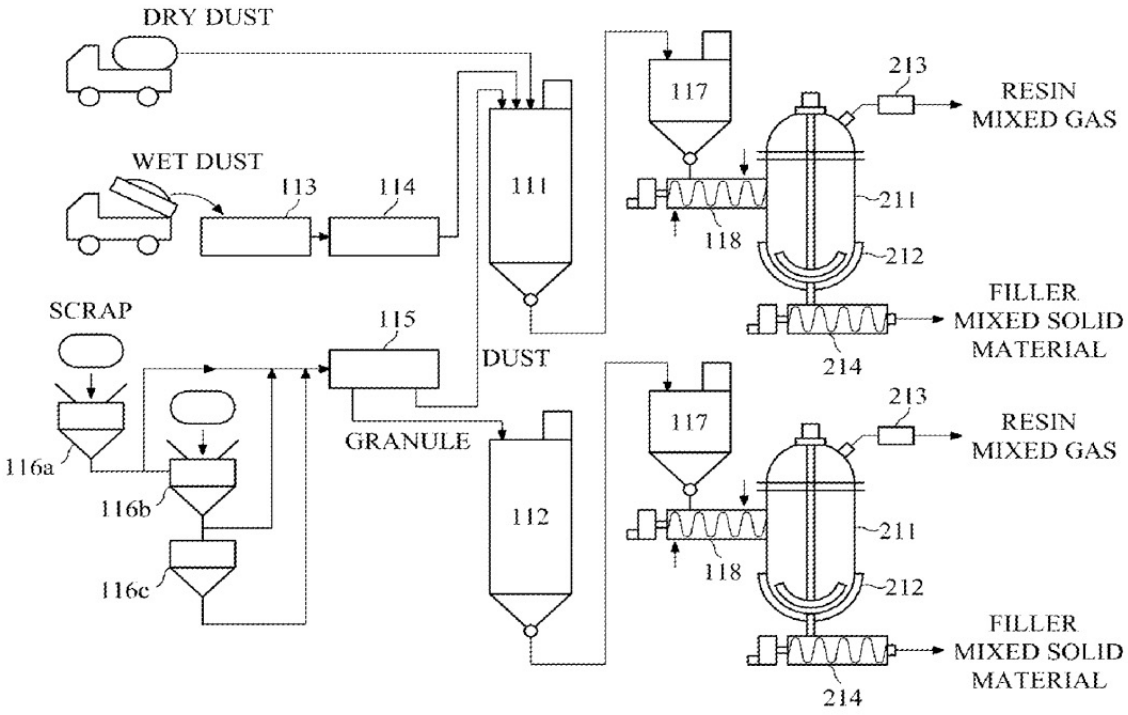

Figure (A.3) Pretreatment (100 section) and Depolymerization (200 section) [3]

A.2.2 Depolymerization (Section 200)

The depolymerization step is quantitatively described in [5]. The reactor concept (Figure A.4) resembles the Plastic Energy mixed plastics recycling; i.e., a stirred-tank reactor. It thermally decomposes the artificial marble wastes while stirring and heating, and then condenses (311, Figure A.7) the pyrolysis gases and recovers the alumina (214).

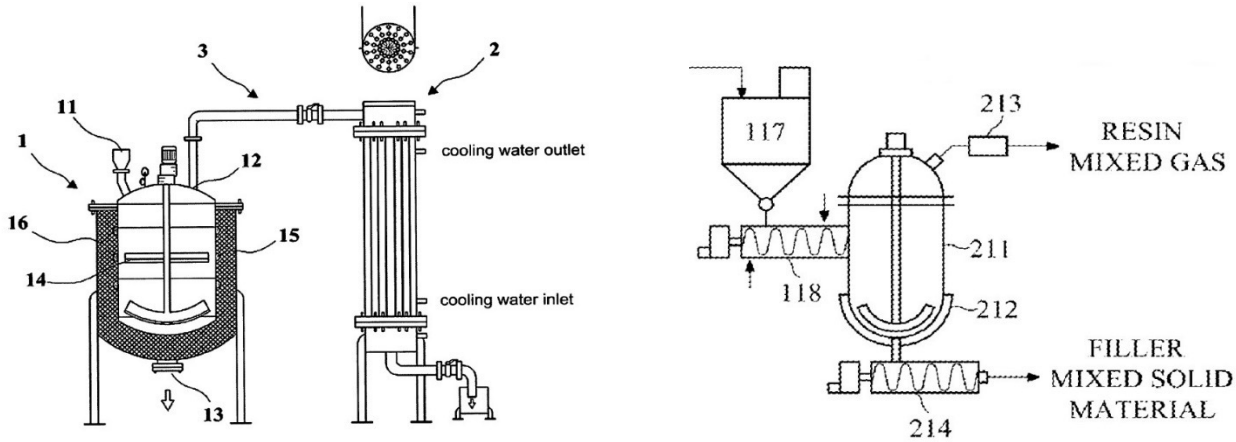

Figure (A.4) Depolymerization reactor and condensation (from [5] left, [3] right)

Because of the presence of $Al(OH)_3$ in the artificial marble, and the known dehydration reaction:

$$2Al(OH)_3 \rightleftharpoons Al_2O_3 + 3H_2O$$

the depolymerization is done in two steps to avoid PMMA hydrolysis.
First, the reactor heats the scraps (or dust) to about 250 °C (Figure A.5a), routing whatever vaporizes during the first heating process to a wastewater treatment. $Al(OH)_3$ starts to decompose to Aluminium OxyHydroxyde/Alumina and water at around 220 °C (on-set dehydration temperature). About 70% of the water is removed during the heating step at 250 °C. Then, progressively increasing the temperature from 250 °C to 400 −450 °C, the PMMA part of the composite starts to depolymerize to MMA. Whatever vaporizes in the meantime: MMA, light gases, water, light impurities (acrylates, propionates, isobutyrate), methacrylic acid, other organic acids, and some heavy-ends is condensed. At least two reactors are operated semi-continuously on the reaction side (as shown in the patent description); and continuously on the purification side, eventually switching the reactors after each batch (Figure A.5b).

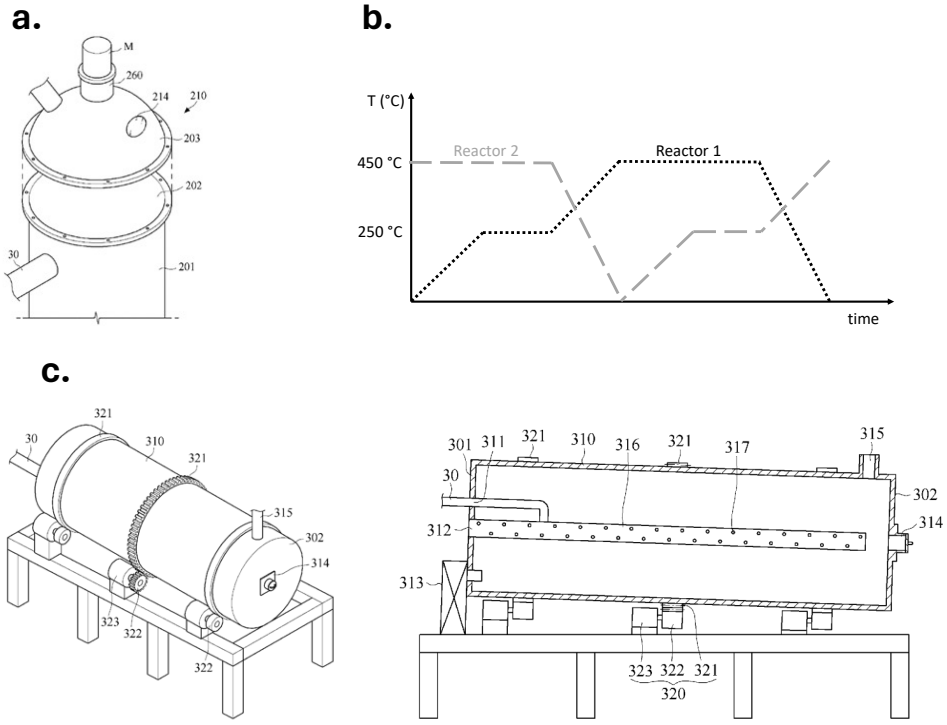

Figure (A.5) Detail of the pyrolysis zone (a) [9]; example of reaction cycles (b); and Alumina calcination furnace (c) from [2])

The pyrolysis gases are condensed and purified by a "three stages distillation tower" [3]. Accordingly, out of 1000 kg of artificial marble (PMMA + $Al(OH)_3$), 440 kg of inorganic alumina (maybe as α-alumina) and a crude MMA, which gives 370 kg of purified r-MMA, are produced.
The PMMA/$Al(OH)_3$ ratio (67:33) is consistent with a 64:35:1 ratio, where 1 is the additives. Since it is impossible to get 370 kg of MMA from only 326.7 kg of PMMA, we assume that the 370 kg corresponds to the MMA-water azeotrope (boiling point: 83 °C at 1 atm, 14 wt% water, 86 wt% MMA). To produce 370 kg of azeotrope, the stream contains 318 kg of MMA and 52 kg of water. However, most probably that stream contains more water than the simple azeotrope.

A.2.3 Purification (Section 300)

The purification section (Figure A.7) is taken from [3]. The pyrolysis vapours from the depolymerization reactor are first filtered (equipment 213, Figure A.7) to remove some elutriated alumina dust (and maybe some carbon) and condensed (311). Then, the crude liquid passes through a first tri-phase separator (312), a cooler (313) to keep the crude at 10 °C to 15 °C, a second tri-phase separator (314) to degas the crude from the uncondensed lights, an additional cleaner (315) for the solid particles, and an oil-water separator (316) to remove part of the water. Prior to the first distillation, the crude is first treated chemically (318), with active carbons/clay to adsorb and remove some impurities originally present in the polymer (e.g. pigment), and then filtered (319) to separate and recover the inorganic material. The crude is then distilled (321) for the first time, to remove some heavy residue, some water, and methacrylic acid (MAA) and other organic acids. The distillate is the MMA/water azeotrope, methanol, and the light impurities (MA, EA, MIB, E/M propionate, and organic acids). After partial condensation (324), the distillate is flashed/decanted (325) to degas the methanol (with some MMA, as an azeotrope [10]), which is sent to a deodorant furnace (329). The cooled MMA-water stream decants in 325, and water is removed with some MMA.

After the first purification, the r-MMA is eventually treated chemically a second time (331) to remove some impurities, and then sent to a second purification section. Again, here the MMA and MMA/water azeotrope distils on top of (341) (for the remaining water traces in crude MMA), then is cooled (in 342), flashed/decanted in (343), degassed from some impurities close to the MMA-water azeotrope (with probably acrylates), cooled in (344), filtered and treated (346) on a water adsorbent (maybe $CaCl_2$) down to 0.35 wt% water, and then finally stored. According to R&E, the MMA content in the r-MMA is above 96.5%, with less than 0.35 wt% of water. R&E recycles 35,000 t/y of artificial marble, made of 35 wt%

PMMA, 1 wt% additives, and 64 wt% $Al(OH)_3$, to produce 6,600 t/y purified r-MMA and 13,860 t/y of alumina; therefore, their global r-MMA yield is only 53.8 wt%.

As a summary, aluminium trihydroxide partially dehydrates at 250 °C. Some water is left with the alumina together with carbon residue. The carbon left should be sufficient to provide the energy for the alumina calcination step. Some small amount of MMA is lost during that initial dehydration. The core of the MMA is produced during the heating at high temperature together with remaining water, and organic impurities. In the purification section, MMA is recovered and purified. The remaining water is decanted and removed. Wastewater treatment is significant on the site, as water is produced at several steps.
In Figure A.6, we report a block flow diagram of the process, with the overall mass flux; the rationale of the balance and our assumptions will be explained in the following sections.

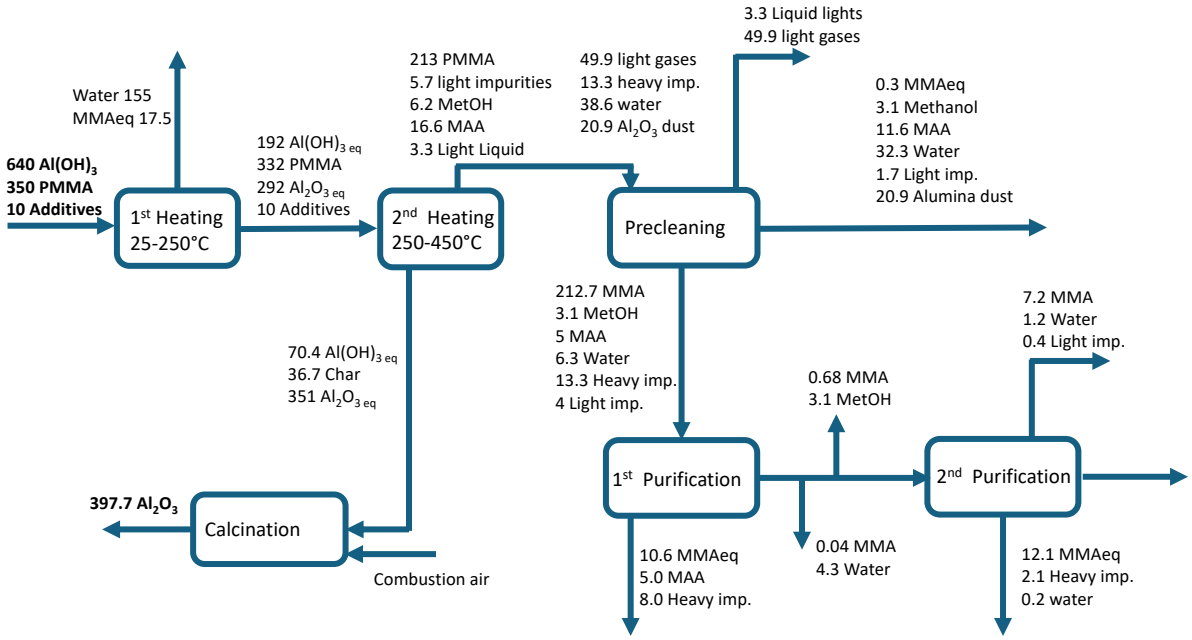

Figure (A.6) Block diagram of the R&E process mass flows

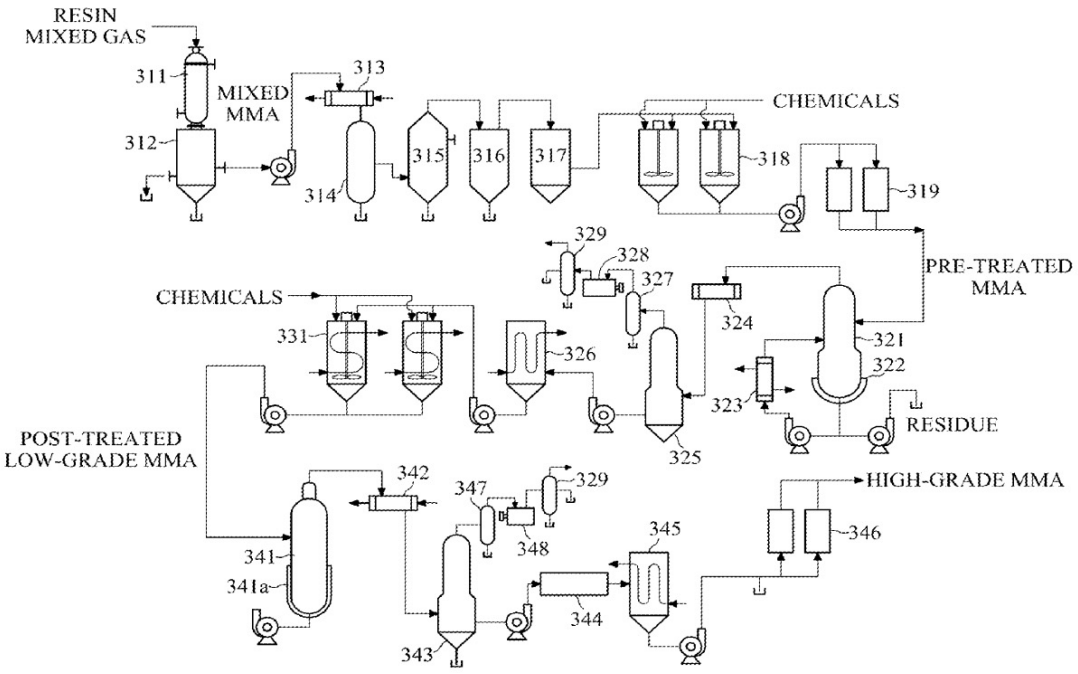

Figure (A.7) Purification section (section 300) [3]

A.3 Mass Balance

We closed the mass balance of the process comprising the purification described in [3], as the data reported in [5] and [4] do not allow us to get a convincing data set (Figure A.8). The global r-MMA yield is 53.8 wt%, and the r-MMA purity is 96.5%, with 0.35 wt% water. The alumina yield is around 95%, with some losses due to the elutriation of the finer particles lost with the pyrolysis gases. For the mass balance, the feed is therefore made of $350\,\mathrm{kg\,h^{-1}}$ PMMA, $10\,\mathrm{kg\,h^{-1}}$ additives, and $640\,\mathrm{kg\,h^{-1}}$ of $Al(OH)_3$, which is virtually able to release 222 kg of water.

We can divide the process into 4 main sections:

- 100: Pretreatment
- 200: Pyrolysis
- 300: Condensation and Purification
- 400: Alumina Calcination

A.3.1 Pyrolysis

For the pyrolysis section, a first dehydration of the artificial marble at 250 °C generates gaseous products which are routed to wastewater treatment. In a second heating stage from 250 °C to 400 °C [3] or 450 °C [5], the gases, which are supposed to be mostly MMA, are collected.

The effect of pyrolysis temperature on the alumina quality suggests that the optimum in terms of chromaticity (colour), surface area, and pore volume is a pyrolysis at 500 °C, which leaves 4-6 wt% of carbon residue on the fillers after pyrolysis [11]. A low carbon residue would mean a lower loss at the pyrolysis, less water is left with the alumina, and if the calcination temperature is properly controlled, one could theoretically get a high surface alumina. However, doing so might over-crack the PMMA, and concurrently require a reactor that is able to reach and withstand this high pyrolysis temperature (500 °C).

The alumina produced has a low surface area ($30-80\,m^2\,g^{-1}$) suggesting that the calcination is difficult to control, due to a higher carbon content corresponding to a pyrolysis done at a lower temperature, more in the order of 450 °C, leaving a higher quantity (>7-8%) of carbon on the filler. 8 wt% of residual PMMA on the alumina would correspond to 10.2% of the initial PMMA, and would then impact the rMMA yield. This is in line with [3], where 8-15 wt% PMMA is left on fillers for the calcination. At lower pyrolysis temperatures ($400-450$ °C), the PMMA residues are not completely charcoaled, and therefore the resulting deposit is brownish.

In the current mass and energy balances, we opted for a pyrolysis temperature of 450 °C, corresponding to 8 wt% carbon residue and an alumina that could still be a high surface alumina if properly calcined. In these operating conditions, the pyrolysis does not dehydrate completely the alumina. After the pyrolysis, the crude alumina is made of 397.3 kg of Al_2O_3, 24.4 kg of water (as alumina oxyhydroxide or $Al(OH)_3$ equivalent), and 36.7 kg of PMMA equivalent as carbon residue.

A.3.2 Alumina Calcination

Depending on the type of hydroxide in the artificial marble, one could produce a different kind of alumina after calcination. When heated, gibbsite can either produce χ-alumina or boehmite (AlO(OH)), therefore only partially dehydrating. When calcined, boehmite will produce γ, δ, or θ-alumina, which are more interesting (especially γ-alumina has high surface area and pore volume, and is in demand as a catalyst support for various applications). Gibbsite does not dehydrate completely during the composite pyrolysis. At 250 °C, the fillers lose at least 10% of their weight in water (data from thermogravimetric analysis), but as the

temperature is kept for some time at 250 °C, we assume a 70 wt% loss of the water at this stage (first heating), or 155 kg.

From the starting 640 kg of $Al(OH)_3$, after the preheating at 250 °C, we end up with 192 kg of $Al(OH)_3$ equivalent and 293 kg of alumina equivalent (which is more like a partially dehydrated/aluminium hydroxide).
After the first dehydration (at 250 °C), in the artificial marble, we still have:

- 95% of the PMMA, or 332.5 kg;
- 30% of the water to be released, or 66.5 kg;
- and all the potential alumina.

After the second heat treatment (250 °C to 450 °C), the alumina residue contains:

- 24.4 kg of water as hydrate of alumina;
- 36.7 kg of char, assuming 8 wt% of carbon in the crude alumina; and
- the complement of not fully dehydrated alumina, 351 kg.

The crude MMA contains:

- 213 kg of MMA;
- 20.9 kg of Al_2O_3;
- 5.7 kg of light impurities (from MMA and additives);
- 6.2 kg of methanol (from MMA hydrolysis);
- 16.6 kg of methacrylic acid (from MMA hydrolysis);
- 3.3 kg of liquid lights;
- 49.9 kg of light gases;
- 13.3 kg of heavy impurities; and
- 36.8 kg of water.

The carbonaceous residue on the crude alumina must provide heat for the calcination. To justify the choice of 8 wt% of carbonaceous residue on the alumina, we analyzed the effect of the content of carbonaceous material left on alumina on the final calcination temperature.

The adiabatic temperature rise is then calculated.
Assuming a Lower Heating Value (LHV) of the carbonaceous material equal to the one of solid PMMA ($24.52\,\mathrm{MJ\,kg^{-1}}$), the combustion of the carbon (or MMA) would have to provide heat for heating the air/diluted air stream, to heat the alumina, dehydrate alumina, and rearrange the alumina crystalline phase.
The heat of combustion of the char is consumed by the remaining alumina dehydration (169 MJ), the crystallization to alpha alumina (53 MJ), 8.2 kg of stoichiometric air (O_2 + N_2) per kilogram of char (to burn the carbon residue assumed to be PMMA). 8 wt% of char (corresponding to 36.7 kg of carbon residue as remaining PMMA) generates $339\,\mathrm{kg\,h^{-1}}$ of flue gas (81 kg CO_2 + 26 kg H_2O + 232 kg N_2).
Therefore, assuming a constant specific heat of $1.2\,\mathrm{kJ\,kg^{-1}\,°C^{-1}}$ for the alumina, and a constant specific heat for the flue gas of $0.823\,\mathrm{kJ\,kg^{-1}\,°C^{-1}}$, the adiabatic temperature rise at calcination (ΔT) increases with the carbon residue. At 8 wt% residue, the adiabatic temperature rise is 890 °C, which is enough to carry the calcination.
For the mass balance, we assumed 8 wt% carbon residue on the crude alumina fillers, which seems reasonable considering the low surface alumina obtained by R&E.

In addition to these, for the pyrolysis we assumed:

- Water released at first dehydration: 155 kg;
- MMA losses at first dehydration: 5% (17.5 kg);
- MMA/PMMA left after the first dehydration: 332.5 kg;
- MMA losses at pyrolysis: 30.6 kg PMMA as carbon char on the fillers, 15% as light gases (49.9 kg), 1% as liquid lights (3.3 kg), 4% as heavies (13.3 kg), 5% as MAA (16.6 kg), 0.5% as impurities (1.7 kg as EA, MA, EP, MP, MIB, odors, and organic acids);
- 60% of the additives become carbon char, and 40% impurities (6 kg and 4 kg respectively).

A.3.3 Purification

In the pre-cleaning part of the purification section (before the distillation), we assumed:

- To remove 30% of the impurities from pyrolysis with the first chemical pretreatment (318/319) with clay/adsorbents.
- The solubility of MAA in water at 20 °C is $97\,\mathrm{g\,L^{-1}}$, therefore all the MAA should be soluble in the water in the first decanter (316). However, we assume that only 70% of

the MAA is separated by decantation, while the rest remains in the crude at this stage (i.e., in stream 10).

- The solubility of water in MMA is 1 wt% [12], but we assumed that the water entrained with the crude is 3 times its solubility limit, as droplets, or because methanol increases the water solubility.
- The solubility of MMA in water is $10.03\,\mathrm{g\,L^{-1}}$ at $15\,^{\circ}\mathrm{C}$ [13] (operating temperature of the decanter 316), and we assumed that 100% of the soluble MMA is lost in the decantation.

In the first distillation section, we assumed:

- The column (321) distills on top the MMA/water azeotrope, along with the methanol, the light impurities, and 40% of the heavy impurities. The residues are the complement of the total water, 60% of the heavy impurities, the rest of the MAA (and organic acids) that was still in the crude, and 5% of the MMA of the crude, that is lost.
- The top of the column is cooled (324) (at around $50\,^{\circ}\mathrm{C}$), and then flashed in (325), what R&E calls the "decanter tank." Here, we separate the methanol along with the MMA at the azeotropic composition [14], and water is decanted at the bottom from the MMA. We assumed that the water is entrained as droplets with the purified crude at its solubility limit in MMA (1 wt% water in MMA). The flash takes the heat from the liquid stream to evaporate the methanol azeotrope.
- We assume to remove some more light impurities in the second chemical treatment (331) (20%, a little less than the first chemical treatment). However, the nature of this treatment is unknown.

Finally, in the second distillation section, we assumed:

- The column (341) distills from the top the MMA and MMA/water azeotrope, and the light impurities remaining. The bottom residue is 6% of the MMA, and 40% of the remaining heavies.
- The top of the column is cooled (342) and flashed (343) to eliminate the MMA/water azeotrope and some odorous impurities (for instance acrylates), with some MMA loss to close the balance.
- The water still present (0.84 kg at this stage) is partially eliminated with a $CaCl_2$ (or magnesium sulfate) treatment (346), to bring it down to the r-MMA specs (0.35 wt% water in r-MMA).

The purified r-MMA stream is then composed of:

- MMA: 96.5 wt%;
- Light impurities: 1.45 wt%;
- Heavy impurities: 1.7 wt%;
- Water: 0.35 wt%.

Treating 1000 $\mathrm{kg\,h^{-1}}$ of artificial marble, the process produces:

- 299 kg of wastewater, with 34.2 kg (or 11.5 wt%) of organics in it;
- 91 kg of by-products to be burned, with (or without) energy recovery;
- 12.6 kg of light impurities/odors/MMAeq to be thermally oxidized on site;
- 188.7 kg of purified r-MMA (96.5 wt% purity) to be sold;
- 397.3 kg of Al_2O_3 to be sold.

Stream		**1**	**2**	3	**4**	**5**	**6**	**7**	**8**	**9a**	**9**
Name	Mol. Weight	Artificial Marble	Dehydration discharge	Preheated Marble	Cracked gas	Fillers/ Crude Alumina	Alumina	Crude MMA	Uncondensed gases	1st precleaning purge	1st decanter purge
Temperature	*(˚C)*	*250*	*250*	*450*	*450*	*25*	*25*	*15*		*15*	*15*
PMMA		350									
MMA	100		17.5	332.5	213			213			0.3
$Al(OH)_3$	78	640		192		70.4					
Char						36.7					
Alpha-Alumina	101.9			292.8	20.9	351.3	397.3			20.9	
Additives		10.0		10.0							
Light Impurities (EA, MA, MIB, Ketones, Pigments)					5.7			5.7		1.7	
Methanol	32.04				6.2			6.2			3.1
MAA	86.06				16.6			16.6			11.6
Light liquids					3.3				3.3		
Light gases (CO_2, CO, Ethylene, C3, CH_4)					49.9				49.9		
Heavy Impurities					13.3			13.3			
Water	18		155.1		38.6	(24.4)		38.6			
Total		**1000**		**827.3**	**367.6**	**458.4**	**397.3**	**293.5**	**53.2**	**22.6**	**47.4**

Figure (A.8) Overall Mass Balance - Streams 1 to 9

Stream		**10**	**11**	12	**13a**	**13**	**22**	**14**	**15**	**16**	**17**	**18**	**19**	**20**	**21**
Name	Mol. Weight	Precleaned Crude	Top 1st Column	Residue 1st Column	Flash to 1st Odor removal	2nd decanter Purge	2nd Chemical Trt purge	Chemicall y treated	Top 2nd Column	Residue 2nd Column	Decant. 2nd Column	Odor Removal 2nd Col.	Dirt rMMA	Water Removal purge	rMMA
Temperature	*(˚C)*		*83*									*83*			
PMMA															
MMA	100	212.7	202.2	10.6	0.68	0.04		201.4	191.3	12.1		7.2	182.0		182.0
$Al(OH)_3$	78														
Char															
Alpha-Alumina	101.9														
Additives															
Light Impurities (EA, MA, MIB, Ketones, Pigments)		4.0	4.0				0.8	3.2	3.2			0.4	2.8		2.8
Methanol	32.04	3.1	3.1		3.1										
MAA	86.06	5.0		5.0											
Light liquids															
Light gases (CO_2, CO, Ethylene, C3, CH_4)															
Heavy Impurities		13.3	5.3	7.98				5.32		2.13			3.19		3.19
Water	18	6.3	6.3	0.0		4.3		2.0	2.0	0.00		1.2	0.84	0.18	0.66
Total		**244**	**219**	**23.6**	**3.8**	**4.3**	**0.8**	**212**	**196**	**14.2**	**0.0**	**8.8**	**188.8**	**0.2**	**188.7**

Figure (A.9) Overall Mass Balance - Streams 10 to 21

A.4 Energy Balance

From our mass balance, we can estimate the main energy consumption of the process. To do so, we assumed:

- $C_{p,l,v}$, calorific value ($\mathrm{kJ\,kg^{-1}\,K^{-1}}$) of liquid and gas MMA = $1.6\,\mathrm{kJ\,kg^{-1}\,K^{-1}}$
- $C_{p,l,v}$, calorific value ($\mathrm{kJ\,kg^{-1}\,K^{-1}}$) of molten PMMA = $1.6\,\mathrm{kJ\,kg^{-1}\,K^{-1}}$
- Heat of fusion (H_f) ($\mathrm{kJ\,kg^{-1}}$) of PMMA = $50.2\,\mathrm{kJ\,kg^{-1}}$
- Heat of depolymerization (H_{dep}) ($\mathrm{kJ\,kg^{-1}}$) of PMMA = $540\,\mathrm{kJ\,kg^{-1}}$
- Temperature of depolymerization = 450 °C
- Heat of condensation/(-vaporization) ($H_{cond,MMA}$) in E-201: $360\,\mathrm{kJ\,kg^{-1}}$
- $C_{p,p}$, calorific value ($\mathrm{kJ\,kg^{-1}\,K^{-1}}$) of PMMA = $2.3\,\mathrm{kJ\,kg^{-1}\,K^{-1}}$
- $C_{p,Al}$, calorific value of $Al(OH)_3$/Alumina system = $1.2\,\mathrm{kJ\,kg^{-1}\,K^{-1}}$ [15,16]
- Hdehydration enthalpy of $Al(OH)_3$ dehydration to $\gamma/\kappa/\chi$ alumina = $2400\,\mathrm{kJ\,kg^{-1}}$ $Al(OH)_3$ [15,16]
- Reflux ratio in both distillation columns $R = 3$
- Artificial marble "melting" temperature = 250 °C
- Dehydration temperature of $Al(OH)_3$ = 250 °C

A.4.1 Pyrolysis

To calculate the total energy needed to depolymerize and dehydrate the artificial marble at the pyrolysis, we can split it into the energy needed for the two components of the solid: PMMA and $Al(OH)_3$, and then sum the two contributions. It will be useful later when we need to split the energy and CO_2 emissions on the 2 products. For the PMMA, we need to heat the PMMA from 25 °C until the melting temperature (250 °C), melt the PMMA, heat the molten PMMA up to the depolymerization temperature (450 °C), and then depolymerize it.
At the same time, we will heat up the $Al(OH)_3$ part of the artificial waste marble, from 25 °C to 250 °C (the dehydration temperature), and then heat up the Al_2O_3 formed to 450 °C.
Therefore, the total energy required for the pyrolysis is:

- For the PMMA part: 593 MJ, and

- For the Alumina/$Al(OH)_3$: 1656 MJ.

The total duty for the pyrolysis is 2249 MJ. Splitting this energy into MMA and crude Alumina by mass allocation, we have:

- 878 MJ to crude MMA,
- 1371 MJ to crude Alumina.

A.4.2 Purification

The reboiler of the first column (321) consumes 264 MJ, while the second column consumes 229 MJ. So, the total energy required for the purification is 493 MJ, that we allocate fully to MMA. The total overall energy for the process is 2742 MJ.

A.4.3 Energy split by mass allocation

The MMA contribution to the total energy of the process is 878 MJ + 493 MJ = 1371 MJ, corresponding to 7.26 $MJ\,kg^{-1}$ of purified r-MMA . This corresponds to the MMA contribution at cracking (by mass allocation) and the purification energy. The Alumina contribution to the total energy of the process is also 1371 MJ, corresponding to 2.99 $MJ\,kg^{-1}$ crude Alumina, or 3.45 $MJ\,kg^{-1}$ of Al_2O_3. This energy represents the Alumina contribution (by mass allocation) at the cracking.

Theoretically, part of this heat could be provided by the by-products combustion. In fact, stream 8, the uncondensed gases from pyrolysis, stream 12, and stream 16, the heavy residue of the two columns, could provide respectively (assuming an LHV = 27.252 $MJ\,kg^{-1}$ for all the streams): 1447 MJ , 639 MJ , and 387 MJ. For a total of 2476 MJ provided by the by-product combustion, around 90% of the total duty required by the process. The reason why the by-products could provide almost all the energy needed is the very low MMA yield (54 wt%).

A.4.4 Water treatment

Although not mentioned directly in the process description, the high amount of wastewater produced (299 kg with 11.5 wt% of organics in it) requires a water treatment on site. As a rule of thumb, in first approximation, the COD (chemical oxygen demand) can be taken equal to the pollutant concentration. In our case, the organics are mainly MMA equivalents, Methanol, and MAA, which means for instance that to oxidize 34.4 $kg\,h^{-1}$ of MMA we

would need 66.4 kg h^{-1} of O_2, so the COD would be around twice the pollutant concentration.

Nevertheless, considering the broad nature of the pollutants (organics somehow close to MMA, MAA, and Methanol), we believe that an appropriate choice could be a catalytic wet air oxidation unit (CWAO). Air oxidizes the wastewater in a catalytic bed, in an exothermic reaction. Then, the hot treated water from the reactor preheats the incoming polluted water. At the same time, the treated water cools down before degassing in a liquid-water separator. Here, we recover the treated water, separating the off-gases on top.
We can split the water produced by mass allocation into r-MMA and Alumina. All the streams (S) coming from the purification section (S9, S9a, S13, S20, S22) can be completely allocated to MMA, for a total of 0.39 kg kg^{-1} wastewater per r-MMA. The wastewater from the alumina calcination (water vapor from char combustion + water vapor from dehydration) can be allocated fully to Alumina for 0.12 kg kg^{-1} of Alumina.

Finally, the wastewater from cracking (172.7 kg) can be split between MMA and Alumina as:

- 0.35 kg wastewater/kg r-MMA, and
- 0.26 kg wastewater/kg Alumina.

For a total of:

- 0.39 + 0.35 = 0.74 kg wastewater/kg r-MMA, and
- 0.12 + 0.26 = 0.38 kg wastewater/kg Alumina.

A.4.5 Cooling water estimates

We must cool the crude MMA generated at the depolymerization and the streams at the distillations. The calcined Alumina is also heated to high temperature and would have to be cooled. However, in the case of the alumina, we are going to assume that the calcination is done in a countercurrent furnace. It means that cold air contacts the hot calcined alumina when it enters the furnace. That way, the alumina is cooled and the air is preheated to the calcination temperature, avoiding water consumption.
For the crude and distilled MMA, the cooling water consumption is proportional to the heat exchanged in the units. For the condensation of the crude MMA from the pyrolysis, one must cool the MMA vapors from 450 °C to the condensation temperature, followed by condensation and finally cooling the MMA liquid to storage temperature.
In addition, we must cool water from the first stage at 250 °C to room temperature, and for

the remaining water heated to depolymerization temperature to storage temperature.
To simplify the calculations, we are going to treat the 2 streams as pure MMA and pure water respectively. The total water consumption is then 363 kg of water.
For the distillations, we take the energy injected at the reboilers as the energy we have to remove from the unit. This corresponds to 493 MJ, and 214 kg of water consumption. The water consumption from cooling is then 3.06 $kg\,kg^{-1}$ of r-MMA. Again, this is the same order of magnitude as for other units processing PMMA scraps and not composites. However, a major difference here is the high amount of water generated by the process itself, which also requires being condensed and cooled.

A.5 CO_2 Emissions

The CO_2 emissions in the process are divided into (Figure A.10):

- CWAO water treatment emissions, from the oxidation of the organic fractions in the wastewater,
- Emissions from the thermal oxidation of the odorous streams,
- Emissions from the calcination of the crude alumina via char combustion,
- Emissions from the combustion of either natural gas or by-products to supply the energy for the cracking and purification.

In each section, we split the emissions by mass allocation into r-MMA and Alumina emissions, and finally, we calculate the global emissions.

A.5.1 Water treatment

The organics in the water treatment will oxidize as follows:

- MMA: $C_5H_8O_2 + 6\,O_2 \longrightarrow 5\,CO_2 + 4\,H_2O$
- MAA: $C_4H_6O_2 + 4.5\,O_2 \longrightarrow 4\,CO_2 + 3\,H_2O$
- Methanol: $CH_3OH + 1.5\,O_2 \longrightarrow CO_2 + 2\,H_2O$

With the light impurities assumed to behave like MMA, the total amount of CO_2 generated is then 73 kg.

Again, the CO_2 produced by the oxidation of the organic species can be split between Alumina and r-MMA by mass allocation. The CO_2 of stream 2 (38.5 kg CO_2eq) is split into:

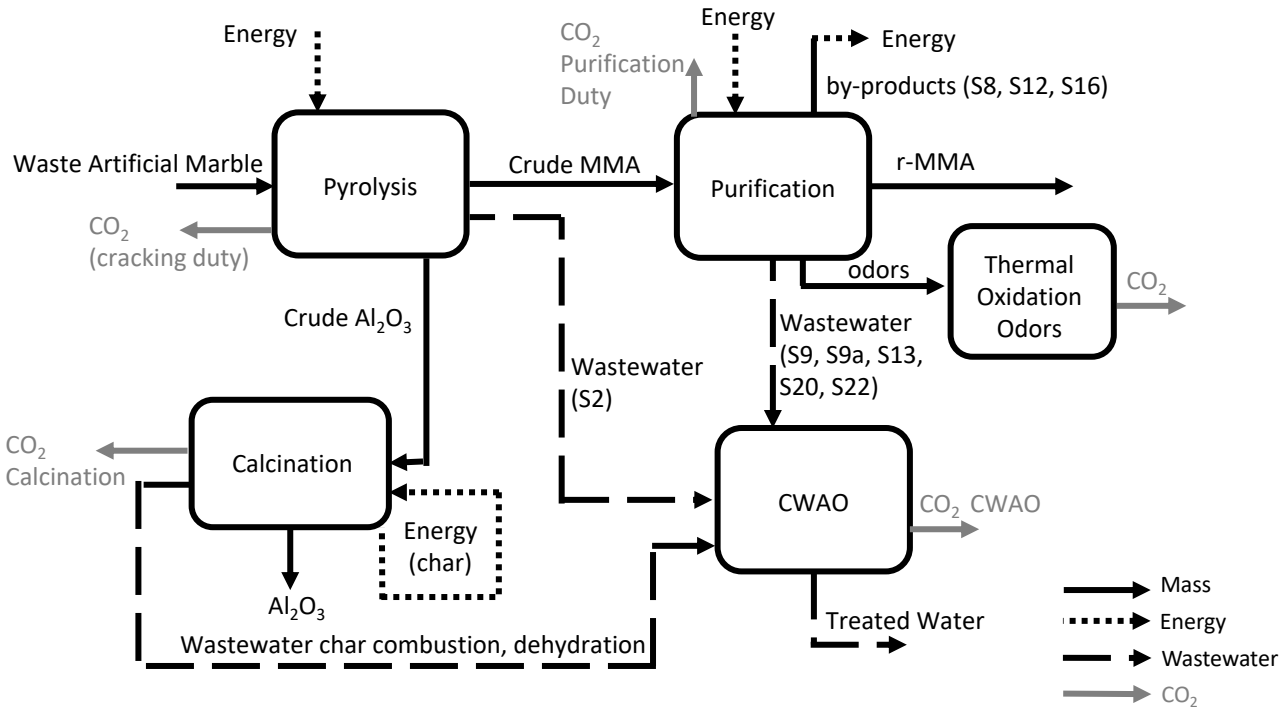

Figure (A.10) Energy, CO_2 and wastewater streams in the process.

- 15 kg to MMA,
- 23.5 kg to Alumina.

The remaining CO_2 (34.5 kg CO_2eq), coming from the purification section, is allocated fully to MMA. Finally, the CO_2 produced in the CWAO section is:

- 23.5 kg CO_2eq allocated to Alumina,
- 49.5 kg CO_2eq allocated to MMA.

A.5.2 Thermal (or catalytic) oxidation of odours

The CO_2 produced by the thermal (or catalytic) oxidation of the odoriferous streams S13a (degassed from 325) and S18 (degassed from 343) comes from the oxidation of Methanol and MMA-equivalent compounds, following the reactions:

- MMA: $C_5H_8O_2 + 6\,O_2 \longrightarrow 5\,CO_2 + 4\,H_2O$
- Methanol: $CH_3OH + 1.5\,O_2 \longrightarrow CO_2 + 2\,H_2O$

Considering all the other impurities behave like MMA, to minimize the CO_2 emissions, we consider that a catalytic exhaust treatment would be used, and it would generate 23 kg CO_2 allocated fully to r-MMA. The amount is small, and a thermal oxidizer would have a limited impact on the process.

A.5.3 CO_2 emissions from calcination

The calcination of crude alumina to Al_2O_3 is fueled by the combustion of the char PMMA residue left on the crude alumina, following the reaction:

- PMMA ($C_5H_8O_2$) + 6 O_2 $\longrightarrow$ 5 CO_2 + 4 H_2O.

Thus, 36.7 kg of PMMA generates 81 kg CO_2eq, allocated completely to Alumina.

A.5.4 CO_2 emissions from natural gas/by-products combustion

Different cases can be considered for the by-products combustion with or without energy recovery. The energy recovery allows minimizing the natural gas consumption but also the CO_2 emissions. In case the by-products contribute for part (90%) of the total duty, natural gas (47.2 MJ kg^{-1}) would provide for the rest of the duty at the cracking section, where we would need the highest temperature. From the by-products, we can recover 2476 MJ of energy (Section A.4.3), while we need to provide 2742 MJ. The natural gas must cover for the surplus of 267 MJ, to be provided at the cracking section.
If we split this surplus by mass allocation, we get:

- 104 MJ to MMA, and
- 163 MJ to Alumina.

The 2476 MJ of by-products fuels the purification (493 MJ completely allocated to MMA), and 1983 MJ required by the cracking. We can split these 1983 MJ by mass allocation into:

- 774 MJ to MMA, and
- 1208 MJ to Alumina.

Assuming the by-product combustion is similar to that of MMA (@27.2 MJ kg^{-1}):

- $C_5H_8O_2$ + 6 O_2 $\longrightarrow$ 5 CO_2 + 4 H_2O.

The CO_2 emitted on-site, in case of energy recovery from by-product combustion, is the sum of CO_2 from by-product combustion, CO_2 from natural gas, CO_2 from CWAO, CO_2 from calcination, and CO_2 from the thermal oxidation of odors (Figure A.1).

Contribution	Kg Natural gas	kWh	MJ	Kg CO_2 eq	Kg CO_2eq/ kg rMMA	Kg CO_2eq/ Kg Alumina
Natural Gas	2.2	29	101	6	0.03	
MMA Contribution (Cracking)						
By-products		353	1267	102	0.55	
MMA contribution (Cracking & Purification)						
1371 MJ is the MMA contribution to the total duty of the process						
By-Products		336	1208	98		0.25
Alumina contribution (Cracking)						
Natural Gas	3.4	45	163	9.3		0.02
Alumina Contribution (Cracking)						
1371 MJ is the Alumina contribution to the total duty of the process						
Char combustion @ 24.5 MJ/kg				81		0.2
(Calcination)						
CWAO				49.5	0.26	
MMA Contribution						
CWAO				23.5		0.06
Alumina Contribution						
Catalytic Oxidation				23	0.12	
Total	**5.6**		**2742**	**398**	**0.96**	**0.53**

Table (A.1) CO_2 emissions

In case of energy recovery from by-products, there is an emission of 398 kg CO_2eq (221 kg CO_2eq from combustion of gas/by-products and 177 kg from calcination, CWAO, and thermal oxidation), with consumption of 5.6 kg of natural gas. Allocating this CO_2 by mass, there will now be 0.96 kgCO_2eq/kg r-MMA, and 0.53 kgCO_2eq/kg Alumina.
In case of no energy recovery from the by-products, and all the energy must be supplied by extra natural gas consumption, the process would generate 1.48 kgCO_2eq/kg r-MMA, and 0.64 kgCO_2eq/kg Alumina. This shows that there is an incentive to try to valorize these side products.

CO_2 emissions could also have been split according to different rules. In the case of Alumina substitution, we calculate the amount of energy needed to calcine gibbsite to alumina, and the corresponding CO_2 emissions that we subtract from the total of the process for the same amount of alumina. When considering the energy recovery case, the impact rises to 1.32 kgCO_2eq/kg r-MMA, higher than when using the mass allocation.
We can also allocate all the emissions to the r-MMA. Indeed, that would be the case when the co-product would have no marketable value and would have to be landfilled, as it could

be the case if the co-product is glass-fiber. When considering the energy recovery case, the CO_2 emissions would rise to 2.11 $kgCO_2eq/kg$ r-MMA, but still lower than for virgin MMA. The last option would be to allocate the CO_2 emissions by market value of the products. Similar alumina could have a market value of about 0.75 USD/kg, while the low purity r-MMA generated in the process is assumed to have a market value of 1.5 USD/kg. When considering the energy recovery case, the CO_2 emissions would split into 1.03 $kgCO_2eq/kg$ r-MMA and 0.51 $kgCO_2eq/kg$ Alumina.

The allocations by mass or market value, or by substitution, give similar values. As long as the co-product of the composite (Alumina in the present case) has a market value, the recycling operation could seem attractive. In fact, there is a limitation to that model. One has to keep in mind that in the present case, there is a cluster of solid surface producers in the same region, and nevertheless supplying three different plants. One of the reasons would be to minimize the transportation cost, but also the CO_2 emissions related to transportation. The longer the distance, the higher the CO_2 emissions.
In a full life cycle analysis, one would have to include the CO_2 emissions linked not only to the transportation, but also to the pretreatment (crushing) of the solid surface scraps. To recover 1 kg of r-MMA, about 6 kg of scraps have to be transported. Solid surfaces are very hard materials, so a much higher energy consumption is expected for the crushing and grinding of that material. That step is certainly mandatory to promote heat and mass transfer. If the scraps have to be transported over a longer distance, the benefit compared to virgin MMA would disappear. Of course, it is even worse when the inorganic filler has no marketable value.

A.6 Conclusion

R&E is a Korean company that collects and recycles 35,000 t/y of waste artificial marble, a mixture of PMMA and $Al(OH)_3$ (64% $Al(OH)_3$, 35% PMMA, 1% additives). From their three plants in Korea, they produce 6,600 t/y of r-MMA (96.5 wt.%) purity, and 13,860 t/y of low surface area Al_2O_3, with a global r-MMA and Alumina mass yield of 0.54 and 0.5, respectively.

Based on the patents [3,5], we rebuilt a process flowsheet and derived mass and energy balances. The process uses a stirred-tank pyrolysis reactor to depolymerize the PMMA part in the artificial marble and concurrently dehydrate the $Al(OH)_3$. The cracked gases, containing MMA, MMA impurities (light and heavy), MAA and other organic acids, methanol, and

water, undergo a pre-cleaning and two distillations to recover a low-quality purified r-MMA (96.5 wt.%). Most of the water released from the $Al(OH)_3$ in the cracking is separated, but the crude MMA still carries a significant quantity of water. The main reason for the complex purification section is the presence of this water (forming a low-boiling azeotrope with MMA), and the high quantity of MMA impurities. Some of these, in particular the acrylates, are generated due to the artificial marble preparing method.

The process produces a high quantity of wastewater (around 0.74 kg wastewater/kg r-MMA and 0.38 kg wastewater/kg Alumina) that has to be treated on-site because of the high pollutant concentration (11.5 wt.%, or COD >115,000 mg/l). Such a high concentration of organics in the water would require a rather expensive wastewater treatment, like for instance a catalytic wet air oxidation unit (CWAO), operating at high pressure.
Despite extensive purification steps, MMA quality remains low, and the co-produced Alumina has a low surface area (30-80 $m^2\,g^{-1}$ at best, from BET). Pyrolysis at less than 500 °C could not only yield a higher surface area alumina but also minimize the losses of PMMA/MMA as carbon residue on the alumina surface. However, looking at the Al_2O_3 datasheet from this process, the pyrolysis is probably done at 500 °C. A high quantity of charred PMMA on the crude alumina (8-10 wt.%) remains and makes the calcination temperature more difficult to control. The process requires around 7.26 $MJ\,kg^{-1}$ purified r-MMA, and 3.45 $MJ\,kg^{-1}$ of Alumina, for a total of 2742 MJ in our case study of 1000 kg of artificial marble treated. Because of the low r-MMA mass yield, the by-products could theoretically cover for around 90% of this duty, reducing the natural gas consumption.
Considering only the emissions inside the boundaries of the plant, in case of energy recovery from the by-products, the total on-site CO_2 emissions would go down to 0.96 $kgCO_2eq/kg$ r-MMA, and 0.53 $kgCO_2eq/kg$ Alumina. On top of that, emissions have to be added for the transportation and the pretreatment (crushing) of the solid surface scraps. To remain attractive versus virgin MMA, that process should collect scraps over a short distance and valorize the co-product (Alumina). Another inorganic filler, like glass fiber, would not necessarily give as good an environmental impact.

A.7 References

1. "R&E Leaflet in English" on their website, `https://www.veolia.co.kr/sites/g/files/dvc2646/files/document/2020/06/R%26E%20Leaflet%20English.pdf` (accessed June 18, 2024).

2. Lee YS, Noh MS, Lee YM, Korean patent application KR101242763, 2013, assigned

to R&E Co. Ltd. Accessible at Patent (101242763) < KIPRIS (Korea Intellectual Property Rights Information Service).

3. Lee YS, Noh MS, Lee YM, US Patent application US2013/0055926 A1, 2013, assigned to R&E.

4. Lee SG and Jeng EK, Korean patent application KR1020080008975, 2008, assigned to R&E. Accessible at Patent (1020080008975) < KIPRIS (Korea Intellectual Property Rights Information Service).

5. Jeon MC, Ahn HG, Kim JG, Jung HM, Jeong SH, Park BJ, US patent application US2009/0099290, 2007. Assigned to Lotte Advanced Materials Co. Ltd.

6. Lee YS, Noh MS, and Lee YM, Korean patent application KR1020120017035, 2012, assigned to R&E Co., Ltd. Accessible at Patent (Crushing apparatus of waste scagliola) < KIPRIS (Korea Intellectual Property Rights Information Service).

7. Lee YS, Noh MS, and Lee YM, Korean patent application KR1020110036934, 2011, assigned to R&E Co., Ltd. Accessible at Patent (101155126) < KIPRIS (Korea Intellectual Property Rights Information Service).

8. Lee YS, Noh MS, and Lee YM, Korean Patent application KR1020120017037, 2012, assigned to R&E Co., Ltd. Accessible at Patent (Purification apparatus of waste scagliola) < KIPRIS (Korea Intellectual Property Rights Information Service).

9. Lee YS, Noh MS, and Lee YM, Korean Patent application KR1020120017036, 2012, assigned to R&E Co., Ltd. Accessible at Patent (Decomposition apparatus of waste scagliola) < KIPRIS (Korea Intellectual Property Rights Information Service).

10. Ishikawa T and Lu BCY, Vapor-liquid equilibria of the methanol-methyl methacrylate system at 313.15, 323.15 and 333.15 K. Fluid Phase Equilibria, 1979, 3, no. 1, 23-34.

11. Kim, BR, Chang WK, Yang GS, and Young SL. A Study on Recovery of Aluminum Oxide from Artificial Marble Waste by Pyrolysis. Korean Chemical Engineering Research, 2012, 50, no. 3, 567-573.

12. Kooi, J. The system methylmethacrylate?methanol?water. Recueil des Travaux Chimiques des Pays?Bas 68, no. 1 (1949): 34-42.

13. Knovel: Yaws' Handbook of Properties for Aqueous Systems, https://app.knovel.com/.../yaws-handb-solubility (accessed June 18, 2024).

14. Knovel Critical Tables (2nd Edition), Two Component Azeotropes (accessed June 18, 2024).

15. Hemingway BS, Robie RA, Fisher JR, Wilson WH, Heat capacities of gibbsite, $Al(OH)_3$, between 13 and 480 K and magnesite, $MgCO_3$, between 13 and 380 K and their standard entropies at 298.15 K and the heat capacities of calorimetry Conference benzoic acid between 12 and 316 K. (1977). J. Res. U.S. Geol. Surv.; 1977, Vol. 5:6.

16. Munro RG. Evaluated material properties for a sintered alpha-alumina. Journal of the American Ceramic Society, 1997, 80, no. 8, 1919-1928.

APPENDIX B SUPPORTING INFORMATION - CHAPTER 4

The supporting information of Chapter 4 are a very long list (over 20 pages) of links and a table with the capital cost references for the database. They are available at: https://chemistry-europe.onlinelibrary.wiley.com/doi/full/10.1002/cssc.202301172.

I decided to not report them here because they render the PDF document too heavy to read, and they do not add anything else to the work.

APPENDIX C SUPPORTING INFORMATION - CHAPTER 5

This annex contains the Supporting Information (SI) for the article "ARTICLE 3 – Waste Artificial Marble Pyrolysis and Hydrolysis" of Chapter 5.
The references are at the end of the section.

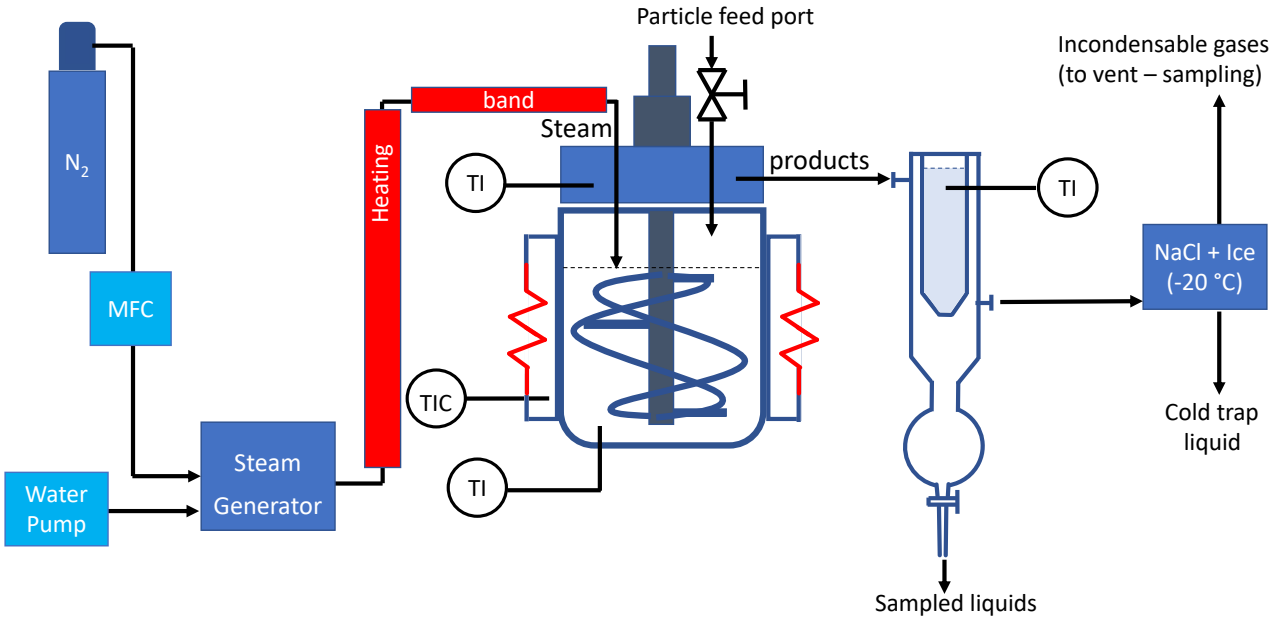

Figure (C.1) Experimental Pyrolysis and Hydrolysis setup

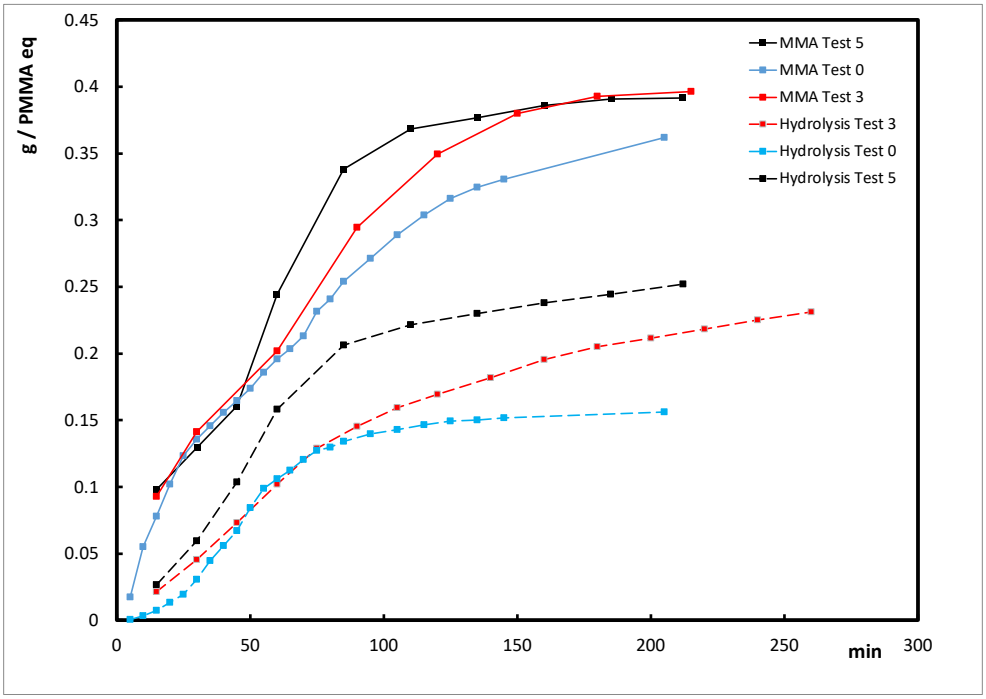

Figure (C.2) Effect of stirring rate - Test 3 vs Test 5 and Test 0 (Benchmark)

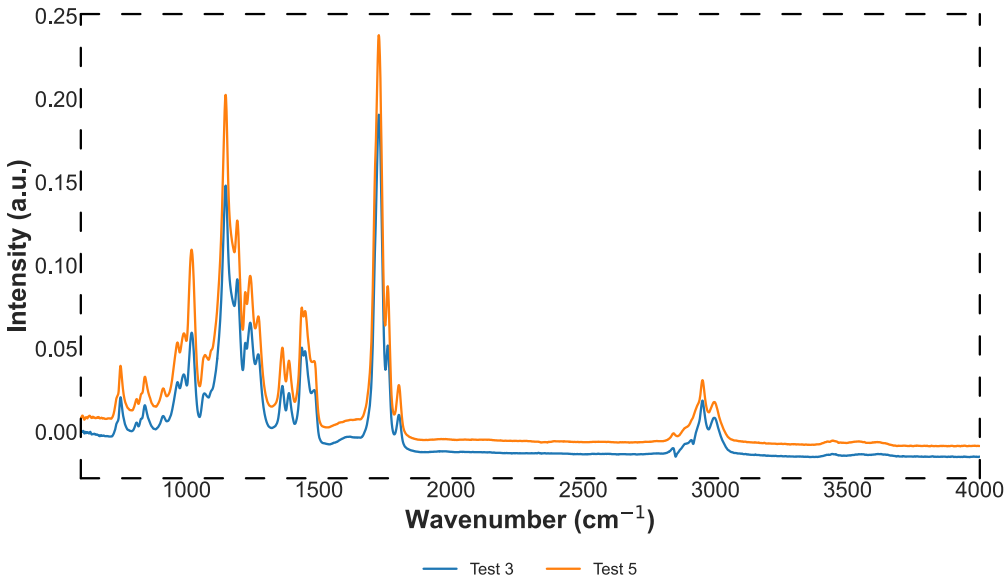

Figure (C.3) FTIR 600 to 4000 cm^{-1} - Test 5 vs Test 3

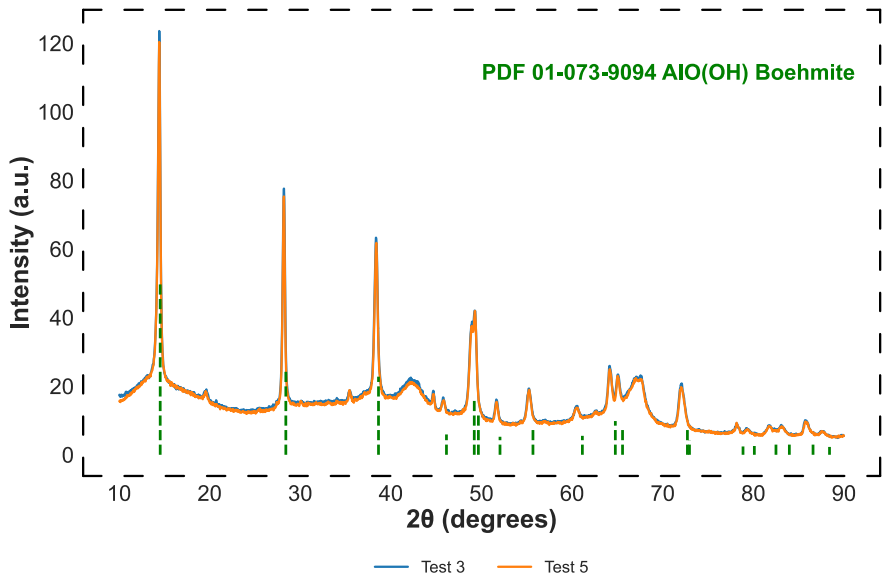

Figure (C.4) XRD Test 5 vs Test 3. The broad and diffuse peaks, represent chi-Alumina that concurrently forms during the dehydration process.

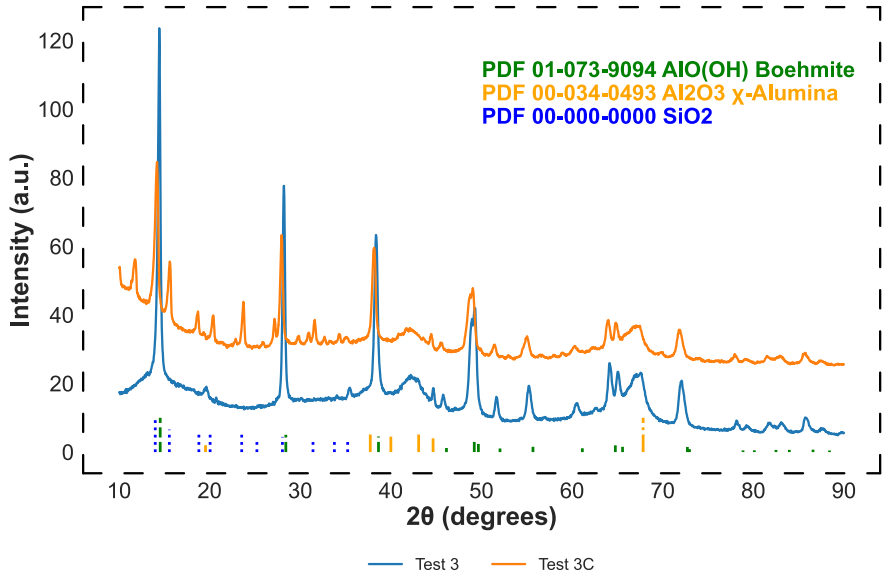

Figure (C.5) XRD Test 3 vs Test 3C, with reference peak positions of Boehmite, Chi-Alumina and SiO_2 .

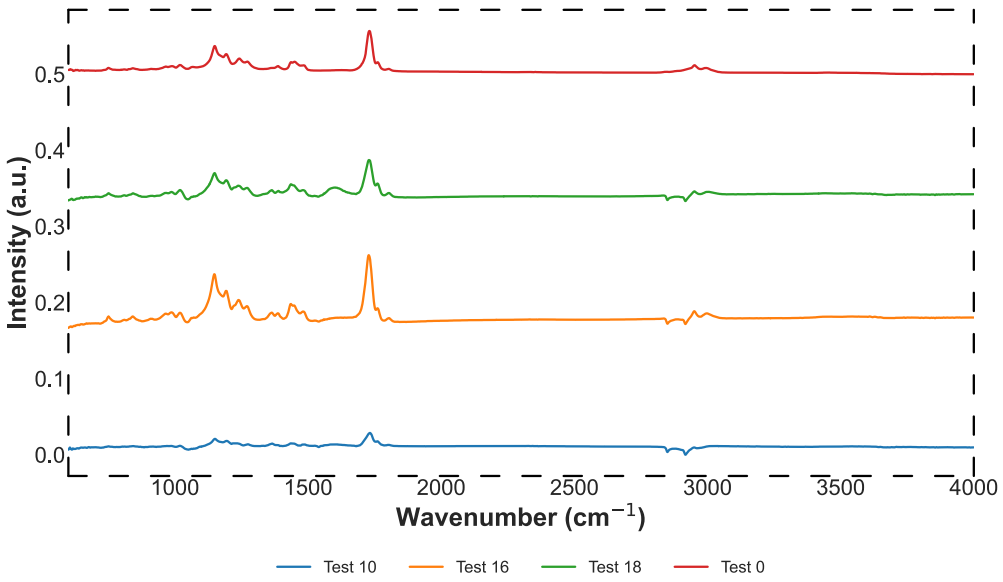

Figure (C.6) FTIR - Effect of heating ramp. Test 16, Test 18, Test 0 and artificial marble. Tests 12 is omitted because there is almost no polymer (flat spectrum). The dashed line corresponds to 1600 cm^{-1}

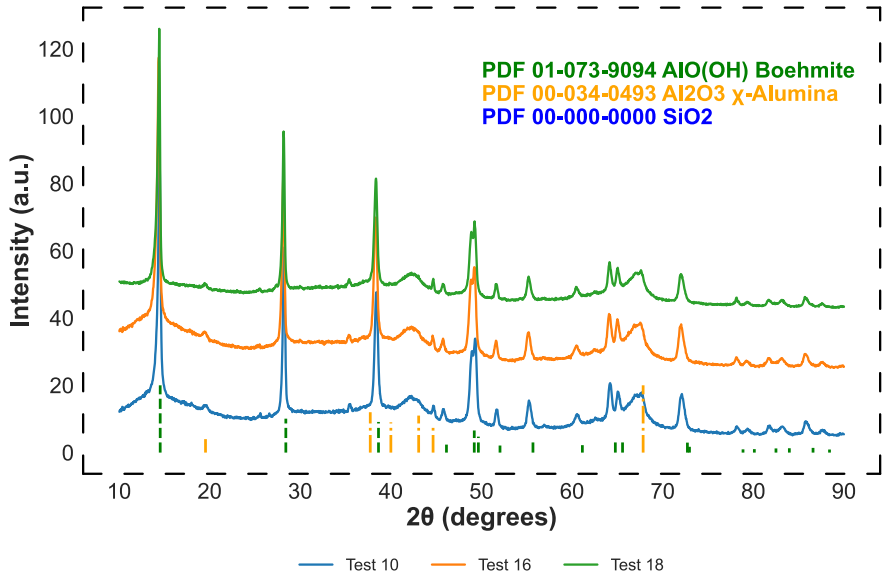

Figure (C.7) XRD - heating ramp effect

TEST	Y_{MMA} (g/g PMMAEQ)	$Y_{HYDROLYSIS}$ (g/g PMMAEQ)	Y_{MAA} (g/g PMMAEQ)	Y_{PRS} (g/g PMMAEQ)	$\bar{Y}_{CHAR}$ (g/g PMMAEQ)	$\bar{Y}_{GAS}$ (g/g PMMAEQ)	$Y_{BUTANOL}$ (g/g PMMAEQ)	$Y_{C16\,H30\,O4}$ (g/g PMMAEQ)	$Y_{ACETONE}$ (g/g PMMAEQ)
0	0.39	0.17	0.01	0.18	0.03	0.20	<0.005	0.03	<0.005
1	0.09	0.13	0.01	0.72	0.01	0.05	0.01	0.01	<0.005
2	0.44	0.22	0.04	0.00	0.03	0.27	0	0.03	0.01
3	0.42	0.24	0.02	0.20	0.02	0.10	<0.005	0.01	0.01
3C	0.24	0.24	0.08	0.27	0.05	0.20	<0.005	0	0.01
4	0.42	0.22	0.04	0.00	0.03	0.30	<0.005	0.02	0.01
5	0.42	0.27	0.04	0.22	0.03	0.06	<0.005	<0.005	0.01
7	0.41	0.32	0.04	0.19	0.03	0.02	0	0.02	0.01
7C	0.25	0.35	0.08	0.26	0	0.14	0	0	0.01
10	0.47	0.36	0.05	0	0	0.14	0.01	<0.005	0.01
12	0.53	0.29	0.05	0.00	0.03	0.14	0.01	<0.005	0.02
16	0.37	0.19	0.02	0.33	0.02	0.09	0.01	0.01	0.01
18	0.66	0.16	0.01	0.09	0.01	0.08	<0.005	<0.005	<0.005

TEST	Liquid and solid Global balance $\frac{\text{Liquid+Solid OUT (g)}}{\text{Composite+steam IN (g)}}$	Solid residue over composite $\frac{\text{Solid Residue (g)}}{\text{Composite IN (g)}}$
0	0.92	0.52
1	0.96	0.73
2	0.83	0.39
3	0.91	0.55
3C	0.81 *	0.63 *
4	0.87	0.41
5	0.93	0.53
7	0.98	0.53
7C	0.93	0.62
10	0.94	0.44
12	0.96	0.39
16	0.88	0.54
18	0.91	0.47

Table (C.1) Overall mass balance. * for the catalyzed test, the inlet mass includes the catalyst. Average on two repetitions. 300 g composite in, made of 44.4 % wt. PMMAeq

C.1 Alumina calcination heat balance

Bohemite transforms into Gamma Alumina in between 500 °C to 750 °C roughly (Figure 5.1b). Therefore we calculated the adiabatic temperature rise DT_{ad} in function of the quantity of polymer in the solid residue, for a given crude boehmite stream (boehmite + pyrolysis in the residue) of 520 kg/hr, containing 10.5 wt.% of polymer.

Assuming a LHV of the carbonaceous material equal to that of solid PMMA ($24.5\,\mathrm{MJ\,kg^{-1}}$ [1[), the combustion of the polymer in the residue would have to provide heat for heating the air/diluted air stream, to heat the alumina, dehydrate alumina, and rearrange the alumina crystalline phase.

The heat of combustion of the residue is:

$$\mathrm{LHV_{psr}} \times \text{residue (kg/hr)} = Q = 24.5\,\mathrm{MJ/kg} \times F\,\text{(kg/hr)}$$

where the carbon residue (kg/hr) is equal to the total flowrate of the crude boehmite stream

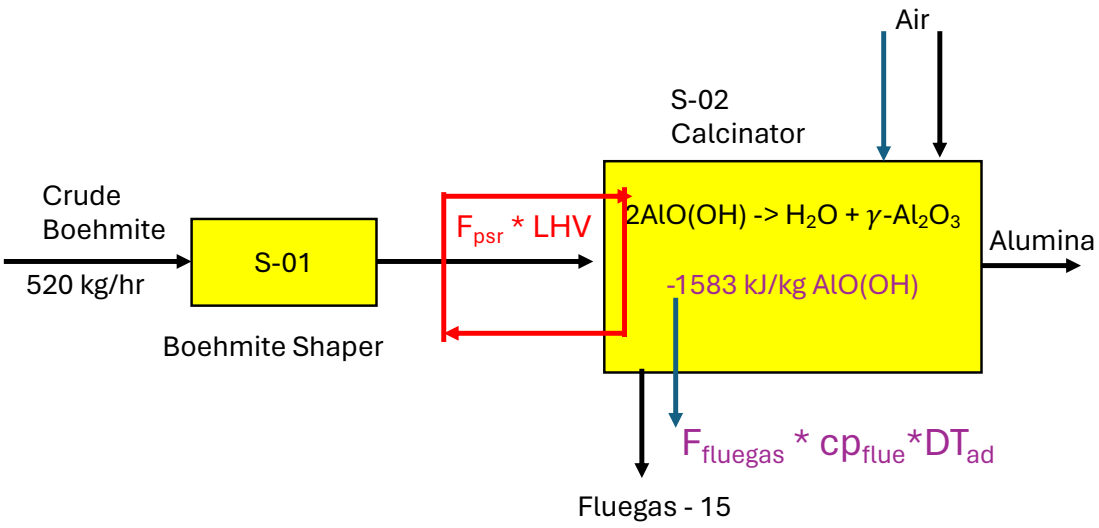

Figure (C.8) Energy balance around calcinator

multiplied by the weight percentage of polymer left on the boehmite.

The energy from the residue combustion will be consumed for (Figure C.8):

$$Q = H_{\text{solid-reaction}} + c_{p,\text{boehmite}} \times F_{\text{boehmite}} \times \Delta T + (F_{\text{air}} + F_{\text{gas}}) \times c_{p,\text{air-gas}} \times \Delta T$$

Where the residue is the weight of carbon (PMMAeq) in the alumina at the exit of the depolymerization/hydrolysis stage; F_{air} is the stoichiometric mass flow of air needed for the combustion, and the term $(F_{\text{air}} + F_{\text{gas}}) \times c_{p,\text{air-gas}} \times \Delta T$ represents the sensible heat lost with the flue gases. The temperature rise ΔT of the calcination as a function of the polymer content in the residue is therefore:

$$\frac{(Q - H_{\text{solid-reaction}})}{(c_{p,\text{boehmite/Alumina}} \times F_{\text{boehmite}} + (F_{\text{air}} + F_{\text{gas}}) \times c_{p,\text{air-gas}})} = \Delta T$$

The solid reaction of boehmite to gamma-Alumina is:

$$2\text{AlO(OH)} \rightarrow \gamma\text{Al}_2\text{O}_3 + \text{H}_2\text{O}$$

and the heat of reaction from the enthalpies of formation is $1585\,\text{kJ}\,\text{kg}^{-1}$ AlO(OH) [2,3], therefore for the transformation of the boehmite, we would need:

$$1585\,\text{kJ/hr} \times 467.7\,\text{kg/hr} = 741\,\text{MJ/hr}$$

With a carbon residue equal to 10.5% of the total weight of the crude boehmite stream (520 kg/hr × 10.5% = 54.6 kg/hr), and assuming that this residue burns similarly to solid PMMA, the combustion will be:

$$\text{PMMA}(C_5H_8O_2) + 6O_2 \rightarrow 5CO_2 + 4H_2O$$

Providing $54.6\,\text{kg}\,\text{h}^{-1}$ * $24.5\,\text{MJ}\,\text{kg}^{-1} = 1340\,\text{MJ}\,\text{h}^{-1}$. This duty has to cover for the boehmite transformation, as well as the flue gas losses in the calcinator.

To control the temperature of calcination, we work with stoichiometric O_2. To burn each $1\,\text{kg}\,\text{h}^{-1}$ of char PMMA ($1/100 = 0.01\,\text{kmol}\,\text{h}^{-1}$), we will need $\frac{6}{100} = 0.06\,\text{kmol}\,\text{h}^{-1}$ of O_2, corresponding to $\frac{0.06}{0.21} = 0.29\,\text{kmol}\,\text{h}^{-1}$, or $8.2\,\text{kg}\,\text{h}^{-1}$ of stoichiometric air ($O_2 + N_2$).

From the complete stoichiometric combustion of $1\,\text{kg}\,\text{h}^{-1}$ of char PMMA, we have:

$$0.06 * 3.76 = 0.03\,\text{kmol}\,\text{h}^{-1} \text{ of } N_2 \ (6.3\,\text{kg}\,\text{h}^{-1}),$$

$$5 * 0.01 = 0.05\,\text{kmol}\,\text{h}^{-1} \text{ of } CO_2 \ (2.2\,\text{kg}\,\text{h}^{-1}),$$

$$4 * 0.01 = 0.04\,\text{kmol}\,\text{h}^{-1} \text{ of } H_2O \ (0.7\,\text{kg}\,\text{h}^{-1}).$$

Thus, we obtain a total of $6.3\,\text{kg}\,\text{h}^{-1}$ + $2.2\,\text{kg}\,\text{h}^{-1}$ + $0.7\,\text{kg}\,\text{h}^{-1}$ = $9.2\,\text{kg}\,\text{h}^{-1}$ of flue gas per kilogram per hour of char PMMA residue.

Therefore, with the combustion and the boehmite transformation, we produce $502\,\text{kg}\,\text{h}^{-1}$ of flue gas.

Table (C.2) Mass balance around the boehmite calcinator

In the calcination operative range, the specific heat of boehmite is $1.5\,\text{kJ}\,\text{kg}^{-1}\,\text{K}^{-1}$ according to the Lawrence-Berkeley equation [4], while for alumina it is around $1.2\,\text{kJ}\,\text{kg}^{-1}\,\text{K}^{-1}$ [5]. Therefore, for the boehmite/alumina system, we took an intermediate value of $1.35\,\text{kJ}\,\text{kg}^{-1}\,\text{K}^{-1}$. For the flue gas, we assumed a specific heat constant equal to $0.65\,\text{kJ}\,\text{kg}^{-1}\,\text{K}^{-1}$ [6].

The adiabatic temperature rise ΔT is given by:

$$\Delta T = \frac{(Q - H_{\text{solid-reaction}})}{(c_{p,\text{boehmite/alumina}} \times F_{\text{boehmite}} + (F_{\text{air}} + F_{\text{gas}}) \times c_{p,\text{air-gas}})}$$

Substituting the values:

$$\Delta T = \frac{(1340 - 741)}{(1.35 \times 520 + 502 \times 0.65)} = 582\,^{\circ}\mathrm{C}$$

Therefore, the final temperature of the alumina is:

$$582\,^{\circ}\mathrm{C} + 25\,^{\circ}\mathrm{C} = 607\,^{\circ}\mathrm{C}$$

This temperature is within the operative range to obtain high surface area alumina, such as gamma-alumina.

Table (C.3) Azeotrope Composition and Boiling Points

Azeotrope	**Composition (% wt.)**	**Normal Boiling Point** (°C)
Methanol/MMA [7, 8]	82/18	64.2
Water/MMA [7, 9]	14/86	83
Methanol/Methyl Iso Butyrate [10]	75/25	64.0
Water/Methyl Iso Butyrate [10]	6.8/93.2	77.7
Water/Butyl Acrylate [11]	38/62	94.3
Water/Butanol/Butyl Acrylate [11]	50/37.6/12.4	92
MAA/Water [12, 13, 14, 15]	76.9/23.1	99.3

Table (C.4) FT-IR ATR Bands, Functional Groups, and Structures for PMMA and PMAA

Wavenumber (cm^{-1})	**Functional Group**	**Polymer**	**Description**
1150 and 1190	C-O-C vibration	PMMA [16; 17]	Ether group
1245	C-C-O vibration	PMMA [16]	Symmetric vibration
1730	C=O stretching vibration	PMMA [17; 18]	Ester carbonyl
2850 to 3100	C-H stretching vibration	PMMA [17; 19]	Symmetrical and asymmetrical methyl stretch
1700	C=O vibration	PMAA [17]	Acidic carbonyl
1800 and 1755	C=O stretching vibration	PMAA anhydride [17; 20; 22]	Acidic anhydride carbonyl (glutaric type), 1755 peak being the most intense
1803 and 1743	C=O stretching vibration	PMAA [20]	Acidic anhydride carbonyl (intermolecular isobutyric anhydride ring), 1803 peak being the most intense
1012-1022 (depending on the source)	C-O-C stretching	PMAA anhydride [21; 23]	Typical of anhydride
2600 to 3500	O-H stretching	PMAA [17; 25]	Broad band with free hydroxyl stretch (around 3500), and self-associated carboxylic groups
1640	Water bending	PMMA-PMAA [24]	Water adsorbed in the presence of acidic comonomer

References

1. Walters, R.N., Hackett, S.M. and Lyon, R.E., 2000. Heats of combustion of high temperature polymers. Fire and materials, 24(5), pp.245-252.

2. Chase, 1998, Chase, M.W., Jr., NIST-JANAF Themochemical Tables, Fourth Edition, J. Phys. Chem. Ref. Data, Monograph 9, 1998, 1-1951.

3. Chen, Qiyuan, and Wenming Zeng. "Calorimetric determination of the standard enthalpies of formation of gibbsite, Al (OH) 3 (cr), and boehmite, AlOOH (cr)." Geochimica et cosmochimica acta 60, no. 1 (1996): 1-5.

4. Lawrence Berkeley Laboratory. (1988). Thermochemical Properties of Gibbsite, Bayerite, Boehmite, Diaspore, and the Aluminate Ion Between 0 and 350 C. NUREG/CR-5271 LBL-21482.

5. Munro, Ronald G. "Evaluated material properties for a sintered alpha?alumina." Journal of the American Ceramic Society 80, no. 8 (1997): 1919-1928.

6. Engineering Toolbox - Carbon Dioxide specific heat of gas vs temperature, and Nitrogen specific heat of gas vs temperature. `https://www.engineeringtoolbox.com/carbon-dioxide-d_974.html`. Accessed on 11 - June - 2024.

7. Knovel Critical Tables (2nd Edition) - Two Component Azeotropes, 2008.

8. Ishikawa, Takeshi, and Benjamin C-Y. Lu. "Vapor-liquid equilibria of the methanol-methyl methacrylate system at 313.15, 323.15 and 333.15 K." Fluid Phase Equilibria 3, no. 1 (1979): 23-34.

9. Gao, Xiaoxin, Chen, Mengyuan, and Wang, Tianyu. "Design and optimization for the separation of a ternary methyl methacrylate-methanol-water mixture to save energy." Energy Sources, Part A: Recovery, Utilization, and Environmental Effects, 2020: 1-10.

10. Horsley, Lee H., and Tamplin, William S. "Azeotropic data-II." ACS Publications, 1973.

11. Niesbach, Alexander, et al. "Esterification of Acrylic Acid and n-Butanol in a Pilot-Scale Reactive Distillation Column Experimental Investigation, Model Validation, and Process Analysis." Industrial & Engineering Chemistry Research 51, no. 50 (2012): 16444-16456.

12. Gould, Robert F. "Azeotropic data-III, copyright, advances in chemistry series, foreword." ACS Publications, 1973.

13. Wilczynski, Robert, and Jerrick Juliette, Jamie. "Methacrylic acid and derivatives." Kirk-Othmer Encyclopedia of Chemical Technology, 2000.

14. Frolov, A.V., et al. "Liquid-Vapor Equilibrium in the Methacrylic Acid-Water System." ZHURNAL FIZICHESKOI KHIMII 36, no. 10 (1962): 2282-2284.

15. Moraru, Mihai Daniel, Bildea, Costin Sorin, and Kiss, Anton A. "Novel eco-efficient process for methyl methacrylate production." Industrial & Engineering Chemistry Research 60, no. 3 (2021): 1290-1301.

16. Cavallo, V., Pruvost, S., Gerard, J.F., Fina, A., 2023. Dispersion of cellulose nanofibers in methacrylate-based nanocomposites. Polymers 15, 3226.

17. Mansur, C.R., Monteiro, E.E., 1998. Characterization of methacrylic polymers by calorimetry and infrared analyses. Journal of applied polymer science 68, 345-354.

18. Kochneva, I., Roshupkin, V., 1991. Ir spectroscopic study of the hydrogen bond network in copolymers of methyl methacrylate with methacrylic acid. Polymer Science USSR 33, 2104-2111.

19. Sain, S., Ray, D., Mukhopadhyay, A., Sengupta, S., Kar, T., Ennis, C.J., Rahman, P.K., 2012. Synthesis and characterization of pmma-cellulose nanocomposites by in situ polymerization technique. Journal of Applied Polymer Science 126, E127-E134.

20. Grant, D., Grassie, N., 1960. The thermal decomposition of polymethacrylic acid. Polymer 1, 125-134.

21. Ho, B., Lee, Y., Chin, W., 1992. Thermal degradation of polymethacrylic acid. Journal of Polymer Science Part A: Polymer Chemistry 30, 2389-2397.

22. Semen, J., Lando, J., 1969. The acid hydrolysis of isotactic and syndiotactic poly (methyl methacrylate). Macromolecules 2, 570-575.

23. Jamieson, A., McNeill, I., 1974. The thermal degradation of copolymers of methyl methacrylate with methacrylic acid. European polymer journal 10, 217-225.

24. Max, J.J., Chapados, C., 2010. Isotope effects in liquid water by infrared spectroscopy IV. no free OH groups in liquid water. The Journal of Chemical Physics 133, 164501.